Electron Transfer and Energy Transfer in Porphyrin-Based Donor-Acceptor Systems

A Thesis
Submitted for the Degree of
DOCTOR OF PHILOSOPHY

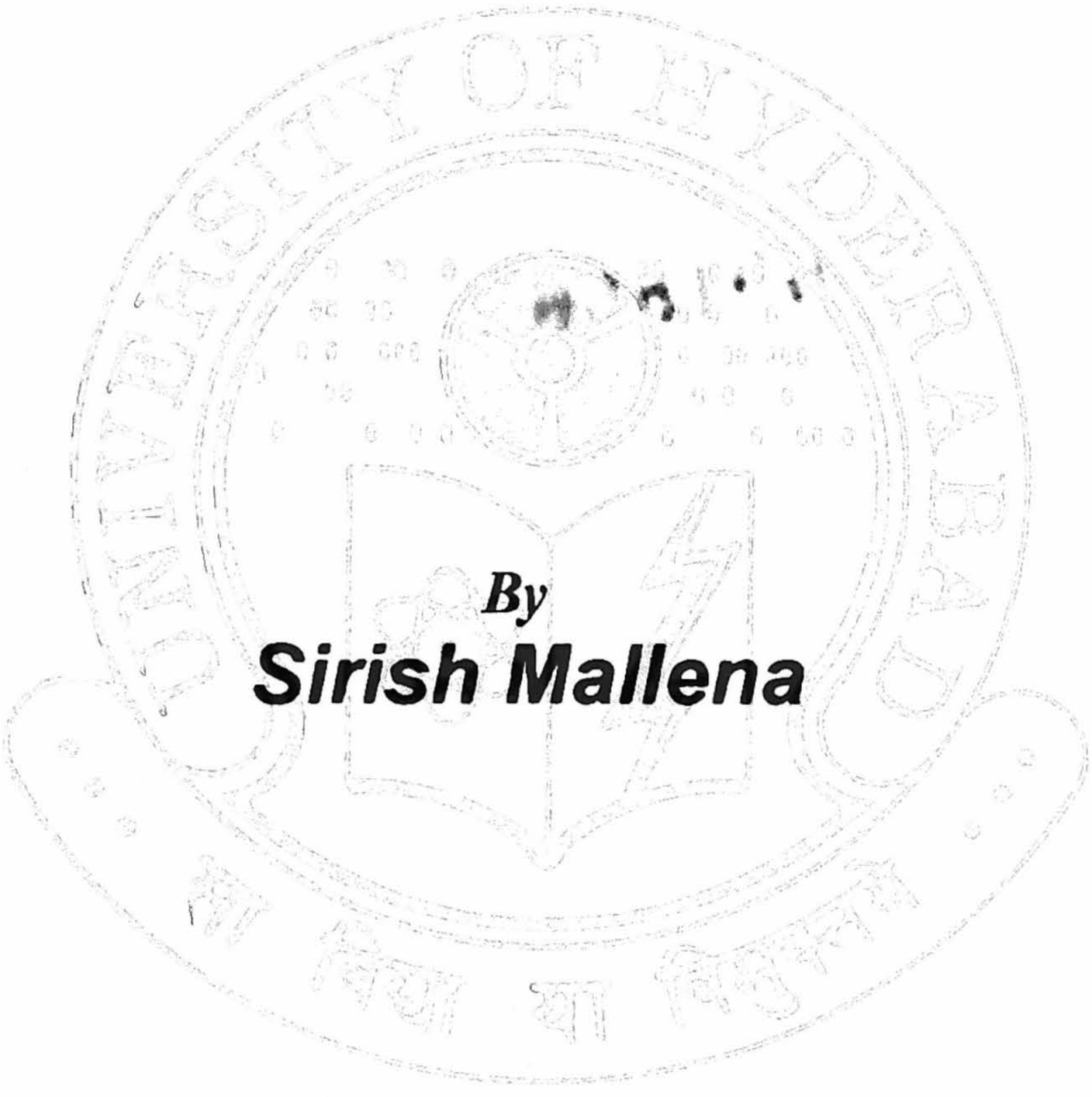

By

Sirish Mallena

School of Chemistry
University of Hyderabad
Hyderabad-500 046
India

December, 1995

Electron Transfer and Energy Transfer in Porphyrin-Based Donor-Acceptor Systems

A Thesis
Submitted for the Degree of
DOCTOR OF PHILOSOPHY

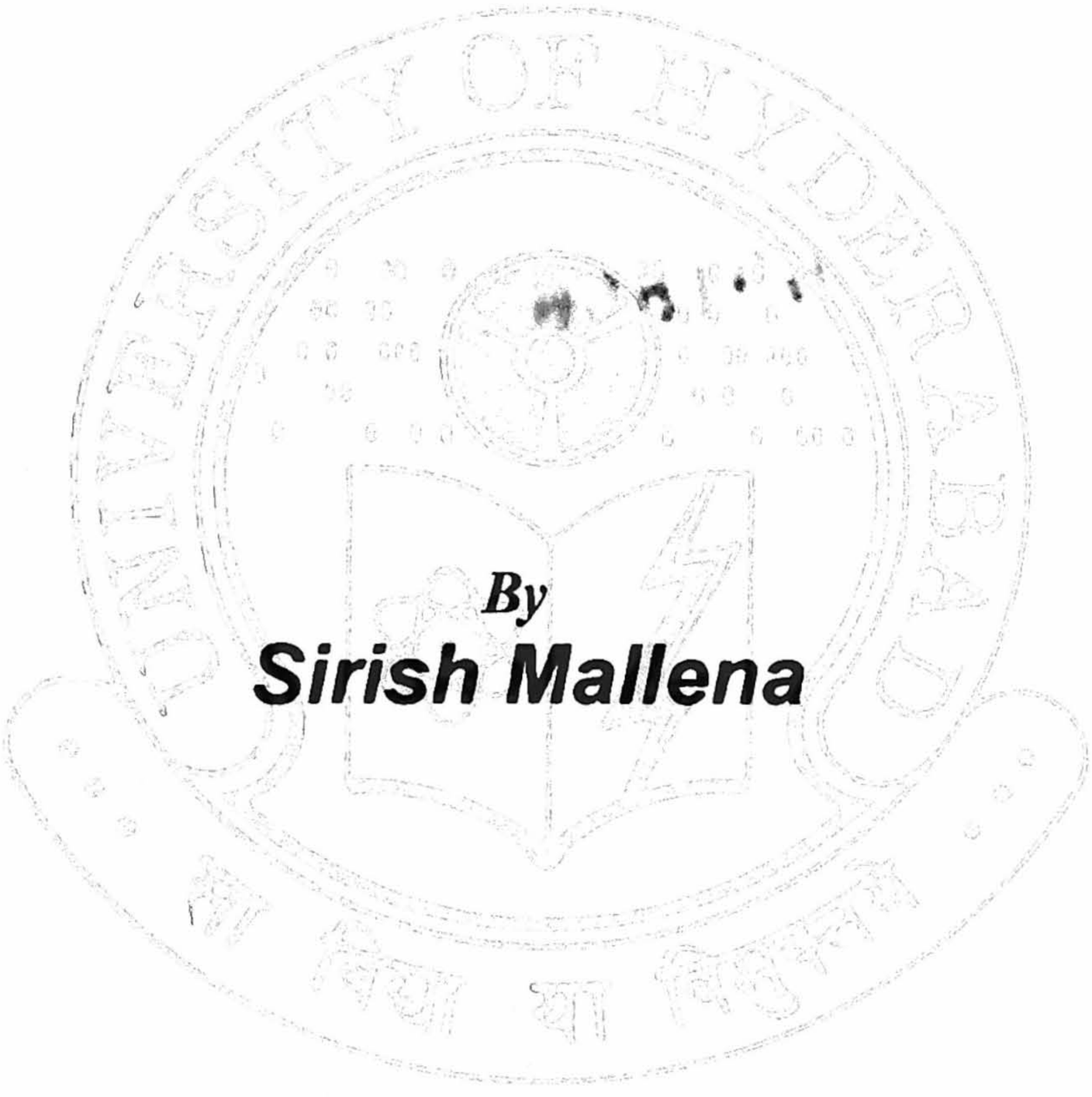

By

Sirish Mallena

School of Chemistry
University of Hyderabad
Hyderabad-500 046
India

December, 1995

Contents

Statement i

Certificate ii

Acknowledgements iii

Synopsis v

CHAPTER 1: Introduction 1

CHAPTER 2: Materials and Methods 43

CHAPTER 3: Photoinduced electron transfer in a series of porphyrin-dinitrobenzene dyad molecules 57

CHAPTER 4: Intramolecular excitation energy transfer in isomeric porphyrin-anthracene dyads 90

CHAPTER 5: Excitation energy transfer in a supramolecular porphyrin bearing four anthracene donor moieties 120

CHAPTER 6: Design, synthesis and singlet state activity of a porphyrin-anthracene supramolecular system assembled by nucleic acid base-pairing 144

CHAPTER 7: Photophysical and DNA cleavage studies of porphyrin-based photosensitizers for PDT 178

CHAPTER 8: Conclusions 222

Appendix 1: List of Publications 232

Statement

I hereby declare that the matter embodied in this Thesis is the result of investigations carried out by me in the School of Chemistry, University of Hyderabad, India under the supervision of Dr. Bhaskar G Maiya.

In keeping with the general practice of reporting scientific observations due acknowledgements have been made wherever the work described is based on the findings of other investigators

M. Sirish

Certificate

Certified that the work **"Electron transfer and energy transfer in porphyrin-based donor-acceptor systems"** has been carried out by **M. Sirish** under my supervision and that the same has not been submitted elsewhere for a degree.

Dean

School of Chemistry

D E A N
School of Chemistry
University of Hyderabad,
P C
HYDE
(A.P.)

Dec 30, 1995

Bhaskar G. Maiya

Thesis Supervisor

Acknowledgements

It is with great pleasure I express my deepest sense of gratitude to Dr Bhaskar G. Maiya, my supervisor for introducing me to the fascinating field of porphyrin chemistry, for his valuable guidance, kind co-operation, constant encouragement and help throughout this work

I owe a debt of gratitude to Professor G. Mehta who was kind enough to provide me with several porphyrin-based PDT agents for further studies I take this opportunity to thank Dr T Sambaiah, my fellow researcher and a friend, who synthesized these compounds

I thank Professor P S Zacharias, Dean and all the faculty members of the school of chemistry for training me in various aspects of chemistry

I am extremely grateful to Dr Aparna Dattagupta for her guidance, immense help, and co-operation while carrying out the biochemical experiments involved in this study I am especially thankful to Mr A Shanavas who helped me a lot during this period

I am grateful to Dr M Durga Prasad and Dr T P Radhakrishnan for their help in the computational work I thank Dr Anunay Samanta for his kind help with the time-resolved fluorescence studies

I also thank Professor N Periasamy, TIFR, Bombay and Dr Deepankar Chattarjee, CCMB, Hyderabad for their help

I would like to acknowledge my fellow researchers and friends Messrs Dr Ch Krishna Mohan Sharma, Dr Ram Dayal Yadav, Dr T Rajender Reddy, Dr G Subramanian, Dr K Venkateswara Rao, Dr B Satish Goud, Mr Bhaskar, Mr G Naga Srinivas Mr M B Viswanath and Mr M Lakshminarayana Rao who made my stay in the campus a memorable one I also thank my labmates and colleagues Messrs, T. Anita

Rao, Satya Prasanna, K. Rajashekar, S. Aruna Giri, L Giri Babu, B L V Prasad and M Ravi

I would like to thank Mr Satyanarayana, Mr. Bhaskar Rao, Mrs. Vijayalakshmi, Venkataramana and Mr Mishraji for their technical asssistance. I also thank Mr. Shetty, Mr. Santosh and other non-teaching staff of the school of chemistry for their help.

The financial assistance from the Council of Scientific and Industrial Research (CSIR) is gratefully acknowledged

The heavenly blessings of my father and best wishes of all my family members and relatives are the source of strength behind my sustenance I owe a great debt of gratitude to them.

Synopsis

This thesis entitled **"Electron Transfer and Energy Transfer in Porphyrin-Based Donor-Acceptor Systems"** deals with studies on photoinduced electron- and energy-transfer reactions of donor-acceptor (D-A) systems in which a porphyrin macrocycle has been used either as a donor or as an acceptor. Main findings of the research carried out here include elucidation of determinants of electron/energy transfer reactions occurring in covalently or non-covalently 'linked' D-A dyads and a pentad as well as demonstration of DNA photocleavage reactions by novel porphyrin-intercalator conjugates

Being the primary process of natural photosynthesis, photoinduced electron transfer (PET) reaction has attracted considerable attention over the past few years and recently, PET reactions occurring in a great variety of porphyrin-based model D-A compounds have been studied However, probably, owing to the difficulty involved in the synthesis of appropriate model compounds, an elucidation of the orientation dependence of electron transfer reactions in such D-A systems has received much less attention. A chapter in this thesis describes the design, synthesis and distance and orientation dependence of PET reactions of a series of covalently linked prophyrin-dinitrobenzene compounds

Intramolecular singlet-singlet excitation energy transfer (EET) is another process that bears relevance to both natural and synthetic systems. During the course of this investigation, it was noticed that studies on EET are relatively few in number compared to those on PET in the literature concerning the photochemistry of porphyrin-based model systems It was

also noticed that while studies that deal with electron transfer from the excited state of a porphyrin to the appended acceptor are numerous, those dealing with the electron transfer from a donor to the porphyrin are scarce. Considering these facts, a systematic investigation into the spectral and photophysical aspects of a series of covalently- or non-covalently 'linked' porphyrin(acceptor)-anthracene(donor) dyads and a pentad system has been undertaken in this study Intramolecular EET and PET reactions have been shown to compete with each other in the fluorescence quenching of all porphyrin (P) -anthracene(A) systems as shown schema-tically in Figure 1 A special emphasis has been given to an elucidation of distance and orientation dependence of energy- and electron-transfer reactions during this investigation.

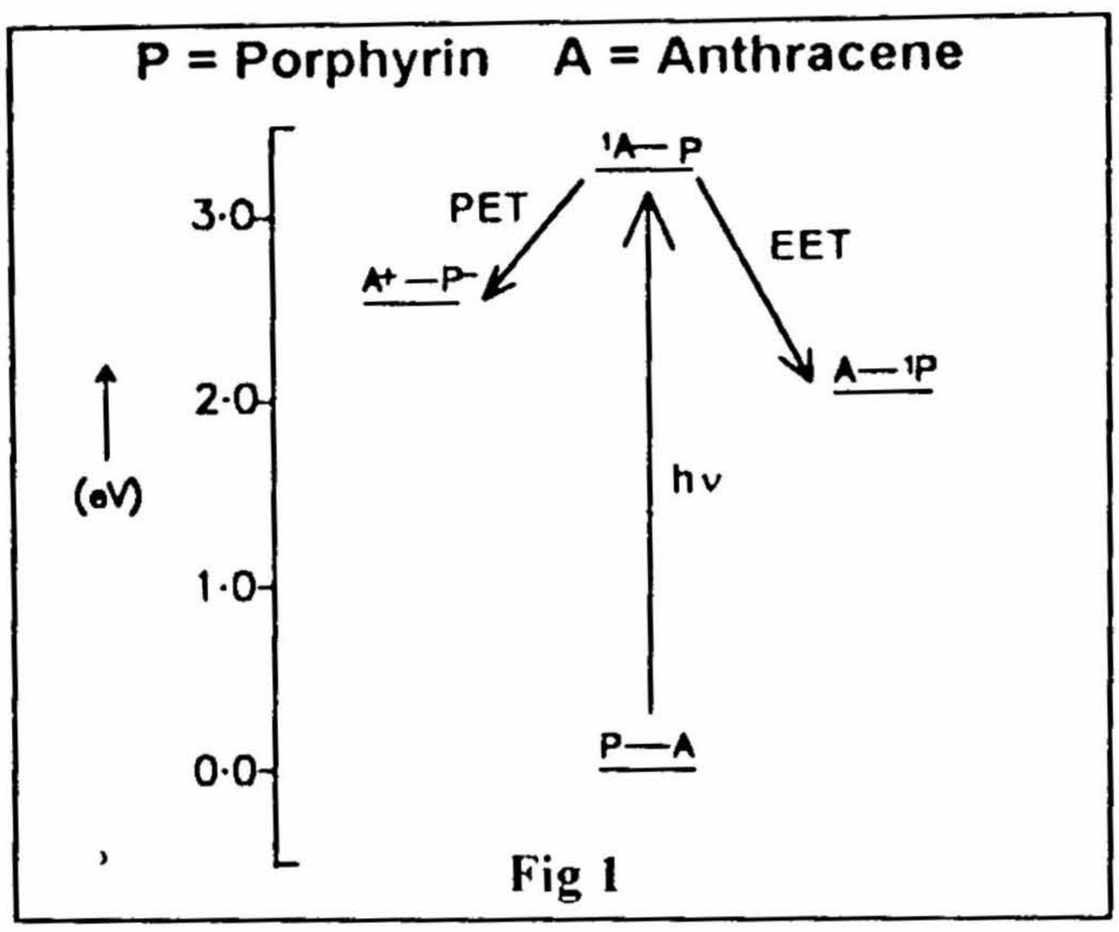

Fig 1

Apart from being the components of photosynthetic model systems, another major application of photochemically active porphyrin systems that is currently finding world-wide interest is in the photodynamic therapy (PDT) PDT, a newly introduced modality for cancer treatment, uses a porphyrin (P) photosensitizer to destroy the malignant tumor under the influence of light The process involves the intravenous injection of a porphyrin which, over a period of time, is selectively retained by the neoplastic tissue Subsequent irradiation of the tissue using the laser light of appropriate frequency generates toxic species such as singlet oxygen

(*via* EET) or superoxide radical (*via* PET) resulting in cell necrosis (Fig. 2).

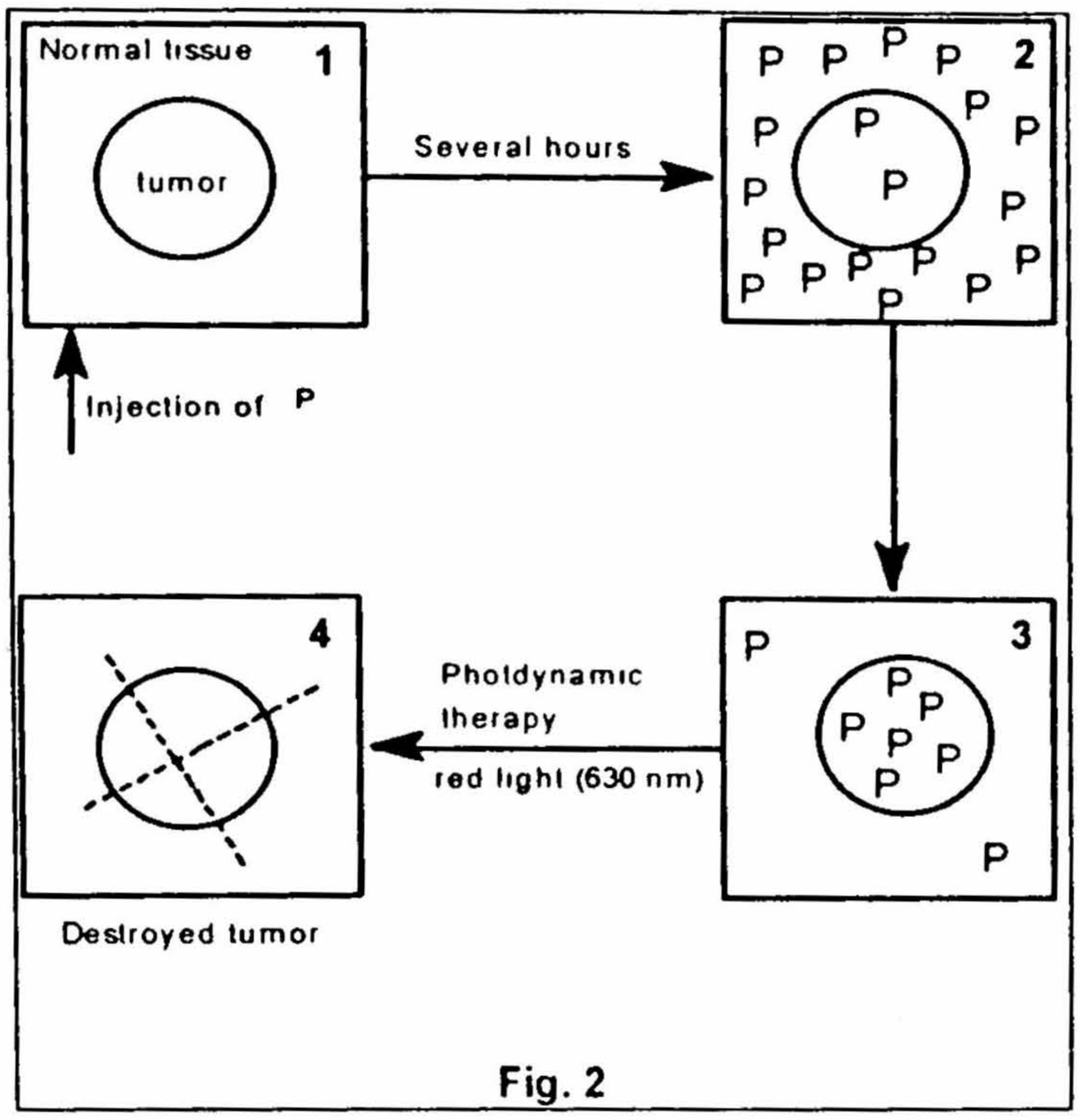

Fig. 2

As the exact mechanism of PDT remains elusive, there exists considerable scope for developing new photosensitizers which would enhance the therapeutic efficacy. Towards this end, spectral, photophysical and DNA-cleavage studies on a series of hybrid molecules in which a porphyrin has been covalently linked to either a DNA intercalator (e g acridone, acridine or phenothiazine) or a DNA-cross linking agent (e g chlorambucil) have been carried out in this study

The thesis has been divided into eight chapters and a brief, chapter-wise account of the results is presented below.

Chapter 1. ***Introduction***

In this chapter, recent literature on the EET and PET reactions of porphyrin-based D-A compounds is reviewed Also given is a brief survey on the development of new photosensitizers for PDT with emphasis laid on the aspects related to photocleavage of DNA.

Chapter 2. *Materials and Methods*

A general description of the synthetic methods and the spectroscopic techniques employed during the research work is presented in this chapter.

Chapter 3. *Photoinduced electron transfer in a series of porphyrin-dinitrobenzene dyad molecules.*

A series of isomeric D-A compounds (see Fig. 3) have been synthesized by linking a 3,5-dinitrobenzene acceptor moiety, *via* an ester bridge, to either para, meta or ortho position of one of the phenyl groups of meso-5,10,15,20(tetra-phenyl)porphyrin (H_2TPP) and its zinc(II) analogue, (ZnTPP). In comparison with the spectral properties of H_2TPP or ZnTPP, these D-A dyads show a broadening of the Soret band in their UV-visible spectra and an upfield shift of the imino proton resonance in their ^1H NMR spectra. These observations suggest the presence of a weak π-π interaction between the nitroaromatic acceptor and the porphyrin donor in these compounds. Low fluorescence quantum yields and short lifetimes observed for the ZnTPP-based dyads have been interpreted in terms of the occurrence of a PET reaction from the singlet porphyrin to the appended nitroaromatic acceptor moiety A detailed analysis of the fluorescence lifetime data obtained in five different solvents for each of the D-A compounds suggests a distance and orientation dependence of the

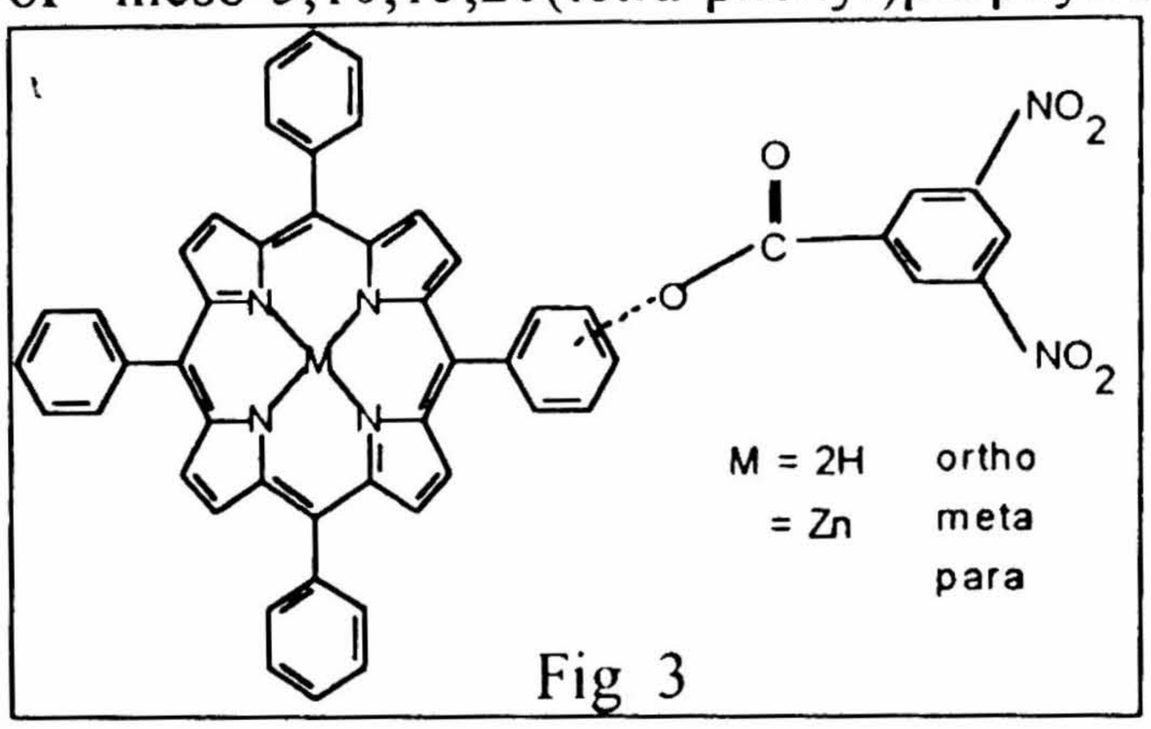

Fig 3

PET reaction in them (J. Photochem. Photobiol. A:Chemistry, 1994, 77, 189-200).

Chapter 4. *Intramolecular excitation energy transfer in isomeric porphyrin-anthracene dyads*

Covalently linked, isomeric porphyrin-anthracene dyads shown in Fig. 4 have been synthesized and fully chara-cterized by spectral and electro-chemical methods When excited at the anthracene absorption maximum, these dyads show a quenching of fluorescence

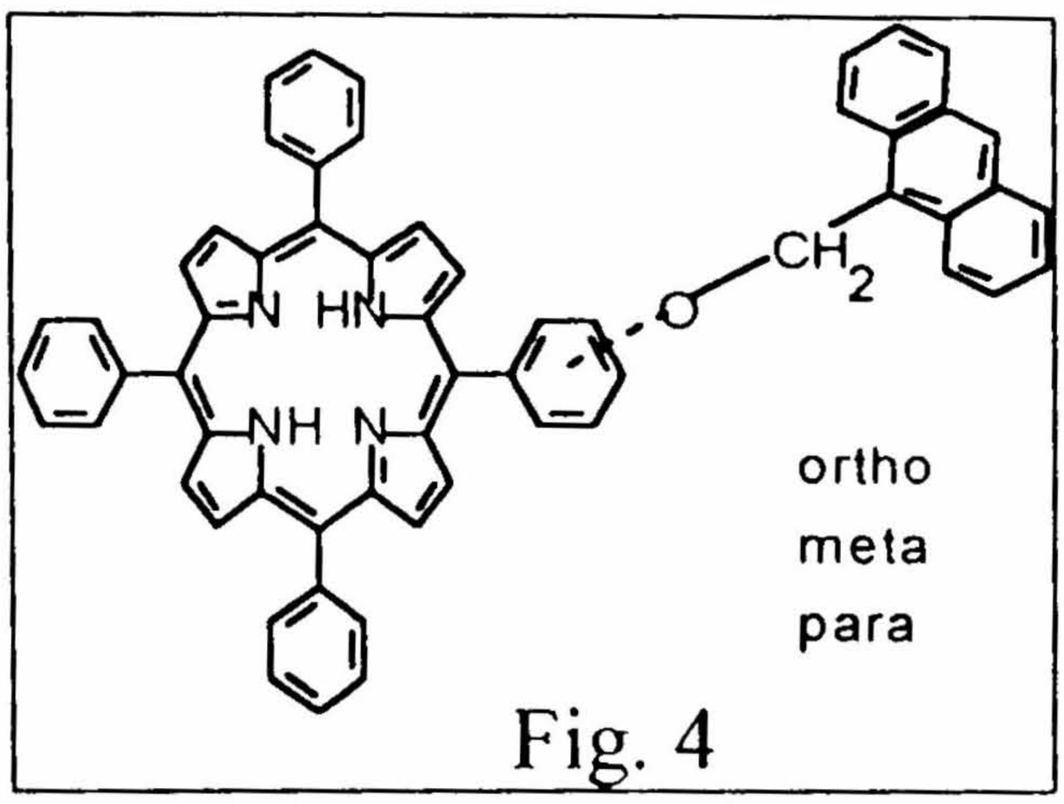

Fig. 4

in comparison with the fluorescence due to free anthracene as shown in Fig 5. Excitation spectra of these compounds obtained when the emission was monitored at the porphyrin emission maximum show bands due to the anthracene moiety thus providing evidence for the existence of intramolecular EET from the anthracene subunit to the porphyrin The energy transfer efficiencies as estimated from an overlay of the normalized excitation spectra with the corresponding absorption spectra, are found to vary with the site of attachment of the anthracene with respect to the porphyrin (o > m > p).

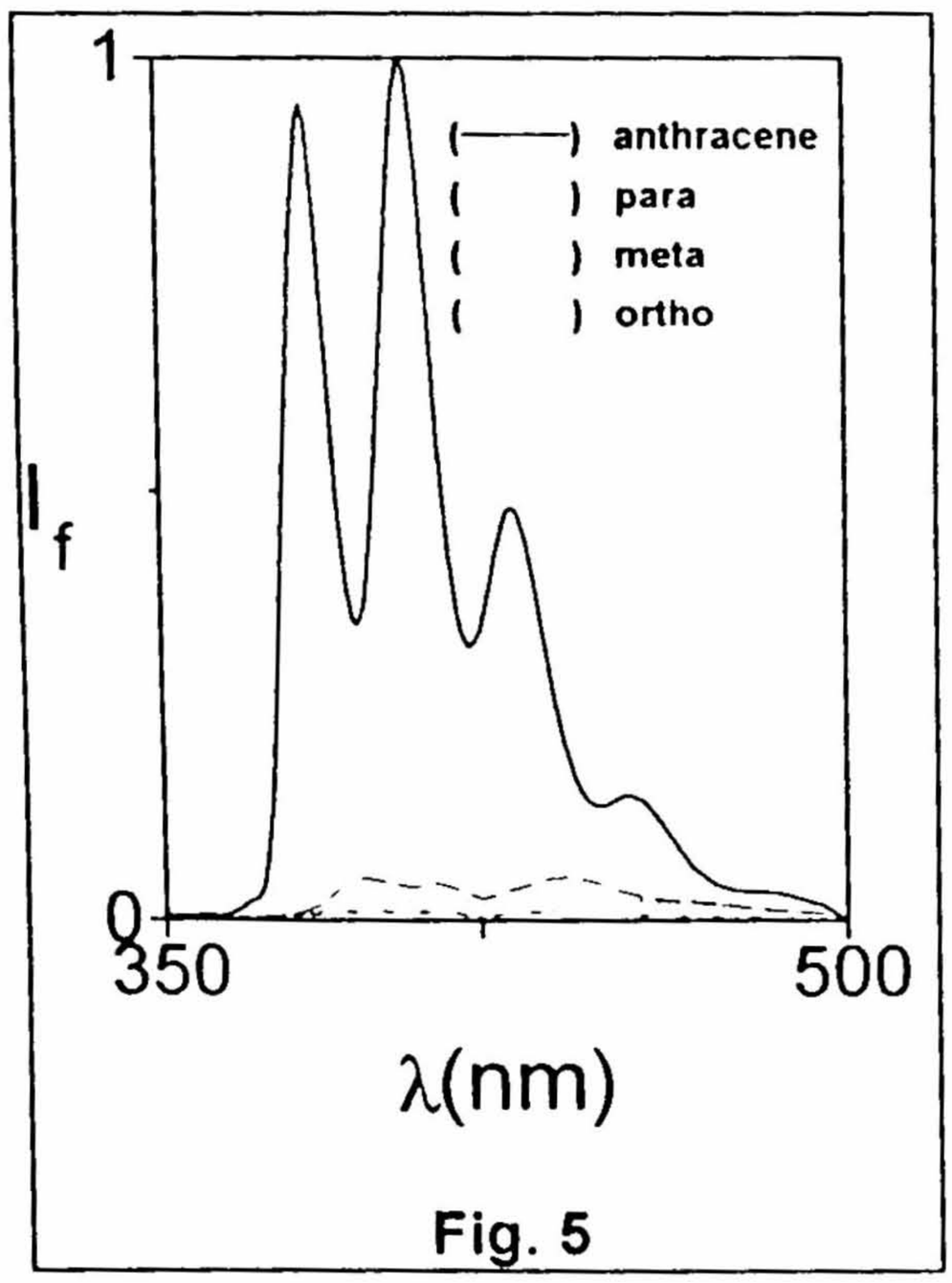

Fig. 5

Interestingly, a detailed analysis of the energy transfer data suggests that neither Forster's dipole-dipole mechanism nor Dexter's electron exchange mechanism could adequately explain this energy transfer Thermodynamic considerations and solvent dependent fluorescence data suggest the participation of a competing PET reaction in the fluorescence quenching of these dyads (J Photochem Photobiol A Chemistry, 1995, 0000)

Chapter 5. ***Excitation energy transfer in a supramolecular porphyrin bearing four anthracene donor moieties.***

Synthesis, characterization and singlet state activity of a supramolecular porphyrin bearing four anthracene moieties (5,10,15,20-tetra-(3-(9-methyloxyphenyl))porphyrin, a D_4-A pentad, Fig 6) are described in this chapter As was the case with the porphyrin-anthracene dyads mentioned above, the observed quenching of the anthrecenes' fluorescence (90-99%) together with the excitation spectral data provide evidence for the occurrence of intramolecular EET from anthracene to porphyrin in this molecule The energy transfer efficiencies measured in various solvents (76%, hexane, 64%, CH_2Cl_2, 36%, CH_3CN) for this pentad system are found to be lower compared to the meta-linked D-A dyad (see Fig 4) which shows a 82-85% efficiency in all the investigated solvents. This observation has been rationalized in terms of the difference between

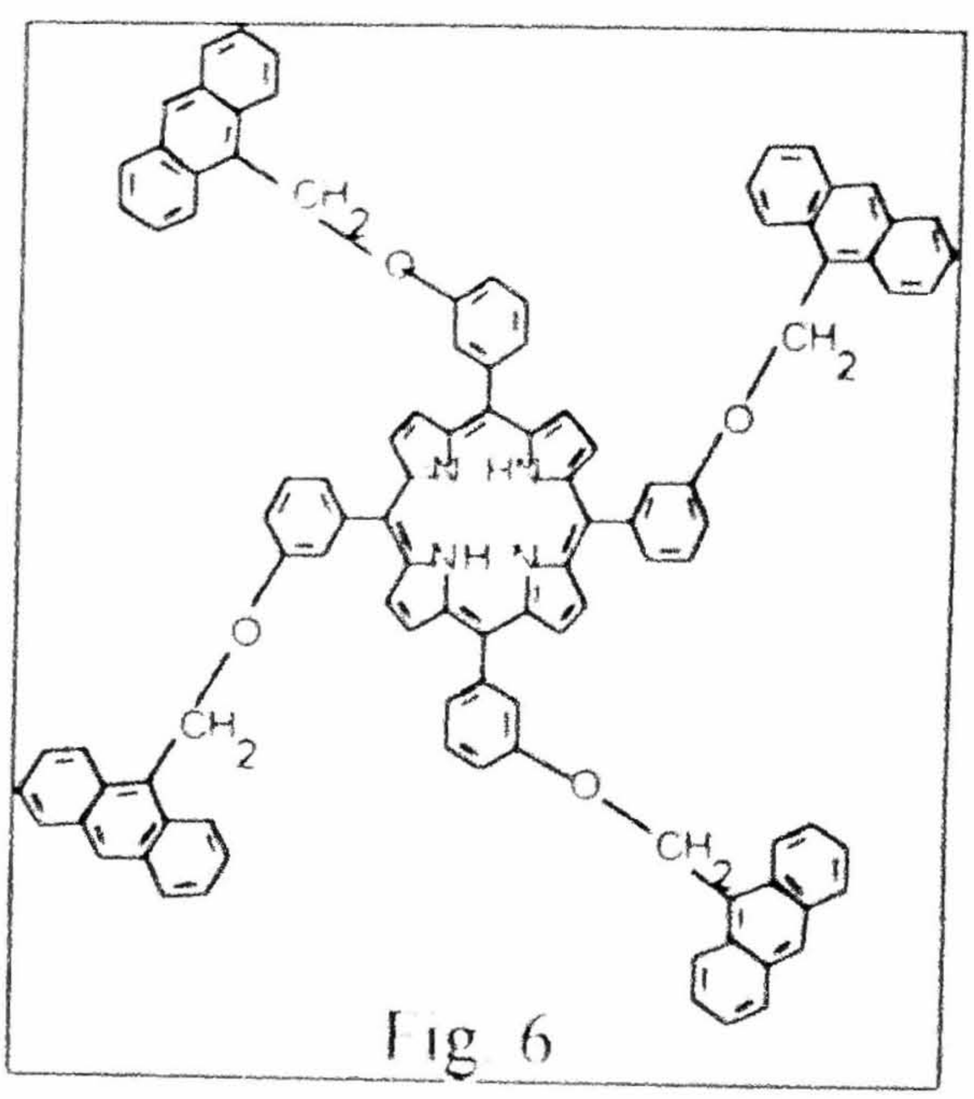

Fig 6

the pentad and the dyad with respect to the number and orientation of the possible D-A conformers in these systems. It is further rationalized that the various D-A orientations that are possible due to linking of four anthracene subunits might promote the excited state processes other than the EET in this supramolecular porphyrin (J Photochem Photbiol A:Chemistry, 1995, 85, 127-135.)

Chapter 6. ***Design, synthesis and singlet state activity of a porphyrin-anthracene supramolecular system assembled by nucleic acid base-pairing.***

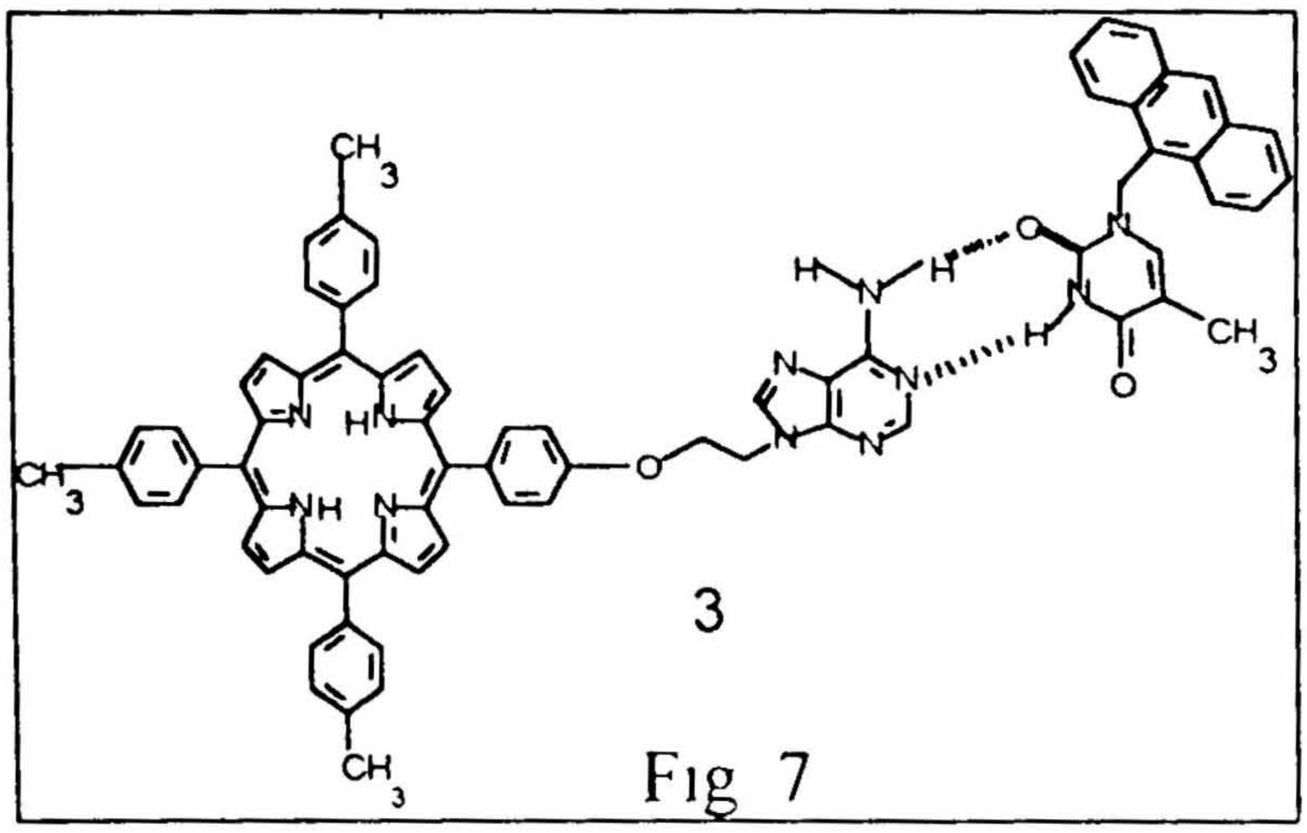

3

Fig 7

Molecular recognition and self assembly have recently become important features of bi- or multi-chromophoric systems which exhibit EET and PET reactions The non-covalently bound D-A system (**3**) shown in Fig 7 is assembled by mixing $CHCl_3$ (or $CDCl_3$) solutions of meso-5(4-(9-ethyloxyadenyl)phenyl))-10,15,20-tritolyl)porphyrin (**1**) and 1-(9-methyl- anthracenyl) thymine (**2**) Binding studies carried out by moni- toring the adenine amino-Hs of **1** (5mM) in the presence of 0 5 - 50 mM of **2** (see Fig 8) and standard data analysis gives the association constant, K, to be equal to (47±5) M^{-1} for the A-T base-pairing. The Stern-Volmer constants obtained from the time-resolved fluorescence quenching studies of **2** by **1** and H_2TTP have been found to be 1100 ± 150 and 2100 ± 300 for **2/1** and **2**/H_2TTP, respectively.

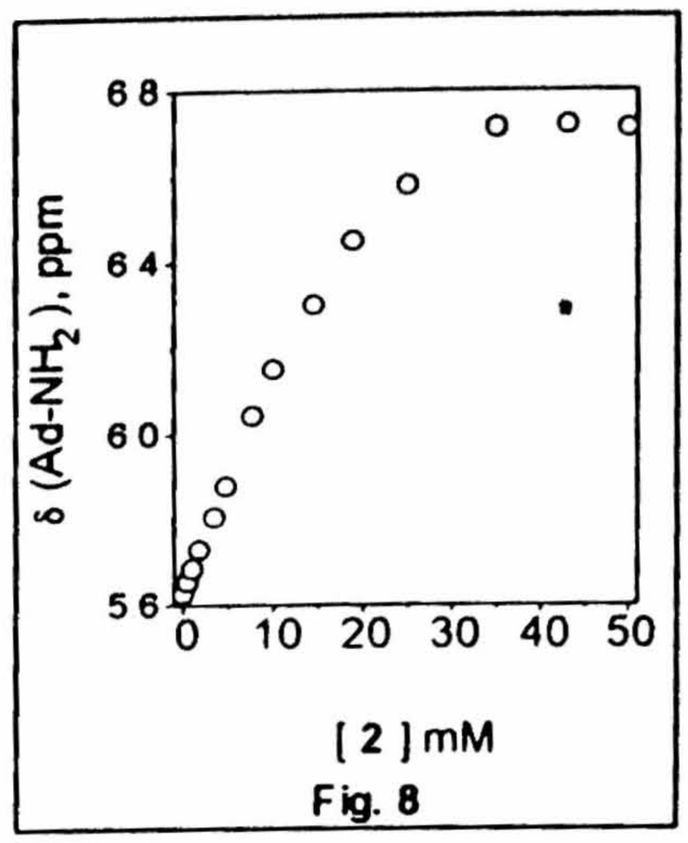

Fig. 8

Similarly, experiments carried out for solutions containing equimolar mixtures of **2** and H_2TTP or **1** at varying concentrations (0.001 - 2 mM in each case) have been found to give shorter lifetimes for solutions containing **2** and H_2TTP in comparison with those obtained for solutions containing **2** and **1**. These results have been interpreted in terms of an exclusive intermolecular quenching reaction between **2** and H_2TTP and of an additional and, obviously less efficient, intramolecular pathway involving the H-bonded complex **3** in the quenching reaction between **2** and **1**. Both PET and EET have been shown to participate in the quenching mechanism.

Chapter 7. ***Photophysical and DNA cleavage studies of porphyrin-based photosensitizers for PDT.***

The photophysical and DNA cleavage studies of a series of photosensitizers in which a porphyrin macrocycle has been linked to either a DNA intercalator or a cross-linking agent (Fig 9) are described in this chapter. The investigated photosensitizers include porphyrins linked to acridone (**1a-e**), 9-aminoacridine (**2a-c**), phenothiazine (**3a-j**) or chlorambucil derivatives (**4a-f**) and are obtained as a kind gift from Professor G Mehta. The similarity of UV-visible absorption spectra of these conjugates with the spectra of the corresponding non-linked constituent components indicates that there exist a minimal ground state interaction between the porphyrin and the utilized intracellular recognition element in each case. Consistent with this observation is the fact that the fluorescence quantum yields and also the

CH3
HN
NH
N
R
R =
n = 2 1a
n = 3 1b
n = 4 1c
n = 5 1d
n = 6 1e
n = 2 2a
n = 3 2b
n = 4 2c
n = 3 3a
n = 4 3b
n = 5 3c
n = 6 3d
n = 3 3e
n = 4 3f
n = 5 3g
n = 3 3h
n = 4 3i
n = 5 3j
n = 3 4a
n = 4 4b
n = 5 4c
n = 6 4d
4e
4f
R = OH 5a
R = 5b

Fig 9

singlet oxygen quantum yields of these hybrid porphyrins are in the same range as those of the reference porphyrin, H_2TPP. Thus, neither the appended intercalator/cross-linking agent nor the intervening spacer unit has an adverse effect on the photosensitising ability of the porphyrin subunit in these systems. However, fluorescence from the acridone and acridine moieties is seen to be quenched in compounds **1a-e** and **2a-c**. Intramolecular EET from the acridone to the porphyrin has been established in the case of porphyrin-acridone systems. The nuclease activity of these sensitizers has been studied using the supercoiled plasmid pBR322 DNA by the gel electrophoresis method. While control experiments in the absence of light show no discernible nicking, on irradiation by the visible light (λ = 550±10 nm), compounds **1a-e**, **3a-j** and **4a-f** all affect the relaxation of the supercoiled form I to the circular form II. A representative result showing the DNA cleavage using compounds **4a-f** is given in Fig. 10. Control experiments also suggest that the non-linked reference compounds do not affect any cleavage of DNA under similar experimental conditions. (J Chem. Soc Perkin Trans. I 1993, 2667.; Tetrahedron Lett. 1994, 4201, J Chem. Soc Perkin Trans. I, 1995, 295.)

Chapter 8. *Conclusions*

A summary of the investigations is presented here

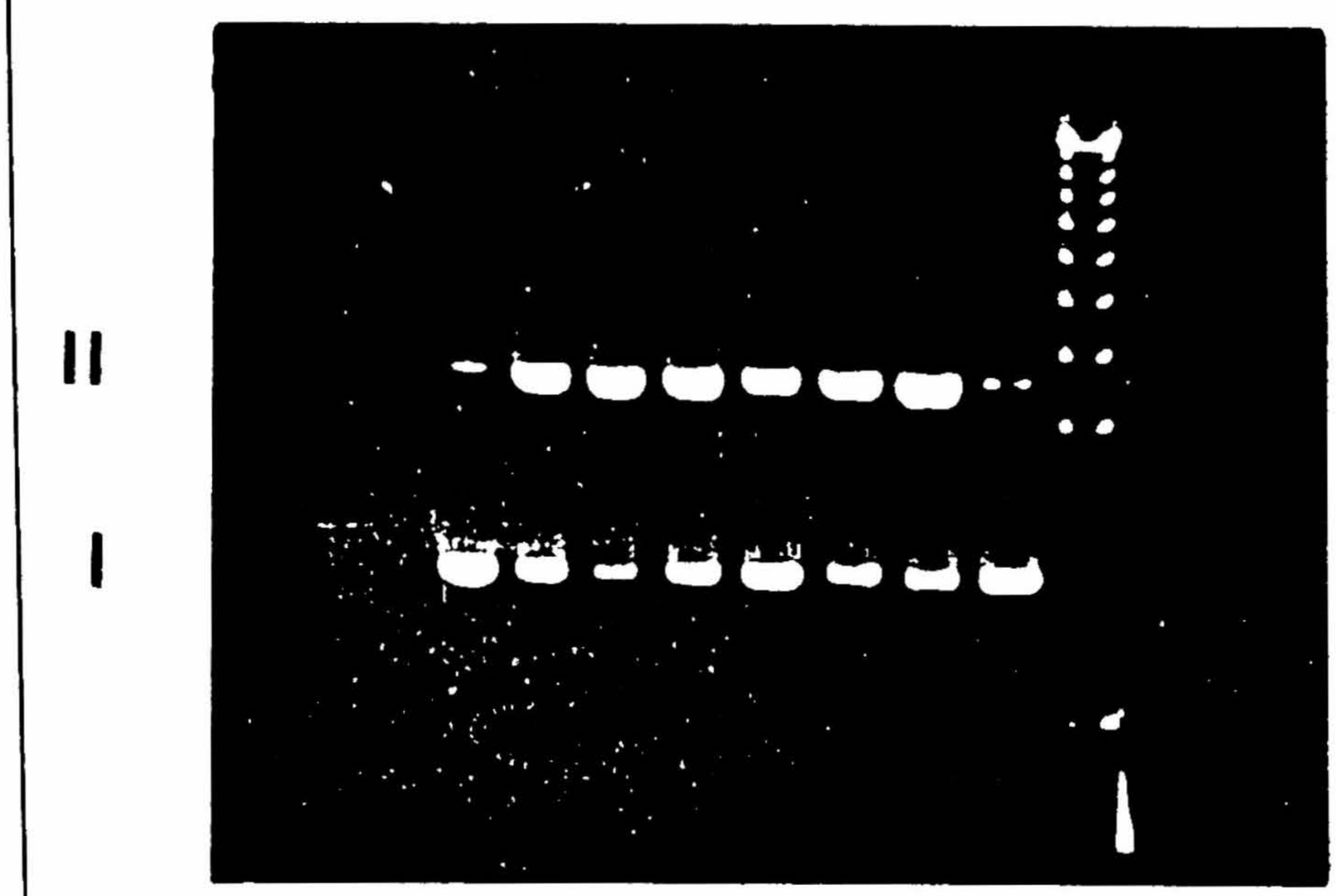

Fig. 10

Fig. 10. Light induced nuclease activity of 4a-f. (From left to right) Lane 1: Untreated pBR 322; Lanes 2, 3, 4, 5, 6 and 7: pBR 322 + 4e, 4a, 4b, 4c, 4d and 4f, respectively, Lane 8 : pBR 322 + chlorambucil, Lane 9 : DNA mol. wt. marker.

CHAPTER 1

Introduction

Porphyrins are involved in many biological and abiological functions including hemoglobin/myoglobin oxygenation, cytochrome activity, antenna function and charge separation reactions of both natural and artificial photosynthetic systems, catalysis of organic reactions, magnetic resonance imaging, photodynamic therapy (PDT) etc Among these functions, photosynthesis and photodynamic therapy are the ones which deal with the photochemistry of these versatile red-light-absorbing chromophores Both these functions are characterized by photoinduced electron transfer (PET) and excitation energy transfer (EET) reactions of porphyrin excited states This thesis deals with studies on PET and EET reactions of donor-acceptor (D-A) systems in which a porphyrin or a metalloporphyrin has been used either as a donor or as an acceptor This chapter first gives a general introduction to the electron transfer and energy transfer processes and then discusses the chemistry of recently reported porphyrin-based D-A compounds and PDT agents with a special reference being given to their PET and EET reactions as applicable to the subject matter of this thesis

1.1 PET and EET - general considerations

Molecules, upon photoexcitation become powerful donors or acceptors and hence, can be involved in electron and/or energy transfer reactions. Photoinduced electron transfer reaction has attracted the interest of chemists in many respects which include synthesis of organic molecules, development of solar energy storage/conversion systems and understanding

of natural/artificial photosynthetic systems.[1-4] Similarly, excitation energy transfer reactions are also important from the point of view of photosynthetic antenna function,[5] polymer photophysics,[6] molecular electronic devices etc.[7] The significant theoretical contributions in the field of electron and energy transfer have added further impetus to the study of these important processes in general.[8-10] Scheme 1.1 depicts pathways through which electron and energy transfer processes can occur. In electron transfer, the excited state(*) can act either as a donor (D) or as an acceptor (A) whereas in energy transfer, the excited state will always be a donor.

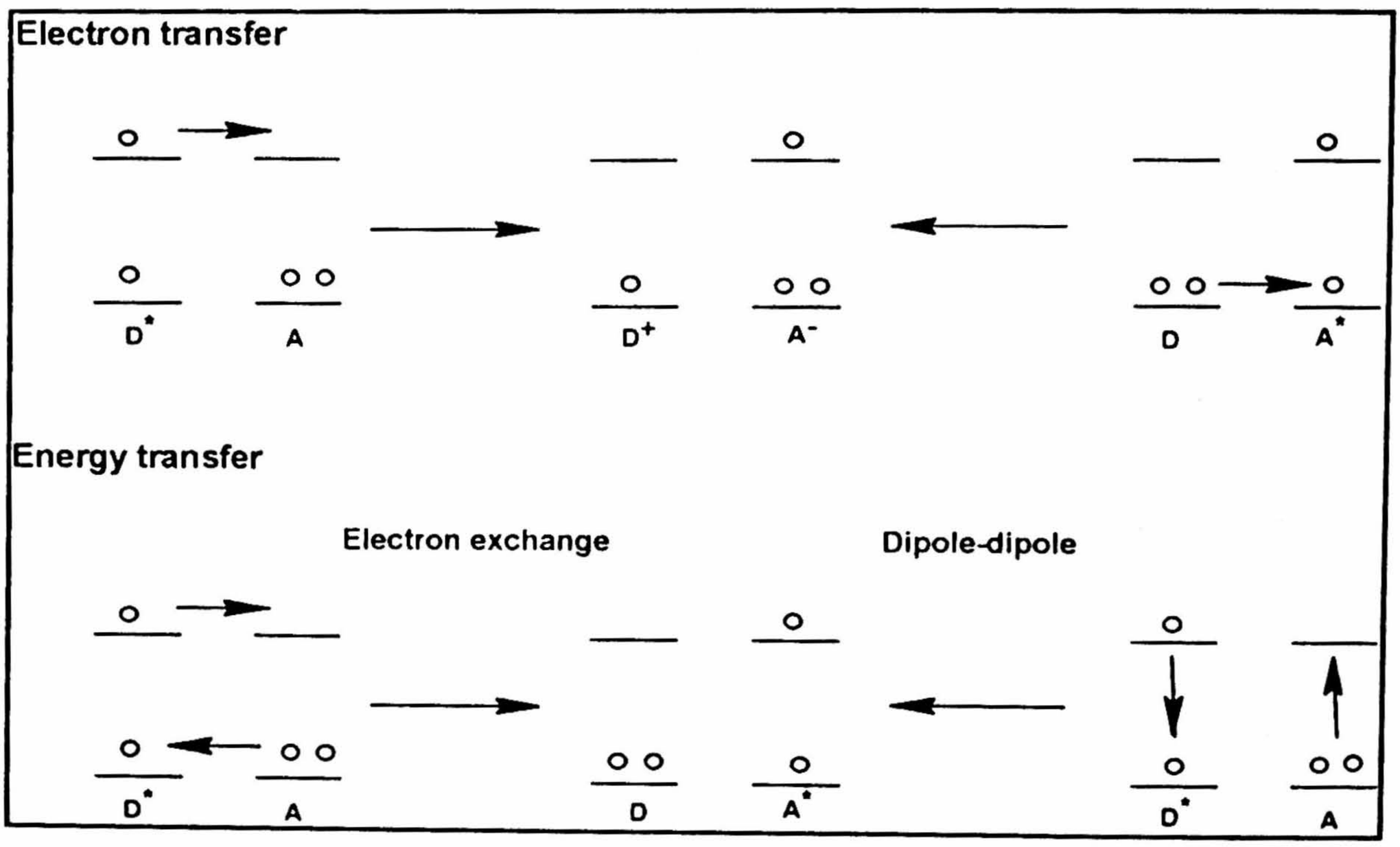

Scheme 1.1

According to Marcus theory of electron transfer reactions, the precursor state (D*-A) must reorganize the nuclear coordinates of both the

complex and the surrounding environment to the point where energy of the reorganized precursor state is the same as that of the successor state immediately following electron transfer.[8] The rate constant for an electron transfer, k_{et}, is given by

$$k_{et} = k_{el}\, \nu_n \exp \frac{-(\lambda + \Delta G^{\varnothing'})^2}{4\lambda kT} \qquad (1.1)$$

where λ is the reorganization energy needed to distort the precursor complex and its surroundings to the equilibrium configuration of the successor complex, k_{el} is the electronic transmission coefficient and ν_n is the frequency of passage (nuclear motion) through the transition state $\Delta G^{\varnothing'}$ is the Gibbs free-energy change for the overall ET reaction with a correction term ΔG_{corr} to account for any specific interactions (such as Coulombic attraction) between $D^{+\cdot}$ and $A^{-\cdot}$ in the product successor complex The relationship between the free energy of activation ($\Delta G^{\#}$), $\Delta G^{\varnothing'}$ and λ is given by

$$\Delta G^{\#} = (\lambda + \Delta G^{\varnothing'})^2/4\lambda \qquad (1.2)$$

Thus, as $\Delta G^{\varnothing'}$ increases, $\Delta G^{\#}$ decreases, and k_{et} is maximal when $-\Delta G^{\varnothing'} = \lambda$ However, in the region where $-\Delta G^{\varnothing'} > \lambda$, k_{et} is predicted to decrease and is termed as "Marcus inverted region".

The reorganization energy λ is usually divided into two contributions

$$\lambda = \lambda_i + \lambda_o \qquad (1\ 3)$$

where λ_i arises from critical internal vibrational modes in the precursor complex and is usually represented by a sum of harmonic potential energies and λ_o accounts for the effect of the surrounding medium. Applying dielectric continuum model, λ_o can be obtained as

$$\lambda_o = e^2/4\pi\varepsilon_0 [(1/2r_D) + (1/2r_A) - (1/r_{DA})] [(1/\varepsilon_{op}) - (1/\varepsilon_s)] \quad (1.4)$$

where r_D and r_A are the radii of the donor and the acceptor respectively, r_{DA} is the D-A center-to-center distance, ε_{op} is the optical dielectric constant and ε_s is the static dielectric constant.

PET reactions have also been treated quantum mechanically. A widely used model assumes a single, averaged effective internal vibrational frequency in the precursor complex that contributes to λ_i and the surrounding medium is treated classically as a dielectric continuum. The rate constant, k_{et}, in this case is given by

$$k_{et} = (2\pi/\hbar)\, H_{ps}^2\, (4\pi\lambda kT)^{-1/2}\, \exp[-(\lambda + \Delta G^{\varnothing'})^2/4\lambda kT] \quad (1\ 5)$$

where H_{ps} is an electronic coupling energy ($H_{ps} = \langle \Psi_p^0 | H_{el} | \Psi_s^0 \rangle$ where H_{el} is the electronic Hamiltonian and Ψ_p^0 and Ψ_s^0 are the electronic wave functions for the precursor and successor complexes, respectively).

As far as EET is concerned, this reaction can operate either by a dipole-dipole (Coulombic) mechanism involving the mutual interaction of electrons or by an exchange mechanism involving mutual exchange of electrons (Scheme 1 1)

Forster has developed an expression for the rate of electronic energy transfer due to dipole-dipole interaction in terms of the experimentally obtainable parameters.[10] According to this theory, the rate constant for energy transfer, $k_{Forster}$ is given by eq. 1.6,

$$k_{Forster} = \frac{8.8 \times 10^{-25} \kappa^2 \phi_D}{n^4 \tau_D R^6} \int \bar{F}_D(\nu) \varepsilon_A(\nu) \nu^{-4} d\nu \qquad (1.6)$$

where, ν is the wave number, $\bar{F}_D(\nu)$ is the spectral distribution of the donor emission in quanta normalized to unity, $\varepsilon_A(\nu)$ is the molar extinction coefficient for the acceptor absorption and n is the refractive index of the solvent. κ^2 is a function of relative orientation of transition dipole moments of the donor and the acceptor ϕ_D is the quantum yield of donor emission, τ_D is the actual donor emission lifetime (in seconds) and R is the distance between the donor and acceptor molecules (in centimetres).

Dexter has derived an expression for the rate of excitation energy transfer in which the initial and final states are coupled through the exchange interaction.[9] According to this theory, the rate of energy transfer, k_{Dexter} is given by

$$k_{Dexter} = (2\pi/\hbar)\, K \exp(-2R/L) \int \bar{F}_D(\nu)\, \bar{\varepsilon}_A(\nu)\, d\nu \qquad (1.7)$$

where K is related to specific orbital interactions, R is the distance between the donor and the acceptor molecules, L is an "effective average Bohr radius" and $\bar{F}_D(\nu)$ and $\bar{\varepsilon}_A(\nu)$ are the spectral distributions of the donor

emission and the acceptor absorption normalized to unity on a wavenumber scale.

From the photophysical point of view, the fundamental processes that take place during the electron/ energy transfer are depicted in Fig. 1.1.

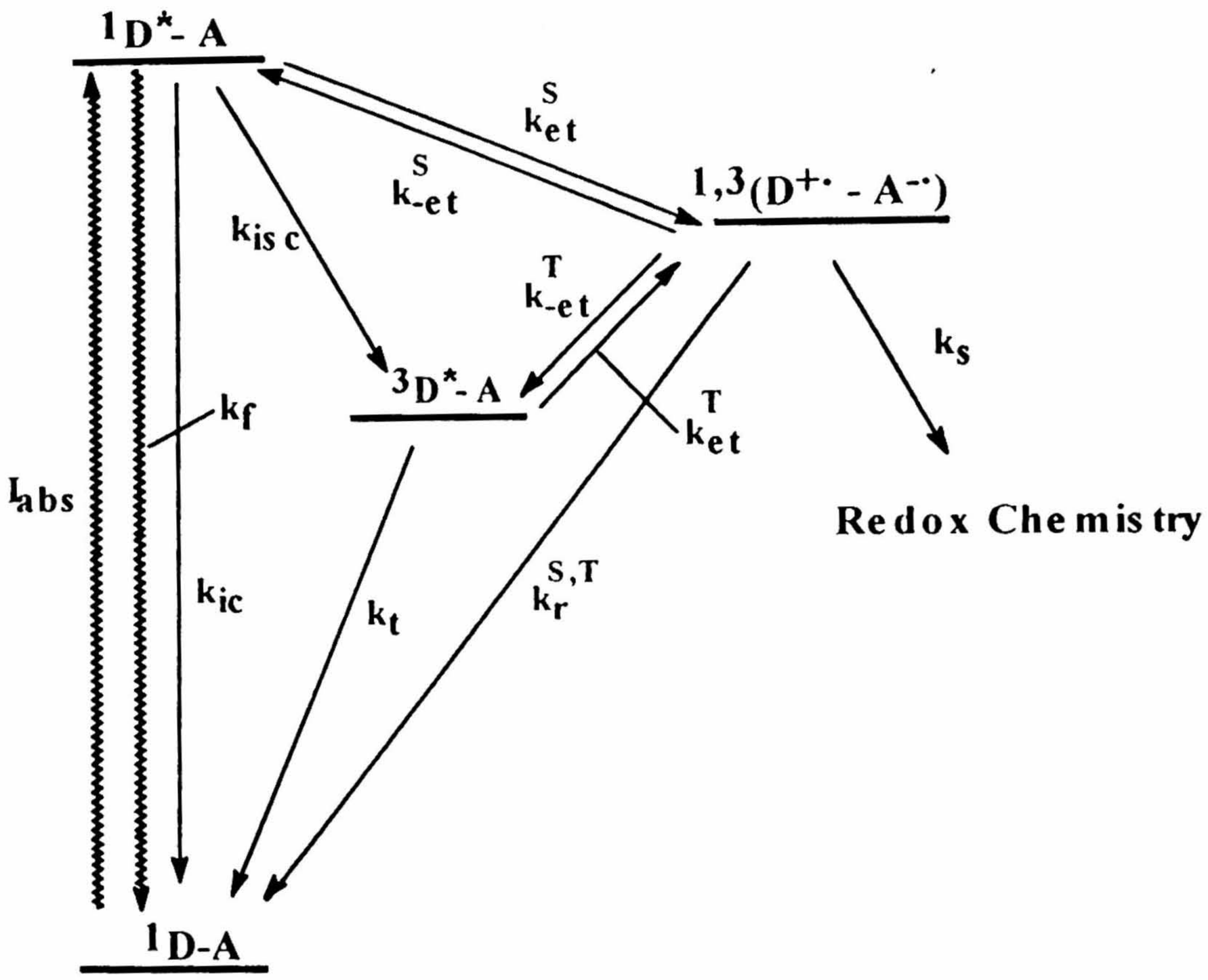

Fig. 1.1

Here, S and T refer to the singlet and the triplet states, respectively. k_f, k_{ic}, k_{isc}, k_s, k_r^S, k_{et}^S and k_{-et}^T are the rate constants for fluorescence, internal conversion, intersystem crossing, redox chemistry, recombination and electron transfer (singlet and triplet), respectively. For an efficient

electron/energy transfer to occur, these processes have to compete with other processes *viz.* fluorescence, internal conversion, intersystem crossing etc. such that

$$k_{et}^{S} >> (k_f + k_{ic} + k_{isc}) \quad (1.8)$$

$$k_s >> (k_r^S + k_{-et}^S + k_{-et}^T) \quad (1.9)$$

Table 1.1 summarizes the determinants of the EET and PET reactions that may be derived from the theories of electron and energy

Table 1.1.

Determinants of electron and energy transfer	
Electron transfer	Distance and orientation (electronic coupling, orbital overlap), Free energy change (driving force), Reorganization in D and A, Orientation polarization of medium
Excitation energy transfer	Distance and orientation (coupling of excited states), Spectral overlap of emission and absorption of D and A, Refractive index of the medium
Processes competing with electron and energy transfer	
Electron transfer	(i) Nonradiative relaxation of D^* by photoisomerization and other conformational changes, Excited state proton transfer, Intersystem crossing, Chemical reactions, (ii) Back reaction to the ground state D, A
Excitation energy transfer	same as (i)

transfer reactions as well as the processes competing with these reactions discussed above.

The following observations that can be made from the information provided in Table 1 1 are of importance for the present study. Both electron- and energy transfer reactions depend on the geometric relation (distance and orientation) between donors and acceptors Excitation energy transfer may occur over wide distances when transition dipole moments are favourably aligned The spectral overlap and the driving force have obvious effects on the transfer rates and are largely determined by the chemical nature of donors and acceptors Nuclear reorganization of donor, acceptor and the surrounding medium accompanying electron transfer is another important factor that governs the rate of electron transfer. Energy transfer also depends on the medium and the Forster type is disfavoured in media with high refractive index

1.2 PET and EET in porphyrin-based D-A systems

Both EET and PET are important and prevalent phenomena in natural photosynthesis. For example, antenna function of the photosynthetic systems involves singlet-singlet (s—s) energy transfer between two chlorophyll (Chl) molecules and also that between carotenoids (Car) and Chl.[5] In addition, carotenoids provide photoprotection by rapidly quenching the triplet states of chlorophyll by triplet-triplet (t t) energy transfer thus preventing chlorophyll-sensitized production of singlet oxygen.[5] These processes are summarized in eqs 1 10-1 15

$$\text{Chl} \xrightarrow{h\nu} {}^{1}\text{Chl}^{*} \qquad (1\ 10)$$

$$^{1}Chl^{*} + Chl \xrightarrow{EET\ (s \rightarrow s)} Chl + {}^{1}Chl^{*} \quad (1.11)$$

$$Car \xrightarrow{h\nu} {}^{1}Car^{*} \quad (1.12)$$

$$^{1}Car^{*} + Chl \xrightarrow{EET\ (s \rightarrow s)} Car + {}^{1}Chl^{*} \quad (1.13)$$

$$^{1}Chl^{*} \longrightarrow {}^{3}Chl^{*} \quad (1.14)$$

$$^{3}Chl^{*} + Car \xrightarrow{EET\ (t \rightarrow t)} Chl + {}^{3}Car \quad (1\ 15)$$

The electron transfer events of photosynthesis take place within a highly specialized reaction center (RC) complex Detailed X-ray structures of several bacterial photosynthetic reaction centers are now known [1] The X-ray crystal structure of bacterial reaction center *Rhodobacter sphaeroides* (Fig. 1.2, a schematic diagram) reveals that the RC comprises of four bacteriochlorophylls including those of the so-called 'special pair', two bacetriopheophytins, two quinones and a carotenoid and that it has two branches. Within 2 - 4 ps of excitation (excitation received from the antenna), singlet state of the 'special pair' transfers an electron to one of the bacteriopheophytin molecules with a quantum yield of unity Bacteriopheophytin then transfers an electron to the nearby quinone, again with a quantum yield of unity, ultimately leading to the generation of a spatially separated, charge transfer state comprising the oxidized 'special pair' and the reduced quinone

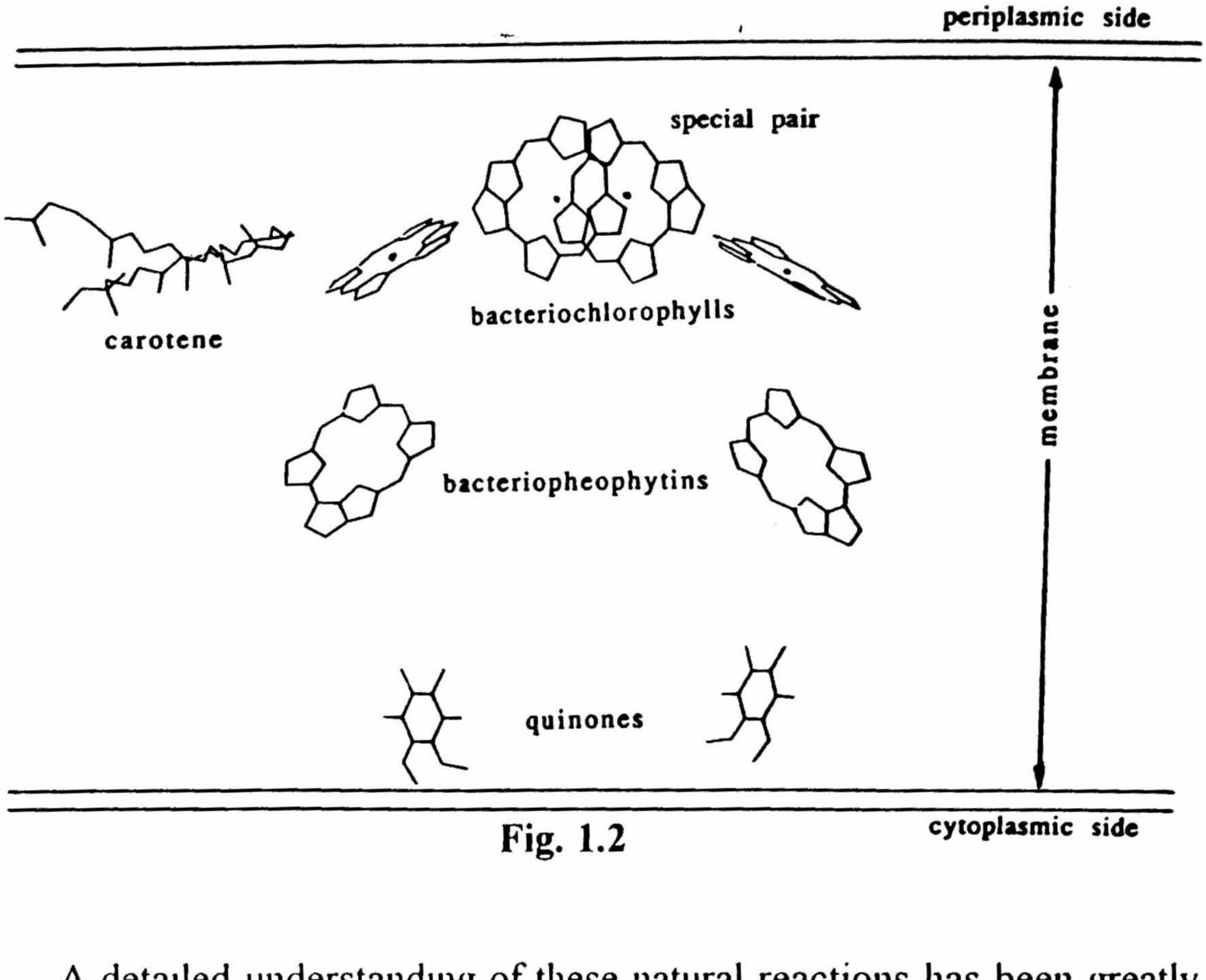

Fig. 1.2

A detailed understanding of these natural reactions has been greatly aided by studies of electron and energy transfer in synthetic model systems. A great variety of porphyrin-based photosynthetic model systems have been synthesized and studied with an aim to simulate the natural photosynthetic reactions. These studies have also helped in testing the current theories of electron- and energy transfer reactions. Sections 1 2.1 and 1.2.2 present a brief survey of the recent studies on covalently and noncovalently bound porhyrin-based D-A systems, respectively.

1.2.1 Covalently linked D-A systems

Earlier reports on EET and PET reactions of porphyrin-based D-A systems are abound with studies on covalently linked complexes and these

have been reviewed in many recent accounts.[12-22] The principal reason behind the study of covalently bound D-A molecules is to eliminate diffusion as a source of kinetic complexity, thus making it possible to study reactions with rate constants that may be substantially faster than diffusion. In addition, distance and orientation effects of PET and EET may also be discerned in such compounds A large number of structures have been reported and variation of such structures forms the basis of discussion presented below.

The first covalently linked cyclic tetrapyrroles were reported in 1972[23] and the first chlorophyll-based dimeric models (**1**) were reported in 1976.[24,25] Since then, several studies on porphyrin- and chlorophyll-based homo-dimers, as model systems for the 'special pair', have appeared in the literature.[12-22,26-29] These systems have been reported to exhibit interesting optical properties and singlet-singlet energy transfer reactions, PET reactions have not been observed in these homo-dimers On the other hand, the hetero-dimers have been reported to show PET reactions For example,

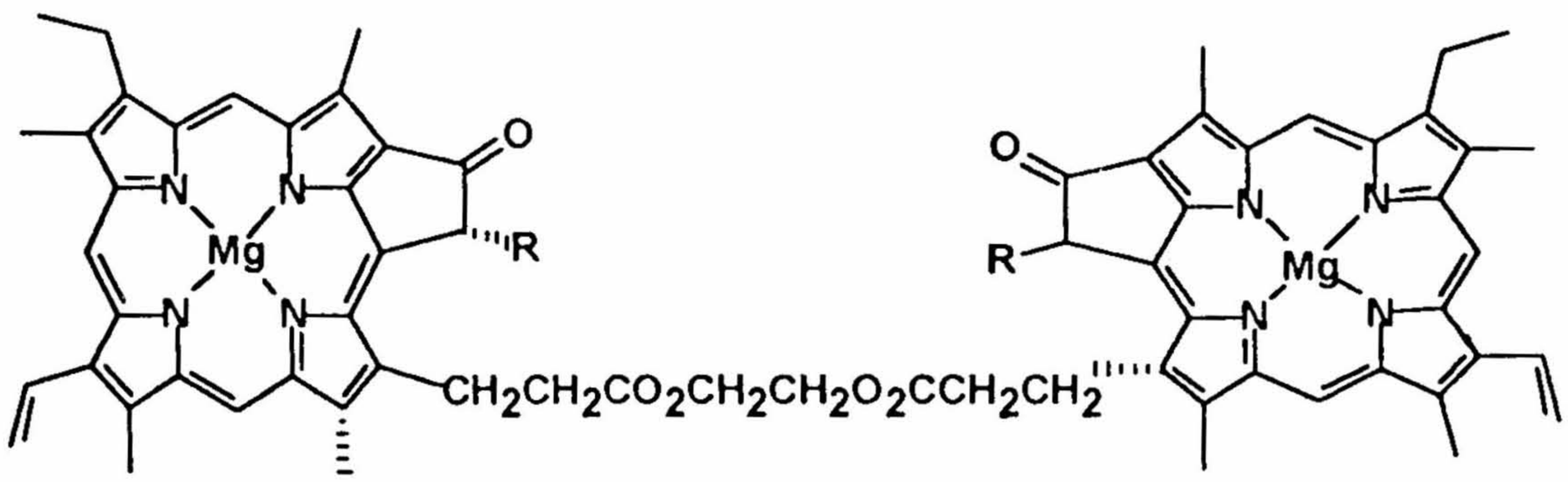

1a R = H
1b R = O_2CCH_3

in their study on the 1,10-phenanthroline bridged bisporphyrin metallodimers, Harriman, Sauvage and co-workers have observed an intramolecular PET reaction with almost unit quantum yield on excitation with the visible light.[30] Recently, rapid (10^{11}-10^{12} s^{-1}) and efficient singlet-singlet energy transfer from the porphyrin to the pheophorbide has been observed in novel, covalently linked porphyrin-pheophorbide hetero-dimers.[31]

In an attempt to mimic photosynthetic energy transfer reactions and to develop molecular devices, porphyrin systems, as energy acceptors, have been covalently linked to carotenoid,[5,17,32,33] cyanine dye,[34] and anthracene[35] donor subunits to generate molecular dyads. Gust et al. have recently synthesized a series of carotenoporphyrin dyad molecules in which the carotenoid is covalently linked to a tetraarylporphyrin at the ortho, meta, or para position of a meso aryl ring (**2**).[32]

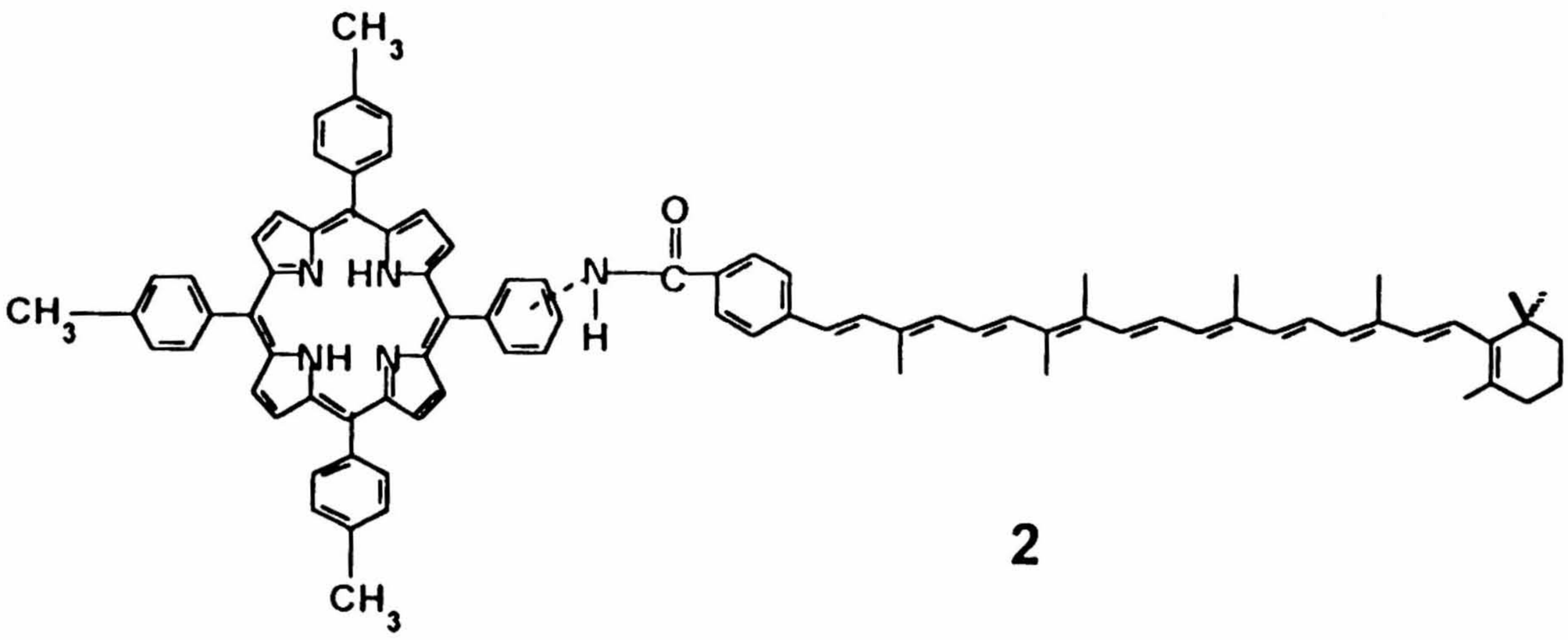

2

Results of steady-state and transient spectroscopic studies have revealed singlet-singlet energy transfer from the carotenoid to the porphyrin and

triplet-triplet energy transfer from the porphyrin to the carotenoid in these dyads

Lindsey et al have synthesized a series of porphyrin-cyanine dye dyads (**3a-c**) to mimic the phycobilisome action of photosynthesis.[34] While an 80% energy transfer efficiency from the dye to the porphyrin was noticed in compounds **3a** and **3b**, the energy transfer occurs with the same efficiency from the porphyrin to the cyanine dye in compound **3c**

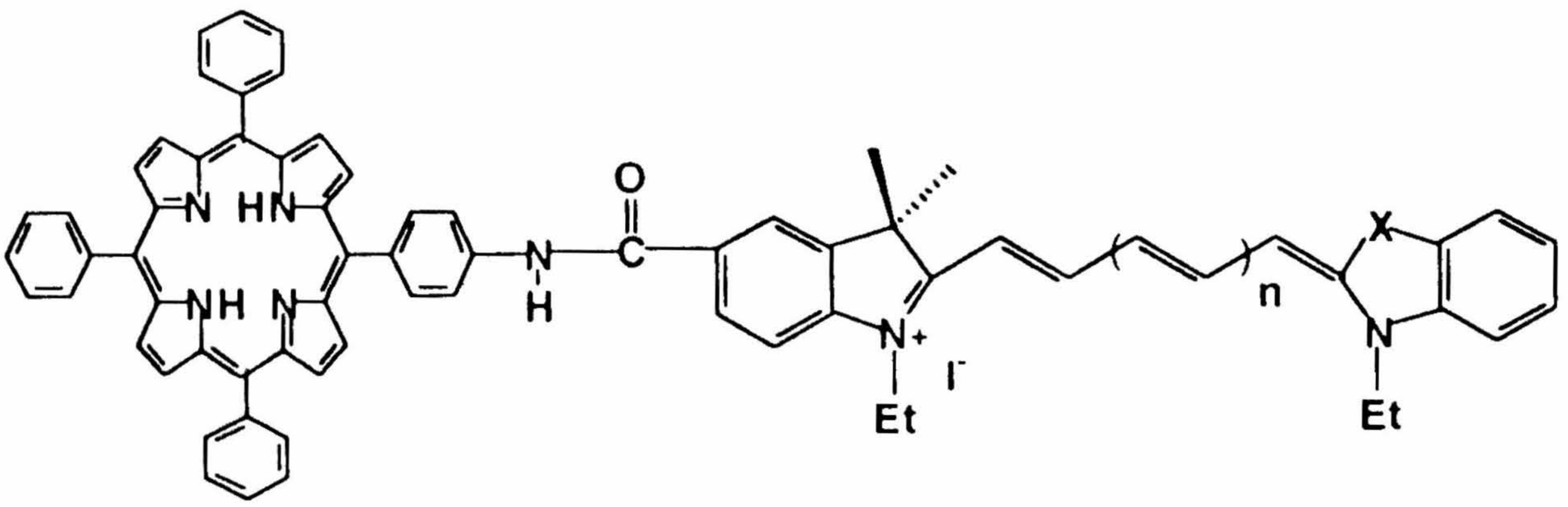

3a : X = O, n = 0 **3b** : X = $C(CH_3)_2$, n = 0 **3c** : X = $C(CH_3)_2$, n = 2

The vast majority of the D-A dyads that were built to simulate the photosynthetic electron transfer are those in which a porphyrin or a metalloporphyrin has been covalently linked to a quinone Compound **4**, that has been reported by Kong and Loach as early as in 1978,[36] typifies the general structural characteristics of porphyrin-quinone (P-Q) dyads A large number of such P-Q systems have now appeared in the literature [12-22] It has been found that, under suitable conditions (e g conducive electronic coupling, thermodynamic driving force, solvent and temperature) these P-Q systems readily undergo PET reaction from the excited singlet state of the

porphyrin to the quinone to generate a charge separated (CS) state $P^{+\cdot}$ - $Q^{-\cdot}$. The amount of chemical potential stored in the CS state is a function of the redox properties of the two moieties involved.

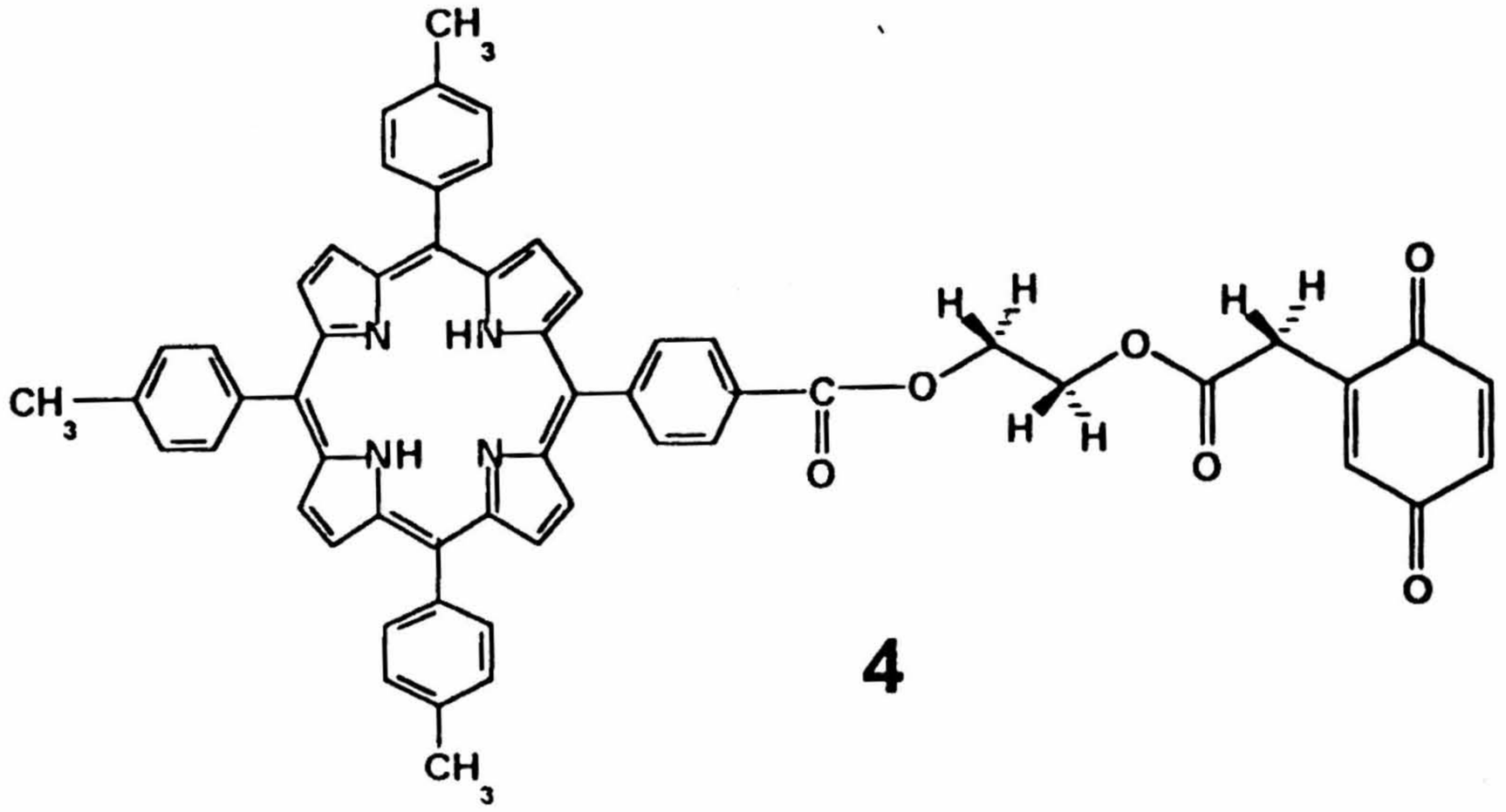

4

In order to further probe the mechanistic details involved in the PET reactions of the porphyrin-acceptor complexes, D-A systems in which a porphyrin is connected to an acceptor other than a quinone (*viz.* nitroaromatics, viologens, pyromellitimides) have also been studied. Photochemistry of these systems have been discussed in recent reviews.[12-22] More recently, fullerenes have been covalently linked to porphyrins.[37-39] For example, Sakata and co-workers have synthesized a porphyrin-C_{60} dyad molecule **5** which shows a PET reaction from singlet excited state of the zinc(II) porphyrin to the appended C_{60}.[38]

Although, the distance dependence of PET reactions has been elucidated in a large number of porphyrin-based D-A systems,[40] only a few studies concerning the effect of D-A orientation have appeared in the ——

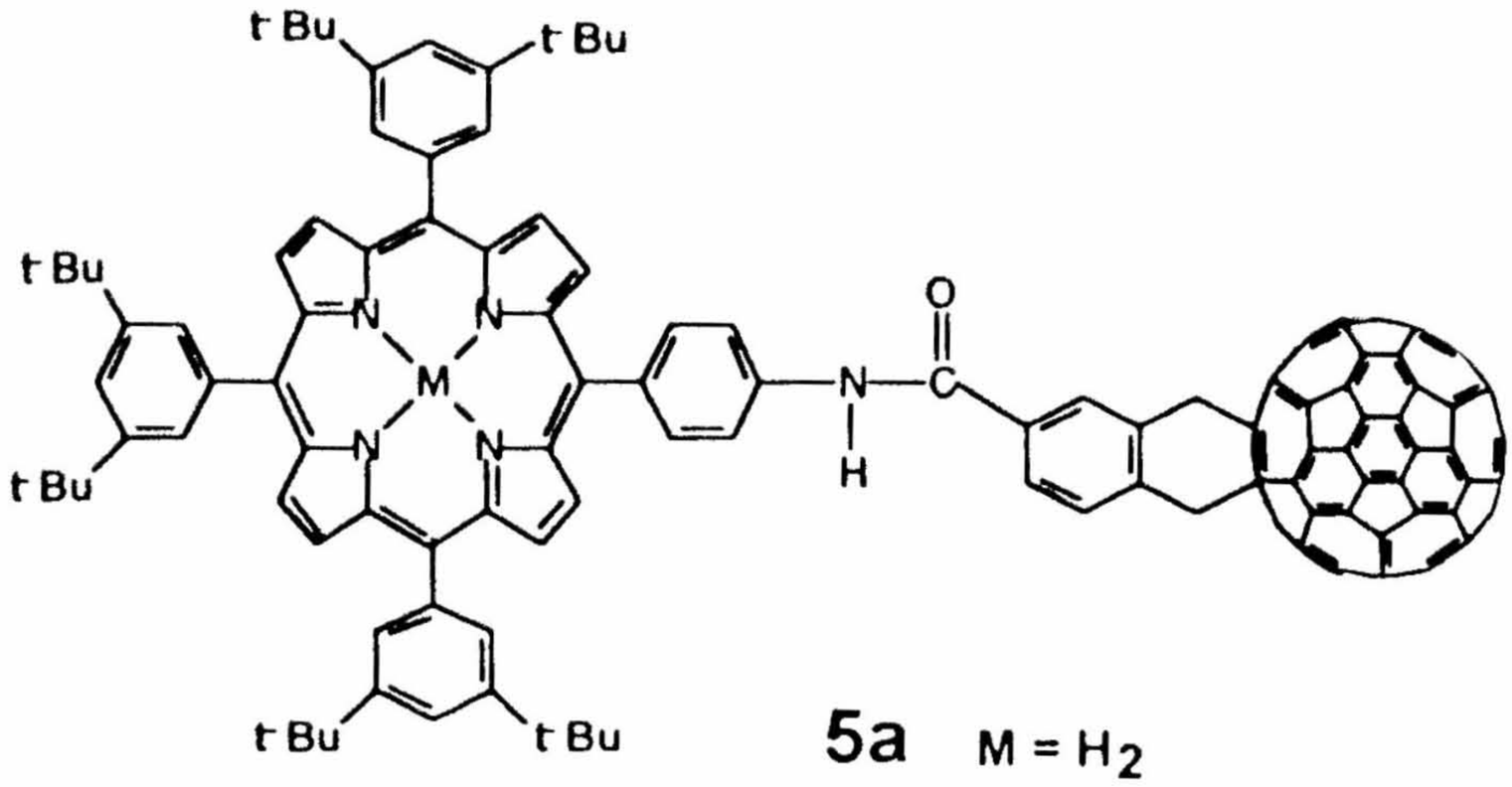

5a M = H_2

5b M = Zn

literature [41-44] Sakata, Wasielewski and co-workers have studied a series of P-Q dyads (**6** and **7**) in which a 1,4-benzoquinone is covalently linked to a zinc porphyrin *via* spiro[4,4]-nonane (SP) or trans-decaline (TD) [44b] The

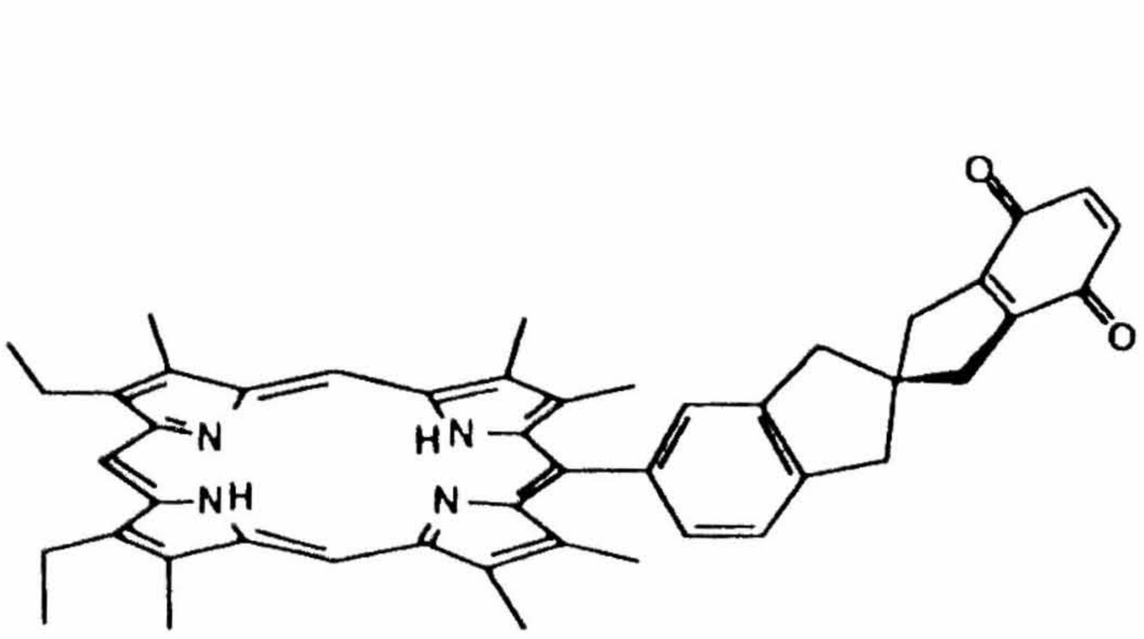

6a (SP - H)

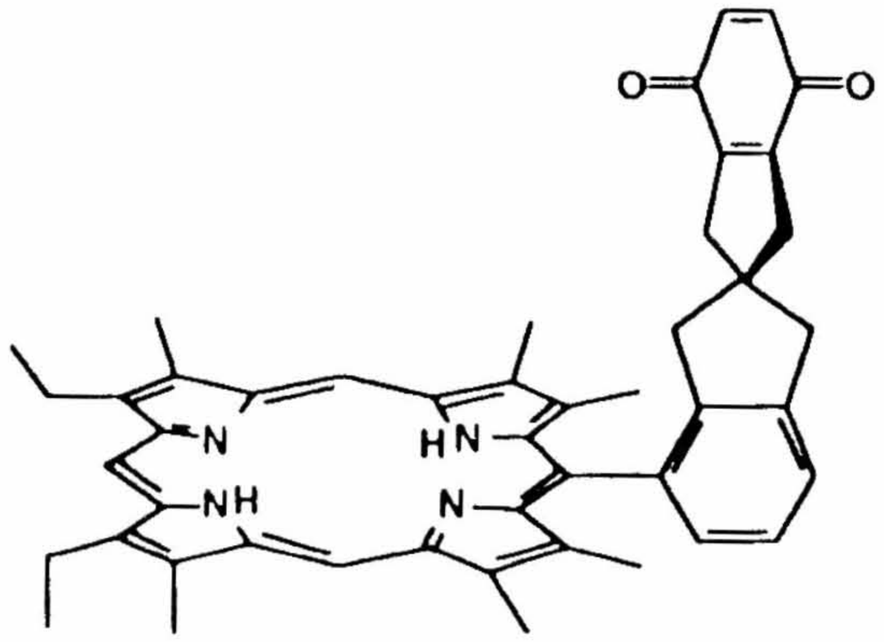

6b (SP - V)

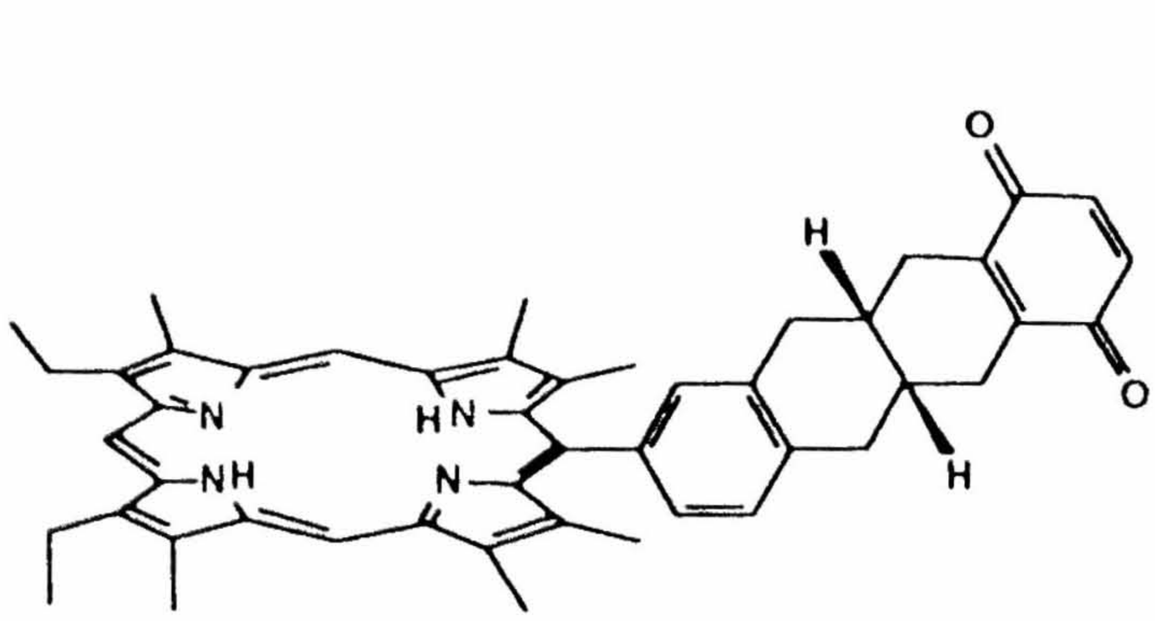

7a (TD - H)

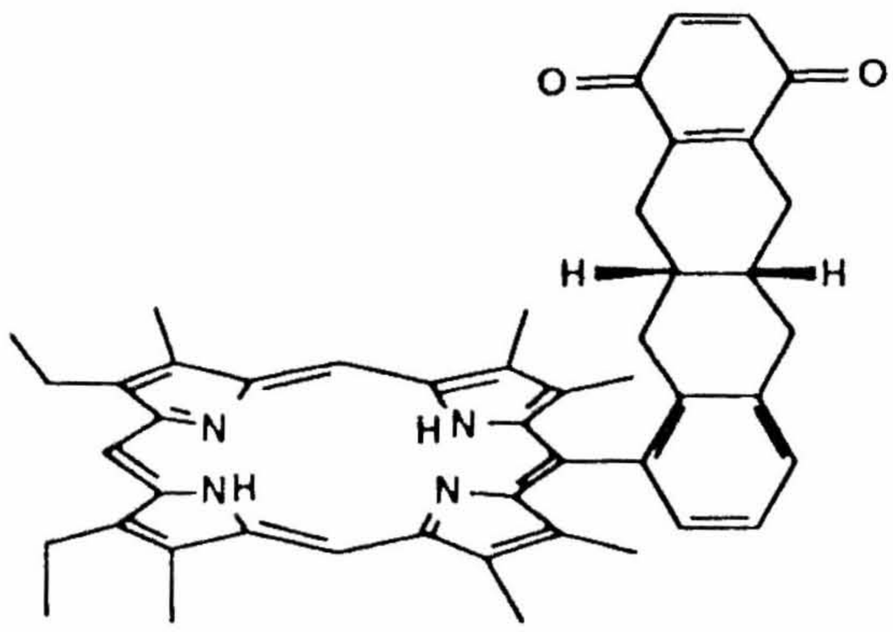

7b (TD V)

ultrafast kinetic measurements revealed that these dyads undergo PET reaction from singlet excited state of the porphyrin to the quinone to form the ZnP^{+} - Q^{-} state The rate constant data obtained in toluene, THF and DMF suggests that the D-A orientation effects observed are due to variation in the sum of the direct, through space interaction between the donor and the acceptor and the indirect, through-solvent interaction

Both "through bond" and "through space" PET reactions can occur in covalently linked systems in which donor and acceptor subunits are separated by semi-rigid spacers Importance of the through bond mechanism can be enhanced by separating the donor/s and acceptor/s by rigid aromatic spacers Influence of the energy of the bridge orbitals has been investigated in a recent study which involves a comparison of compounds **8a** and **9a** (unsubstituted bridges) with **8b** and **9b** (electron donating methoxy substituents on the bridges) by means of absorption, fluorescence, and transient absorption spectroscopy [41a,b] It was found that the rate of recombination from the charge-separated state is a factor of 3 to 4 larger for **8b/9b** than for **8a/9a** The influence exerted by the substituents indicates that

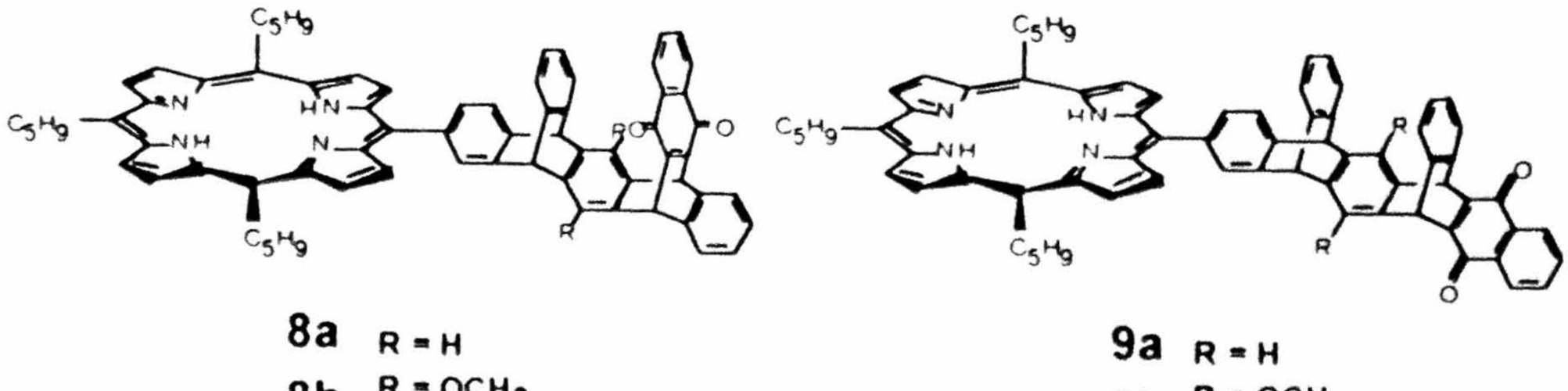

8a R = H
8b R = OCH_3

9a R = H
9b R = OCH_3

the bridge takes part in the ET reaction. The importance of the solvent and the spacer on the PET reactions in a series of porphyrin-peptide-quinone dyads has been reported recently [41c]

D-A triads, tetrads and pentads have been assembled by covalently linking porphyrin (P), carotene (C) and quinone (Q) or other acceptor moieties and EET and PET reactions in these compounds have been studied [5,17,19,45-49]

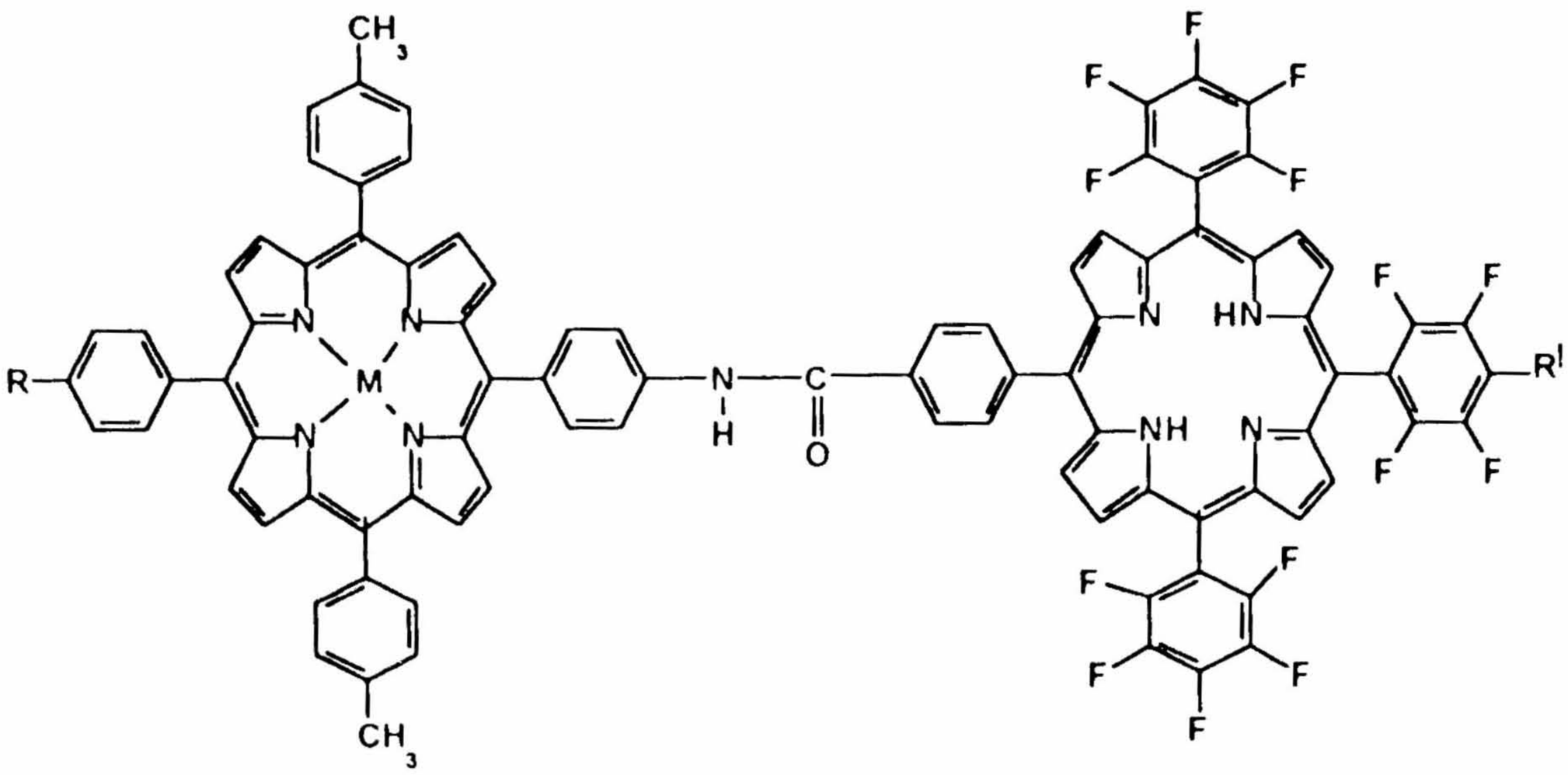
CH3
F
F
F

For example, in triad (**10**), interporphyrin singlet-singlet energy transfer occurs with rate constants ranging from 8.1 x 10^8 to 2.3 x 10^{10} s^{-1}. It has been suggested that energy transfer involves a contribution from an electron exchange mechanism. Interporphyrin PET was seen to produce C - P_a^+ - P_b^- CT state with a rate constant of 3 5 x 10^9 s^{-1} and with a quantum yield (ϕ_{CS}) of 0.68. The triad was also seen to undergo a subsequent electron transfer step to give a final C^+ - P_a - P_b^-state (ϕ_{CS} = 0.32) whose lifetime was estimated to be 250 ns [46] Very recently, Gust and co-workers have come up with a novel strategy for slowing down the charge recombination reactions in C-P-Q triads based on coupling photoinduced electron transfer to a change in proton chemical potential.[47a]

For tetrad **11**, a PET between the two porphyrins was found to be thermodynamically unfavourable but, a series of PET reactions producing the final C^+ - P_a - P_b - Q^- has been established This final state was produced with a quantum yield of 0 25 and it lived for 2.9 ms. These data suggest that large spatial separation of the cation and the anion would be needed to place the charges on adjacent chromophores for a long time.[48]

The pentad system C - P_{Zn} - P_{H2} - Q_a- Q_b **12**, displayed a singlet-singlet energy transfer from the zinc porphyrin to the free-base porphyrin with a rate constant of 2.3 x 10^{10} s^{-1} and with a quantum yield of 0.90. When excited into the free-base porphyrin absorption maximum, the pentad yielded an initial CS state C - P_{Zn} - P_{H2}^+ - Q_a^- - Q_b with a quantum yield of 0.85 in $CHCl_3$ solutions. Subsequent ET steps lead to a final CS state C^+ - P_{Zn} - P_{H_2} - Q_a - Q_b^- which was formed with an overall quantum yield of 0 83

(τ =55 ms) This artificial photosynthetic system could preserve a significant fraction ($\cong$ 1 0 eV) of the initial excitation energy (1 9 eV) in its CS state [49]

Recently, Sessler et al[50] and Osuka et al[51] have reported porphyrin trimers and quinone-linked porphyrin trimers Based on the fluorescence spectroscopic data, PET reactions from the porphyrin singlet state to the appended quinone acceptor have been indicated in both cases More recently, Sessler, Capuno and Harriman have reported that rapid energy transfer occurs between the porphyrin subunits within the quinone-linked trimeric porphyrin supramolecular array **13** and that this process is slow with respect to electron transfer between a directly linked porphyrin-quinone couple [52]

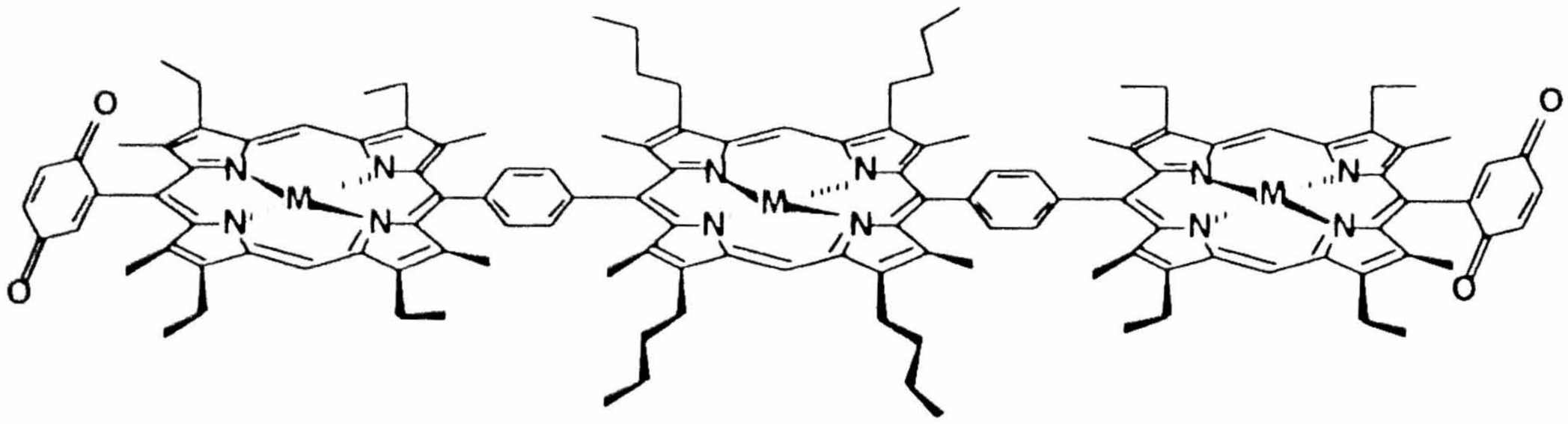

13a M = 2H
13b M = Zn

Harriman, Sauvage and co-workers have adopted a new strategy that is based on metal ion chelation to synthesize versatile molecular triads wherein two different porphyrins have been assembled around a central ruthenium(II) bis(terpyridyl) complex (**14**) [53-55] Results of ultrafast transient absorption and emission spectroscopy have been interpreted in terms of multistep electron- and energy transfer reactions in this triad

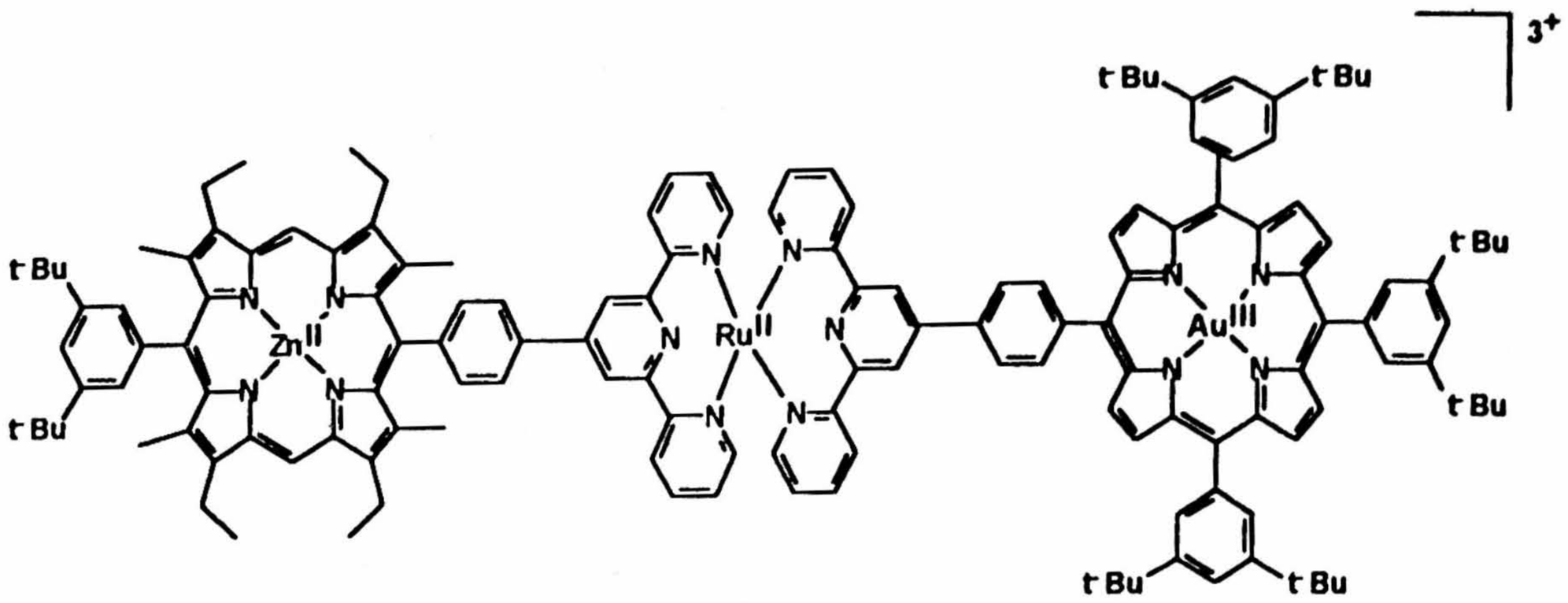

14

Recently, Lindsey and co-workers have reported a versatile porphyrin pentamer **15**, as a model for the photosynthetic antenna function, wherein the four phenyls of a central porphyrin molecule is flanked by another porphyrin molecule *via* an acetylene bridge [56a] Singlet-singlet and triplet-triplet energy transfer from the outer porphyrins to the core porphyrin has been observed in this supramolecular porphyrin.

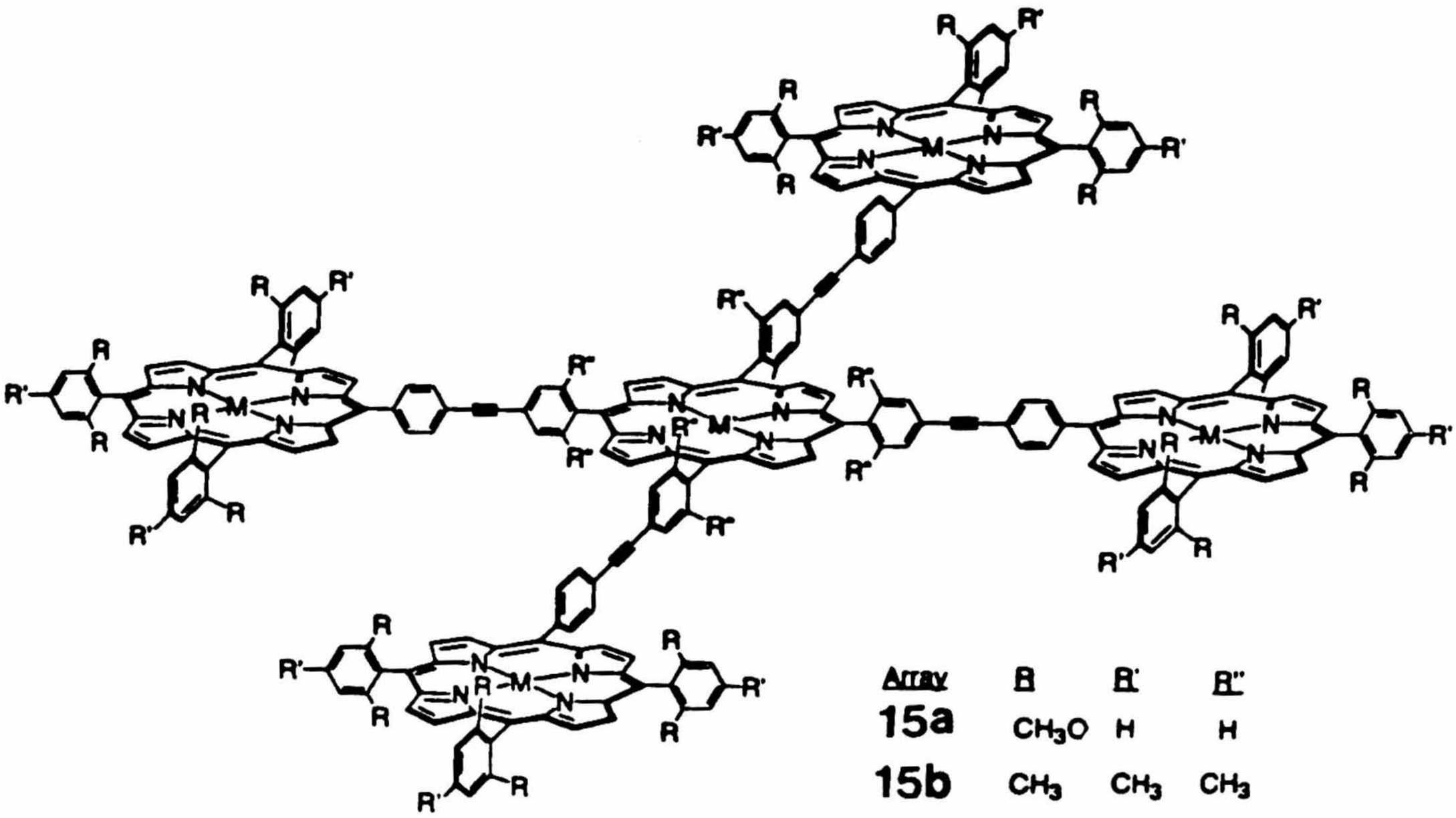

Array	R	R'	R''
15a	CH_3O	H	H
15b	CH_3	CH_3	CH_3

1.2.2 Non-covalently bound D-A systems

D-A systems bound by noncovalent interactions can be expected to provide a better understanding of the biological energy/electron transfer processes as these processes in natural systems proceed through complex noncovalently bound protein pathways. This consideration has led to the construction of porphyrin-based D-A systems that are characterized by either coordinative, H-bonding or nucleic acid base-pairing interaction between the donor and the acceptor.[57-64]

Linked porphyrin-crown ether systems have been employed for the construction of photosynthetic model systems.[58,59] For example, It has been demonstrated that irradiation of a Ag ion containing porphyrin-crown ether results in ET from the porphyrin to the Ag ion with subsequent ejection of elemental silver from the crown.[58] More recently Sun et al [59] have synthesized and studied a porphyrin that is covalently linked to a redox active crown ether-quinone (CEQ) It has been assumed that the structural changes involving coordinative interaction between the Zn porphyrin and the CEQ have a profound influence on the ET properties of this P-Q dyad

H-bonding interactions have also been employed to construct supramolecular D-A assemblies. For example, bis- or tetrakis-(2-hydroxy naphthyl)porphyrin has been reported to spontaneously form face-to-face

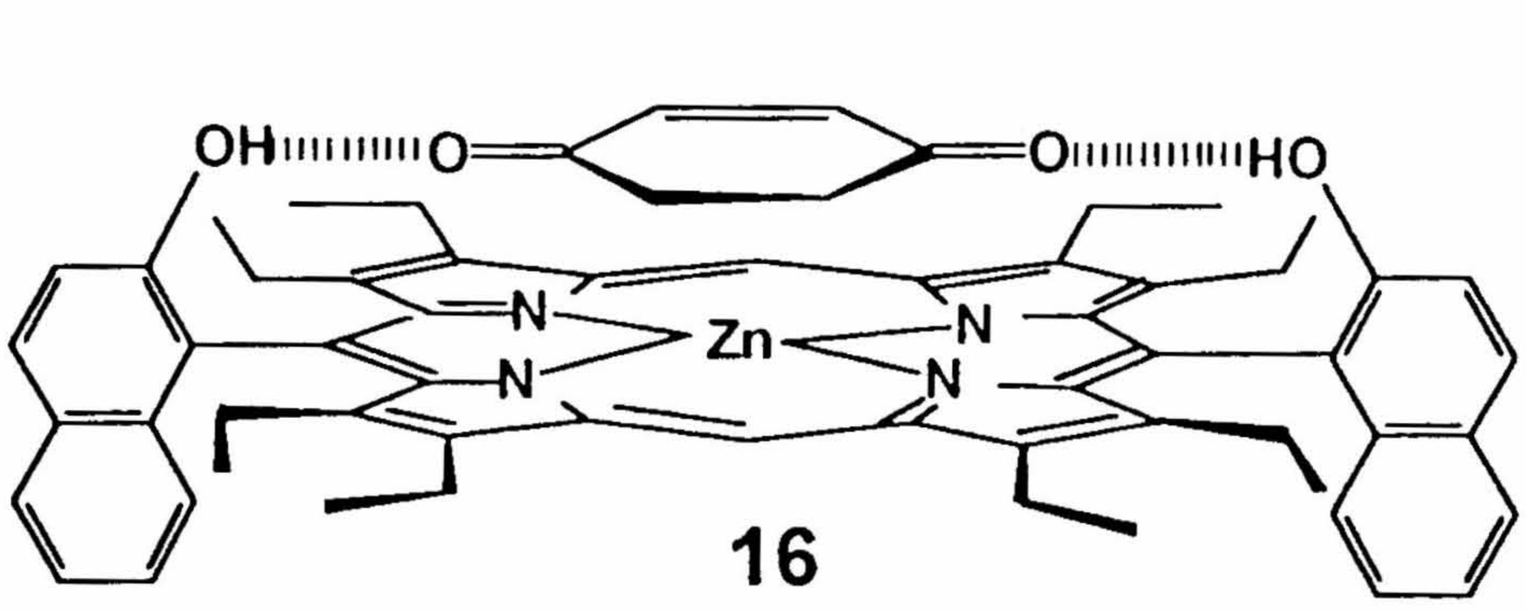

16

adducts with various quinones through one-, two- or multi-point hydrogen bonding depending on the substrate and a PET reaction from porphyrin to quinone in these systems has been elucidated.[60] Steady state fluorescence spectroscopic studies carried out on **16** indicated an efficient PET reaction from the porphyrin to the H-bonded quinone.[60c]

An interesting and probably, biologically 'more relevant' approach for the construction of photosynthetic model systems involves nucleic acid base-pairing. This approach has been employed to synthesize porphyrin-porphyrin (P-P) and porphyrin-quinone (P-Q) energy and electron transfer systems.[61-63] For example, Sessler, Harriman and their co-workers have demonstrated the occurrence of electron/energy transfer reactions in P-Q (**17**) and P-P (**18**) systems wherein the self-association of cytosine (C) and complementary base-pairing between cytosine and guanine (G) residues respectively, have been employed to assemble individual donor and acceptor subunits.[61a,c] Although these dimers are linked by flexible spacer units, they have been shown to be stable enough to exhibit efficient electron and energy transfer reactions. Finally, carboxylate-carboxylate and amidinium-carboxylate salt bridged porphyrin-dinitrobenzene dyads have been reported recently. A PET from the porphyin donor to the nitroaromatic acceptor has been elucidated in these novel systems.[64]

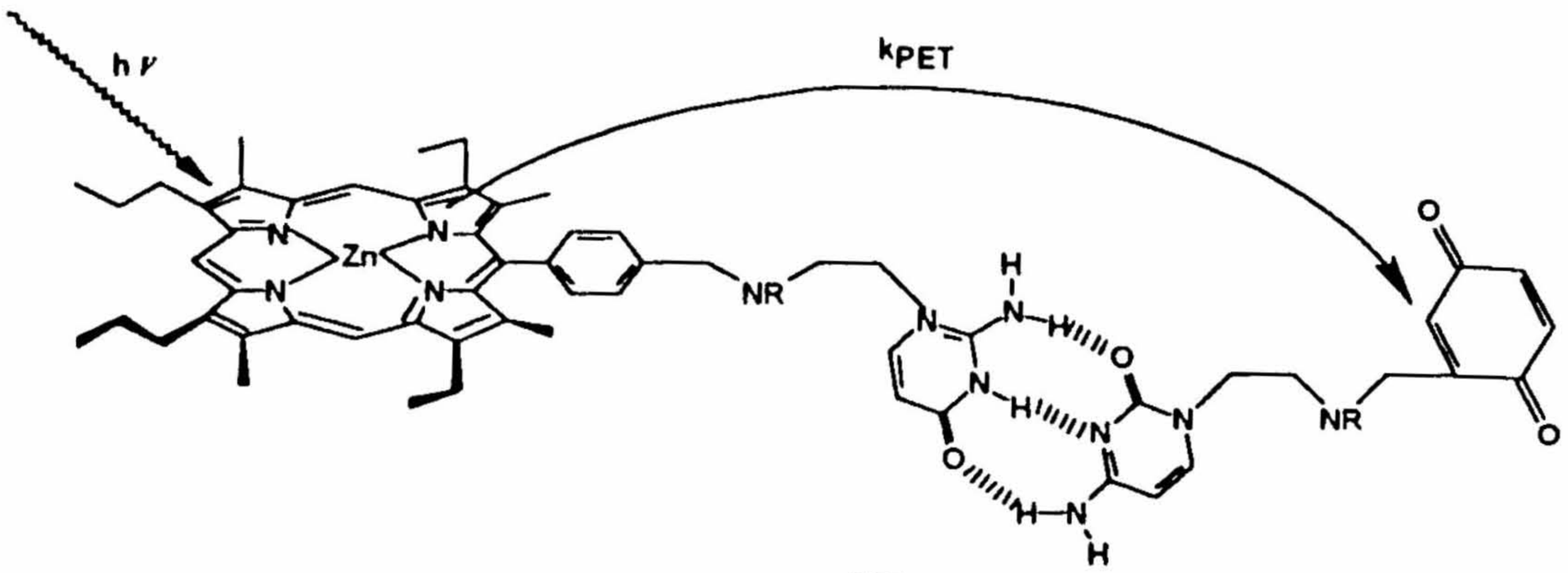

R = $CH_2C_6H_4O(CH_2)_2OCH_2OCH_3$

17

R = $CH_2C_6H_4O(CH_2)_2OCH_2OCH_3$

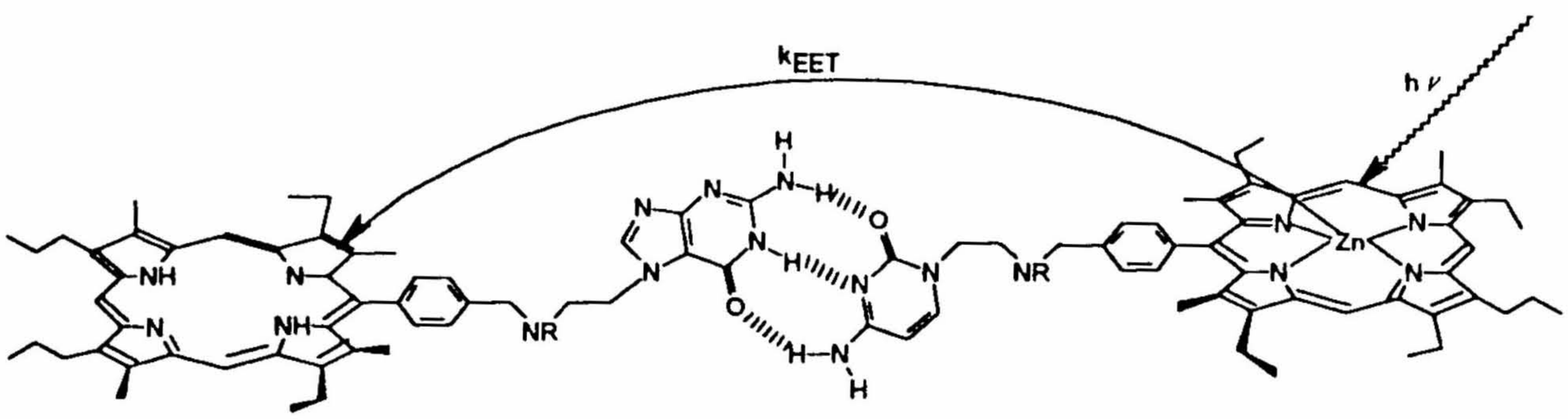

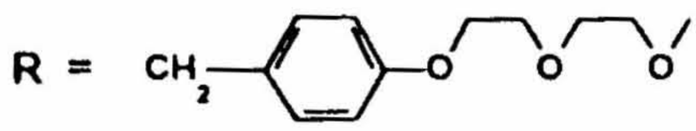

18

R^1 = $CH_2CH_2OCH_2CH_2OCH_3$

R^1 CH_2

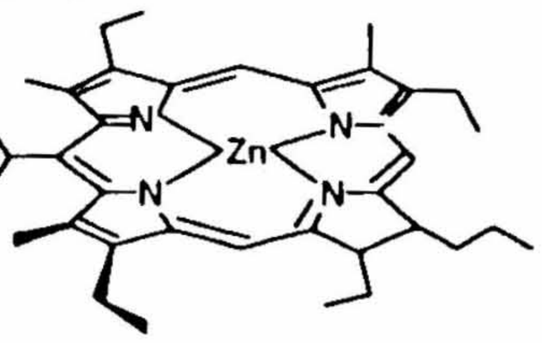

1.3 Photodynamic therapy

The use of visible light as a therapeutic agent in clinical medicine is termed as phototherapy.[65] The use of photo-activated drugs in the treatment of malignant tumors, destruction of arterial plaque, curing of psoriatic lesions, eradication of viral contaminants etc. is known as photodynamic therapy (PDT). The technique of PDT in cancer therapy involves the intravenous injection of a photosensitizer (P), which over a period of time, is

selectively retained by the neoplastic tissue. Subsequent irradiation with visible light using a laser generates singlet oxygen (or other cytotoxic species) within the tumour, ultimately leading to cell necrosis and tumor regression.[66] A diagrammatic representation of the action of PDT in cancer therapy is shown in Fig. 1 3.

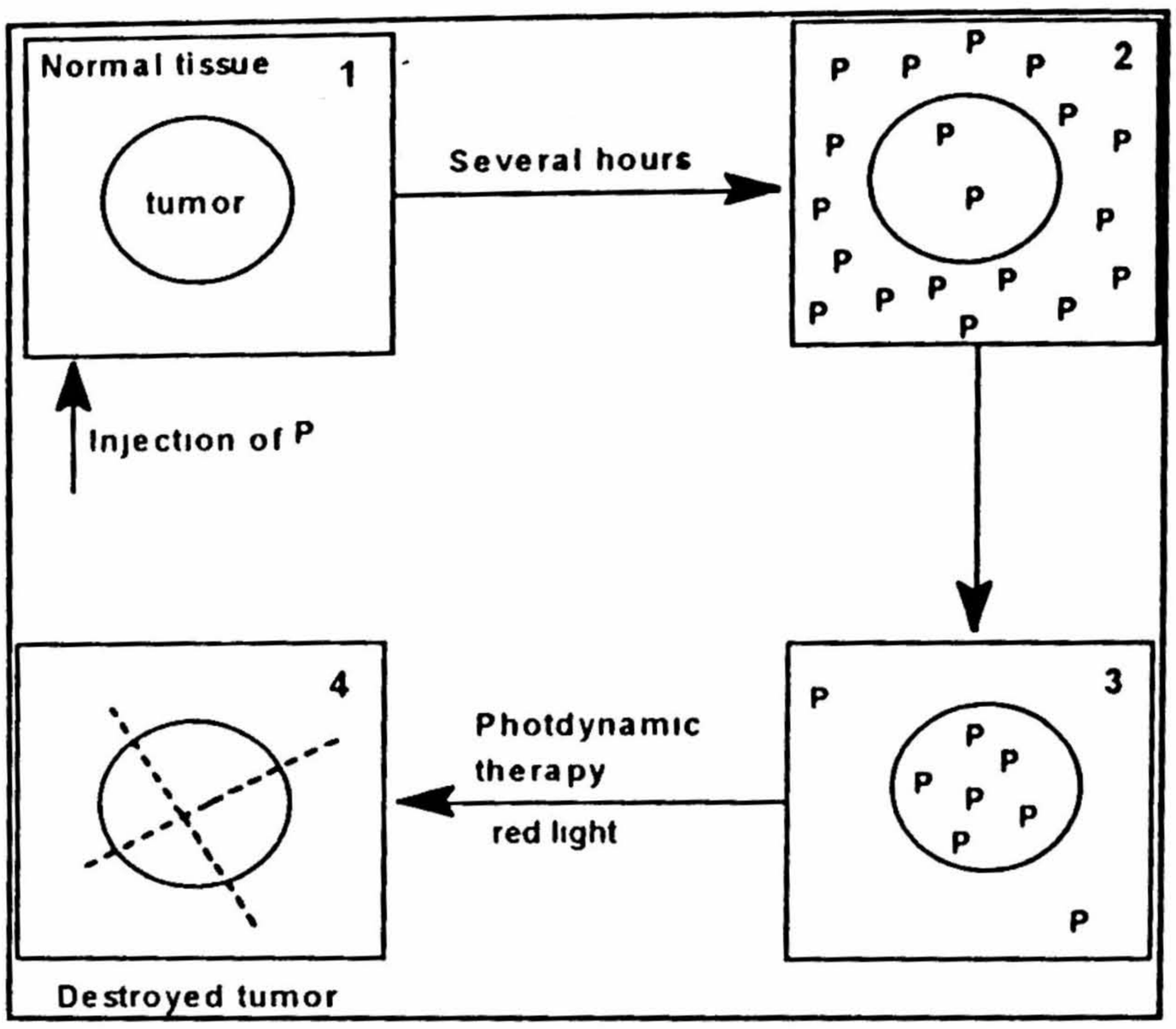

Fig. 1.3

Two different kinds of mechanisms, Type I and Type II, have been proposed for the PDT action and in both the mechanisms involve the formation of excited triplet sensitizer (^3S).

$$S \xrightarrow{h\nu} {}^1S \qquad (1.18)$$

$$^1S \xrightarrow{ISC} {}^3S \qquad (1.19)$$

TYPE I

$$^{*}3_S + R \longrightarrow S^{+} + R^{-} \quad (1.20)$$

$$^{3}S + R \longrightarrow S^{-} + R^{+} \quad (1.21)$$

TYPE II

$$^{3}S + {}^{3}O_2 \longrightarrow S + {}^{1}O_2 \quad (1.22)$$

$$^{1}O_2 + \text{Biomolecules} \longrightarrow \text{Products} \quad (1\ 23)$$

In the Type I mechanism, ^{3}S interacts directly with the substrate molecule (R), either by hydrogen atom abstraction or by electron transfer to produce the reactive radical species. These radicals may interact with oxygen to produce cytotoxic products such as $O_2^{-\cdot}$, $OH^{\cdot}$, H_2O_2, etc. In the Type II mechanism, ^{3}S reacts with the ground state triplet oxygen producing singlet oxygen, which is a highly reactive species that selectively attacks electron rich substrates to give peroxides or other oxidized species. Recent *in vitro* and *in vivo* studies indicate that generation of singlet oxygen is a crucial step in the PDT cytotoxicity [66-69]

An ideal photosensitizer for PDT should fulfil the following minimum criteria.

1. It should be a single, nontoxic, stable compound of known chemical structure, which is retained with a high degree of selectivity in malignant tumours compared with the normal tissue.

2. It should have a strong absorption peak in the part of the spectrum where light penetrates the living tissue best and where the photon energy is still high enough to produce singlet oxygen (i.e 600 to 1100 nm).

Porphyrins, the well-known photosensitive dyes already used by the nature (Section 1.2), possess most qualities that are expected in an ideal PDT photosensitizer. Indeed, porphyrins and related compounds are the best known PDT photosensitizers to date and this Section reviews some recent advances made in this field.[69]

Among the first generation photosensitizers, hematoporphyrin derivative (HpD) and its commercial variant, photofrin II® have been used for clinical testing.[66,70] HpD is a complex mixture of hematoporphyrin (Hp), hydroxyethylvinyl deuteroporphyrin (Hvd) and protporphyrin together with dimers and higher oligomers of these porphyrins joined with ether or ester linkages. photofrin II® is a purified preparation of the active fraction of HpD. Despite the utility of photofrin II, it has three important disadvantages which are given below.

1. It is a complex and variable mixture of porphyrin oligomers linked with ether, ester or carbon-carbon linkages, which are not stable either during storage or after administration

2. It has only one weak absorption peak in the relevant part of the spectrum at about 630 nm, but absorbs much more strongly at shorter wavelengths in the visible and near UV regions

3. It is not very selective and causes skin photosensitivity

It was therefore found desirable to develop new photosensitizers and the second generation sensitizers include modified phthalocyanines and naphthalocyanines,[71] chlorins and bacteriochlorins,[72] purpurins,[73] benzoporphyrin derivatives,[74] porphycenes and expanded porphyrins,[75] and picket fence porphyrins.[76] Representative structures of these are shown below (**19-24**).

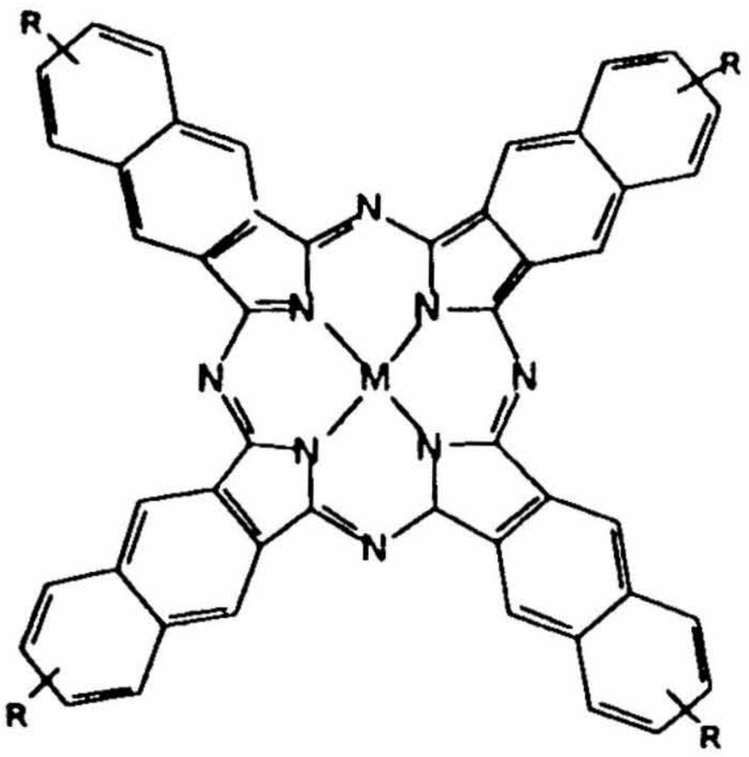

Phthalocyanine

19

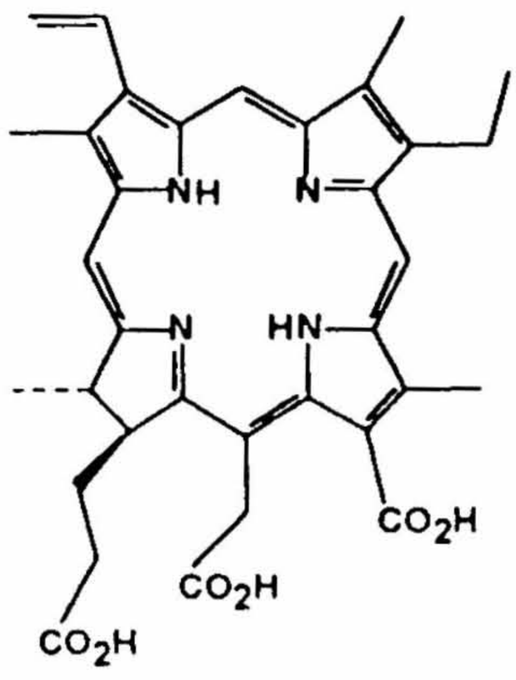

Chlorin e_6

20

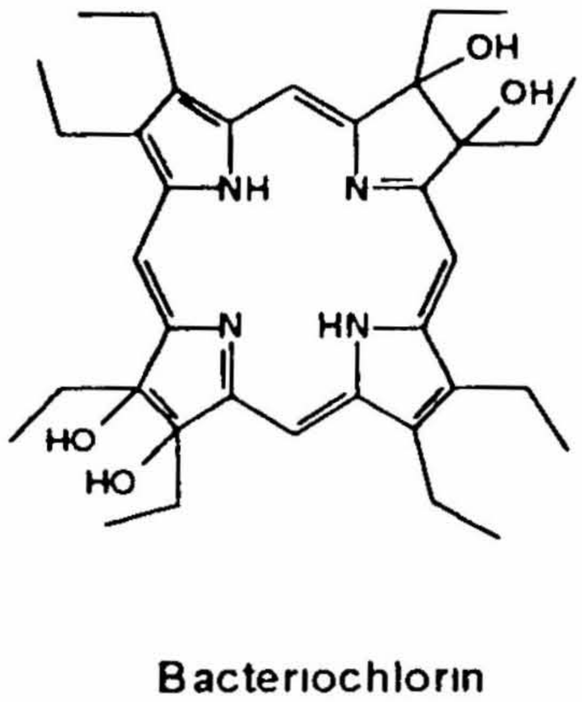

Bacteriochlorin derivative

21

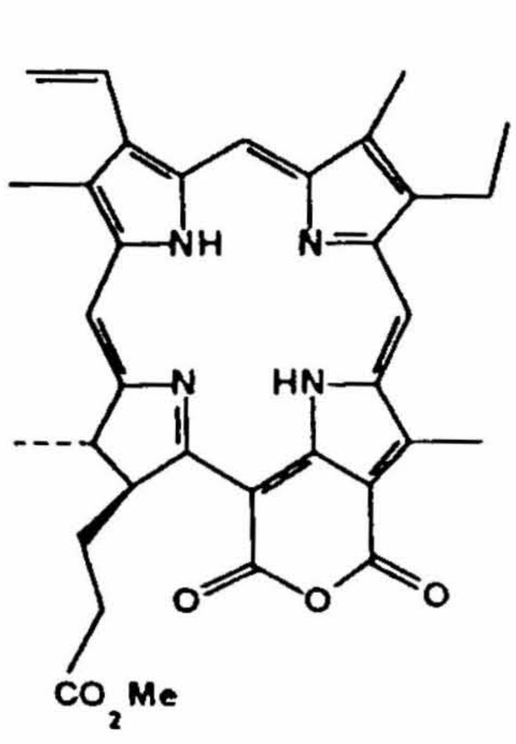

Purpurin 18-methyl ester

22

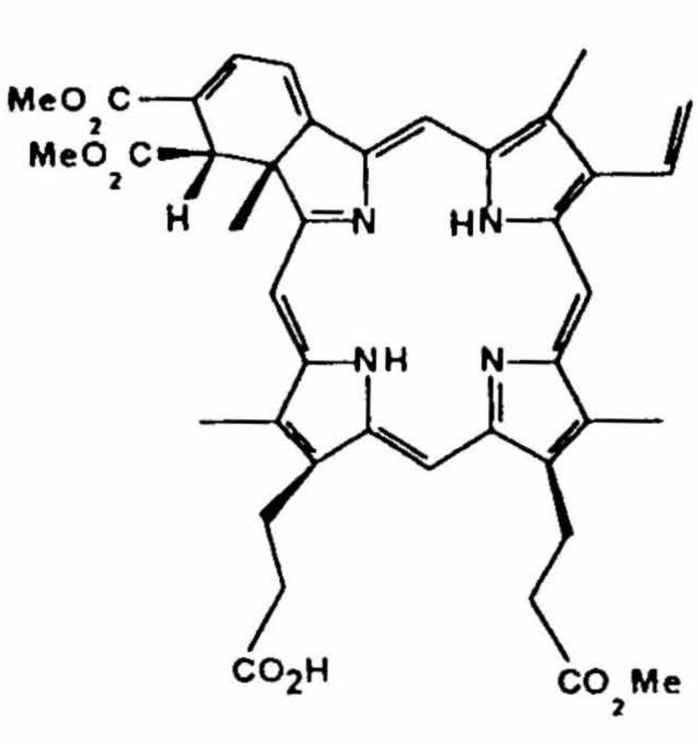

Benzoporphyrin derivative

23

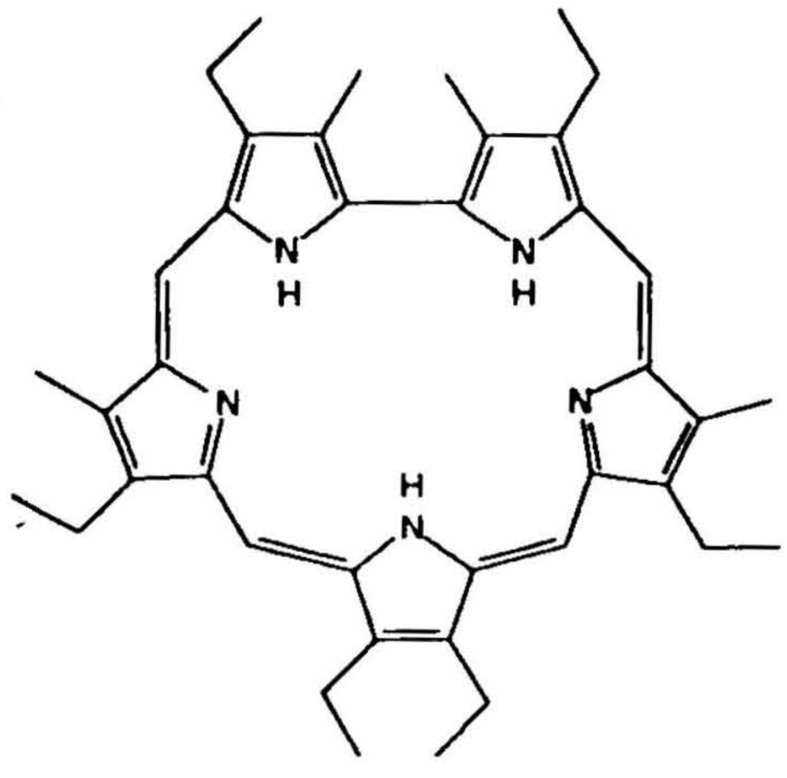

Sapphyrin

24

Many of these second generation photosensitizers, although are efficient $^1O_2$ generators and also absorb strongly in the tissue-transparent region, suffer severly from their inability to accumulate selectively in tumours. One possible way to circumvent the problem of low accumulation of a given porphyrin-based drug in the cells is to equip the drug with an intracellular recognition element *viz* a DNA or membrane binding agent. Thus, porphyrin conjugates endowed with oligonucleotide,[77] monoclonal antibody,[78] ellipticene,[79] or other intracellular recognition elements[80] have been reported recently.

Oligodoxynucleotides (ODN) are considered as new tools in the selective inhibition of gene expression and as potential drugs in anticancer or antiviral therapy. Mastruzzo et al.[77b] have studied photochemical effects induced in a 24-mer RNA by a complementary antisense ODN that is covalently linked to a porphyrin. It was found that ODN-porphyrin conjugates (**25**) induce sequence-specific cross-linking reactions on the target HIV RNA and that the free base porphyrins are more efficient than the zinc derivatives.

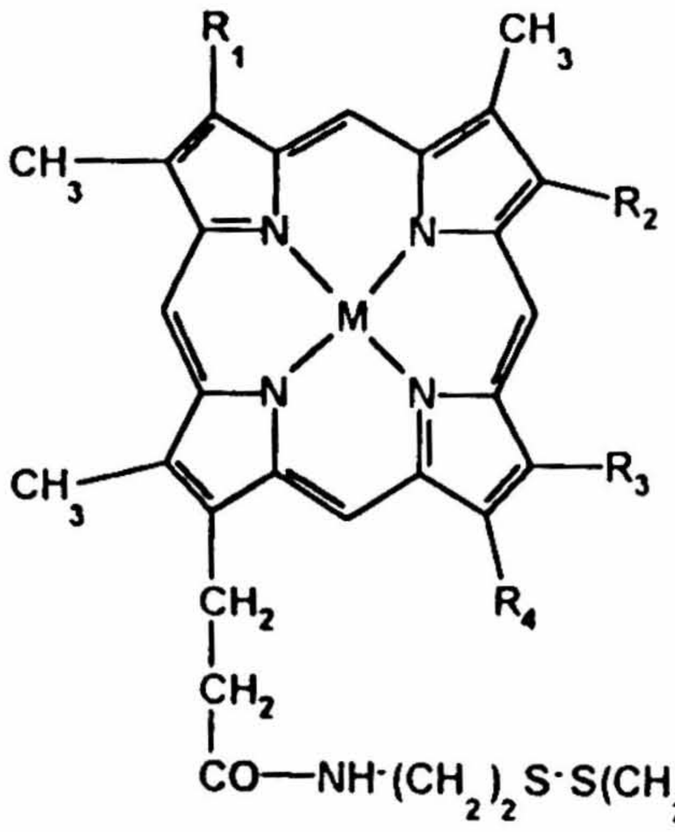

M = 2H or ZN

POR	R_1	R_2	R_3	R_4
25a	Me	Et	Et	Me
25b	Vi	Vi	Me	Pr

Monoclonal antibodies have been used to target the DNA as these possess the property of localizing in tumor cells [81] The strong interaction of the antibodies with porphyrins has also been studied with regard to the use of such conjugates in PDT [78,82] Netropsin, a DNA minor groove binding agent, has been linked to an intercalating cationic porphyrin, meso-tetrakis(4-N-methylpyridyl)porphine (TMPyP-4) [80c] In order to optimize the intercalation of the porphyrin moiety, theoretical computations of porphyrin-netropsin DNA interactions have been performed Other groove binders such as ellipticene etc have also been linked to porphyrins but, these conjugates have been used to cleave DNA *via* chemical means [79]

Photocleavage of DNA has been observed in studies with the so-called 'expanded' porphyrins In their recent study using pBR 322 plasmid DNA assay, Sessler et al have compared the photocleavage capabilities of expanded porphyrins, viz lutetium (III) texaphyrin complex (LuTx, **26**) and the nonmetallated sapphyrin (**27**), with that of TMPyP-4 (**28**), a known photocleaving agent [83] At wavelengths above 300 nm, all the three compounds showed efficient photocleavage However, when the shorter wavelengths were blocked out with a 700 nm filter, **26** showed 93% cleavage efficiency while **27** and **28** showed only 8 and 17% cleavage efficiencies, respectively It has been further found from the sequence specific DNA studies of **26** that the sites of reaction lie across the minor groove of DNA

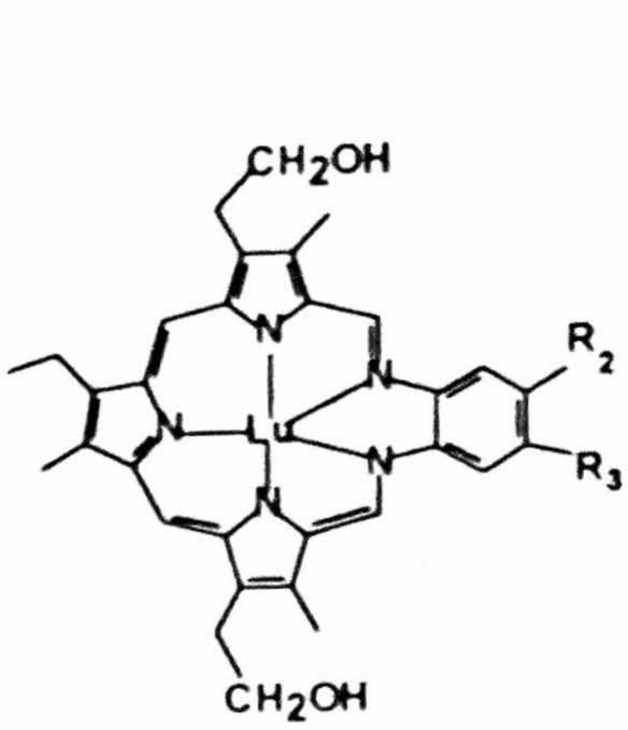

$R_2 = R_3 = OCH_2CH_2CH_2OH$

$R_2 = OCH_2CO_2H$, $R_3 = H$

$R_2 = OCH_2CO$-RNA(2'-OMe), $R_3 = H$

26

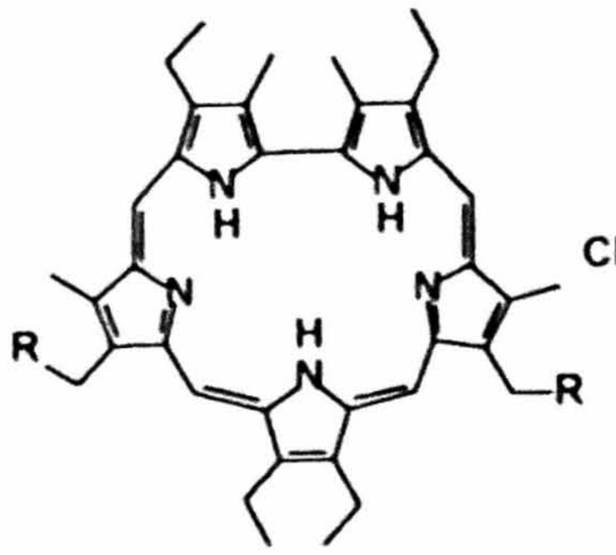

$R = CH_2CON(CH_2CH_2OH)_2$

27

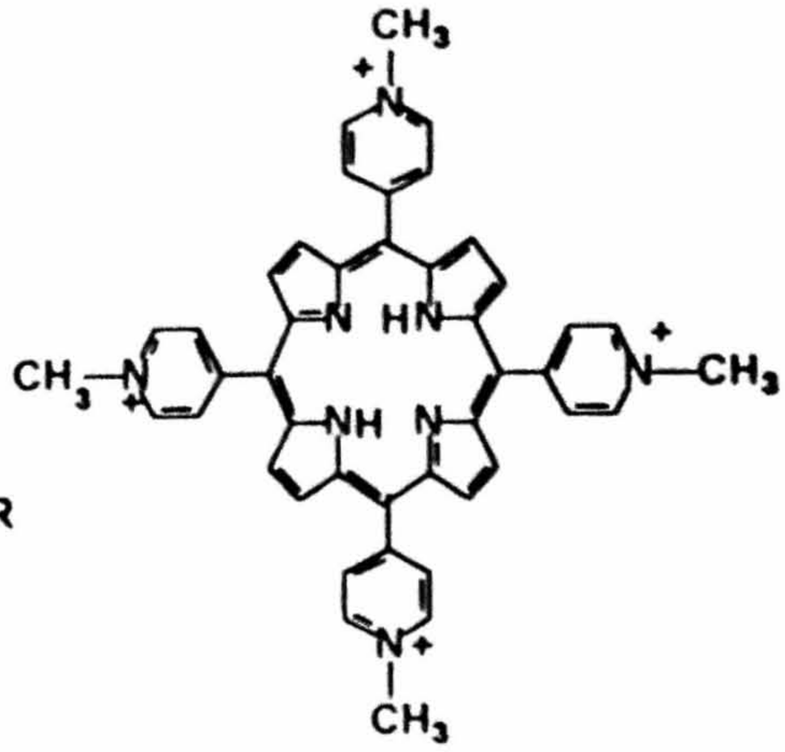

28

1.4 Summary

The principles involved in EET and PET reactions, discussion on the recent porphyrin-based D-A compounds and a brief introduction to PDT have been presented in this chapter

This thesis has been divided into eight chapters

Chapter 1 gives a general introduction to EET and PET reactions including a discussion on the porphyrin-based D-A compounds It also gives a brief account of new photosensitizers for PDT

Chapter 2 details various materials and spectroscopic methods used in this work

Chapter 3 deals with the synthesis and a detailed study on the mechanism of PET in a series of isomeric porphyrin-dinitrobenzene compounds

Chapter 4 presents the synthesis and studies on EET reactions of a series of covalently-linked porphyrin-anthracene molecular dyads.

Chapter 5 deals with the synthesis and fluorescence studies of a supramolecular porphyrin-anthracene molecular pentad.

Chapter 6 presents the synthesis and photophysical studies of a bichromophoric system that is assembled *via* a two-point H-bonding between a porphyrin-adenine and an anthracene-thymine conjugates.

Chapter 7 presents studies on 'porphyrin-intracellular recognition element' conjugates in which a porphyrin is covalently linked to either a DNA intercalator (acridone, aminoacridine, phenothiazine) or DNA cross-linking agent (chlorambucil). Photophysical data and DNA cleavage reactions of these novel conjugates have been specifically discussed in this chapter

Chapter 8 presents general conclusions based on the studies carried out in this work.

1.5 References

1 *Photoinduced Electron Transfer, Parts A-D;* Fox, M A , Channon, M., Eds.; Elsevier. Amsterdam, 1988

2. *Photoinduced Electron Transfer* A series in *Topics in Current Chemistry* Mattay, J., Ed.; Springer-Verlag. New York, 1991.

3. Marcus, R A.; Sutin, N. *Biochim Biophys. Acta* **1985**, 811, 265.

4. *Photosynthesis;* Amesz, J , Ed ; Elsevier. Amsterdam, 1987

5. Gust, D.; Moore, T. A ; Moore, A L *Acc Chem Res* **1993**, 26, 198

6 Guillet, J. E In *Polymer Photophysics and Photochemistry,* Cambridge University Press. Cambridge, 1985

7. Yamamoto, M.; Ito, S.; Ohmori, S. In *Photochemical Processes in Organized Molecular Systems;* Honda, K., Ed.; Elsevier: Amsterdam, 1991; p 329.

8. (a) Marcus, R. A. *J. Chem. Phys.* **1956**, 24, 966. (b) Marcus, R. A. *J. Chem. Phys.* **1965**, 43, 679. (c) Marcus, R. A. In *Light Induced Charge Separation in Biology and Chemistry;* Gerischer, H.; Katz, J. J., Eds.; Verlag Chemie Berlin, 1979, p 15. (d) Marcus, R. A. *Angew. Chem., Int. Ed. Engl.* **1993**, 32, 1111 and references therein.

9. Dexter, D. L. *J. Chem. Phys.* **1953**, 21, 836.

10. Forster, Th. *Discuss. Faraday Soc.* **1959**, 27, 7.

11. (a) Deisenhofer, J ; Epp, O.; Mikki, K.; Huber, R., Michel, H. *J. Mol. Biol.* **1984**, 180, 385. (b) Deisenhofer, J. Epp, O., Mikki, K.; Michel, H. *Nature* **1985**, 318, 618. (c) Chang, C. H ; Tiede, D.; Tang, J., Smith, U ; Norris, J Schiffer, M. *FEBS Lett.* **1986**, 205, 82. (d) Allen, J. P.; Feher, G.; Yeates, T. O., Rees, D. C , Deisenhofer, J , Michel, H., Huber, R *Proc. Natl. Acad Sci. USA* **1986**, 83, 8589. (e) Allen, J. P.; Feher, G.; Yeates, T. O , Komiya, H ; Rees, D C.; *Proc Natl. Acad. Sci. USA* **1987**, 84, 5730 (f) Yeats, T O., Komiya, H , Chirino, A , Rees, D C ; Allen, J. P.; Feher, G. *Proc. Nat.l. Acad. Sci USA* **1988**, 85, 7993. (g) El-Kabbani, O ; Chang, C. H.; Tiede, D. M.; Norris, J ; Schiffer, M. *Biochemistry* **1991**, 30, 5361. (h) Ermler, U.; Fritzsch, G ; Buchanan, S. K.; Michel, H. *Structure* **1994**, 2, 925. (i) Deisenhofer, J.; Epp, O.; Sinning, I.; Michel, H. *J. Mol. Biol.* **1995**, 246, 429.

12. Connolly, J. S In *Photochemical Conversion and Storage of Solar Energy;* Rabani, J., Ed.; The Weizman Science Press: Jerusalem, 1982, Part-A, p. 175.
13. *Photochemistry of Polypyridine and Porphyrin Complexes;* Kalyanasundaram, K., Academic Press: London, 1992.
14. Harriman, A. In *Supramolecular Photochemistry;* Balzani, V., Ed.; D. Reidel: Boston, 1987, p 207.
15. Connolly, J. S.; Bolton, J. R. In *Photoinduced Electron Transfer, Part A;* Fox, M. A.; Channon, M., Eds ; Elsevier: Amsterdam, 1988, Chapter 6.2.
16. Wasielewski, M R. In *Photoinduced Electron Transfer, Part D;* Fox, M A ; Channon, M Eds ; Elsevier Amsterdam, 1988, Chapter 1.4
17. Gust, D., Moore, T A *Science* **1989**, 244, 35
18. Fox. M A *Photochem Photobiol* **1990**, 52, 617
19. Gust, D.; Moore, T. A *Top. Curr Chem.* **1991**, 159, 103
20. Wasielewski, M. R *Chem Rev.* **1992**, 92, 435.
21. Fox, M. A. *Chem Rev.* **1992**, 92, 365.
22. Kurreck, H.; Huver, M *Angew. Chem . Int Ed Engl* **1995**, 34, 849
23. Schwartz, F. P.; Gouterman, M ; Muljiani, Z ; Dolphin, D H *Bioinorg Chem.* **1972**, 2, 1.
24. (a) Boxer, S. G.; Closs, G. L. *J Am. Chem. Soc.* **1976**, 98, 5406. (b) Wasielewski, M R.; Studier, M. H.; Katz, J. J *Proc Natl Acad. Sci USA* **1976**, 73, 4282
25. Wasielewski, M R.; Studier, M. H , Katz, J J *Proc Natl Acad. Sci. USA* **1976**, 73, 4282

26. Boxer, S. G. *Biochim. Biophys. Acta* **1983**, 726, 265.

27. Morgan, B.; Dolphin, D. *Structure and Bonding* **1987**, 64, 115.

28. (a) Krishnan, V. In *Solvation Dynamics and Charge Transfer Reactions;* Bagchi, B ; Krishnan, V., Eds.; World Scientific: Singapore, 1991, p. 123. (b) Osuka, A.; Maruyama, K.; Yamazaki, I.; Tamai, N.; *Chem. Phys. Lett.* **1990**, 165, 392. (c) DeGraziano, J. M.; Liddel, P. A.; Leggett, L ; Moore, A. L.; Moore, T. A.; Gust, D. *J. Phys. Chem.* **1994**, 98, 1758.

30. Chambron, J. -C., Harriman, A., Heitz, V.; Sauvage, J -P. *J. Am. Chem. Soc.* **1993**, 115, 7419.

31. Raghavan, M., Krishnan, V *Chem. Phys. Lett.* **1993**, 205, 19.

32. Gust, D.; Moore, T. A ; Moore, A. L.; Devadoss, C ; Liddell, P. A.; Hermant, R., Nieman, R. A , Demanche, L J ; DeGraziano, J. M.; Gouni, I *J Am Chem Soc* **1992**, 114, 3590

33. Osuka, A.; Yamada, H., Maruyama, K ; Mataga, N.; Asahi, S.; Ohkouchi, M. T.; Okada, T.; Yamazaki, I.; Nishimura, Y. *J. Am. Chem. Soc.* **1993**, 115, 9439.

34. Lindsey, J. S.; Brown, P. A ; Siesel, D. A. *Tetrahedron* **1989**, 45, 4845.

35. Effenberger, F., Schlosser, H.; Bauerle, P., Maier, S.; Port, H.; Wolf, H. C. *Angew Chem., Int. Ed. Engl.* **1988**, 27, 281.

36. Kong, J., Loach, P. A In *Frontiers of biological energetics: From electrons to tissues;* Dutton, P. L ; Leigh, J. S.; Scarpa, H. Academic Press: New York, Vol 1, p 173.

37. Liddel, P. A.; Sumida, J. P.; MacPherson, A. N.; Noss, L.; Seely, G. R.; Clark, K. N.; Moore, A L.; Moore, T. A., Gust, D. *Photochem. Photobiol.* **1994**, 60, 537.

38. Imahori, H.; Hagiwara, K.; Aiyama, T.; Taniguchi, S., Okada, T.; Sakata, Y. *Chem. Lett.* **1995**, 265.

39. Drovetskaya, T.; Reed, C. A. *Tetrahedron Lett.* **1995**, 36, 7971.

40. (a) Wasielewski, M. R.; Niemczyk, M. P. *J. Am. Chem. Soc.* **1984**, 106, 5043. (b) Wasielewski, M. R.; Niemczyk, M. P.; Svec, W. A., Pewitt, E. B.; *J. Am. Chem Soc.* **1985**, 107, 1080. (c) Wasielewski, M. R.; Niemczyk, M. P., Svec, W. A., Pewitt, E. B., *J Am Chem Soc* **1985**, 107, 5562 (d) Joran, A R.; Leland, B A.; Geller, G G ; Hopfield, J. J ; Dervan, P. B *J. Am Chem. Soc* **1984**, 106, 6090. (e) Lindsey, J S., Mauzerall, D C ; Linschitz, H *J. Am Chem Soc* **1983**, 105, 6528.

41. (a) Wasielewski, M. R , Niemczyk, M P., Johnson, D G ; Svec, W A ; Minsek, D. W. *Tetrahedron* **1989**, 45, 4785 (b) Wasielewski, M R , Johnson, D. G ; Niemczyk, M. P.; Gaines, G L.; O'Neil, M. P.; Svec, W. A *J. Am Chem. Soc.* **1990**, 112, 6482. (c) Hayashi, T , Takimura, T.; Hitomi, Y.; Ohara, T , Ogoshi, H *J. Chem Soc , Chem Commun.* **1995**, 545.

42. Cave, R.; Marcus, R. A ; Siders, P *J. Phys Chem.* **1986**, 90, 1436

43. (a) Oliver, A. M ; Craig, D. C.; Paddon-Row, M N , Kroon, J , Verhoeven, J. W. *Chem. Phys. Lett.* **1988**, 150, 366 (b)Oevering, H.; Verhoeven, J. W., Paddon-Row, M N., Warman, J. M *Tetrahedron* **1989**, 45, 4751.

44. (a) Sakata, Y.; Tsue, Y.; Goto, S.; Misumi, T.; Asahi, S.; Nishikawa, T.; Okada, T.; Mataga, N. *Chem. Lett.* **1991**, 1307. (b) Sakata, Y.; Tsue, H.; O'Neil, M. P ; Wiederrecht, G. P.; Wasielewski, M. R. *J. Am. Chem. Soc.* **1994**, 116, 6904. (c) Higashida, S.; Tsue, H.; Sugiura, K.; Kaneda, T.; Tanaka, Y.; Taniguchi, S.; Okada, T.; Sakata, Y. *Chem. Lett.* **1995**, 515.

45. Moore, T. A.; Gust, D.; Mathıs, P ; Mialocq, J. C.; Chachaty, C.; Benasson, R. V , Land, E. J., Doizi, D.; Liddell, P. A.; Lehman, W. R.; Nemeth, G. A., Moore, A. L *Nature* **1984**, 307, 63.

46. Gust, D.; Moore, T. A , Moore, A. L., Gao, F , Luttrull, D., DeGraziano, J. M ; Ma, C X , Markings, L R.; Lee, S. -J ; Trier, T. T ; Bittersman, E., Seely, G R., Woodward, S.; Bensasson, R. V.; Rougee, M.; De Schryver, F. C ; Vander, M *J Am. Chem. Soc.* **1991**, 113, 3638

47. (a) Hung, S. -C., Macpherson, A. N , Lın, S ; Liddell, P. A.; Seely, G. R.; Moore, A. L , Moore, T A ; Gust, D. *J. Am. Chem. Soc.* **1995**, 117, 1657. (b) Gosztola, D., Yamada, H., Wasielewski, M. R *J Am. Chem. Soc.* **1995**, 117, 2041.

48. Gust, D.; Moore, T. A.; Moore, A. L ; Markıngs, L. R ; Seely, G. R.; Ma, X.; Trier, T. T ; Gao, F *J. Am. Chem. Soc.* **1988**, 110, 7567.

49. Gust, D.; Moore, T. A , Moore, A. L ; Lee, S. -J , Bittersman, E.; Luttrull, D. K,, Rehms, A. A ; DeGrazino, J M.; Ma, X C.; Gao, F.; Belford, R. E.; Trier, T. T. *Science* **1990**, 248, 199.

50. Sessler, J. L ; Capuano, V L. *Angew. Chem., Int. Ed. Engl.* **1990**, 29, 1134.

51 Osuka, A , Nagata, T , Maruyama, K *Chem Lett* **1991**, 481

52 Sessler, J L ; Capuano, V L , Harriman, A *J Am Chem Soc* **1993**, 115, 4618

53 Harriman, A , Heitz, V , Ebersole, M , van Willigen, H *J Am Chem Soc* **1991**, 113, 719

54 (a) Brun, A M , Harriman, A , Heitz, V , Sauvage, J -P , *J Am Chem Soc* **1991**, 113, 8657 (b) Chambron, J -C , Harriman, A , Heitz, V , Sauvage, J -P *J. Am Chem Soc* **1993**, 115, 6109 (c) Chambrom J C , Harriman, A , Heitz, V , Sauvage, J -P *J Am Chem Soc* **1993**, 115, 7419 (d) Harriman, A , Heitz, V , Sauvage, J -P *J Phys Chem* **1993**, 97, 5940

55 Harriman, A , Odobel, F , Sauvage, J -P *J Am Chem Soc* **1995**, 117, 9461-72

56 (a) Prathapan, S , Johnson, I E , Lindsey, J S *J Am Chem Soc* **1993**, 115, 7519 (b) Wagner, R W , Lindsey, J S *J Am Chem Soc* **1994**, 116, 9759

57 (a) Brun, A M , Harriman, A *J Am Chem Soc* **1994**, 116, 10383 (b) Lehn, J -M *J Chem Soc , Chem Commun* **1994**, 2313 (c) Hunter, C A *Chem Soc Rev* **1994**, 101 (d) Hunter, C A , Sarson, D L *Angew Chem , Int Ed Engl* **1994**, 33, 2313 (e) Anderson, S , Anderson, H L , Bashall, A , McPartlin, M , Sanders, J K M *Angew Chem , Int Ed Engl* **1995**, 34, 1096 (f) Anderson, H L , Waltor, C J , Ferran, A V , Hay, R A , Lowden, P A , Sanders, J K M *J Chem Soc , Perkin Trans 1* **1995**, 2275 and references therein (g) Rao, T A , Maiya, B G *J Chem Soc , Chem Commun* **1995**, 939 (h)

Funatsu, K.; Kimura, A.; Imamura, T.; Sasaki, Y. *Chem. Lett.* **1995**, 765. (e) Imahori,; H.; Yoshizawa, E.; Yamada, K.; Hagiwara, K.; Okada, T.; Sakata, Y. *J. Chem. Soc., Chem. Commun.* **1995**, 1133. (f) Arimori, S.; Murakami, H.; Takeuchi, M.; Shinkai, S. *J. Chem. Soc., Chem. Commun.* **1995**, 961. (g) Kuroda, Y.; Kato, Y.; Higashioji, T.; Hasegawh, J. Y , Kawanami, S.; Takahashi, M.; Shiraishi, N.; Tanabe, K.; Ogoshi, H *J Am. Chem. Soc.* **1995**, 117, 10950 and references therein.

58. Lehn, J. -M *Supramolecular Photochemistry;* Balzani, V., Ed.; NATO ASI Ser Ser C 1987, 214, 290

59. Sun, L.; von Gersdorff, J., Niethammer, D.; Tian P.; Kurreck, H. *Angew. Chem., Int. Ed. Engl.* **1994**, 33, 2318.

60. (a) Aoyama, Y , Asakawa, M.; Matsui, Y., Ogoshi, H. *J. Am. Chem. Soc.* **1991**, 133, 6223. (b) Hayashi, T., Asai, T , Hokazono, H., Ogoshi, H. *J. Am. Chem. Soc.* **1993**, 115, 1220 (c) Hayashi, T ; Miyahara, Hashizume, N , Ogoshi, H. *J Am Chem. Soc.* **1993**, 115, 2049. (d) Hayashi, T , Miyahara, T., Aoyama, Y.; Nonoguchi, M., Ogoshi, H. *Chem. Lett.* **1994**, 1749. (e) Hayashi, T ; Miyahara, T ; Aoyama, Y.; Kobayashi, M ; Ogoshi, H. *Pure and Appl. Chem.* **1994**, 66, 797. (f) Mizutani, T.; Murakami, T ; Matsumi, N ; Kurahashi, T.; Ogoshi, H. *J. Chem. Soc., Chem. Commun.* **1995**, 1257.

61. (a) Harriman, A.; Magda, D. J., Sessler, J. L *J. Chem. Soc., Chem. Commun.* **1991**, 345. (b) Harriman, A., Magda, D. J.; Sessler, J. L. *J. Phys. Chem.* **1991**, 95, 1530 (c) Harriman, A ; Kubo, Y.; Sessler, J. L.

J. Am. Chem Soc **1992**, 114, 388. (d) Sessler, J. L.; Wang, B.; Harriman, A. *J. Am Chem Soc* **1993**, 115, 10418.

62. Drain, M.; Fischer, R.; Nolen, E G.; Lehn, J. -M. *J. Chem Soc., Chem. Commun.* **1993**, 243.

63. (a) Hisatome, M.; Maruyama, N.; Furutera, T.; Ishikawa, T.; Yamakawa, K. *Chem. Lett.* **1990**, 2251. (b) Kus, P ; Knerr, G., Czuchajowski, L. *Tetrahedron Lett.* **1990**, 36, 5133. (c) Hisatome, M.; Ikeda, K.; Kishibata, S., Yamakawa, K *Chem. Lett.* **1993**, 1357.

64. (a) Turro, C ; Chang, C K ; Leroi, G. E.; Cukier, R. I ; Nocera, D G *J. Am. Chem Soc.* **1992**, 114, 4013 (b) Kirby, J P ; van Dantzig, N A , Chang, C. K ; Nocera, D G *Tetrahedron Lett.* **1995**, 36, 3477

65. Finsen, N. R *Phototherapy* (Sequeira, J. H trans), Arnold London, 1901.

66. (a) *Photodynamic Therapy Basic Principles and Clinical Applications*, Henderson, B. W., Dougherty, T J., Eds.; Marcel Dekker New York, 1992.

67. (a) Girotti, A W *Photochem Photobiol* **1983**, 38, 745 (b) Dolphin, D. *Can. J. Chem.* **1994**, 72, 1005

68. (a) Gomer, C. J *Photochem Photobiol.* **1983**, 37S, 91 (b) Bohn, F ; Marston, G.; Truscott, T G.; Wayne, R. P *J Chem Soc Faraday Trans.* **1994**, 90, 2453

69. Bonnett, R. *Chem Soc Rev* **1995**, 19

70. (a) Girard, A ; Gasparro, F *Spectrum* **1993**, 6, 28 (b) Dougherty, T J.; Marcus, S. L. *Eur J. Cancer* **1992**, 28A, 1734

71. (a) Shopova, M.; Mantareva, V.; Krastev, K.; Hadjiolov, D.; Milev, A.; Spirov, K.; Jor, G.; Ricchelli, F. J. *Photochem. Photobiol., B. Biol.* **1992**, 16, 83. (b) Bishop, S. M.; Khoo, B. J.; MacRobert, A. J.; Simpson, M. S. C.; Phillips, D.; Beeby, A. *J. Chromatogr.* **1993**, 646, 345. (c) Boyle, B. W.; Leznoff, C. C.; van Lier, J. E. *Br. J. Cancer* **1993**, 67, 1177. (d) Segalla, A.; Milanesi, C.; Jori, G.; Capraro, H. -G.; Isele, U.; Schieweck,, K. *Br. J. Cancer* **1994**, 69, 817.

72. (a) Kostenich, G. A.; Zhuravkin, I. N.; Zhavrid, E. A. *J. Photochem. Photobiol B. Biol.* **1994**, 22, 211. (b) Bonnett, R.; Benzie, R.; Grahn, M. F.; Salgado, A , Valles, M. A. *Proc SPIE* **1994**, 2078, 171. (c) Leach, M. W., Higgins, R. J ; Autrey, S. A ; Bogganim J. E., Lee, S. -J. H.; Smith, K M. *Photochem Photobiol.* **1993**, 58, 653. (d) Pandey, R. K.; Shiau, F -Y , Ramachandran, K., Dougherty, T. J , Smith, K. M. *J Chem. Soc , Perkin Trans I* **1992**, 1377 (e) Richter, A. M , Kelly, B., Chow, J.; Liu, D. J., Towers, G. M. N , Dolphin, D ; Levy, J. G. *J. Natl. Cancer Inst.* **1987**, 79, 1327.

73. Morgan, A. R., Garbo, G. M.; Keck, R. W , Skalkos, D.; Selman, S. H. *Photochem. Photobiol* **1990**, 6,133.

74. (a) Ritcher, A. M.; Watterfield, M. E.; Jain, A. K.; Allison, B.; Sternberg, E D ; Dolphin, D.; Levy, J. G. *Br. J Cancer* **1991**, 63, 87. (b) Hunt, D. W. C.; Jiang, J. -H.; Levy, G. J ; Kabn. A. H. *Photochem. Photobiol.* **1995**, 61, 417

75. (a) Vogel, E.; Kocher, M.; Schmickler, H.; Lex, J. *Angew. Chem., Int. Ed. Engl.* **1986**, 25, 197 (b) Leung, M ; Richert, C., Gainarra, F.; Lumper, W , Vogel, E ; Jochanji, D.; Goetz, A E *Br. J. Cancer* **1993**,

68, 225 (c) Sessler, J L ; Hemmi, G , Mody, T. D , Murai, T., Burrell, A ; Young, S W *Acc Chem Res* **1994**, 27, 43 and references therein

76 (a) Hegan, W J ; Barber, D. C ; Whitten, D G ; Kelly, M ; Albrecht, F.; Gibson, S L., Hilf, R *Cancer Res.* **1988**, 48, 1148. (b) Barber, D C., Van Der Meid, K R ; Gibson, S. L , Hilf, R , Whitten, D G *Cancer Res* **1991**, 51, 1836 (c) Lawrence, D. S ; Gibson, S L ; Nguyen, M L ; Whittemore, K R , Whitten, D G ; Ressell, H *Photochem Photobiol* **1995**, 61, 90

77. (a) Bigey, P , Pratviel, G , Meunier, B *J Chem Soc , Chem Commun* **1995**, 181. (b) Mastruzzo, L , Woisard, A , Ma, D D F , Rizzarelli, E , Favre, A ; Doan, T L *Photochem Photobiol* **1994**, 60, 316 (c) Le Doan, T Praseuth, D , Perrouault, L , Chassignol, M , Thuong, N T , Helene, C *Bioconjugate Chem* **1990**, 2, 108 (d) Fedorova, O S , Savitskii, A P , Shoikhet, K G , Ponomarev, G V *FEBS Lett* **1990**, 259, 335

78 Milgrom, L R , O'Neill, F *Tetrahedron* **1995**, 51, 2137

79 (a) Ding, L , Moghadam, G E , Cros, S , Auclair, C , Meunier, B *J Chem Soc , Chem Commun* **1989**, 1711 (b) Moghadam, G E , Ding, L., Tadj, F., Meunier, B *Tetrahedron* **1989**, 45, 2641 (c) Ding, L , Moghadam, G E , Meunier, B *Biochemistry* **1990**, 29, 7868

80 Perreee-Fauvet, M , Gresh, N *Tetrahedron Lett* **1995**, 36, 4227 (b) Mathews, S E , Pouton, C W , Threadgill, M D *J Chem Soc , Chem Commun* **1995**, 1809 (c) Herbelin, G A , Perreee-Fauvet, M , Gaudemer, A , Helissey, P , Renault, S G , Gresh, N *Tetrahedron Lett*

1993, 45, 7263. (d) Hashimoto, Y.; Lee, C. -S.; Shudo, K.; Okamoto, T. *Tetrahedron Lett.* **1983**, 24, 1523.

81. *Principles of Cancer Biotherapy;* Oldham, R. K., Ed.; Raven: New York, 1987.

82. (a) Harada, A.; Okamoto, K.; Kamachi, M.; Honda, T.; Miwatani, T. *Chem. Lett.* **1990**, 919. (b) Harada, A.; Shiotsuki,K.; Fukushima, H.; Yamaguchi, H.; Kamachi, M. *Inorg. Chem.* , **1995**, 34, 1070.

83. Magda, D.; Wright, M.; Miller, R. A.; Sessler, J. L.; Sansom, P. I. *J. Am. Chem. Soc.* **1995**, 117, 3629.

CHAPTER 2

Materials and Methods

1 Introduction

In this chapter, a listing of all the materials employed at different ages of the investigation and procedures for purification of the utilised hemicals/solvents are given. Also given is a brief description of physico-hemical techniques employed in this study.

:.2 Materials

Pyrrole, was procuied form Aldrich Chemicals (U.S.A) and was listilled (129-131 °C) over KOH before use.

Phenol, o-, m-, and p-hydroxy benzaldehydes, p-tolualdehyde, and 3,5-dinitrobenzoyl chloride were obtained from E Merck (India)

Adenine, thymine, 1,3-Diphenylisobenzofuran (DPBF) and Tetrabutyl-ammonium perchlorate (TBAP) were procured from Aldrich Chemicals (U.S.A).

9-chloromethylanthracene was obtained from Fluka (U.S.A).

1,2-dibromoethane was procured from Sisco Chem. (India) and was distilled under vacuo before use.

The supercoiled DNA, pBR 322 (Cesium Chloride purified), was obtained from Bangalore Genei (India)

Agarose (Low Melt (65°C) Preparative Grade for DNA gels) and Hind III, a restriction enzyme were procured from Bio-Rad (U.S.A).

Tris-acetate, sucrose and ethylenediaminetetraacetate (EDTA, disodium salt) were of AR grade, obtained from Sisco Research Laboratories (India).

Ethidium bromide and bromophenol blue were procured from Sigma Chemicals (USA).

Zinc (II) acetate tetrahydrate, copper (II) acetate monohydrate were of AR grade obtained from B D H. (India) and were used as such.

Potassium chloride was of AR grade (B.D.H., India) and was used as such.

Aluminium oxide (basic and neutral) and silica gel used for column chromatography were obtained from Acme Synthetic Chemicals (India).

The drying agents employed at various stages of purification procedures are anhydrous sodium sulfate, calcium chloride, calcium hydride, magnesium turnings and anhydrous magnesium sulfate. These were procured from either B D H (India) or Ranbaxy (India).

Other common chemicals used are benzaldehyde, potassium carbonate, potassium hydroxide. These are of LR grade from B D.H. (India). The mineral acids such as hydrochloric acid, sulphuric acid and nitric acid are of AR grade.

The gases utilised in this study, nitrogen and oxygen, were obtained from Indian Oxygen Limited. Nitrogen was further purified by using the pyrogallol and BASF catalyst before use.

2.3 Solvents

The common solvents used for the synthesis were purified according to the standard procedures.[1,2]

Acetic acid and propanoic acid were obtained from E Merck (India) and were used as such.

Dimethyl formamide and dimethylsulfoxide were obtained from E. Merck (India) and were purified using flash distillation over calcium hydride under vacuum.

Benzene was of recrystallisable grade from Ranbaxy (India). It was dried over calcium chloride, distilled and stored over sodium wire.

Chloroform and methanol used for the spectroscopic studies were of AR grade from B.D.H. (India).

Methylene chloride used for spectroscopic and electrochemical studies was purified rigorously. The LR Grade solvent obtained from B.D.H (India) was washed twice with sulfuric acid, and then with water This was followed by washing twice with sodium carbonate solution and water again. It was dried over anhydrous $CaCl_2$, and distilled from calcium hydride before use.

Pyridine was of LR grade from Ranbaxy (India) and was refluxed over KOH for an hour and then distilled.

The other solvents used were acetone, ethanol, acetonitrile, toluene, and tetrahydrofuran They were purified according to the known procedures before use.[1,2]

$CDCl_3$ (99.8%) and DMSO-d_6 (99.8%) were obtained from Aldrich Chemicals (U.S.A) and were used as such for the ^1H NMR measurements

2.4 Physical methods

Various instrumental methods that were used to elucidate the molecular structure of the porphyrins and their metallodervatives synthesised in this study are infrared, electronic absorption and emission, proton magnetic resonance, electron paramagnetic resonance and mass

spectroscopic methods and electrochemical techniques. A general outline of these methods is given below.

The infrared spectra were recorded either on a Perkin-Elmer Model 1310 or a Jasco Model 5300 FT-IR spectrophotometers. The spectra of the solid samples were recorded by dispersing the sample in Nujol-mull or in KBr disc (pellet technique).

The UV-visible spectra were recorded with either a Perkin-Elmer Lambda 3B, a Shimadzu Model 160A or a Jasco model 7800 spectrophotometer. The concentration of the porphyrins used for this purpose ranged from ca. 2×10^{-6} (Soret bands) to 5×10^{-5} M (Q bands).

The steady state fluorescence spectra of the compounds were recorded either on a Hitachi Model F-3010, or a Jasco Model FP 777 spectrofluorometer using 1 cm quartz cell Right angle detection technique was employed for these measurements. The excitation and emission slit widths usually employed were both 2 nm. The concentration of the samples were such that the optical densities at the excitation wavelengths were less than ca. 0.2 for emission spectra and about 1×10^{-7} M (or the optical density at emission wavelength, $\lambda_{em} < 0\ 02$) for excitation spectra. A rhodamine 6G quantum counter was employed for spectral corrections at wavelengths < 600 nm. Fluorescence quantum yields (ϕ_f) were estimated by integrating the areas under the fluorescence curves using the expression of Austin and Gouterman,[3]

$$\phi_{sample} = \frac{A_{sample} \times O.D_{standard}}{A_{standard} \times O\,D_{sample}} \times \phi_{standard} \qquad (2.1)$$

where A is the area under the corrected emission spectral curve, O.D. is the optical density of the compound at wavelength of the exciting light. The fluorescence standards employed were either meso-5,10,15,20-tetraphenyl porphyrin (H_2TPP) and its zinc (II) complex (ZnTPP) (ϕ_{H_2TPP} = 0.13 and ϕ_{ZnTPP} = 0.033)[4] for excitation into the porphyrin absorption maxima of the free-base and zinc (II) porphyrin derivatives, respectively or anthracene ($\phi_{anthracene}$ = 0.24) [5,6] for excitation into the non-porphyrinic chromophores' absorption maxima Refractive index corrections have been incorporated while estimating the ϕ_f values in various solvents [7]

While estimating the percentage energy transfer efficiency, excitation spectrum of a given porphyrin derivative was overlapped with its absorption spectrum after correcting for the instrument response function and after normalizing the spectrum in the 500-600 nm region[16] The excitation spectrum of H_2TPP may well (±5%) be overlapped with its absorption spectrum in the wavelength region 220-600 nm under the experimental conditions λ^2 corrections were applied whenever the data obtained as wavelengths were converted into wavenumbers [5]

The proton magnetic resonance (^1H NMR) spectra were recorded either on a JEOL JNM FX-100 spectrophotometer or a Bruker NR-200 AF-FT NMR spectrometer using $CDCl_3$ as the solvent and tetramethylsilane (TMS) as an internal standard In cases where not specified, the concentration of the sample employed was ≈ 1 0 x 10^{-3} M

The electron paramagnetic resonance (EPR) spectra were recorded on a JEOL JM-FE3X spectrometer. Diphenylpicrylhydrazide (DPPH) was used as a g-marker. The spectra were recorded for ca 1 0 x 10^{-3} M solutions of the copper (II) porphyrins in toluene at 100±3 K For the on-line irradiation experiments in the ESR cavity, a 150 W PTI Model A1010

xenon lamp coupled with a PTI Model LPS 2020 power supply was used. The samples (5.0×10^{-4} M) were irradiated with broad band visible light. The UV irradiance was cut off using glass filters ($\lambda_{irradiation} > 400$ nm). Light beam was focused into the ESR cavity through a focusing light-guide.

The FAB mass spectra were recorded on a JEOL SX 102/DA-6000 mass spectrometer/data system.

The cyclic- and differential pulse voltammetric experiments were performed with a Princeton Applied Research (PAR) Model 174A/175 polarographic analyzer/universal programmer which was coupled with a PAR Model RE 0074 X-Y recorder. Both the working and the counter electrodes were platinum A saturated calomel electrode (SCE) served as the reference electrode. A 'salt-bridge' containing the same concentration of base electrolyte as that of bulk solution was positioned between the deaerated (N_2 purged) bulk-test-solution and the reference electrode to reduce the effect due to liquid junction potentials. TBAP was used as the supporting electrolyte in all the cases. Half-wave potentials in the cyclic voltammetric experiments were measured as the average of the cathodic and anodic peak potentials for all the reversible processes. Unless otherwise stated, all the potentials were measured *vs.* SCE. Ferrocene could be reversibly oxidised at 0.48 V in CH_2Cl_2, 0.1 M TBAP under these experimental conditions.

2.4.1 Fluorescence lifetime measurements

Fluorescence lifetime measurements were carried out by the time-correlated single photon counting (TCSPC) technique[8] using two different instruments.

The first set-up, that is available at the Tata Institute of Fundamental Research (Bombay),[9] has been employed for measuring the life time data

given in Chapter 3. Here, the excitation light source was a tunable picosecond dye laser pulse derived from a cavity dumped dye laser, pumped synchronously by the KTP frequency doubler (SP 3220) of the cw mode-locked Nd-YAG laser obtained from Spectra Physics Inc USA (Model 3460). The sample was excited by 4 ps laser pulses at a repetition rate of 800 kHz. The fluorescence was detected at the magic angle (54.7°C) with respect to polarisation of the incident laser beam by a Hamamatsu microchannel plate (R2809U-01) at a rate of less than 2 x 10^4 s^{-1}. The dark count rate of the photomultiplier was typically about 200 s^{-1} Fluorescence decay data were collected at a resolution of 42 ps per channel on a Tracor Northern model TN-7200 multichannel analyser Instrument response functions were obtained using a suspension of MgO in water

The second set-up namely IBH 5000 is fully a commercial one obtained from IBH Consultants (U.K.) This instrument has been used for obtaining the life time data given in Chapter 6. Here, the excitation source was a H_2-discharge coaxial nanosecond flash lamp with a pulse width of 1 4 ns and the photomultiplier was Hamamatsu 3235 The count rates employed ranged typically from 10^2 to 10^3 s^{-1}. The dark count was < 40 s^{-1}

The fluorescence decays of all the samples studied were fitted to either a single-exponential or a multiexponential decay function Deconvolution was carried out by the method of iterative reconvolution of the instrument response function and the assumed decay function [9,10] The goodness of the fit of the experimental data to the assumed decay function was judged by the standard statistical tests (i e. random distribution of weighted residuals, the autocorrelation function and the values of reduced χ^2). The error estimates of the lifetimes, obtained by single-exponential fits, and of the mean lifetime (defined as $< \tau_1 > = \sum A_1\tau_1$, where $\sum A_1 = 1$),

obtained by multiexponential fits, were less than 10%. Although no specific effort has been made here to estimate the error limit on the relative amplitudes (A_i), it is believed that they should be less than 2%-3%.

2.4.2 Singlet oxygen quantum yield (ϕ_Δ) measurements

A 2.5 ml of DMF (saturated with AR grade molecular oxygen) solution containing 1 0 x 10^{-6} M of a given porphyrin as sensitiser and 0.5-1.0 x 10^{-4} M DPBF was taken in a 1 cm path-length quartz cuvette and irradiated at 550 nm. A 150W Xe arc lamp (PTI Model A1010) coupled with a PTI Model S/N 1366 monochromator (10 nm band-pass) was used as the source of irradiation. It should be noted that porphyrin is the only chromophore that absorbs at this wavelength and DPBF, the singlet oxygen scavenger, does not absorb appreciably in this region. The solution was stirred during the irradiation period The depletion of DPBF due to its reactions with singlet oxygen was monitored at 410 nm spectrophotometrically. The total depletion of DPBF was restricted to 10-15% of its original concentration and an average of five or six depletion rate runs were used for quantum yield measurements. H_2TPP (ϕ_Δ = 0.60) has been employed as the standard and the details of the calculation are given in chapter 7.

2.5 Agarose gel electrophoresis of plasmid DNA

Electrophoresis through agarose is the standard method used to separate, identify or purify DNA fragments.[11-13] The technique is simple, rapid to perform and capable of resolving fragments of DNA that cannot be separated by other procedures such as density gradient centrifugation. The

location of DNA within the gel can be determined directly by staining with low concentration of the fluorescent intercalating dye ethidium bromide. Using this technique, bands containing as little as 1-10 ng of DNA can be detected by direct examination of the gel in the UV-light.[14] Agarose gels are usually run in a horizontal configuration in an electric field of constant strength and direction. When an electric field is applied across the gel, DNA, which is negatively charged at neutral pH, migrates toward the anode. This technique has been employed to investigate the DNA photocleavage by the porphyrin derivatives described in chapter 7.

2.5.1 Buffers used

Water used for these experiments was triply distilled using a quartz distillation set-up and then autoclaved before use

2.5.1.1 Tris-acetate ethylenediaminetetraacetate (TAE) electrolyte buffer (50 x stock)

A 48.4 g of tris base was dissolved in 100 ml of water. A 7.44 g of EDTA disodium salt was dissolved in 50 ml of water and the pH was adjusted to 8.0 using sodium hydroxide This pH-adjusted EDTA solution was added to tris solution followed by the addition of 11.42 ml of glacial acetic acid. The volume was made up to 200 ml and the resulting buffer was stored at 4 ^{o}C.

2.5.1.2 Sample buffer (6X)

A 0.25% bromophenol blue in 40% sucrose/H_2O was used as the sample buffer. This buffer was prepared by first dissolving a 2 g of sucrose in 3 ml of water and by then adding a 12 5 mg of bromophenol blue to this

solution. The volume was made up to 5 ml. The resulting buffer was stored at 4 °C.

2.5.1.3 Ethidium bromide stock solution (10 mg/ml)

A 100 mg of ethidium bromide was dissolved in 10 ml of water by stirring in dark for several hours. The resulting solution was stored in a brown bottle at the ambient temperature. A working concentration of 0.5 μg/ml was used for staining the gel after electrophoresis.

2.5.2 Gel configuration and gel casting

A horizontal slab gel electrophoresis chamber for submerged mini gels obtained from Broviga Inc , India, (a 3 5 x 7.5 inches polystyrene snap-lock box) was used to carry out the agarose gel electrophoresis. Platinum wire was used for each of the two electrodes that are glued in place with silicone rubber cement. A platform composed of four lantern slides glued together in a stack is cemented in the center of the box. A gel plate of 7 cm X 10 cm in size rests on this platform so that the gel is submerged just beneath the surface of the electrophoresis buffer. The standard TAE buffer is used for the electrophoresis. The details of gel casting are given below.

A 400 mg of low-melt, fine quality agarose was added to 50 ml of TAE buffer. The slurry was then heated on a boiling-water bath until the agarose dissolved completely The solution was then cooled to 50 °C. Both ends of the gel mold was closed with a clean autoclaved tape and a small quantity of agarose solution was applied with a pasteur pipette along the edges of the gel mold so as to seal completely Remaining warm agarose solution was poured onto the gel mold and immediately the comb was clamped into position near one end of the gel The teeth of the comb formed

the sample wells Care was taken to see that at least 0.5-1.0 mm of agarose was left between the bottom of the teeth and the base of the gel, so that the sample wells are completely sealed. After 35-40 minutes (by which time the gel was completely set), the comb and the autoclaved tape were removed carefully and the gel was mounted in the electrophoresis tank A 200 ml of working buffer (TAE) was poured into the gel until the gel was covered to a depth of about 1mm.

2.5.3 Assay for photocleavage of DNA

In an Eppendorf tube, pBR 322 DNA (100 μM, per nucleotide) in tris-HCl buffer (pH 8.0) was mixed with an equimolar concentration of the porphyrin dissolved in the same buffer containing 10% V/V DMF in a total volume of 10 μl The mixture was then incubated for 1 h at 25 °C in the dark. Each solution thus prepared was transferred to a 2 mm diameter glass capillary for irradiation The samples were irradiated for 1 h with visible light ($\lambda > 400$ nm) using a 150 W xenon arc lamp (PTI Model A1010) The UV light was cut off by using appropriate UV filters and cold water was circulated in order to keep the temperature < 10 °C inside the capillary tube throughout the irradiation The irradiated solutions were then transferred to Eppendorf tubes containing 2 μl of 0 25% bromophenol blue in 40% sucrose/H_2O as sample buffer and were loaded onto a 0 8% agarose gel The gel was run with standard tris-acetate buffer, pH 8 0, at 40 V for 5 h, after which it was stained with a 0 5 μg/mL solution of ethidium bromide for 30 minutes The gel was then visualised under a UV trans-illuminator and was photographed with a 400 ASA (B/W) film using 35 mm SLR camera The negatives were quantitatively scanned with a UVP gel documentation system

GDS 2000. The DNA bands were read as integrated peak areas using the software package SW2000 Version 2.

The percentage of cleavage (C) was calculated using the expression[15]

$$C = \frac{[\text{Form II}] + 2[\text{Form III}]}{[\text{Form I}] + [\text{Form II}] + 2[\text{Form III}]} \times 100 \qquad (2.2)$$

Form I DNA, as supplied, was contaminated with approximately 15-20% of form II. The relaxation resulting from irradiation of DNA alone was always less than 5%.

2.6 General considerations

The geometry optimisation of the molecules was carried out by using molecular mechanics program PCM4 or PH4. Error estimation of the data, reconstruction of various spectra, calculations of equilibrium constants by the ^{1}H NMR method, various regression analysis etc. which appear throughout this dissertation, have been carried out on an IBM compatible PC 486 using the available in-house soft-ware

Care was taken to avoid the entry of direct, ambient light into the samples in all the spectroscopic and electrochemical experiments. Unless otherwise specified, all the experiments were carried out at 293 ± 3 K.

Care was taken to avoid the direct human contact of DNA and ethiduim bromide solutions. All solutions containing ethidium bromide and other hazardous chemicals were decontaminated before disposal. Protective

goggles and safety mask were used to minimise the exposure to obnoxious chemicals, ultraviolet light etc

Standard error limits involved in various measurements (unless otherwise stated).

λ_{max} (absorption/fluorescence)	± 1 nm
logε	± 10%
^{1}H NMR chemical shifts	± 0.01 ppm
ϕ_f	± 10%
ϕ_Δ	± 10%
$E_{1/2}$	± 0 03 V

2.7 Summary

A brief account of various solvents and chemicals used in this study is given in this chapter. Also given here is a description of spectroscopic and other physical methods employed in this study

2.8 References

1 *Vogel's text book of practical organic chemistry*, ELBS England, 1989

2 Perrin, D. D , Armanego, W L F , Perrin, D R *Purification of Laboratory Chemicals*, Pergamon Oxford, 1986

3 Austin, E , Gouterman, M *Bioinorg Chem* **1978**, 9, 281

4 Quimby, D. J.; Longo, F R *J Am Chem Soc* **1975**, 19, 5111

5 Demas, J. N.; Crosby, G A *J Phys Chem* **1971**, 75, 991

6 Murov, S. L., In *Handbook of Photochemistry*, Marcel Dekker New York, 1973

7. Lackowicz, J. R. *Principles of Fluorescence Spectroscopy;* Plenum: New york, 1983.
8. *Time-correlated Single Photon Counting;* O'Connor, D. V.; Philips, D. Academic Press: London, 1984.
9. Periasamy, N.; Doraiswamy, S.; Maiya, B. G.; Venkataraman, B. *J. Chem. Phys.* **1988**, 88, 1638.
10. Bevington, R. *Data Reduction and Analysis in Physical Sciences;* McGraw-Hill: New York, 1969.
11. Maniatis, T.; Fritsch, E. F., Sambrook, J. *Molecular Cloning A Laboratory Manual;* CSH. New York, 1984.
12. Fisher, M. P.; Dingman, C. W. *Biochemistry* **1971**, 10, 895.
13. Ajay, C ; Borst, P *Biochim Biophys. Acta* **1972**, 269, 192.
14. Sugden, P. A. B., Sambrook, J. *Biochemistry* **1973**, 12, 3055.
15. Kerwin, S. M. *Tetrahedron Lett.* **1994**, 35, 1023.
16. **Lindsey, J. S.; Brown, P. A.; Siessel, D. A.** ***Tetrahedron*** **1989**, 45, 4845.

CHAPTER 3

Photoinduced Electron Transfer in a Series of Porphyrin-Dinitrobenzene Dyad Molecules

3.1 Introduction

A great variety of donor-acceptor (D-A) compounds, in which a hydrocarbon or a porphyrin is covalently linked to an electron acceptor, have been synthesized and studied over the past few years [1,2] Examples of such D-A systems include covalently linked porphyrin-quinone systems which also serve as important models for the photoinduced electron transfer (PET) reactions which occur in photosynthetic reaction center complexes However, in order to gain more insight into the mechanisms of PET reactions, acceptors other than quinones have also been linked to porphyrins For example, polynitrobenzene,[3-5] alkyl and aryl viologen[6-14] and pyromellitic anhydride[15] subunits have been used as acceptors in porphyrin-based covalently linked D-A systems In many such compounds, the observed fluorescence quenching of the porphyrin fluorophore has been attributed to a PET reaction from the porphyrin donor to the appended acceptor

Several previous studies on porphyrin-based D-A systems have attempted to elucidate the effect of D-A distance and orientation on the rates of PET reactions [1,2,16-18] In the majority of such studies, a distance dependence of PET reactions has been unequivocally demonstrated On the other hand, possibly because of the problems involved in the synthesis of relevant model systems, studies concerning the orientation effects have been scarce [16-18] In this context it can be noted here that, in their elegant study, Sakata and coworkers have recently demonstrated an exclusive orientation

effect of the PET reactions in a series of porphyrin-quinone compounds in which the donor and the acceptor moieties are linked by rigid spacer/s.[17] On the other hand, conformational heterogeneity of porphyrin-acceptor dyads in which the donor and the acceptor subunits are held together by 'semi-flexible' linkages can be advantageously employed for a demonstration of the distance and orientation effects on the PET reactions.

This chapter describes the synthesis, characterisation and conformational control of the fluorescence quenching of a series of free base and zinc(II) porphyrins linked to dinitroaromatic acceptor units. The dinitrobenzene subunit has been linked at the ortho, meta or para position of one of the aryl groups of meso-5,10,15,20-(tetraphenyl)porphyrin (H_2TPP) or its zinc(II) derivative (ZnTPP) *via* an ester linkage (see scheme 3.1). A detailed analysis of both steady state and time-resolved fluorescence data suggests that a PET reaction is possible in the zinc(II) porphyrin series and that conformational control exists on the rates of PET reactions in these D-A dyads.

3.2 Experimental details

3.2.1 Synthesis of meso-5-(4-,3-, or 2-hydroxyphenyl)-10,15,20-triphenyl porphyrin (1a, 1b and 1c)

Pyrrole (2.68 g, 0.04 mol) was added to refluxing propanoic acid (500 ml) containing 3.18 g (0.03 mol) of benzaldehyde and 1.34 g (0.011 mol) of o-, m- or p-hydroxybenzaldehyde. The mixture was refluxed for 45 minutes and left overnight. The propanoic acid was removed from the reaction mixture under reduced pressure leaving behind a black-violet residue. It was washed with hot water, dried in air and chromatographed on basic alumina column using $CHCl_3$ as the eluent to remove H_2TPP. Mono-

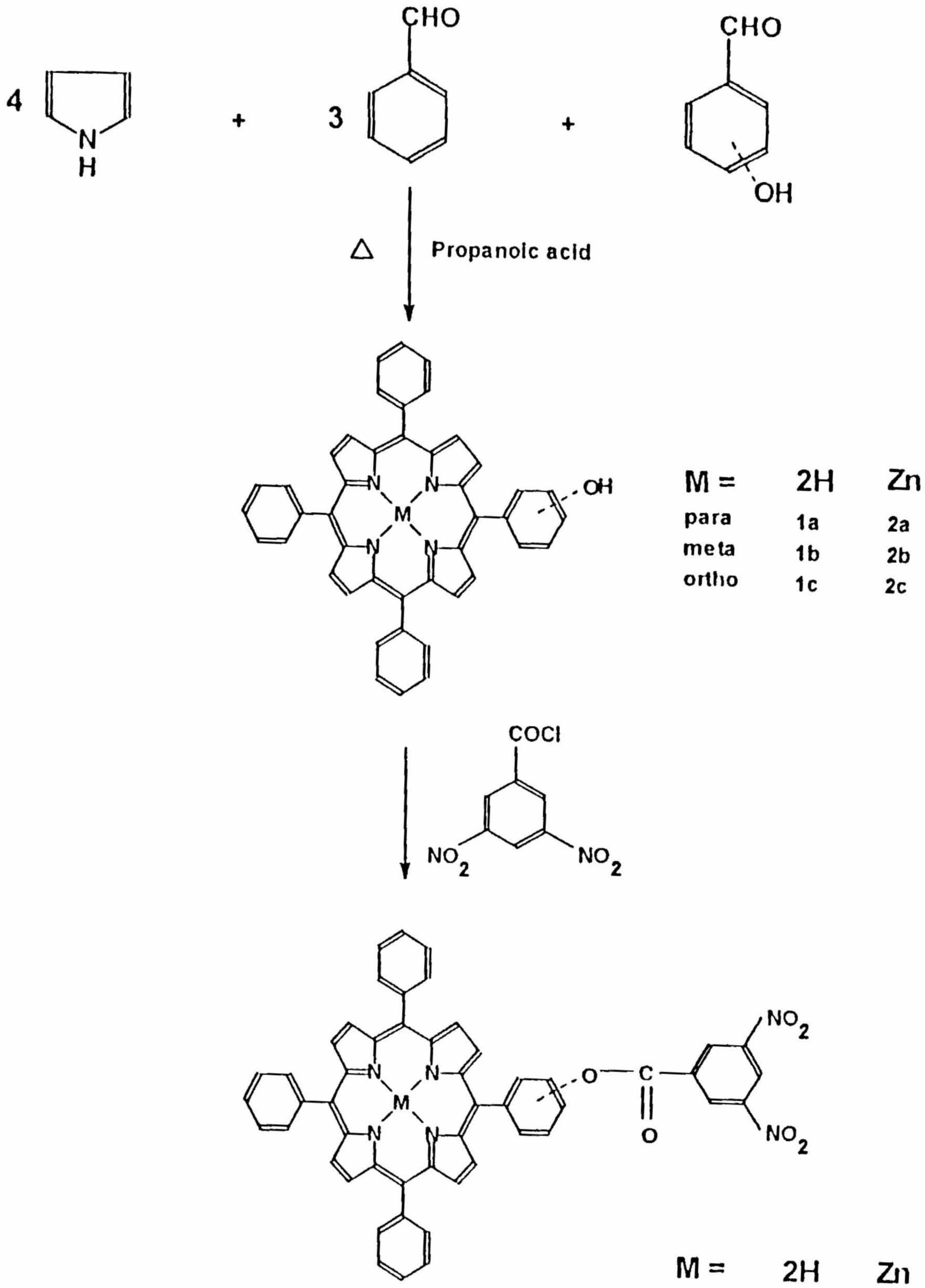
4
N
H
+
3
CHO
+
CHO
OH
Δ
Propanoic acid
N
N
M
N
N
OH
M = 2H Zn
para 1a 2a
meta 1b 2b
ortho 1c 2c
COCl
NO2
NO2
O
C
O
NO2
NO2
M = 2H Zn
para 3a 4a
meta 3b 4b
ortho 3c 4c

Scheme 3.1

(hydroxyphenyl)triphenyl porphyrin was eluted out of the column when $CHCl_3$-CH_3OH (95.5 V/V) was used as the eluent. Evaporation of the solvent under reduced pressure yielded a 0.25 g of the product in each case. Yield ≅ 10%.

UV-visible spectral data in $CHCl_3$: λ_{max} , nm (log ε)

1a : 418 (5.63), 515 (4.21), 550 (3.90), 590 (3.72), 648 (3.70).

1b : 417 (5 57), 514 (4.17), 549 (3.79), 588 (3.66), 646 (3.64)

1c : 417 (5 59), 514 (4.21), 549 (3.77), 588 (3.69), 645 (3.43)

3.2.2 Synthesis of meso-5-(4-,3- or 2-hydroxyphenyl)-10,15,20-tri- phenyl porphyrinato zinc(II) (2a, 2b, and 2c)[20]

A solution of **1a-c** (0 1 g, 0 16 mmol) in 50 ml of $CHCl_3$ was added to a solution of zinc(II)acetate tetrahydrate (0.2 g, 0.78 mmol) in 5 ml of methanol and the resulting mixture was refluxed for 1h. The progress of the reaction was monitored spectrophotometrically At the completion of the reaction, the solvent was evaporated and the residue dissolved in a minimum volume of $CHCl_3$ and was loaded on an alumina column. Eluting with $CHCl_3$-CH_3OH (95:5 V/V) and evaporating the solvent gave almost quantitative (> 95%) yield of the desired zinc(II) porphyrins.

UV-visible spectral data in $CHCl_3$: λ_{max} , nm (log ε)

2a : 420 (5.70), 548 (4 21)

2b : 421(5.66), 549 (4 09)

2c : 420(5.56), 549 (4 31)

3.2.3 Synthesis of meso-5-(4-, 3-, or 2-(3,5-dinitrobenzoyl)phenyl) 10, 15,20-triphenyl porphyrin (3a, 3b or 3c)

Either **1a**, **1b** or **1c** (0.1 g, 0.16 mmol), 3,5-dinitrobenzoyl chloride (0.1 g, 0.46 mmol) and pyridine (≅0 2 ml, as catalyst) were dissolved in 15 ml of dry CH_2Cl_2 and the mixture was stirred for 2 h at 25 °C The solvents were evaporated and the residue redissolved in 10 ml of $CHCl_3$. It was loaded onto an alumina column and eluted with $CHCl_3$. The fast moving first fraction was collected and was identified as the desired product in each case (yield ≅ 50%) .

All the isomeric D-A porphyrins gave identical CHN data: (obsd.) C, 73.90; H, 3.88; N, 9 94. Calcd for ($C_{51}H_{32}N_6O_6$) C, 74.3; H, 3.88, N, 10.19 Their UV-visible and proton nuclear magnetic resonance (^{1}H NMR) spectral data are summarised in Tables 3.1 and 3.2, respectively.

These free base porphyrins were converted to their zinc(II) derivatives (**4a-c**) using a procedure similar to that described above for **2a-c**.[20]

For the time-resolved fluorescence experiments the excitation wavelength used was typically 585 nm, corresponding to the Q band of the zinc porphyrins, and the fluorescence was collected at 600 nm Typical concentrations of the porphyrins ranged between 5 x 10^{-5} and 10^{-6} M Analysis of the lifetime data was carried out as described in chapter 2.

Each investigated porphyrin was purified on a short alumina column before spectral measurements were made. All the spectroscopic and electrochemical experiments have been carried out as described in chapter 2

3.3 Results and discussion

3.3.1 Ground state properties

The UV-visible spectra of ZnTPP and **4b** are given in Fig 3 1 and the λ_{max} and log ε values of each synthesized porphyrin are given in Table 3 1.

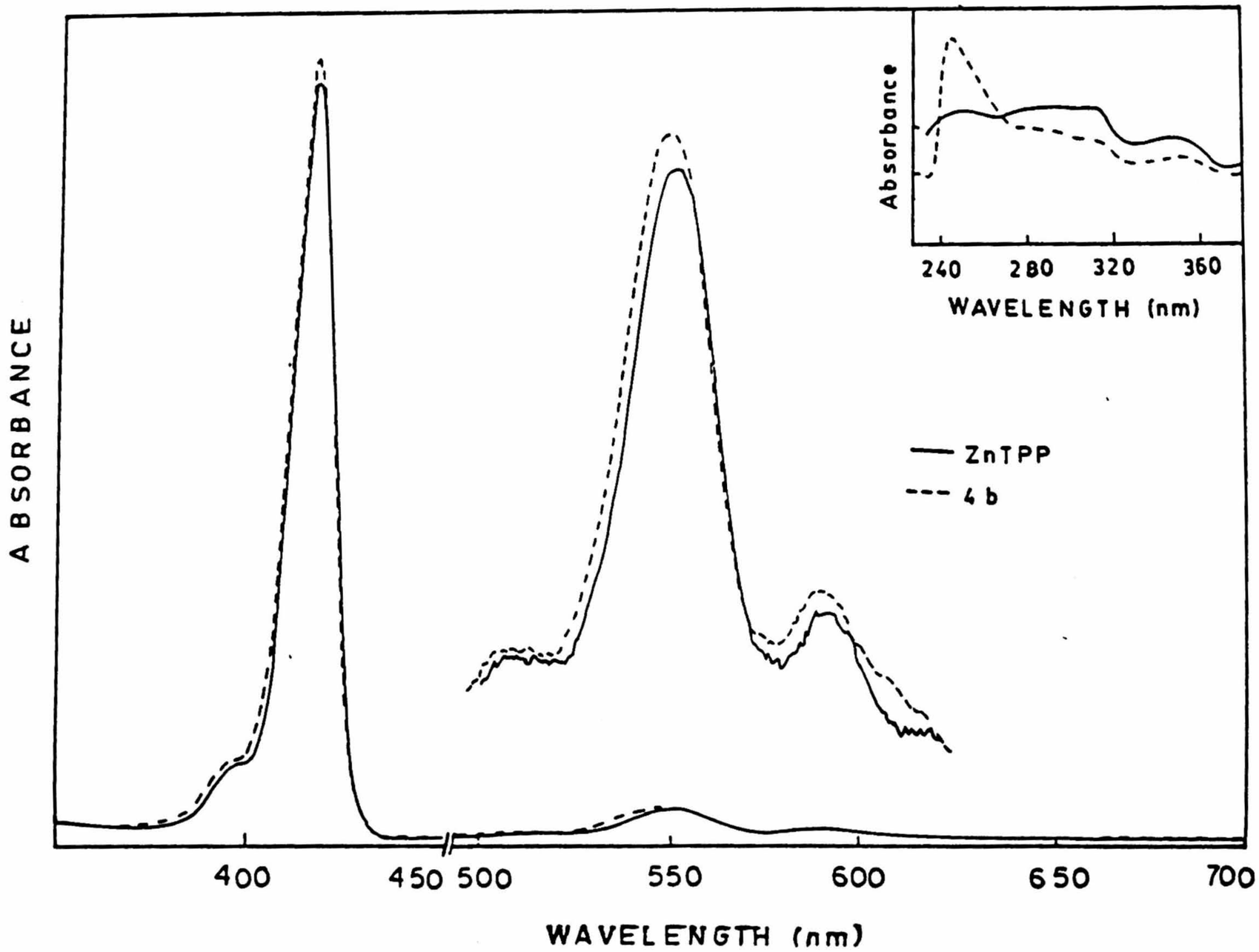

Fig. 3.1. UV-visible spectra of ZnTPP (———) and 4b (-------) in CH_2Cl_2. The inset shows the spectra in the UV region.

Table 3.1 UV-visible data in CH_2Cl_2

Compound	λ_{max}, nm (log ε)					
	Porphyrin transitions					Nitroarene transition
	Q_1	Q_2	Q_3	Q_4	B	
H_2TPP	644 (3 44)	587 (3 61)	548 (3 76)	510 (4 13)	416 (5 56)	—
3a	648 (3 40)	590 (3 49)	549 (3 63)	514 (3 97)	415 (5 36)	236 (5 52)
3b	645 (3 42)	587 (3 42)	547 (3 56)	510 (3 93)	417 (5 34)	236 (5.47)
3c	643 (3 34)	586 (3 60)	546 (3 67)	512 (4 10)	415 (5 49)	236 (5 59)
ZnTPP	—	584 (3 51)	549 (4 23)	—	419 (5 67)	—
4a	—	584 (3 45)	547 (4 26)	—	419 (5 69)	246 (4 45)
4b	—	585 (3 48)	547 (4 23)	—	419 (5 67)	247 (4.43)
4c	—	586 (3 46)	548 (4 24)	—	419 (5 65)	247 (4 50)
3,5-DNBC[a]	—	—	—	—	—	228 (4 32)

(a) 3,5-DNBC 3,5-dinitrobenzoyl chloride

Inspection of Fig 3.1 and Table 3.1 reveals that, within experimental error, the λ_{max} and log ε values of the D-A systems are similar to or marginally different from those of the individual donor and acceptor components. For example, Fig. 3.1 shows that theλ_{max} values of the D-A porphyrins are not considerably shifted from those of ZnTPP. The data given in Table 3.1 shows that the log ε values of the D-A porphyrins are slightly lower than those of the individual components. Furthermore, the full width at half-maximum *(fwhm)* values of Soret bands of the D-A porphyrins are broadened by about 2-4 nm compared with the corresponding values of the non-linked porphyrins. Interestingly, maximum broadening is observed for the ortho isomer **3c**.

The ^{1}H NMR spectral data of the H_2TPP-based D-A compounds (**3a-c)** are summarised in Table 3 2 Peaks at 8 84-8.88 ppm (m), 8 15-8 26 ppm (m) and 7.76-7 79 ppm (m) in the three spectra correspond to the porphyrin β -pyrrole, o-phenyl and p- and m-phenyl proton resonances, respectively These peak positions are similar to those found for the corresponding proton resonances in the hydroxyporphyrins or H_2TPP (Table 3 2).[24] The -NH (imino) proton resonance positions of the D-A porphyrins (-2.85 to -3.04 ppm) can be compared with those of the corresponding parent hydroxyporphyrins or with that of H_2TPP which occurs at -2.80 ppm.[4,24] Conceivably, -NH protons of the D-A porphyrins experience the ring current of the dinitroaromatic moiety and thus their resonances are shifted upfield. This supposition is further substantiated by the ^{1}H NMR signal positions of the acceptor protons. The proton resonances of 3,5-dinitrobenzoyl chloride appear at 9 28 ppm (m) The same proton resonances appear at 9 22 ppm (m), 8.55 ppm (m) and 7.92 ppm (m) for **3a**, **3b** and **3c**, respectively. The acceptor protons of the D-A compounds experience a large ring current effect of the porphyrin and hence appear at a more upfield shifted position

Table 3.2 ^{1}H NMR data in $CDCl_3$ (TMS)

Compound	δ (ppm)				
	Porphyrin protons				Acceptor protons
	β-pyrrole	o-phenyl	m- & p-phenyl	-NH	2,4,6-phenyl
H_2TPP	8 83 (s, 8H)	8 36 (m, 8H)	7.86 (m, 12H)	-2 80 (s, 2H)	—
3a	8 88 (m, 8H)	8 26 (m, 8H)	7 79 (m, 11H)	-2 85 (s, 2H)	9 22 (m, 3H)
3b	8 87 (m, 8H)	8 24 (m, 8H)	7.77 (m, 11H)	-3 00 (s, 2H)	8 55 (m, 3H)
3c	8 84 (m, 8H)	8 15 (m, 7H)	7.76 (m, 12H)	-3 04 (s, 2H)	7 92 (m, 3H)
3,5-DNBC[a]	—	—	—	—	9 28 (m, 3H)

(a) 3,5-DNBC 3,5-dinitrobenzoyl chloride

than when they are not linked to the porphyrin

It is well known that intermolecular interaction of H_2TPP (or ZnTPP) with nitroaromatic acceptors shifts the λ_{max} values, reduces the log ε values and alters the ^{1}H NMR spectral peak positions of the porphyrin [25 26] These

spectral changes have been interpreted in terms of π-π interactions between the porphyrin and the nitroaromatic acceptor. On the basis of the similarities found between the spectral data of the D-A porphyrins investigated in this study and the intermolecular complexes of porphyrins with nitroaromatic acceptors, it can be suggested that weak π-π interactions exist in these linked porphyrin-nitroarene systems. However, the data on these ester-bridged isomeric D-A compounds do not suggest any trend in the magnitudes of the π -π interactions as observed previously for the ether-linked porphyrin-nitroarene systems.[3,4] The -NH proton resonance position and the broadening of the Soret band found for the ortho isomer **3c** suggest that the intramolecular D-A interaction is at a maximum in this case.

The cyclic voltammograms (CH_2Cl_2, 0.1 M TBAP) of ZnTPP and the three ZnTPP-based D-A systems **4a-c** are given in Fig. 3.2 and redox potentials of all the investigated systems are summarised in Table 3.3 As shown in Fig 3.2, ZnTPP undergoes a reversible, one-electron oxidation at 0.80 V (with respect to SCE) and a reversible one-electron reduction at -1.35 V (E_{pa}-E_{pc} = (60 ± 5) mV, i_{pa}/i_{pc} = 0 9-1.0 and $i_p/\gamma^{1/2}$ values are constant in the scan rate (γ) range 50-500 mV s^{-1}). Both of these electron transfer reactions are known to involve the porphyrin ring.[27] The three D-A porphyrins show a reversible oxidation at 0 81 V and a quasi-reversible reduction (E_{pa}-E_{pc} = 80 - 100 mV i_{pa}/i_{pc} = 0.7-0 9 in the scan rate range 50-500 mV s^{-1}) in the potential range -0.73 to -0.78 V. The oxidation peaks for these porphyrins occur at potentials similar to the oxidation potential of ZnTPP and hence they are ascribed to electron abstraction from the porphyrin macrocycle. However, the reduction reactions of the D-A compounds occur close to the potentials at which either 1,3-dinitrobenzene (1,3-DNB) or 3,5-dinitrobenzoic acid (3,5-DNBA) (or the acid chloride, 3,5-DNBC) are

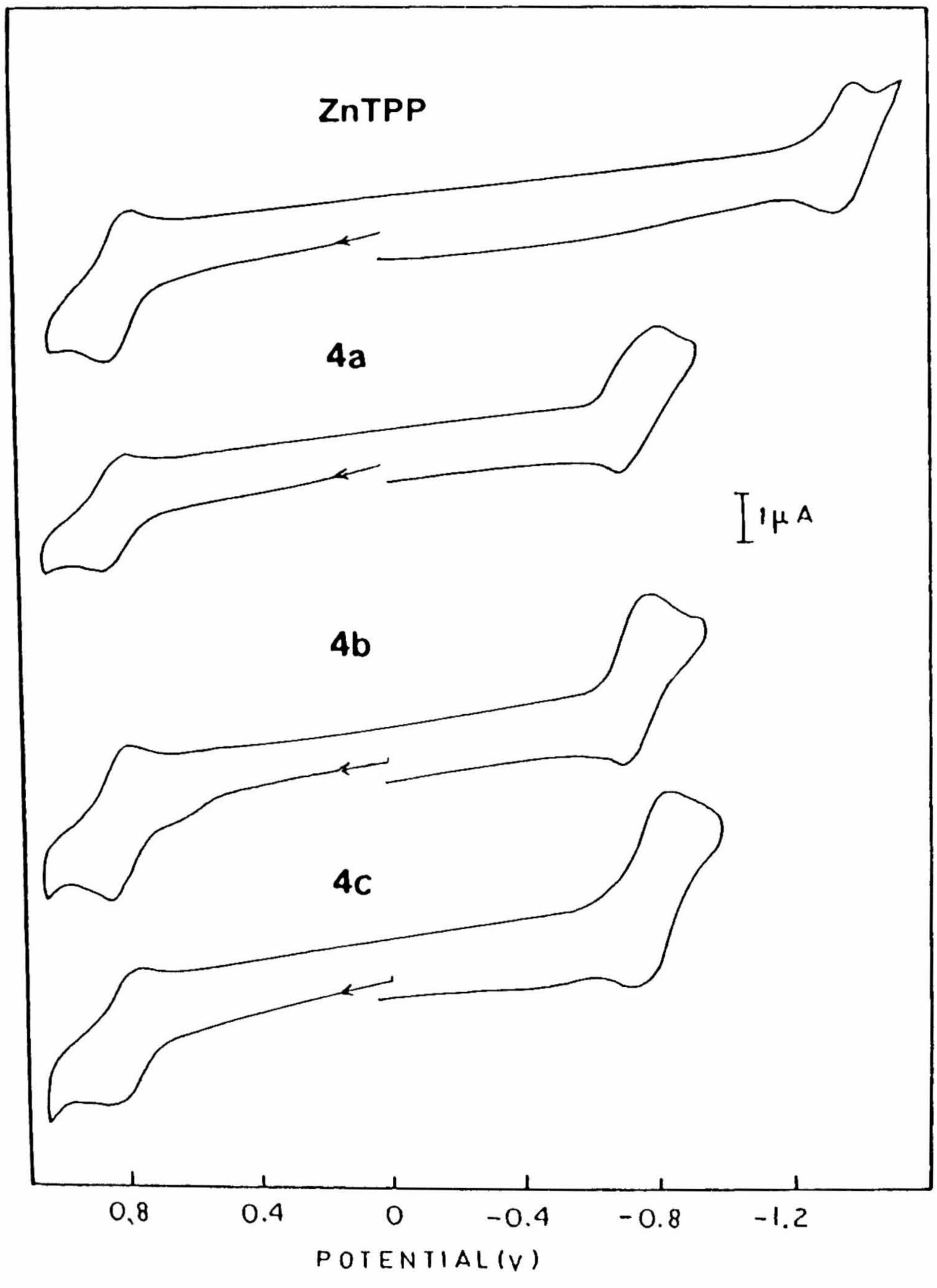

Fig. 3.2. Cyclic voltammograms (scan rate, 100 mV s^{-1}) of ZnTPP, **4a**, **4b** and **4c** in CH_2Cl_2, 0 1 M TBAP The potential axis is referenced with respect to SCE

reduced under similar experimental conditions (see Table 3.3). Therefore, the reduction of these ZnTPP based D-A porphyrins involves electron addition to the dinitroaromatic subunit. A similar interpretation can be made of the redox potential data of **3a-c**. The E_{CT} values (i.e the difference between the potentials of porphyrin oxidation and dinitroaromatic unit reduction or energy of the P^+-DNB^- state) have been calculated using the redox potential data and they are given Table 3 3

Table 3.3 Redox potential, E_{CT} and ΔG_{PET} data in CH_2Cl_2

Compound	**P → P+** (V)	**P → P-** (V)	**E_{CT}** (eV)	**ΔG_{PET}** (eV)
H_2TPP	1 06	-1 19	—	—
3a	1.09	-0 71	1 80	-0.09
3b	1 09	-0 71	1 80	-0 09
3c	1 13	-0 73	1 86	-0.03
ZnTPP	0 80	-1 35	—	—
4a	0 81	-0 73	1 54	-0 53
4b	0.81	-0 78	1 54	-0.53
4c	0.81	-0 78	1.59	-0.47
1,3-DNB	—	-0 84	—	—
3,5-DNBA	—	-0 91	—	—
3,5-DNBC	—	-0 97	—	—

Error limits: E_{CT} and ΔG_{PET}, ± 10%

3.3.2 Singlet state properties

3.3.2.1 Steady state flourescence

The fluorescence emission and excitation spectra of **3a-c** and **4a-c** are similar in shape to the corresponding spectra of H_2TPP or ZnTPP.[28] The λ_{max} and *fwhm* values of these D-A porphyrins are also within ± 2 nm of the corresponding values of H_2TPP or ZnTPP (see Fig. 3.3). This observation together with the fact that the absorption spectra of the D-A porphyrins are similar to the absorption spectra of the non-linked analogues suggest that E^s (0-0 spectroscopic transition energy or energy of the singlet excited state) values of the D-A porphyrins are not significantly different from those of the non-linked porphyrins. Thus, using the reported values of E^s of ZnTPP or H_2TPP[29] and the E_{CT} values taken from Table 3.3, free energy changes for the PET reactions (ΔG_{PET}) originating from the singlet excited states of these D-A porphyrins have been calculated using eq. 3.1.

$$\Delta G_{PET} = E_{1/2}^{ox} - E_{1/2}^{red} - E^s \qquad (3.1)$$

where $E_{1/2}^{ox}$ and $E_{1/2}^{red}$ are the oxidation potential of the donor and reduction potential of the acceptor, respectively. The ΔG_{PET} values for **3-c** are in the region (-0.06 ± 0.03) V and those of **4a-c** are in the region (-0.50 ± 0.03) V. Clearly, the more negative values for **4a-c** suggest that PET reactions from their singlet excited states are thermodynamically allowed

Quenching of porphyrin fluorescence has been observed in these isomeric D-A dyads. This is illustrated in Fig 3.3 where the fluorescence spectra of H_2TPP (Fig. 3.3a) and ZnTPP (Fig 3.3b) have been compared with those of the corresponding D-A systems. Relative fluorescence quantum yields (ϕ_f) have been calculated for each porphyrin in five different solvents

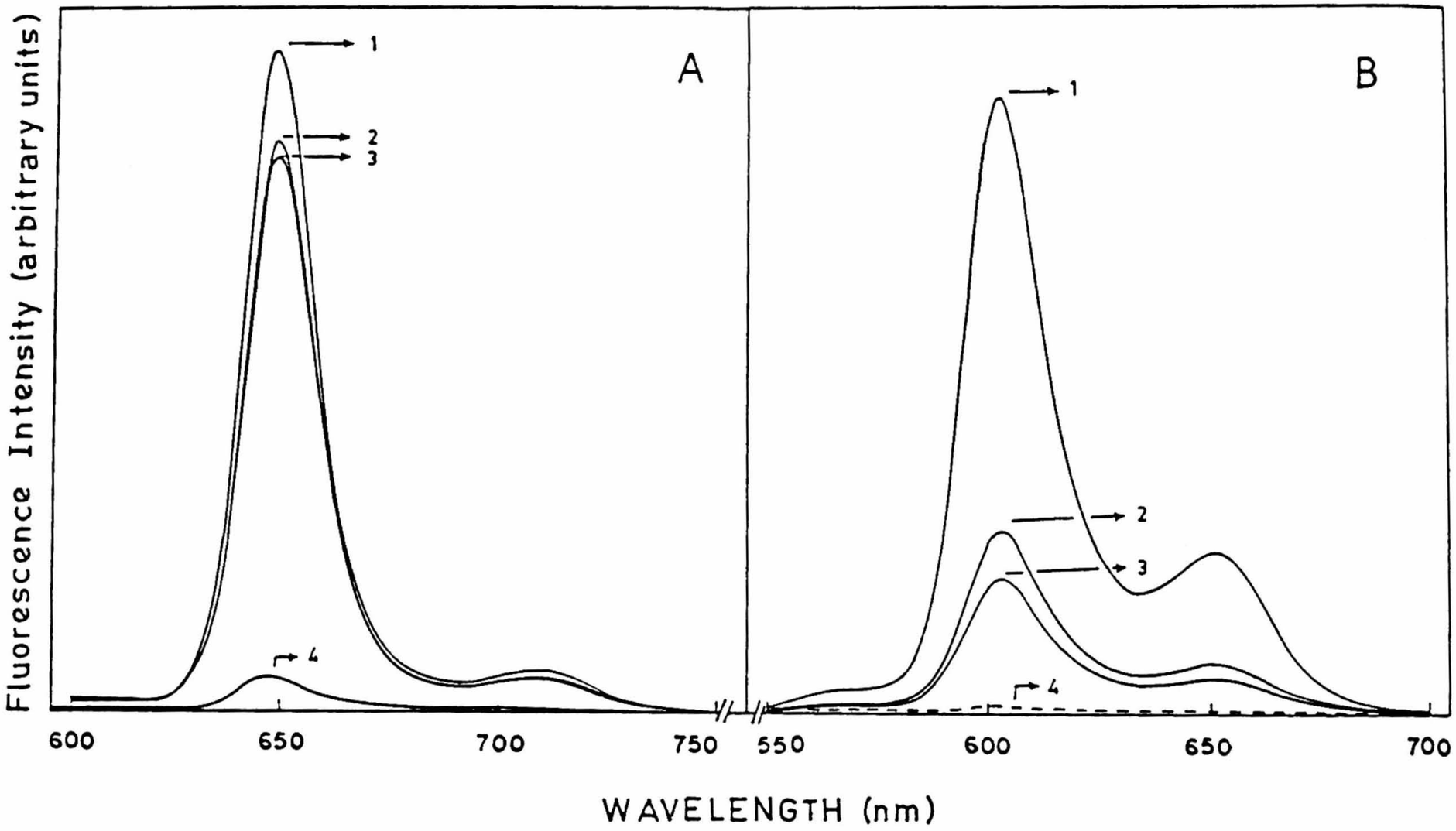

Fig.3.3. Fluorescence emission spectra. (A) H_2TPP (1) , **3b** (2), **3a** (3) and **3c** (4) in dimethylsulfoxide. (B) ZnTPP (1), **4b** (2), **4a** (3) and **4c** (4) in

using either ZnTPP or H_2TPP as the standard (ϕ_f taken to be unity) An inspection of Fig 3 3 and the quantum yield data summarized in Table 3 4 suggests that

i) fluorescence quenching is minimal for **3a** and **3b**,

ii) decrease in ϕ_f values is more pronounced for **4a-c** compared to that for **3a-c** in each investigated solvent, and

iii) in each solvent, ϕ_f values vary with respect to the site of attachment of the acceptor subunit to the donor porphyrin as **(4b)3b** > **(4a)3a** > **(4c)3c**.

Table 3.4 Steady state fluorescence data in various solvents [a,b]

Compound	**Toluene**		**CH_2Cl_2**		**Acetone**		**CH_3CN**		**DMSO**	
	λ_{max} (nm)	**ϕ_f**	**λ_{max} (nm)**	**ϕ_f**	**λ_{max} (nm)**	**ϕ_f**	**λ_{max} (nm)**	**ϕ_f**	**λ_{max} (nm)**	**ϕ_f**
H_2TPP	649	1 00	640	1 00	646	1 00	646	1 00	648	1 00
3a	650	0 94	648	0 81	648	0 93	648	0 80	650	0 81
3b	650	1 20	648	0 80	648	1 20	648	1 12	650	0 87
3c	648	0 37	648	0 04	646	0 06	646	0 03	648	0 05
ZnTPP	596	1.00	601	1 00	600	1 00	603	1 00	605	1 00
4a	596	0 92	593	0 16	600	0 18	604	0 22	605	0 12
4b	596	0 88	592	0 19	601	0 24	604	0 30	605	0 15
4c	595	0 02	592	0 01	600	0.01	604	0 01	605	0 01

(a) ϕ_f values of ZnTPP and H_2TPP were taken to be unity in each solvent and the ϕ_f values of D-A systems were estimated relative to these values

(b) Less intense bands at about 710 nm and 645 nm were observed for H_2TPP- and ZnTPP-based systems, respectively

Electronic energy transfer, exciplex formation and PET reactions can be perceived as possible pathways of fluorescence quenching in these systems. There is no spectral overlap between the emission of the porphyrin and the absorption of the nitroaromatic acceptor and hence, electronic energy transfer from the porphyrin to the acceptor cannot contribute to the observed quenching in these D-A systems. Similarly, the fluorescence spectra show no evidence for emission from an exciplex. Nonetheless, the possibility of the formation of a non-fluorescent exciplex in these systems cannot be ruled out.

Supportive, but not unequivocal, evidence for the participation of an electron transfer quenching in these isomeric systems comes from the on-line irradiation/electron paramagnetic resonance (EPR) method.[30] On-line visible light irradiation of CH_2Cl_2 solutions of the zinc (II) derivatives **4a-c** in an EPR cavity at (100 ± 3) K gave featureless broad signals which disappear when the light source is turned off. A representative spectrum is illustrated in Fig. 3.4. The g values of the signals are (2 0033 ± 0.0002) and $\Delta H_{p.p}$ (peak-to-peak width) values are (0 6 ± 0.1) mT. A change of temperature and/or the EPR spectrometer settings did not seem to improve the quality of the signals, thus restricting a detailed interpretation of the spectra to the 'structure' of the species responsible for them. However, it should be noted that ZnTPP, H_2TPP and free-base compounds **3a-c** all did not give EPR signals under similar experimental conditions. Therefore, the signals obtained only for the ZnTPP-based isomeric porphyrins **4a-c** can be ascribed to the photoproduced $ZnTPP^+$ -DNB^- radical-ion pairs EPR characterisation of the photoproduced radicals in porphyrin-nitroarene[3] and porphyrin-quinone systems[30,31] has been carried out previously. Thus, the fluorescence and EPR data of the compounds **4a-c** can be rationalised in terms of a PET reaction occurring in these systems.

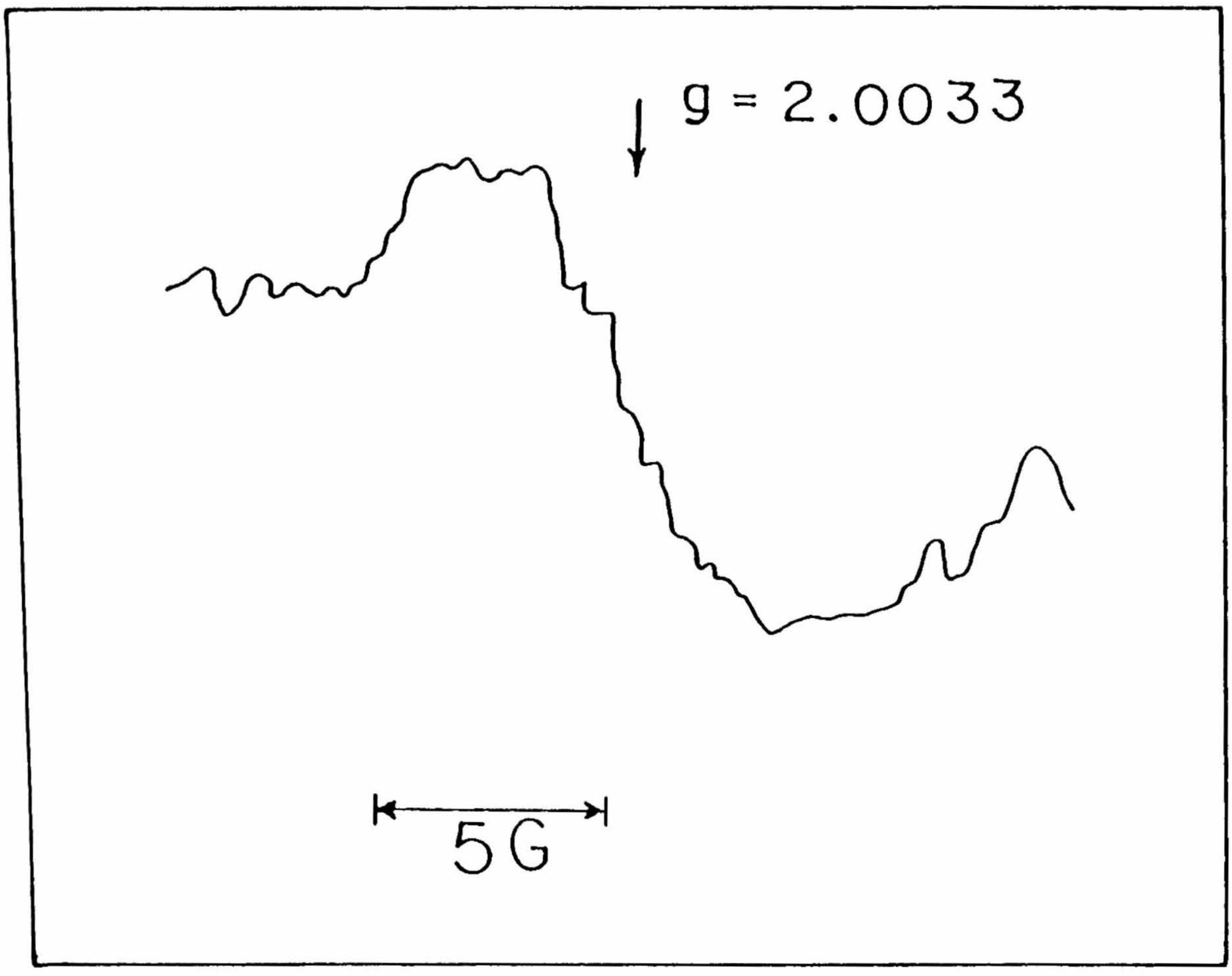

Fig. 3.4. EPR spectrum of the light-generated (λ_{irr} > 400 nm) radical in CH_2Cl_2 observed for **4a** (5 x 10^{-4} M) at (100 ± 3) K EPR settings: time constant 0.064s; scan time 4 min, modulation frequency, 100 kHz, modulation amplitude, 0.2 mT, microwave power, 2mW; microwave frequency, 9.046 GHz.

For compounds **3a-c**, ΔG_{PET} values are more positive and hence PET reaction is expected to be weak. Accordingly, as far as **3a** and **3b** are concerned, the fluorescence quenching is minimal (see Table 3.4). However, the case of **3c** seems to be complex. The centre-to-centre *(ctc)* distance between the donor and the acceptor (R_{DA}) is less for this ortho isomer than for the other two *(vide infra)* and it is possible that a PET reaction may contribute more to the quenching of **3c** than to **3a** or **3b**. On the other hand, PET reaction is more endoergic in the ortho isomer than in the meta and para isomers as suggested by the ΔG_{PET} values (see Table 3.3). Thus, the observed quenching (maximum, about 97%) in **3c** is far stronger than that which can be reconciled by the supposition that the PET reaction is the only mechanism of quenching in this D-A system Intermolecular quenching of H_2TPP by several nitroaromatic acceptors is known to involve mechanisms such as π-π interaction, hydrogen bonding, etc.[25,26] In view of this it can be expected that, in addition to a weak PET reaction, mechanisms such as π-π interaction, hydrogen bonding, etc might be involved in the fluorescence quenching of **3c**.

3.3.2.2 Time-resolved fluorescence

Time-resolved fluorescence data were obtained only for the zinc(II) porphyrin-based D-A systems for which the ΔG_{PET} values suggest an exoergic PET reaction

The fluorescence decay curves for compounds **4a-c** in toluene are shown in Fig 3.5. The time-resolved fluorescence data of ZnTPP and the three investigated isomeric D-A compounds in five different solvents are given in Table 3.5

001806

Jadia Gandhi Memorial Library ★ University of Hyd-34 ★

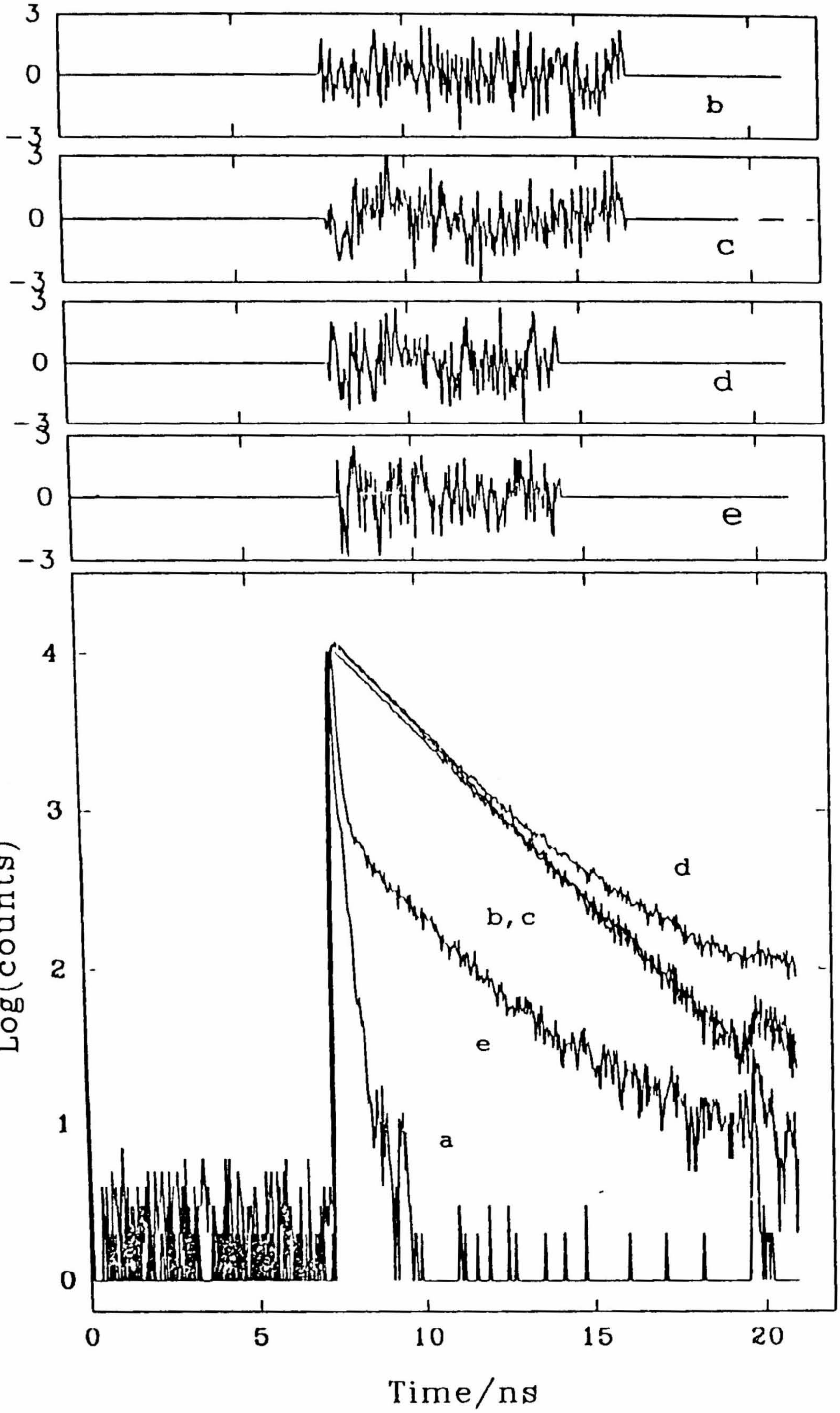

Fig. 3.5. Time-resolved fluorescence decay curves for ZnTPP (b), **4a** (c), **4b** (d) and **4c** (e) in toluene. Trace (a) shows the instrument response function.

Table 3.5 Fluorescence decay parameters of ZnTPP and ZnTPP-based isomeric D-A porphyrins in various solvents.

Porphyrin	Toluene		CH_2Cl_2		Acetone		CH_3CN		DMSO	
	A_i (χ^2)	τ_i (ns)	A_i (χ^2)	τ_i (ns)	A_i (χ^2)	τ_i (ns)	A_i (χ^2)	τ_i (ns)	A_i (χ^2)	τ_i (ns)
ZnTPP	1.00 (1 02)	1 96	1 00 (1 10)	1.69	1 00 (1 16)	2 05	1 00 (1.14)	1 91	1 00 (1.08)	1 91
4a	1 00 (1.11)	1.94	0 97 0 03 (1 23)	0 40 1 53	0.98 0 02 (0 97)	0 80 2 03	0 87 0 13 (1 18)	0 81 1 93	0.97 0.03 (1.17)	0.34 1.74
4b	0 28 0.72 (1 22)	1.53 2 15	0.98 0 02 (1 40)	0.46 2.27	0 84 0 16 (1 37)	0.84 2 24	0.84 0.16 (1 20)	0 84 2.09	0.98 0 02 (1.17)	0.47 2.15
4c	0.94 0 06 (1.26)	0.24 2 12	0.37 0 56 0.07 (1.21)	0.26 1 42 2.10	0 73 0 20 0 07 (1.24)	0.05 1.48 2.77	0.63 0 30 0.07 (0.96)	0 06 1 66 2 18	0.75 0 21 0.04 (1.04)	0 09 1.40 2.27

(a) Analysis using a three-exponential decay did not improve the quality of fit in these cases.

A single-exponential decay function given by

$$f(t) = A \exp(-t/\tau) \qquad (3.2)$$

was found to be adequate to describe the decay of ZnTPP in each solvent and **4a** in toluene. For all other cases, where values of A_i and τ_i (i = 2 or 3) are given, a two- or three- exponential decay function

$$f(t) = \Sigma A_i \exp(-t/\tau_i) \qquad (3.3)$$

has been used since the fit for a single-exponential decay was clearly inadequate. A three-exponential fit was necessary only for **4c** and the fractional amplitude of one of the three components was very low in this case (4-7%).

The intramolecular D-A compounds studied in this work are linked by 'semi-rigid' ester bridges. This gives rise to a flexibility of the distance and orientation of the acceptor with respect to the porphyrin plane and permits the possibility of several conformations. In these conformations, the D-A distances and their mutual orientations may be different. In principle, the excited state reaction coefficients for each of these conformations may differ.

Thus, it is possible that a class of conformations exist in which both the *ctc* distances and relative D-A orientations are favourable for efficient quenching, such conformations can be termed "closed" conformations. Other conformations in which D-A distances and orientations are not as conducive for efficient quenching can be termed "extended" (or "open") conformations. Furthermore, it is also possible that each of these two classes of structure may exist as an ensemble of several physical conformations which are related by slight modification of the structure.[32] Such a model, in which several non-

equilibrating conformations exist within the lifetime of the fluorophore, leads to the following predictions.

i) in cases in which only "extended" conformers exist, the fluorescence decay can be fitted to a single-exponential function and the lifetime of the donor in the D-A compound will be similar to that of the free donor subunit.

ii) in cases in which both "closed" and "extended" conformers coexist, the fluorescence decay can be fitted to a multiexponential (usually biexponential) equation. As, by definition, the *ctc* distances and orientations are conducive for efficient quenching in "closed" forms, the rate coefficients are larger compared to those of the corresponding "extended" forms.

In several previous studies on intramolecular D-A systems with flexible linkages, the fluorescence decay data have been interpreted using a model which predicts multiexponential behaviour as described above. Analysis of the data given in Table 3 5 reveals that this model can be fitted to the decay of **4a-c** described in this study. Therefore, the following observations can be made.

i) **4a** exists as an "extended" form in toluene and shows a single-exponential decay with a lifetime close to that of ZnTPP.

ii) The shorter lifetime components observed in the biexponential decays of **4a** in solvents other than toluene, of **4b** in all the solvents and of **4c** in toluene correspond to the "closed" forms. The longer lifetime components in these cases correspond to the "extended" forms of the compounds. The fractional

amplitudes of the "closed" forms are large in both meta and para isomers compared with those of the "extended" forms.

iii) For **4c**, in solvents other than toluene, a three-exponential fit, with two lifetimes shorter than that of ZnTPP and a lifetime similar to that of ZnTPP, was found. In this case, two distinctly different "closed" forms could coexist, both of which show shorter lifetimes than that of ZnTPP The component having a lifetime close to that of ZnTPP could then be ascribed to the "extended" form of the compound However, the amplitude of this component is very small which suggests that, owing to the conformational architecture of the complex, the acceptor moiety is forced to be in close proximity to the donor in this ortho-linked compound

3.3.2.3 Conformational effects

In order to get more insight into the possible structures of the conformers in the three isomeric D-A systems, molecular mechanics calculations were carried out[38] Structures were minimised for **3a-c** and the lowest energy structures obtained for the three cases are shown in Fig 3 6 The *ctc* distances for the conformers shown in Fig 3 6 are 6 54, 11 47 and 12 53 A° for the ortho, meta and para isomers, respectively Similarly, the dihedral angles 1 2 3 4 (see Fig 3 6) are 41 86°, 162 38° and 141 79° for the three isomers Intuitively, it can be suggested that these lowest energy conformers having the closest D-A approach represent the "closed" conformers

From the steady state fluorescence quenching results, it can be expected that PET reaction provides a major contribution to the decrease in the fluorescence lifetimes of **4a-c** The observed multiexponential

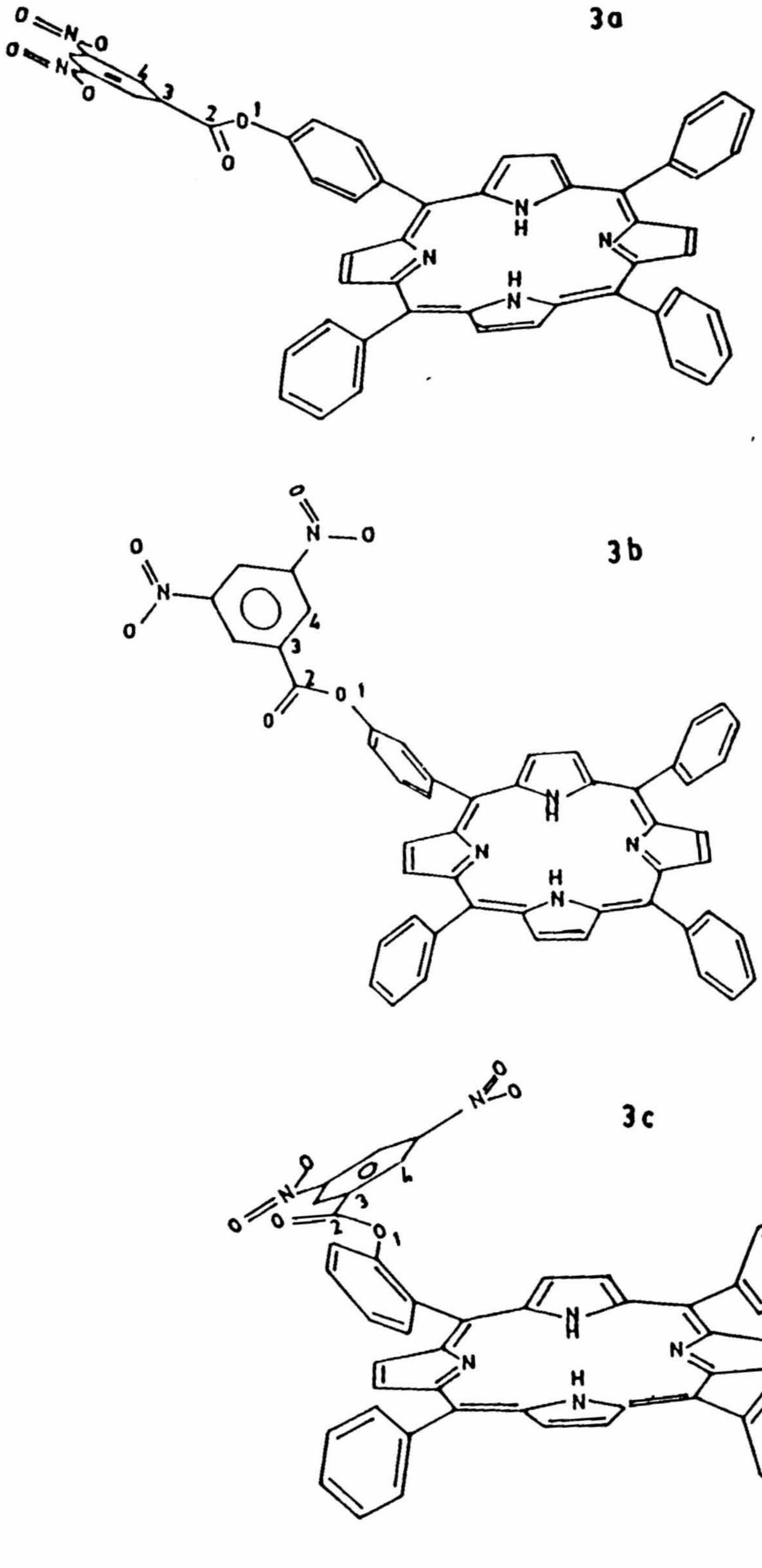

Fig. 3.6. Minimum energy conformations of the D-A systems as derived from the MMX calculations

fluorescence decay and the structures generated by molecular mechanics calculations permit an evaluation of the influence of D-A distance and orientation on the rates of electron transfer reactions in these systems.

The dependence of electron transfer on the D-A separation distance (r) is given by

$$k_{et} = \gamma \exp(-\beta r) \qquad (3.4)$$

where γ (s^{-1}) depends on the energetics of the reaction, including the Franck-Condon factors, and β (A^{o-1}) is a function of the overlap integral of the wavefunctions of the donor and acceptor orbitals.[33] Orientation effects have also been studied theoretically using a variety of models.[34,35] For aromatic D-A pairs, it has been shown that the D-A orientations can influence the electronic matrix element for a non-adiabatic electron transfer, by and large, coplanar mutual orientations favour rapid electron transfer

The relevant rate constant (k_{et}^{TR}, obtained by time-resolved fluorescence data) for intramolecular electron transfer between the singlet excited state of the porphyrin and the appended dinitroaromatic moiety in the isomeric D-A systems has been calculated using eq 3 5

$$k_{et}^{TR} = \tau^{-1} - \tau_0^{-1} \qquad (3.5)$$

where, τ_0 is the lifetime of the longer lived component and τ is the shortest lifetime observed in the multiexponential decay for the D-A compounds in each solvent (Table 3 5) The k_{et}^{TR} values thus calculated for the "closed" forms of the systems are given in Table 3.6

Table 3.6 ΔG_{PET}corr values and PET rate constants as derived from time resolved (k_{et}^{TR}) and steady-state (k_{et}^{SS}) fluorescence methods **4a-c**[a]

	4a	**4b**	**4c**
	Toluene (ε=2.38)		
ΔG_{PET}^{corr}(eV)	0:27	0.20	-0.18
k_{ct}^{TR} (x 10^{-9})	b	0.19	3.70
k_{ct}^{SS} (x 10^{-9})	0 05	0.06	25.0
	CH_2Cl_2 (ε=8 03)		
ΔG_{PET}^{corr}(eV)	-0 34	-0 37	-0.46
k_{ct}^{TR} (x 10^{-9})	1 85	1 73	3.37
k_{ct}^{SS} (x 10^{-9})	3 10	2 52	59.0
	Acetone (ε=20 7)		
ΔG_{PET}^{corr}(eV)	-0 45	-0.48	-0.51
k_{ct}^{TR} (x 10^{-9})	0.76	0.74	19.6
k_{ct}^{SS} (x 10^{-9})	2 22	1 54	48 0
	CH_3CN (ε=37 5)		
ΔG_{PET}^{corr}(eV)	-0 50	-0 52	-0.53
k_{ct}^{TR} (x 10^{-9})	0 72	0 71	16 2
k_{ct}^{SS} (x 10^{-9})	1 86	1 22	52.0
	DMSO (ε=46.7)		
ΔG_{PET}^{corr}(eV)	-0 51	-0.54	-0 54
k_{ct}^{TR} (x 10^{-9})	2 36	1.66	10.70
k_{ct}^{SS} (x 10^{-9})	3 84	2.96	52 0

(a) Error limits : ΔG_{PET}^{corr}, k_{ct}^{TR}, ± 10%, k_{ct}^{SS}, ± 20%

(b) The fluorescene lifetime in this case was similar to that of ZnTPP.

PET reaction rates can also be estimated using the steady state fluorescence data.

$$k_{et}^{SS} = (\phi_0 - \phi_f)/\phi\tau_0 \qquad (3.6)$$

where, ϕ_0 and τ_0 refer to the fluorescence quantum yield and lifetime of ZnTPP respectively and ϕ_f is the fluorescence quantum yield for the isomeric D-A porphyrin. The measured ϕ_0 values for ZnTPP are 0.036, 0.030, 0.032, 0.029 and 0.032 in toluene, CH_2Cl_2, acetone, CH_3CN and DMSO respectively. Using these ϕ_0 values and the relative quantum yield data given in Table 3.4, the ϕ_f values for **4a-c** have been calculated in each solvent. The τ_0 values were taken from Table 3.5 The estimated k_{et}^{SS} values are given in Table 3.6.

Table 3.6 also gives the ΔG_{PET}^{corr} values, where

$$\Delta G_{PET}^{corr} = E_{ox} - E_{red} - E_{0\text{-}0} + \Delta G_s \qquad (3.7)$$

and

$$\Delta G_s = (e^2/2)(1/r_D + 1/r_A)(1/4\pi\varepsilon_0\varepsilon - 1/4\pi\varepsilon_0\varepsilon_r) - e^2/4\pi\varepsilon_0\varepsilon R_{DA} \qquad (3\ 8)$$

In eqs. 3.7 and 3.8, E_{ox} and E_{red} are the oxidation and reduction potentials of the donor and acceptor respectively, measured in CH_3CN, r_D (7 A^o) and r_A (3.5 A^o) are the effective radii of the donor cation and acceptor anion respectively and ε_r and ε are the dielectric constants of CH_3CN and other

solvents, respectively. It can be noted that estimation of the ΔG_{PET}^{corr} values in low polarity solvents is risky, and the values listed in Table 3.6 for low polarity solvents should be regarded only as rough estimates.

Inspection of Table 3.6 reveals several interesting aspects of PET reactions in these isomeric D-A systems.

i) In general, the ΔG_{PET}^{corr} values correlate well with the polarity of the solvent.

ii) The k_{et}^{TR} and k_{et}^{SS} values for a given isomer correlate with the ΔG_{PET}^{corr} values.

iii) The high k_{et} values in CH_2Cl_2 (a less polar solvent) are similar to that observed by Liu et al.[36] for their linked porphyrin-peptide-quinone compound in chlorinated solvents.

iv) In each solvent, although the k_{et}^{SS} values for the para and meta isomers are similar in magnitude to the corresponding k_{et}^{TR} values, they are much higher for the ortho isomer The reasons for this are not known at present, but it can be expected that static quenching mechanisms, including the formation of a non-fluorescent exciplex, may be operative in the ortho isomer. Furthermore, the large errors involved in the estimation of the ϕ_f values of this weakly fluorescent compound may also be responsible for the observed high k_{et}^{SS} values. In general, the order obtained for the variation of k_{et} values is the same (i.e. **4b** < **4a** < **4c**) for both steady state and time-resolved measurements.

v) The above order can be contrasted with that of the *ctc* distances, i.e **4a** > **4b** > **4c**. Clearly, the k_{et} values for these isomeric D-A systems do not follow the predicted distance dependence (eq. 3.4). Thus, it is necessary to invoke an orientation dependence to explain the observed trend of the k_{et} values It is possible that, although the *ctc* distance in **4b** is shorter than that for **4a**, the relative D-A orientation in the former case may not be favourable for efficient electron transfer. Hence, the k_{et} values are smaller for the meta isomer than for the para isomer in each solvent. On the other hand, both distance and orientation are favourable for an efficient electron transfer in the ortho isomer which has high k_{et} value in all the solvents

The complex multiexponential decay observed for the ortho isomer merits further discussion It has been noted previously in the case of a "directly" linked porphyrin-anthraquinone compound, that when the lifetimes become very short, the decay profiles often cannot be fitted satisfactorily with multiple (up to four) exponential components [37] This feature has been interpreted as being due to the distribution of the PET rate constants which, in turn, reflect the distribution of the reaction energetics arising out of hindered rotational oscillations of the linked anthraquinone moiety at the site of attachment It is possible that such hindered rotational oscillations of the dinitroaromatic subunit exist in **4c** as it is connected at a sterically unfavourable ortho site of the porphyrin and that such structural oscillations are manifested in terms of the multiexponential fluorescence decay for this system

Finally, the equilibrium constant K,

$$K = A_{closed}/A_{open} \qquad (3.9)$$

which is equal to the ratio of the amplitudes (A) of the short- and long-lived components does not seem to correlate with either the polarity or the viscosity of the solvent (see Table 3 5)

3.4 Summary

Isomeric D-A compounds **3a-c** and **4a-c** have been synthesized by linking a 3,5-dinitroaromatic acceptor subunit, *via* an ester bridge, to either para, meta, or ortho position of one of the aryl groups of meso-5,10,25,20-(tetraphenyl)porphyrin (H_2TPP) and its zinc (II) derivative (ZnTPP) UV-visible and ^{1}H NMR spectra have suggested the existence of weak intramolecular π-π interaction in these compounds Low fluorescence quantum yields and short lifetimes have been obtained for the zinc(II) derivatives **4a-c** in comparison with the corresponding values for ZnTPP Multiexponential fluorescence decays obtained in five different solvents for these systems have been interpreted in terms of the coexistence of "closed" and "extended" forms of the D-A structures that do not equilibrate within the singlet state lifetime of the donor porphyrin A PET reaction from the ZnTPP donor to the appended 3,5-dinitroaromatic acceptor has been suggested to occur The apparent PET rate constants obtained from time-resolved and steady state fluorescence data vary as **4b** < **4a** < **4c** This observation is inconsistent with the known distance dependence of k_{et} and indicates an orientation influence on the PET reactions

3.5 References

1 Wasielewski, M R *Chem Rev* **1992**, 92, 435

2 Gust, D , Moore, T A *Top Curr Chem* **1991**, 159, 105

3. Maiya, B. G.; Krishnan, V. *J. Phys Chem.* **1985**, 89, 5225.
4. Maiya, B. G.; Krishnan,V *Chemistry and Industry;* Festchrift Volume in honour of Professor of K. K. G. Menon, Oxford & IBH: Bombay, 1987; p 303.
5. Gonazlalez, M. C.; McIntosh, A. R.; Bolton, J. R.; Weedon, A. C. *J Chem. Soc., Chem Commun* **1984**, 1139.
6. Blondeel, G. K.; Kekuerleire, D. D.; Harriman, A.; Milgrom, L. R. *Chem Phys. Lett.* **1985**, 118, 77.
7. Shafirovich, V. Y.; Amouyal, E.; Delaire, J. J. *Chem Phys Lett* **1991**, 178, 24
8. Kanda, Y.; Sato, H ; Okada, T ; Mataga, N *Chem Phys Lett* **1986**, 129, 306
9. McMohon, R J.; Force, R K ; Patterson, H. H ; Wrighton, M S *J Am Chem. Soc.* **1988**, 110, 2670
10. Franco, C.; McLendon, G *Inorg. Chem.* **1984**, 23, 2370
11. Wang, X. D ; Zhan, B W , Bai, J W , Cao, Y., Xiao, X R ; Xu, J M *J Phys. Chem* **1992**, 96, 2886.
12. Irvine, M P.; Harrison, R J.; Beddard, G S , Leighton, P , Sanders, J K M *Chem Phys.* **1986**, 104, 315.
13. Nakamura, H.; Motonaga, A ; Ogata, T.; Nakao, S , Matsuo, T. *Chem. Lett* **1986**, 1615
14. Batteas, J D.; Harriman, A , Kanda, Y , Mataga, N , Nowak, A K *J Am Chem. Soc.* **1990**, 112, 126
15. Cowan, A ; Sanders, J K M ; Beddard, G S , Harrison, R J *J Chem Soc., Chem. Commun* **1987**, 55.

16. Maiya, B. G. In *Solvation Dynamics and Charge Transfer;* Bagchi, B.; Krishnan, V., Eds , World Scientific: Singapore, 1991; p 123 and references therein.

17. (a) Sakata, Y., Tsue, H., Goto, Y.; Misumi, S.; Asahi, T.; Nishikawa, S.; Okada, T.; Mataga, N. *Chem Lett.* **1991**, 1307. (b) Borovkov, V. V.; Ishida, A.; Takamuku, S.; Sakata. Y. *Chem. Lett.* **1993**, 145. (c) Himahori, H.; Tanaka, Y , Okada, T.; Sakata, Y. *Chem. Lett.* **1993**, 1215. (d) Snikin, M. V.; Borovkov, V. V.; Ishida, A.; Wasa, K.; Sakata, Y. *Chem. Phys. Lett.* **1994**, 226, 337. (e) Higashida, S.; Tsue, H.; Sugiura, K., Kaneda, T., Tanaka, Y , Taniguchi, S.; Okada, T ; Sakata, Y. *Chem. Lett* **1995**, 515 and references therein.

18 Osuka, A , Morikawa, S., Maruyama, K , Hirayama, S ; Minami, T. *J. Chem Soc , Chem Commun.* **1987**, 359

19. Perrin, D. D , Armanego, W L F , Perrin, D. R In *Purification of Laboratory Chemicals,* Pergamon Oxford, 1986.

20. Rothemund, P.; Mennotti, A R *J Am Chem Soc.* **1948**, 70, 697

21. Little, R. G , Anton, J. A., Loach, P. A.; Iber, J. A. *J. Heterocycl. Chem.* **1975**, 23, 243.

22. Periasamy, N ; Doraiswamy, S.; Maiya, B. G.; Venkataraman, B. *J. Chem. Phys.* **1988**, 88, 1638.

23. Bevington, R. In *Data Reduction and Analysis in Physical Sciences;* McGraw-Hill. New York, 1969

24. Katz, J J. In *Porphyrins and Metalloporphyrins,* Smith, K. M., Ed ; Elsevier. Amsterdam, 1975, chapter 10

25. Chandrasekhar, T K , Krishnan, V *Inorg. Chem.* **1981**, 28, 2782.

26. Gouterman, M , Stevenson, P E *J Chem Phys* **1962**, 37, 2266.

27. Kadish, K M. *Prog. Inorg Chem.* **1986**, 34, 435.

28. Gouterman, M In *The Porphyrins*, Dolphin, D., Ed.; Academic. New York, 1979, Vol. 3, chapter 1.

29. Wasielewski, M. R ; Niemczyk, M P. *J. Am. Chem Soc* **1984**, 106, 5043.

30. (a) Levstein, P. R.; van Willigen, H. *Chem. Phys Lett.* **1991**, 187, 415
(b) Ebersole, M., Levstein, P. R , van Willigen, H *J. Phys Chem* **1992**, 96, 9310.

31. McIntosh, A R.; Siemiarezu, A ; Bolton, J. R.; Stillman, M J.; Ho, T F ; Weedon, A. C. *J. Am. Chem. Soc* **1983**, 105, 7215

32. Van der Auwear, M., Gilbert, A ; De Schryver, F C. *J. Am Chem.Soc* **1980**, 102, 4007.

33. Larsson, S , Volosov, A *J Chem Phys.* **1986**, 85, 2548 and references therein.

34. Cave, R J.; Siders, P , Marcus, R A. *J. Phys Chem* **1986**, 90, 1436

35. Brunschwid, B S., Sutin, N *J Am Chem Soc* **1989**, 111, 7454

36. Liu, J -Y., Schmidt, J A , Bolton, J R. *J. Phys Chem* **1991**, 95, 6924

37. Cormier, R A.; Posey, M. R.; Bell, W. L., Fonda, H N , Connolly, J S *Tetrahedron* **1989**, 45, 4831

38. **Structures were optimized using PCM4 in such a way that the energies of any two successive optimizations remain the same. No structural parameters have been held constant.**

CHAPTER 4

Intramolecular Excitation Energy Transfer in Isomeric Porphyrin-Anthracene Dyads

4.1. Introduction

Studies on excitation energy transfer (EET) reactions occurring in donor-acceptor (D-A) systems having short (3-6 A°) and intermediate (6-20 A°) D-A separations are of current interest.[1-8] Much of the impetus for such studies seems to have come from the importance of EET in both natural[9] and functionally-active synthetic systems [10-13] Thus, because of their relevance to many research areas including biomimetic photosynthesis, molecular electronics etc. EET reactions occurring in porphyrin-based systems have attracted considerable attention Intramolecular EET has been elucidated in a great variety of bis- and multi-porphyrin arrays[9,14,15] but, only a few studies have dealt with energy transfer in porphyrins attached to other hydrocarbon moieties.[14,16-21] In this regard, it can be noted that only examples of porphyrin-based dyads in which detailed mechanisms of intramolecular singlet-singlet energy transfer reactions are known have been restricted to covalently linked porphyrin-cyanine dye,[16] porphyrin-carotene[17-20] and porphyrin-molecular wire-anthracene[21] systems. More importantly, although studies which inquire into the influence of D-A distance and orientation on the efficiency of the intramolecular electron transfer in porphyrin-based D-A systems have been numerous,[9 14] similar studies dealing with the EET in porphyrin-based energy-transfer dyads are relatively unknown.

During the course of the present research, it became evident that the synthetic manoeuvrability of porphyrins and well-defined spectral as well as

photochemical properties of porphyrin and other hydrocarbon donor systems could provide an opportunity to build energy-transfer dyads of the type 'porphyrin-spacer-hydrocarbon (nonporphyrinic)' that are characterised by short or intermediate D-A separations and varying mutual orientations This has been realised here and this chapter describes the synthesis and photophysical properties of a series of covalently linked D-A dyad molecules wherein an anthracene (donor) moiety is linked covalently at the para (**2a**), meta (**2b**) or ortho (**2c**) position of one of the phenyl groups of meso-5,10,15,20-(tetraphenyl)porphyrin (H_2TPP) *via* an ether bridge (see scheme 4 1)

4.2. Experimental

Precursors **1a-c** were synthesized as described in Chapter 3 (Section 3 2 1)

4.2.1 Synthesis of meso-5-(4-(9-methyloxyanthracenyl)phenyl)-10,15,20 triphenyl porphyrin (2a)

A 0 063 g (0 1 mmol) of compound **1a** and 0 025 g (0 11 mmol) of 9-chloromethylanthracene were dissolved in 10 ml of dimethylformamide (DMF) To this was added a 0 5 g (0 5 mmol) of K_2CO_3 and the contents were stirred for 24 h at 25 °C The solvent was evaporated under reduced pressure and the residue was dissolved in chloroform and applied onto an alumina (neutral, activity 1) column The desired product was eluted using $CHCl_3$ as the eluent Solvent was evaporated and the product recrystallized in $CHCl_3$ C_2H_5OH (1 1 v/v) mixture Yield ≅ 60%

Meso-5-(3-(9-methyloxyanthracenyl)phenyl) 10, 15, 20-triphenyl porphyrin (**2b**) and meso-5-(2-(9-methyloxyanthracenyl)phenyl)10,15,20-

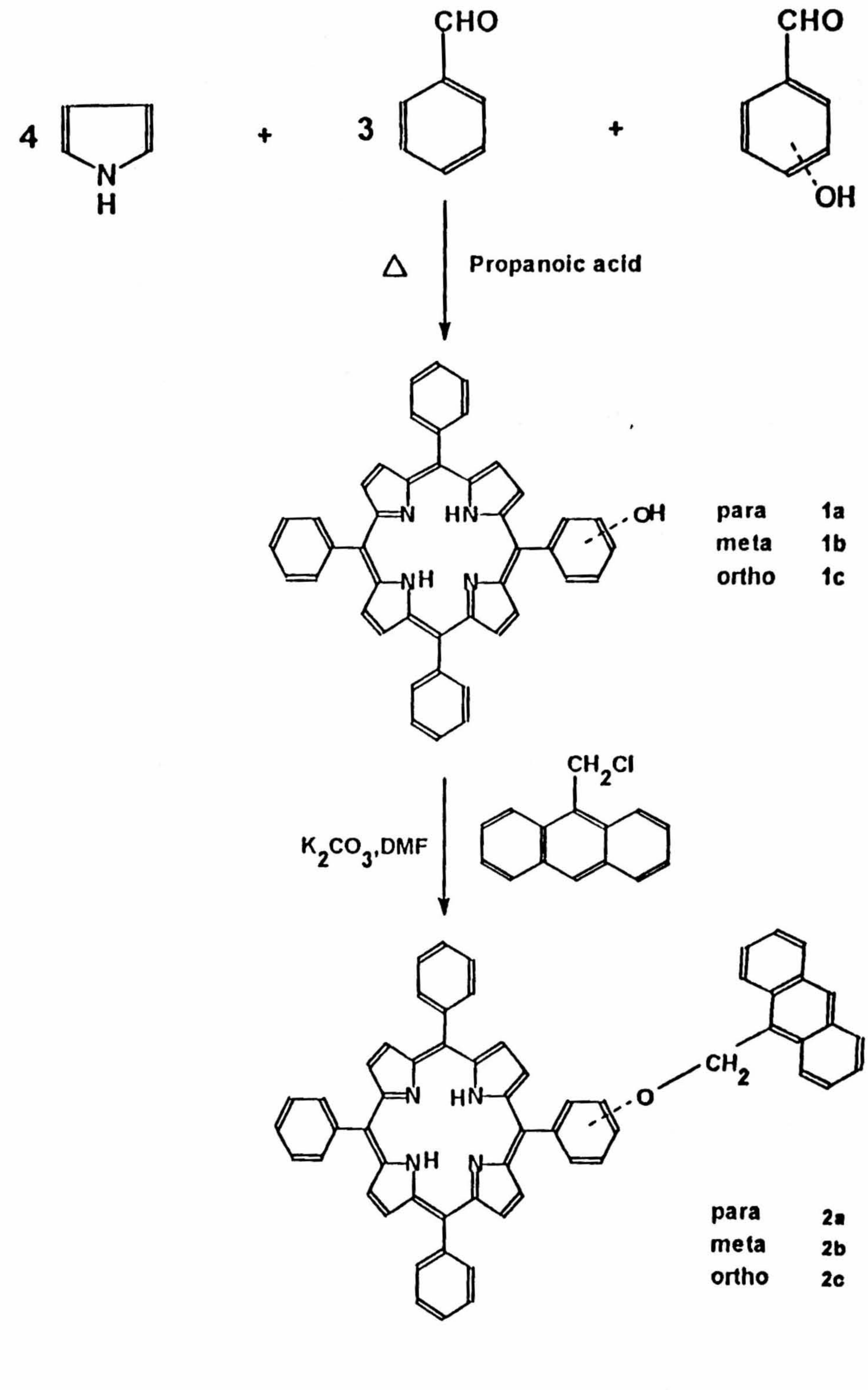
4
+
3
+
CHO
CHO
OH
N
H
Δ
Propanoic acid
N
HN
NH
N
OH
para 1a
meta 1b
ortho 1c
CH_2Cl
K_2CO_3,DMF
O
CH_2
para 2a
meta 2b
ortho 2c

Scheme 4.1

triphenyl porphyrin (**2c**) were synthesized using analogous procedure described above for **2a** (yield : 50-60%)

4.2.2 Synthesis of 9-methyloxyphenylanthracene (3)

This reference compound was synthesized by condensing phenol and 9-chloromethylanthracene in the DMF, K_2CO_3 milieu and was purified as described above for **2a** (yield: ≅ 80%). Melting point, 145 ± 2°C. Analytical data: obsd.: C, 88.60; H, 5.67 calcd. for $C_{20}H_{14}O$: C, 88.70, H, 5.60.

Each investigated porphyrin was purified on a short alumina column before spectral measurements were made All the spectroscopic and electrochemical experiments have been carried out as described in chapter 2

4.3. Results and discussion

4.3.1 Ground state properties

UV-visible spectral data of the covalently linked dyads and that of their constituent individual components (i e H_2TPP and anthracene or **3**) are summarised in Table 4 1 Fig 4 1 shows the UV-visible spectra of **2b**, H_2TPP and anthracene Spectra of **2a** and **2c** are similar to that of **2b** As can be seen from Fig. 4.1 and Table 4 1, spectra of the linked compounds show bands due to anthracene subunit's absorption between 200 and 400 nm and those due to porphyrin absorption between 400 and 700 nm. Data given in Table 4 1 also suggests that while the λ_{max} values of these dyads are within the same range as those of the constituent individual components, their log ε values are slightly altered in comparison with those of anthracene (or **3**) and H_2TPP

Table 4.1 UV-visible data in CH_2Cl_2

Compound	λ_{max}, nm (log ε)							
	Porphyrin transitions					Anthracene transitions		
	Q_1	Q_2	Q_3	Q_4	B	I	II	III
Anthracene						378 (3.84)	359 (3.88)	255 (5.19)
3						387 (4 07)	367 (4.09)	257 (5.29)
H_2TPP	645 (3 67)	590 (3 61)	548 (3.76)	514 (4 22)	417 (5 56)			
2a	648 (3.68)	592 (3.67)	552 (3 83)	517 (4 21)	419 (5.67)	373 (4.72)	355 (4 61)	259 (5.38)
2b	648 (3.53)	591 (3 53)	551 (3 73)	516 (4.03)	419 (5 55)	368 (4.57)	355 (4.34)	257 (5 25)
2c	645 (3.51)	591 (3.72)	551 (3.82)	516 (4.24)	418 (5 41)	368 (4.31)	355 (4.06)	258 (4.95)

Furthermore, the log ε values, in general, seem to follow the order **2c** < **2b** < **2a**. These observations are consistent with the presence of a weak π-π interaction between the two π-systems in this series of porphyrin-anthracene dyads. From a comparison of the spectra given in Fig. 4 1, it is clear that the

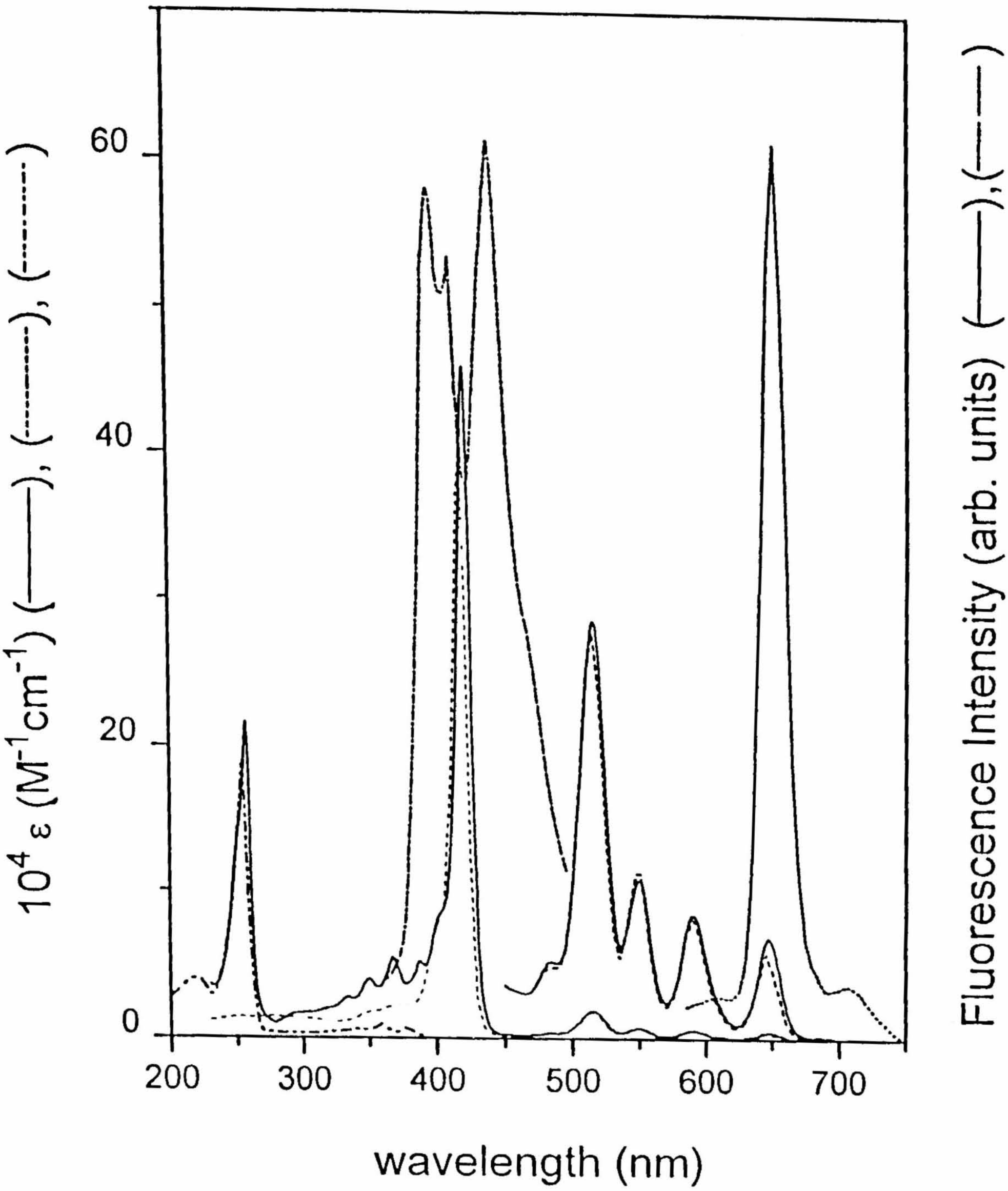

Fig 4.1. UV-visible spectra of H_2TPP (-------), **2b** (———) and anthracene (– –·–), and fluorescence spectra of **2b** obtained on excitation at the anthracene (250 nm) absorption peak (– – – –) and the porphyrin (420 nm) absorption peak (·····) The solvent was CH_2Cl_2. Fluorescence spectra were normalized for clarity

absorption of the two chromophores are well separated and that there exists an opportunity for the excitation into either an exclusive anthracene band (ca. 250 nm) or an exclusive porphyrin band (ca. 550 nm) in these dyads.

Fig. 4.2 compares the ^{1}H NMR spectra ($CDCl_3$, TMS) of the three isomeric D-A compounds. Relevant data are summarised in Table 4.2. Salient features of the spectra that provide evidence for a proximity of the anthracene with the porphyrin in these dyads follow. Firstly, whereas the pyrrole-β protons of H_2TPP resonate at 8 83 ppm (s, 8H)[22,23] those of **2a**, **2b** and **2c** resonate at 8 83 (s, 8H), 8 82 (s, 8H) and 8.73 (s, 8H) ppm, respectively. Similarly, in comparison with the resonance due to the central imino protons of H_2TPP (-2.80 ppm, (s, 2H)), the corresponding resonance in the spectra of the dyads is seen to be upfield shifted by 0.01, 0 04 and 0.16 ppm for **2a**, **2b** and **2c**, respectively Secondly, resonances due to protons at positions 2, 3, 6, 7 of the anthracene subunit also follow a similar trend in that **2a**, **2b** and **2c** show peaks due to these protons at 8 29 (m, 4H), 8.16 (m, 4H) and 6.50 (m, 4H) ppm, respectively. This complementary shielding of the protons on the porphyrin ring and those on the anthracene ring can be explained in terms of the ring current effect exerted by these two aromatic moieties on each other [24] It is interesting that this effect follows a trend that is determined by the site of attachment of the donor to the acceptor, *viz.* **2c** > **2b** > **2a**. Consistent with this analysis is the trend observed for peaks due to the spacer -OCH_2 protons which occur at 6.19 (s, 2H), 6.09 (s, 2H) and 5.56 (s, 2H) ppm for **2a**, **2b** and **2c**, respectively. As the ring-current effects are known to be significant at 'short' distances,[24] the observed mutual shielding of protons on the constituent components of these dyads indicates a proximity of the two π-systems. It can be noted here that the π-system on the porphyrin might also include the meso-

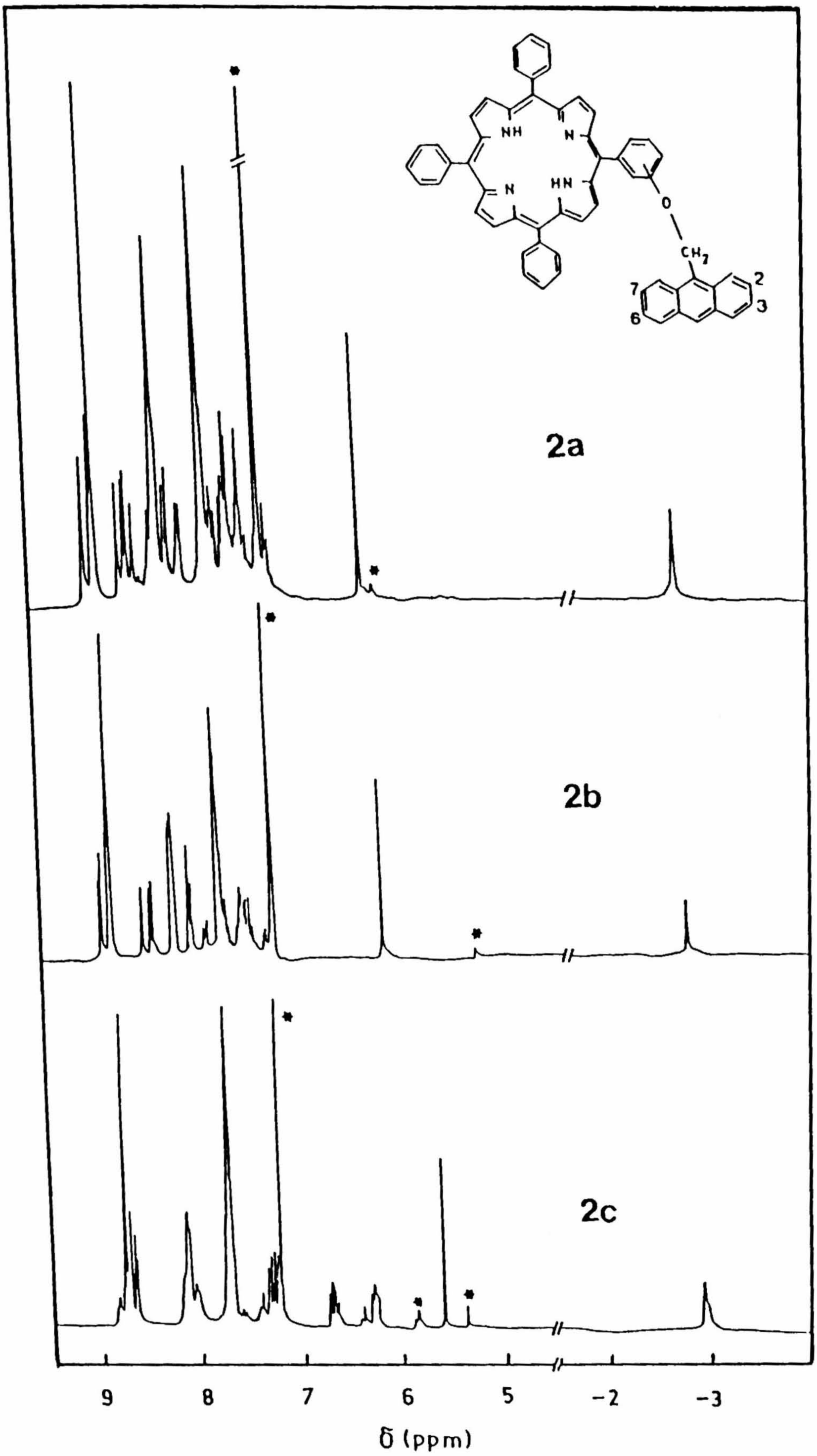

Fig. 4.2. ^{1}H NMR spectra of **2a**, **2b** and **2c** Peaks marked with * are due to solvent or impurities.

aryl ring on it that is linked to the anthracence moiety and that the ^{1}H NMR chemical shifts represent an equilibrium between several D-A conformations present in solution under these experimental conditions.

Table 4.2 ^{1}H NMR data in $CDCl_3$ (TMS).

Compound	δ(ppm)							
	Porphyrin protons				Anthracene protons			
	β-pyrrole	o-phenyl	m-, p-phenyl	-NH	2,3,6,7	1,4,5,8	9	-CH_2
3					8.12 (m, 4H)	7.32 (m, 4H)	8.44 (s, 1H)	5.96 (s, 2H)
H_2TPP	8.83 (s, 8H)	8 30 (m, 8H)	7 80 (m, 12H)	-2 80 (s, 2H)				
2a	8.83 (m, 8H)	8.15 (m, 8H)	7 71 (m, 11H)	-2 81 (s, 2H)	8.29 (m, 4H)	7 39 (m, 4H)	8.54 (s, 1H)	6 19 (s, 2H)
2b	8.82 (m, 8H)	8.15 (m, 8H)	7.65 (m, 11H)	-2.84 (s, 2H)	8.16 (m, 4H)	7.44 (m, 4H)	8.45 (s, 1H)	6.09 (s, 2H)
2c	8.73 (m, 8H)	8.09 (m, 7H)	7 68 (m, 11H)	-2.96 (s, 2H)	6.50 (m, 4H)	7.25 (m, 4H)	8.63 (s, 1H)	5.56 (s, 2H)

Table 4.3 summarises the redox potential data of these isomeric D-A porphyrins measured in CH_2Cl_2, 0.1 M TBAP (with respect to SCE) by the differential-pulse-voltammetric method. As seen from the data given in this Table, while the porphyrin part of each compound could be oxidised and reduced at (1.02± 0.03) V and (-1.24 ± 0.03) V respectively, the anthracene part could be oxidised at (1.41 ± 0.03) V and the reduction of it was not observed within the solvent limit (ca -1.8 V) under the experimental conditions employed here Thus, the redox potential data seems to be insensitive to the molecular structures of these compounds. Nonetheless, based on the consistency observed in the UV-visible and ^1H NMR data described above, it can be suggested that there exists a weak π-π interaction between the donor and the acceptor in these systems and that the extent of this interaction is sensitive to a change in the D-A distance and the orientation.

Table 4.3 Redox potential data in CH_2Cl_2, 0.1 M TBAP.

Compound	**An → An$^+$**	**P → P$^+$**	**P → P$^-$**	**ΔG_{PET}**
	(V)	(V)	(V)	(eV)
3	1.36	——	——	——
H_2TPP		1.06	-1.24	
2a	1.44	1.01	-1 26	-0 50
2b	1.44	1 04	-1 24	-0 52
2c	1.38	0 99	-1 24	-0 58

4.3.2 Singlet state properties

Fluorescence spectra of the three isomeric D-A dyads were measured in three solvents, hexane, CH_2Cl_2 and CH_3CN. When excited at the porphyrin absorption maximum (420 nm), the spectra obtained for the three isomeric dyads were seen to be similar to the spectrum of H_2TPP. However, excitation into the anthracene absorption maximum (250 nm) of these compounds resulted in fluorescence bands that are red-shifted, and also less intense in comparison with the bands due to free anthracene (Fig. 4.3). The red shifts observed here can be a consequence of substitution at the 9-position of anthracene as was the case for previously studied 9-substituted anthracene derivatives.[25] Consistent with this supposition is the fact that the band maxima of **3**, a 9-substituted anthracene derivative, also occur at red-shifted (392, 415 and 438 nm) positions to those of anthracene, (382, 403, and 427 nm) in CH_2Cl_2. From an overlay of the absorption and fluorescence spectra of the three dyads, the 0-0 spectroscopic transition energies ($E_{0\text{-}0}$) of the anthracene moiety (3.20 ± 0.05 eV) and the porphyrin moiety (1.95 ± 0.05 eV) were obtained and these values are similar to the $E_{0\text{-}0}$ values of anthracene[26] and H_2TPP,[27] respectively.

A major difference between the fluorescence data of the dyads and those of H_2TPP and anthracene lies in the magnitude of fluorescence quantum yield (ϕ_f) values. Whereas ϕ_f for an excitation into the porphyrin moiety ($\phi_f = 0.12 \pm 0.1$) was similar to that of H_2TPP,[28] fluorescence from the anthracene part of each dyad was found to be strongly quenched (up to 99%) in comparison with the fluorescence of free anthracene in all the three investigated solvents (Fig. 4.3). The evaluated quenching efficiency (Q, eq. 4.1) and k_{obs} values (eq. 4.2) are given in Table 4.4.

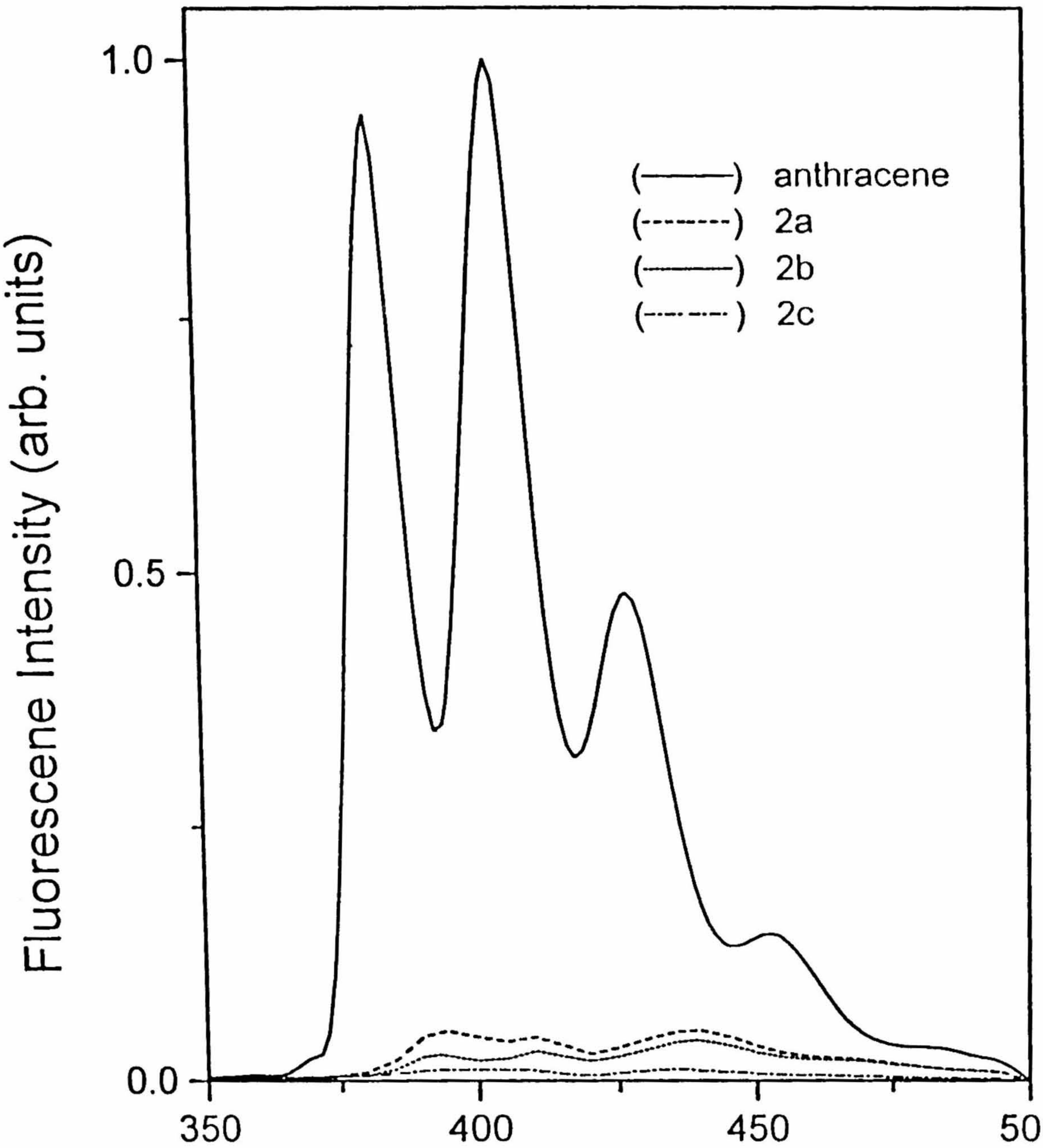

Fig. 4.3. Fluorescence spectra of equiabsorbing solutions (optical density at $\lambda_{ex} = 0.11$) of anthracene and **2a-c** ($\lambda_{ex} = 250$ nm).

Table 4.4 Energy transfer data [a]

Compound	%Q	$\%T_{obs}$	k_{obs}	k_{En}(obs)	$k_{Forster}$ $(10^9\ s^{-1})$[b]		
			$10^9\ s^{-1}$	$10^9\ s^{-1}$	κ^2(I)	κ^2(II)	κ^2(III)
	Hexane (n=1 375, ε=1 88)[c]						
2a	97	60	6 60	0.31	1 30	2.61	0.69
2b	98	84	10 00	1 07	4 75	3 151	0 69
2c	99	100	20 20	20 20	20 11	13 13	13.68
	CH_2Cl_2 (n=1 425, ε=8 93)[c]						
	91	52	1 94	0 21	0.77	1 55	0.41
2a	93	82	2 60	0 86	2 82	1 87	1 00
2b	99	100	19 04	19 04	11 95	7 80	8 13
2c							
	CH_3CN (n=1 344, ε=37 50)[c]						
2a	97	42	6 10	0 14	1 40	2 80	0 74
2b	98	85	9 20	1 07	5 10	3 38	1 82
2c[d]	99	100	18 70	18 70	21 60	14 10	14.67

(a) Error limits %Q, k_{obs} ±5%; $\%T_{obs}$, k_{EN} (obs) ±10%, $k_{Forster}$ ±7%.

(b) κ^2(I) and κ^2(II) values are 1 25, 1 82, 0 28 and 2 59, 1.20, 0 64 respectively for **2a**, **2b** and **2c** κ^2(III) = 2/3 in all the cases.

(c) n and ε refer to refractive index and dielectric constant of the solvents respectively

(d) Considering that %Q is 99 and the $\%T_{obs}$ = 100 for this isomer, k_{obs} is taken as k_{EN} (obs) in these cases.

$$Q = [\phi_f(\mathbf{A}) - \phi_f(\mathbf{2a\text{-}c})] / \phi_f(\text{anthracene}) \quad (4.1)$$

$$k_{obs} = [Q/(1-Q)] / \tau(\text{anthracene}) \quad (4.2)$$

where ϕ_f(anthracene) and ϕ_f(**2a-c**) refer to the fluorescence quantum yields for anthracene and the three isomeric dyads (λ_{exc} = 250 nm), respectively and τ (anthracene) is the singlet state life time of anthracene (= 4.9, 5.2 and 5.3 ns in hexane, CH_2Cl_2 and CH_3CN, respectively[26])

It should be noted that this quenching is not due to the competitive absorption of incident light by the porphyrin part of the dyads. This is because, at 250 nm the contribution of porphyrin absorption is insignificant compared with the absorption due to the anthracene moiety in each compound (compare the absorption data of the dyad and H_2TPP at 250 nm in Fig. 4.1).

Among the various photophysical processes that can explain the fluorescence quenching in these isomeric dyads, exciplex formation, energy transfer and electron transfer processes are of importance. The existence of weak π-π interaction *(vide supra)* can, in principle, manifest itself in the formation of an exciplex but no evidence for the separate emission from an exciplex was noticed for these weakly fluorescent dyads. Therefore, a detailed consideration will be given for the participation of energy transfer and electron transfer reactions.

There exists a strong overlap between the emission of anthracene and the absorption of porphyrin in these dyads (see Fig. 4.1) and this fact suggests that quenching of the anthracene fluorescence in them can be due to an intramolecular EET from the singlet anthracene to the porphyrin. Indeed, excitation of ca. 10^{-7} M solution of each dyad at 250 nm resulted in an appearance of well-defined porphyrin emission bands in all the three solvents

On the other hand, only weak fluorescence could be noticed when a solution of H_2TPP (or 1:1 mol/mol mixture of H_2TPP and anthracene) having the same concentration was excited at the same wavelength. This is illustrated in Fig. 4.4 which shows the emission spectra (λ_{exc} = 250 nm) of **2a**, H_2TPP and an equimolar mixture of H_2TPP and anthracene.

Conclusive evidence for intramolecular EET comes from the excitation spectral measurements. When emission was recorded at the porphyrin emission maximum (650 nm), the excitation spectra of the D-A dyads showed bands characteristic of anthracene absorption. Fig. 4.5 shows an overlay of the corrected and normalized excitation spectra of the three compounds with the corresponding absorption spectra in CH_2Cl_2. A comparison of the excitation and the absorption spectra in the 45.5 x 10^3 to 37 0 x 10^3 cm^{-1} (220-270 nm) region gives the energy transfer efficiencies ($\%T_{obs}$) for these compounds in the three investigated solvents and these data are summarized in Table 4 4. The rates of energy transfer ($k_{EN}(obs)$) have been calculated from the expression

$$k_{EN}(obs) = [T_{obs} / (1 - T_{obs})] / \tau(anthracene) \qquad (4\ 3)$$

An inspection of Fig 4.5 and Table 4.4 suggests that $k_{EN}(obs)$ (and $\%T_{obs}$) values follow the order **2c** > **2b** > **2a** and that in the case of **2a** and **2b**, they are less than the k_{obs} (or Q) values.

Intermolecular energy transfer between anthracene and H_2TPP is not obvious. The addition of 0 2 x 10^{-6} to 2 x 10^{-6} M of H_2TPP to a 1.0 x 10^{-6} M solution of anthracene resulted in an apparent decrease (by about 5-10%) of fluorescence (λ_{exc} = 250 nm) in the anthracene emission region and a

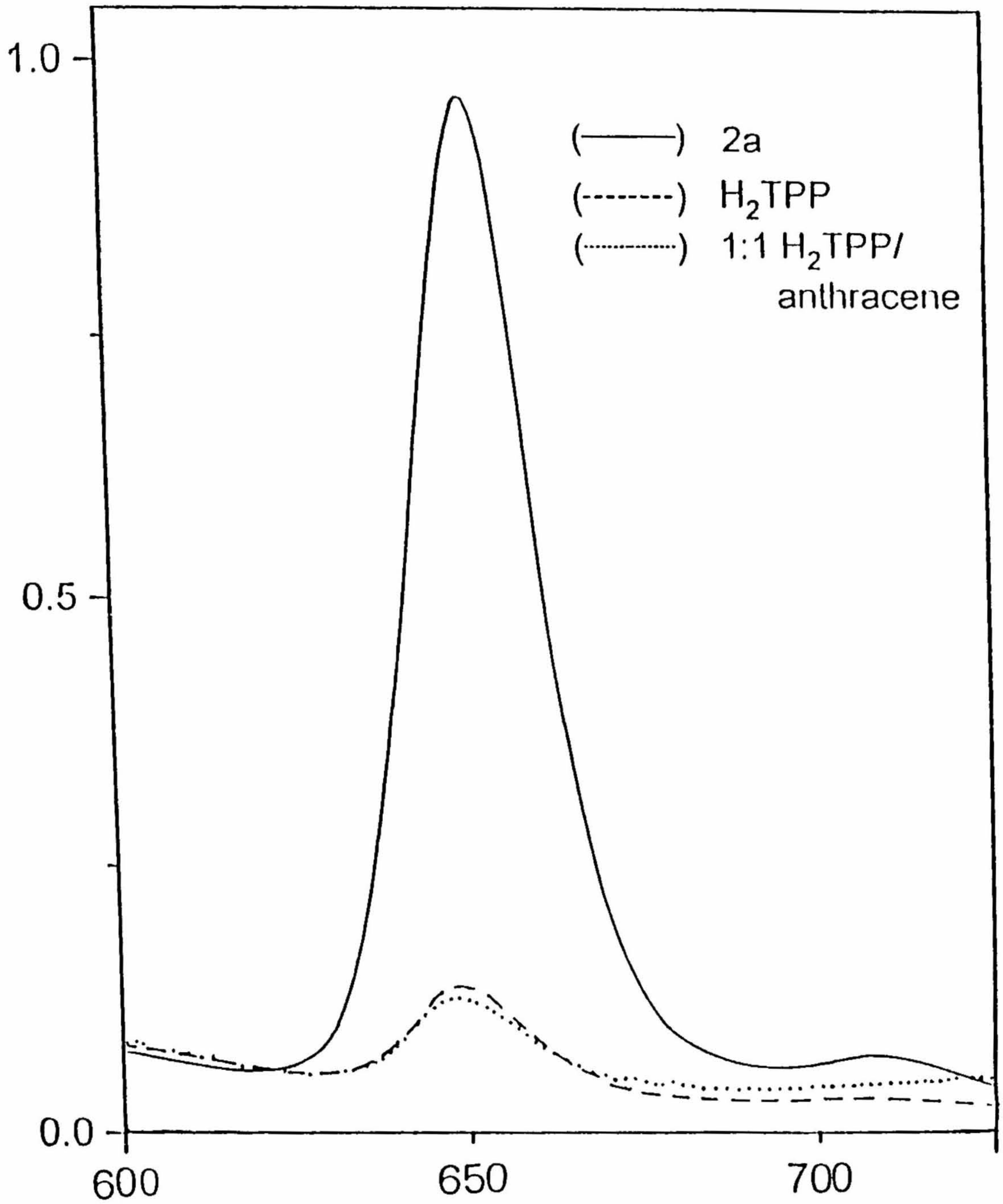

Fig. 4.4. Fluorescence spectra of 10^{-7} M solutions of **2a**, H_2TPP and 1:1 (mol/mol) mixture of H_2TPP and anthracene (λ_{ex} = 250 nm).

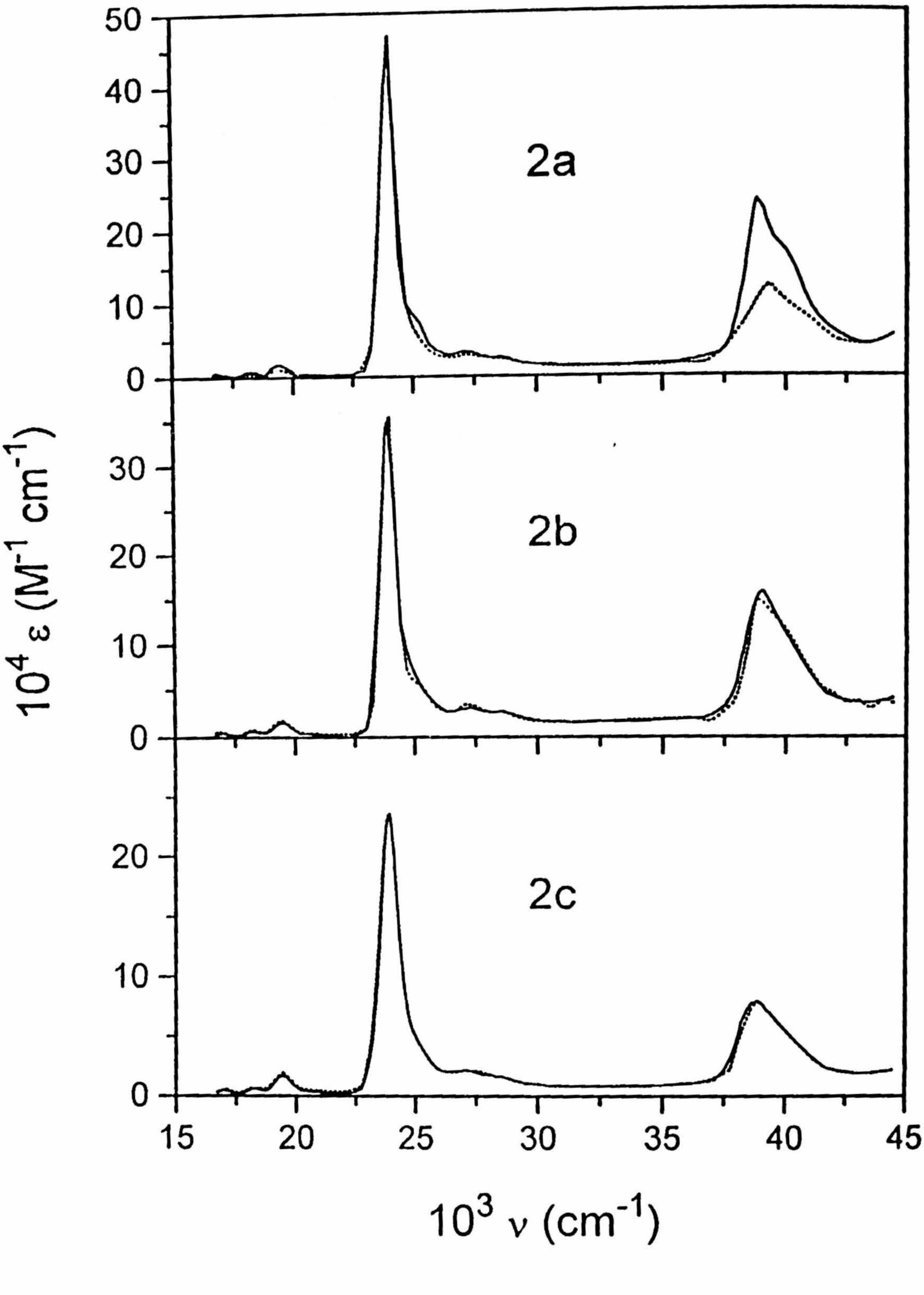

Fig. 4.5. Overlay of the excitation (·····) and the absorption (——) spectra of **2a-c** in CH_2Cl_2 (λ_{em} = 650 nm). The excitation spectra were corrected for the instrument response function and were normalized with respect to the absorption spectra between 16.6 x 10^3 cm^{-1} (600 nm) and 20.0 x 10^3 cm^{-1} (500 nm).

concomitant, progressive increase of fluorescence in the porphyrin emission region. Within the experimental error, the increase in porphyrin emission observed in the presence of anthracene is the same as that obtained in the concentration dependent (0.2 x 10^{-6} to 2.0 x 10^{-6} M) emission of H_2TPP (λ_{exc} = 250 nm) in the absence of anthracene. Moreover, the excitation spectrum (λ_{em} = 650 nm) obtained for 1:1 (mol/mol) mixture of anthracene and H_2TPP is indistinguishable from the spectrum obtained for H_2TPP alone. Collectively, these results suggest that the energy transfer efficiency between anthracene and porphyrin is more efficient in an intramolecular than in an intermolecular situation.

Having established the energy transfer in these isomeric dyads, it is of interest to elicit a mechanistic interpretation of the EET by employing the obtained data. EET reactions in bichromophoric D-A systems can proceed mainly through two types of mechanisms. (i) over large D-A separations and in the absence of any interchromophore interactions, they may occur *via* a Coulombic interaction between the transition dipoles of excited donor and ground state acceptor (Forster mechanism[29]) and (ii) in situations where there is some degree of interchromophore orbital overlap, they can also be mediated by overlap dependent electronic coupling, one of which is the quantum mechanical exchange interaction (Dexter mechanism[30]). Both Forster and Dexter mechanisms require, among the other things, that the rate of energy transfer be proportional to a spectral overlap (J) of the donor emission and the acceptor absorption [29,30] Overlap integrals $J_{Forster}$ (eq 4.4) and J_{Dexter} (eq. 4.5) for the present D-A pair in the three investigated solvents have been estimated to be (2 64 ± 0.12) x 10^{-16} cm^6 $mmol^{-1}$ and (1 40 ± 0.08) x 10^{-4} cm, respectively and in both the cases, no direct correlation of these integrals could be made with the k_{EN}(obs) (or %Tobs) values

$$J_{Forster} = \frac{\int F(\upsilon)\,\varepsilon(\upsilon)\,\upsilon^{-4}\,d\upsilon}{\int F(\upsilon)\,d\upsilon} \qquad (4.4)$$

$$J_{Dexter} = \frac{\int F(\upsilon)\,\varepsilon(\upsilon)\,d\upsilon}{\int F(\upsilon)\,d\upsilon\,\varepsilon(\upsilon)\,d\upsilon} \qquad (4.5)$$

($F(\upsilon)$ is the fluorescence intensity of the energy donor at wavenumber $\upsilon(cm^{-1}$), and ε is the molar extinction coefficient ($mmol^{-1}$ cm^{-1}) of the energy acceptor).

On the other hand, Forster mechanism predicts that the rate constant $k_{Forster}$ for the EET follows eq. 4.6.

$$k_{Forster} = \frac{8.8 \times 10^{-25}\,\kappa^2\,\phi_D\,J_{Forster}}{n^4\,\tau\,R^6} \qquad (4\ 6)$$

Here, n is the solvent refractive index, ϕ_D and τ are the fluorescence quantum yield and the fluorescence lifetime (in s) of the isolated donor, κ^2 is an orientation factor and R (Rc, the center-to-center distance) is the distance (in cm). The possibility of Forster mechanism being operative in the EET of these dyads can be tested by comparing the experimental rates of energy transfer ($k_{EN}(obs)$) with those calculated ($k_{Forster}$) by application of eq. 4.6.

While doing so, it has been assumed that the orientation factor, κ^2 (eq. 4.7), cannot be uniquely defined for the present intramolecular systems.

$$\kappa^2 = (\cos\gamma - 3\cos\alpha \cos\beta)^2 \qquad (4.7)$$

where α and β are the angles made by the transition dipoles of anthracene and porphyrin in these dyads with the line joining the centres of the transitions, γ is the angle between the two transition dipoles. It was found necessary to employ three different κ^2 values while applying eq. 4.6 for these bichromophoric molecules and a rationale behind this is briefly discussed below.

While the transition dipole of the ^1S state of anthracene lies on the molecule's short axis,[2] that of the porphyrin is known to lie along a line joining two opposing pyrrole nitrogens.[31] Thus, for a given porphyrin-anthracene conformation in these dyads there are two possibilities (essentially equally populated) depending upon which nitrogen atoms are protonated.[18] For the evaluation of an equitable κ^2, the optimized molecular structures (MMX) of the three dyads have been employed (Fig. 4.6). Assuming that the orientation between the donor and the acceptor π-planes is the same as that shown in Fig. 4.6, two κ^2 (κ^2 (I) and κ^2(II)) values can be calculated for each dyad. On the other hand, it can be argued that the anthracence moiety assumes an average orientation in its excited state with respect to the porphyrin plane and in such a case, κ^2 (κ^2(III)) will be 2/3. Thus, in all, substitution of these κ^2 values into eq. 4.6 gave three different $k_{Forster}$ values for each dyad (Table 4.4).

A comparison of the $k_{Forster}$ with the k_{EN}(obs) values in Table 4.4 reveals that no correlation between the theory and the experiment can be

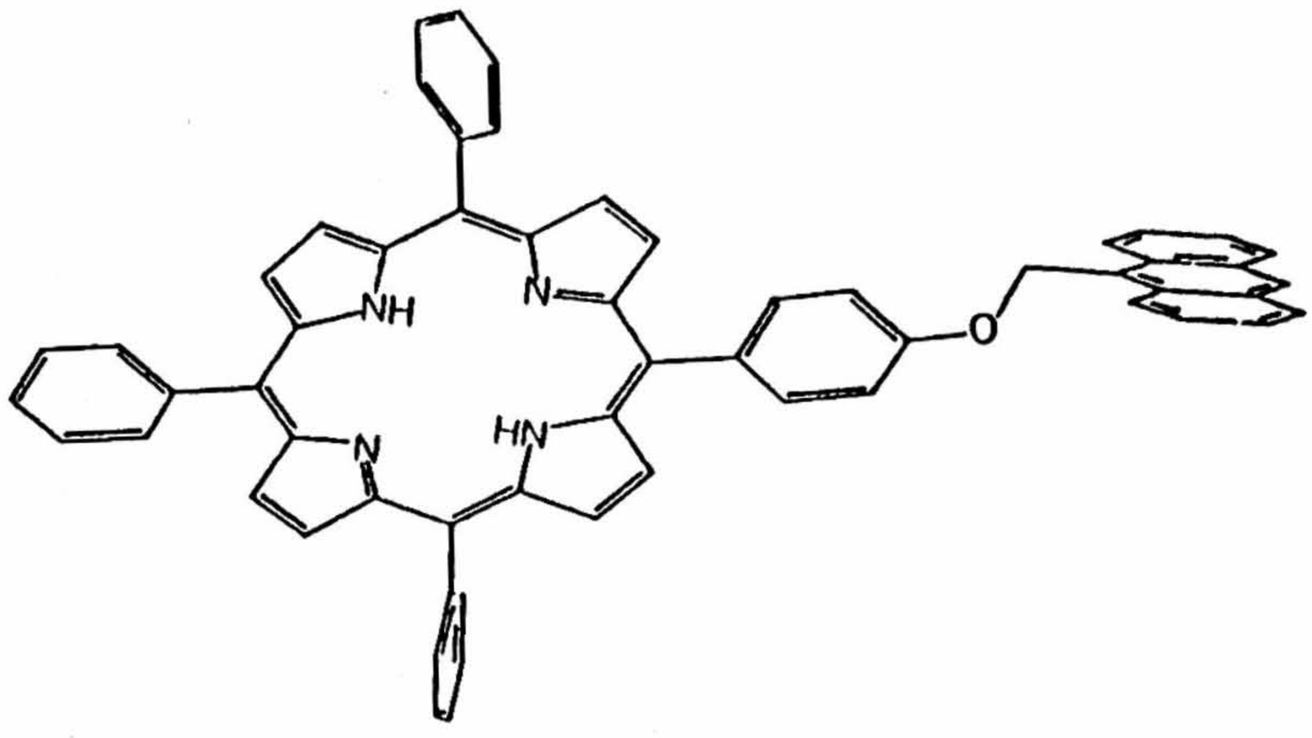

2a

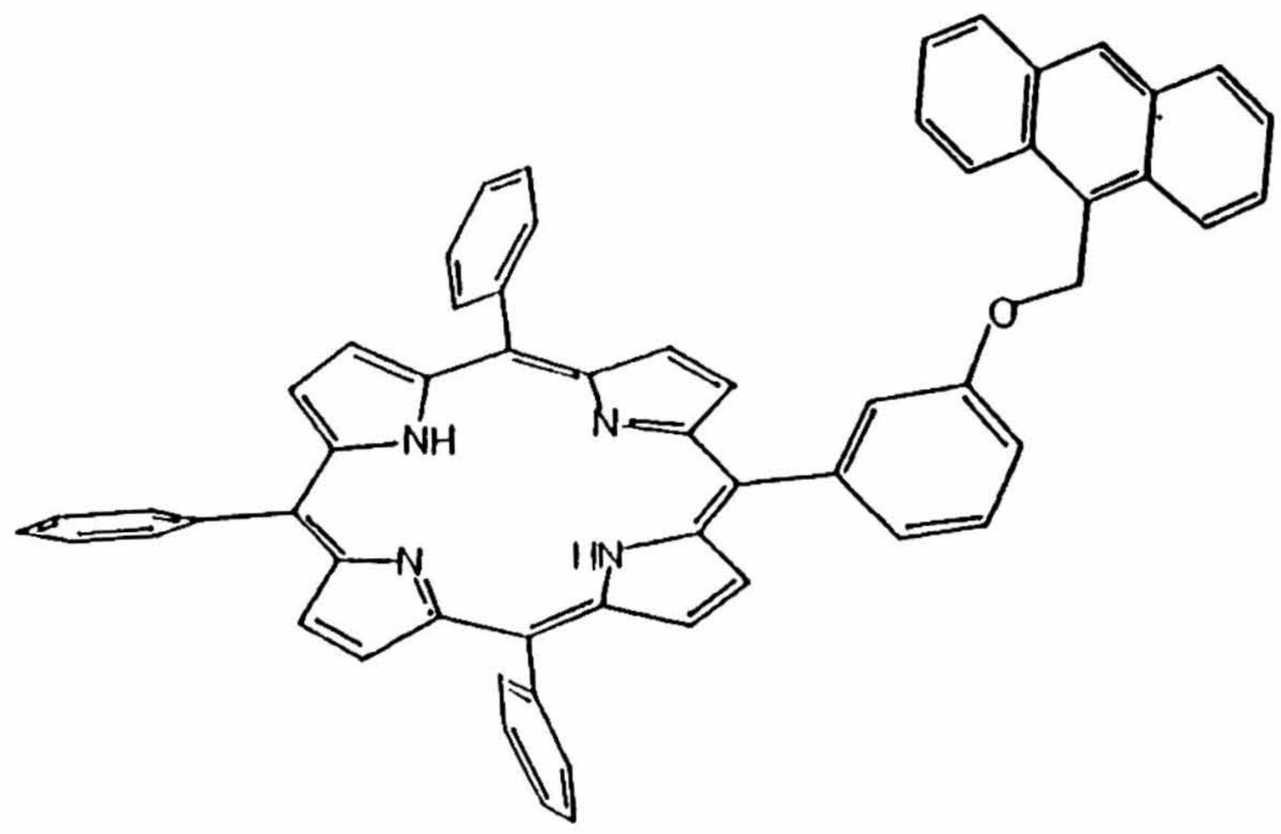

2b

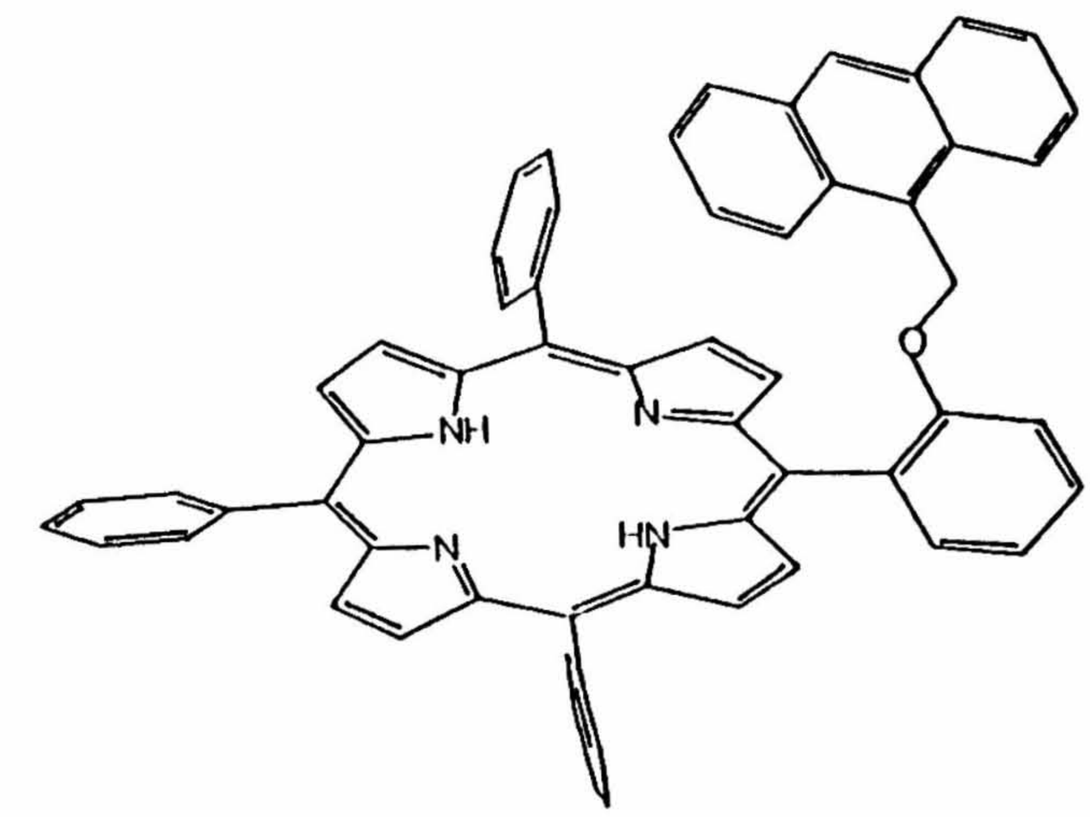

2c

Fig. 4.6. Minimum energy conformations of **2a-c** as derived from the MMX calculations.

made for these dyads under any given set of parameters (i. e. isomer, κ^2 and solvent). Similarly, k_{EN} (obs) values do not show a good correlation with the $k_{Forster}$ values calculated for EET from the ^2S state of anthracene (evaluations of J and κ^2 values pertained to long-axis polarised transition of the chromophore). Finally, the data given in this Table also suggests that k_{EN}(obs) values do not bear an inverse relationship with the refractive index (n) of the solvents as dictated by eq. 4.6. Collectively, all of these observations clearly suggest that the rates of EET in these systems are inadequately explained by Forster mechanism.

The estimated edge-to-edge approach distances (R_e) between the anthracene and the porphyrin as obtained from the MMX calculations for **2a**, **2b** and **2c** are 7.96, 7.20 and 5 08 A^o respectively. These short R_e distances may facilitate D-A orbital interactions, and promote Dexter's exchange process.[30] In addition, Dexter's mechanism involves both the lowest unoccupied molecular orbitals (LUMOs) and highest occupied molecular orbitals (HOMOs) of the donor and the acceptor, and electron exchange can occur in either a concerted process or *via* stepwise electron transfer reactions involving radical intermediates of the type D^+A^- and D^-A^+. In this regard, it can be argued that if neither electron transfer step can occur to an orbital at a higher energy level, the HOMO and LUMO of the acceptor must be either isoenergitic with or sandwiched between the levels of the HOMO and the LUMO of the donor. The later situation is found to hold good for the compounds under study as shown by the energy level diagram shown in Fig 4.7a. It can be seen that the porphyrin energy levels (P^+ and P^-) are sandwiched between those of anthracene (A^+ and A^-) and that electron exchange energy transfer from the singlet anthracene to the porphyrin subunit

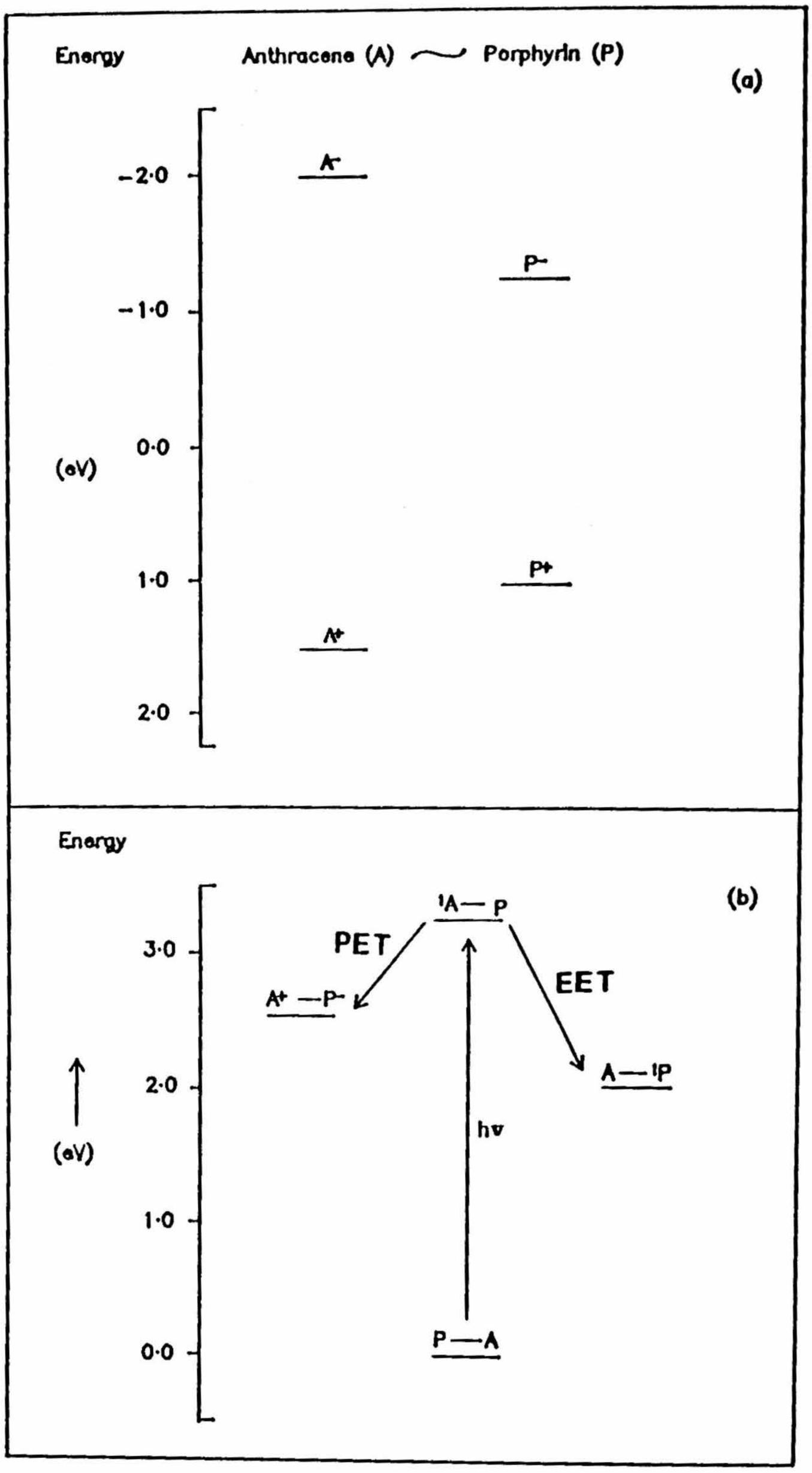

Fig. 4.7. (a) Energy levels of porphyrin (P) and anthracene (A) as derived from the electrochemical redox potential data. The reduction potential of anthracene was taken from ref. 32. (b) Energy level diagram showing both energy (EET) and electron (PET) transfer reactions from the singlet excited state of the anthracene moiety to the porphyrin in the D-A dyads. The A^+ - P^- state positioned in the figure is in CH_2Cl_2 and is sensitive to a change of solvent.

in the three isomeric dyads is possible on thermodynamic grounds. Thus, both the distance and thermodynamic criteria indicate the possibility of the involvement of electron exchange mediated energy transfer in these cases. Furthermore, it can be expected that the weak intramolecular π-π interaction observed for these dyads *(vide supra)* is likely to contribute to the electron-exchange mechanism. Despite these, it is not generally correct to consider exclusively a Forster or a Dexter mechanism for a singlet-singlet interchromophore EET and that this is especially so for systems having intermediate D-A separations such as those investigated in this study Thus, based on the analysis of the EET data presented here, it is reasonable to expect that contribution from the exchange-mediated mechanism increases as one moves from para to meta and to ortho isomer in these D-A systems with the ortho isomer showing the highest contribution

The free-energy change for an electron transfer (ΔG_{PET}) from the singlet anthracene to the porphyrin (eq. 4.8) in these systems as calculated by employing the redox potential and E_{0-0} data given in Table 4 3 is found to be exoergic by (0.53± 0.05) eV in each case (eq. 4.9)

$$A^{*}\text{-}P \longrightarrow A^{+}\text{-}P^{-} \qquad (4\ 8)$$

$$\Delta G_{PET} = E_{1/2}(A^{+}/A) - E_{1/2}(P/P^{-}) - E_{0-0} \qquad (4\ 9)$$

where $E_{1/2}(A^{+}/A)$ and $E_{1/2}(P/P^{-})$ refer to the oxidation potential of anthracene and the reduction potential of porphyrin, respectively. Fig 4.7b, which is based on eqs. 4.8 and 4.9, clearly illustrates the possibility of a PET from the singlet anthracene to the porphyrin in these dyads

Further evidence for the participation of PET reaction comes form the following two observations which can be made from the data given in Table 4.5

i) k_{EET}(obs) (or $^{0}\tau_{-ts}$) is less than k_{-ts} (or Q) for the meta- and more so for the para isomer in each investigated solvent and

ii) the ratio $^{0}\tau_{-ts}/^{0}Q$ seems to depend on the D-A distance and orientation as well as on the solvent polarity

The latter observation is illustrated in Fig. 4.8, an analysis of which clearly suggests that while the observed quenching of the anthracene fluorescence in **2c** can be explained almost entirely on the basis of an EET ($^{0}\tau_{-ts}/^{0}Q \approx 1$), the $^{0}\tau_{-ts}/^{0}Q$ ratio values of **2b** and **2a** imply a parallel quenching mechanism to be operative in these isomers. In addition, the Figure also suggests a solvent polarity dependence of $^{0}\tau_{-ts}/^{0}Q$: the more polar the solvent, the lower is the ratio. This fact coupled with the negative ΔG_{EET} values suggest that a PET reaction competes with the EET in these porphyrin-anthracene dyads. In principle, invoking this competing electron transfer mechanism can explain the excess quenching observed for the meta and para isomers that can not be reconciled solely on the basis of an energy transfer quenching. In such a case, the observed trend for the $^{0}\tau_{-ts}/^{0}Q$ (i.e. $Q > m$-
p) implies that while the energy transfer is the dominant quenching mechanism at shorter distances, it is the electron transfer that takes over at larger distances. Interestingly, the co-occurrence of energy and electron transfer observed here (Fig. 4.7b) for the porphyrin-anthracene dyads is

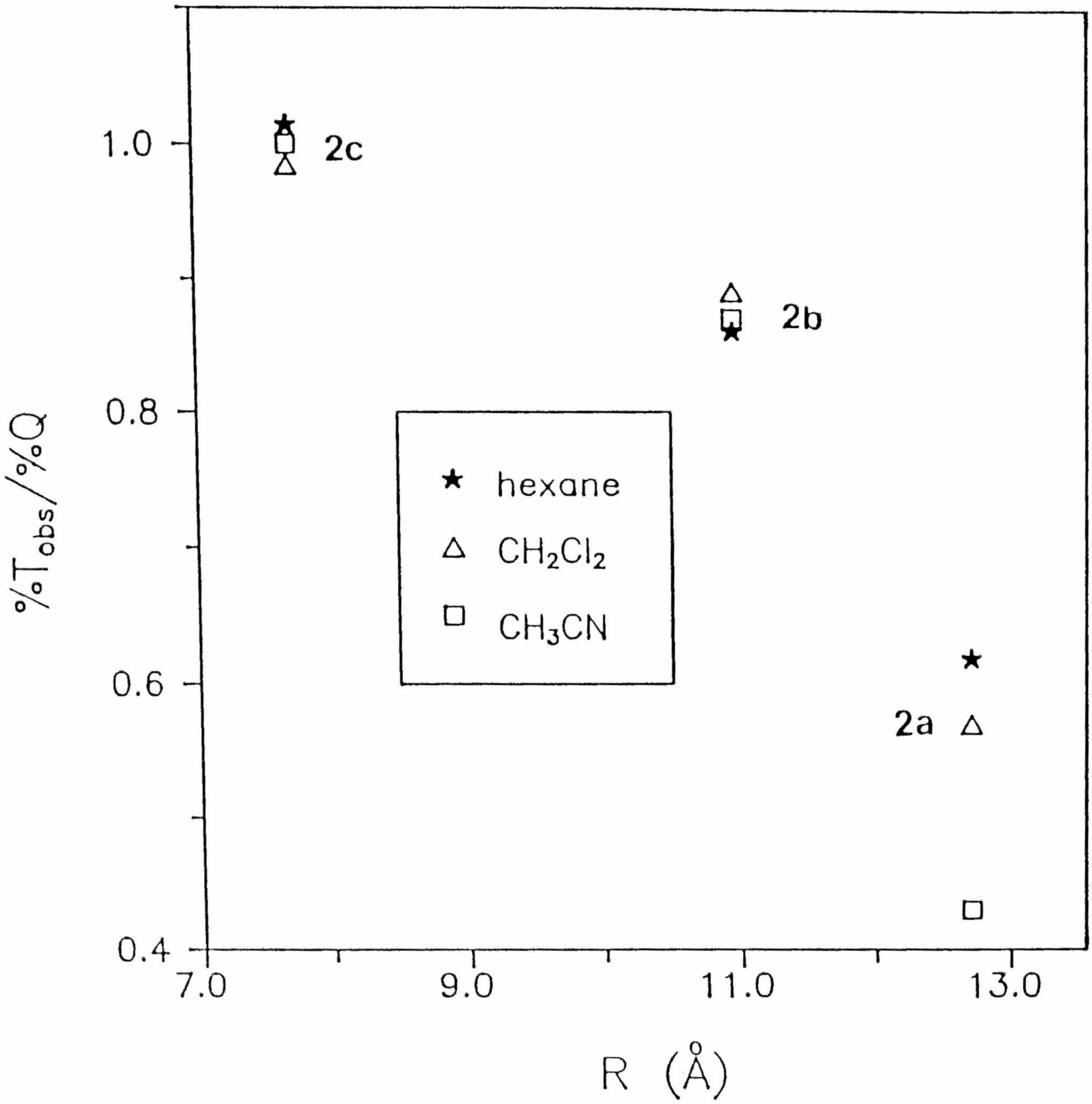

Fig. 4.8. Illustration of the D-A structure as well as solvent dependence of the intramolecular energy and electron transfer reactions in compounds **2a-c**

reminiscent of what has been reported earlier for natural chlorophyll-carotene[33,34] and synthetic porphyrin-carotene[17-19] systems.

4.4 Summary

Isomeric D-A dyads, **2a-c** in which an anthracene donor moiety is covalently linked, *via* a short ether bridge, to either ortho, meta or para position of one of the aryl groups of H_2TPP have been synthesized and characterised by spectral and electrochemical methods. UV-visible and ^1H NMR spectral data of these D-A systems suggest the presence of weak intramolecular π-π interaction between the porphyrin and the anthracene Fluorescence from the anthracene subunit in each dyad is found to be quenched in comparison with the fluorescence of free anthracene Excitation spectral data provides evidence for an intramolecular EET from the singlet anthracene to the porphyrin and the energy transfer efficiency is found to be dependent on the site of attachment (i e ortho (**2c**) > meta (**2b**) > para (**2a**)) of the donor to the acceptor Detailed analysis of the data suggests that Forster's dipole-dipole mechanism does not adequately explain this energy transfer and that an electron exchange mediated mechanism can, in principle, contribute to the intramolecular EET in these short ether bridged dyads Finally, arguments based on the thermodynamic considerations and also the solvent dependent fluorescence data reveal that while quenching of the fluorescence in **2c** could be explained solely on the basis of EET, invoking an intramolecular electron transfer reaction can rationalise the observed quenching in **2b** and **2a.**

4.5 References

1 Scholes, G D , Ghiggino, K P *J Phys Chem* **1994**, 98, 4580

2. Scholes, G. D.; Ghiggino, K. P., Oliver, A M.; Paddon-Row, M N. *J. Phys. Chem.* **1993**, 97, 11871

3. (a) Levy, S. -T.; Spesier, S *J. Chem. Phys.* **1992**, 96, 3585 (b) Levy, S. -T.; Rubin, M. D.; Speiser, S. *J. Am Chem Soc* **1992**, 114, 10747

4. Valeur, B.; Pouget, J.; Bourson, J.; Kaschke, M.; Ernsting, N. P. *J. Phys Chem.* **1992**, 96, 6545.

5. Kroon, J.; Oliver, A. M.; Paddon-Row, M. N.; Verhoeven, J W. *J. Am Chem. Soc.* **1990**, 112, 4868

6 Oevering, H ; Verhoeven, J W , Paddon-Row, M N , Cotsaris, E *Chem. Phys Lett.* **1988**, 143, 487

7. Andrews, D. L.; Sherborne, B S *J Chem. Phys* **1987**, 86, 4011

8. Craig, D. P.; Thirunamchandran, T *Acc. Chem Res* **1986**, 19, 10

9 (a) Wasielewski, M R *Chem Rev* **1992**, 92, 435 (b) Gust, D , Moore, T. A. *Adv. Photochem* **1991**, 16, 1

10. Balzani, V ; Scandola, F In *Supramolecular Photochemistry.* Ellis Horwood: Chichester, 1991

11. Yamamoto, M., Ito, S , Ohmori, S In *Photochemical Processes in Organized Molecular Systems.* Honda, K , Ed , Elsevier Amsterdam, 1991.

12. Kalyanasundaram, K In *Photochemistry in Microheterogeneous Systems;* Academic : New York, 1987

13. Guillet, J. E.; In *Polymer Photophysics and Photochemistry.* Cambridge University : Cambridge, 1985

14. Boxer, S. G. *Biochim Biophys Acta* **1983**, 723, 965.

15. Sessler, J. L.; Capuano, V. L.; Harriman, A *J Am. Chem Soc.* **1993**, 115, 4168, and references therein

16. Lindsey, J. S.; Brown, P. A.; Siesel, D. A. *Tetrahedron* **1989**, 45, 4845.

17. Gust, D.; Moore, T. A.; Bensasson, R. V.; Mathis, P.; Land, E. J. Chachaty, C.; Moore, A. L.; Liddell, P A.; Nemeth, G. A. *J. Am. Chem. Soc.* **1985**, 107, 3631.

18. Gust, D.; Moore, T. A.; Moore, A. L.; Devadoss, C.; Liddell, P. A.; Hermant, R.; Nieman, R A.; Demanche, L. J.; DeGraziano, J. M.; Gouni, I.; *J. Am. Chem. Soc* **1992**, 114, 3590.

19 Hermant, R , Liddell, P A., Lin, S ; Alden, R. G.; Kang, H. K.; Moore, A. L ; Moore, T A ; Gust, D *J Am. Chem. Soc.* **1993**, 115, 2080

20. Osuka, A.; Yamada, H , Maruyama, K , Mataga, N , Asahi, Ohkouchi, M. T.; Okada, T.; Yamazaki, I ; Nishimura, Y. *J. Am. Chem. Soc.* **1993**, 115, 9439.

21. Effenberger, F., Schlosser, H.; Bauerle, P ; Maier, S.; Port, H.; Wolf, H C. *Angew Chem., Int Ed Engl.* **1988**, 27, 281

22 Sirish, M ; Maiya, B G *J. Photochem. Photobiol , A: Chemistry* **1994**, 77, 189.

23. Rao, T. A.; Maiya, B. G. *Polyhedron* **1994**, 13, 1863.

24. Abraham, R J , Fell, S. C. M , Smith, K. M. *Org. Mag. Reson.* **1977**, 9, 367.

25. Singh, A K.; Roy, M. *J. Photochem. Photobiol. B Biol.* **1991**, 8, 325.

26. Lifetimes are either measured in this laboratory as described in Chapter 2 or taken from : Murov, S L , In *Handbook of Photochemistry;* Marcel Dekker: New York, 1973.

27. Bergkamp, M. A.; Dalton, J ; Netzel, T. L. *J. Am. Chem. Soc.* **1982**, 104, 253.

28. Quimby, D J , Longo, F R *J. Am Chem Soc.* **1975**, 97, 5111.

29. Forster, Th. *Discussions Faraday Soc.* **1959**, 27, 7.

30. Dexter, D. L. *J. Chem. Phys.* **1953**, 21, 836.

31. Gouterman, M. *J. Mol. Spectrosc.* **1961**, 6, 138.

32. Mann, C. K. In *Electrochemical Reactions in Nonaqueous Systems*, Marcel Dekker, New York, 1970.

33. Beddard, G. S.; Davidson, R. S.; Trethewey, K. R. *Nature* **1977**, 267, 373.

34. Deming-Adams, B. *Biochim. Biophys. Acta* **1990**, 1020, 1.

CHAPTER 5

Excitation Energy Transfer In a Supramolecular Porphyrin Bearing Four Anthracene Donor Moieties

5.1 Introduction

In the previous chapter, intramolecular excitation energy transfer (EET) occurring in covalently linked dyads in which a tetraphenyl porphyrin is linked to an anthracene donor at *only one* of its meso-phenyl rings has been presented. The architectural symmetry of the porphyrin skeleton, however, permits more than one energy donor to be attached to its periphery and the ensuing supramolecular, bichromophoric, pentad system is expected to show an 'antenna effect' Attempts have been made earlier to build porphyrin-based antenna systems. For example, pentads comprising of a central core-porphyrin that is linked to four peripheral porphyrin units have been reported [1-3] Free base- or metallo-porphyrins attached to four photon-harvesting hydrocarbon moieties have also been known, naphthalene,[4,5] anthracene,[5,6] phenanthrene,[7] pyrene[7] and pyrazole[8] groups have been linked directly to four meso-carbon centres of a porphin In the last three cases, steady state fluorescence spectroscopy has indicated intramolecular energy transfer from the attached hydrocarbon units to the central porphyrin [8-10] An analysis of the results described in all of these studies suggests that neither the attached hydrocarbon moiety nor the porphin itself retains its individual characteristics in these systems In this sense, donor-acceptor (D-A) systems in which the energy donors are linked directly to the

porphyrin periphery cannot be accurately described to possess an antenna function.

Thus it can be suggested that, in order to exhibit an antenna function, it is essential to have multicomponent structure in which the donors and the acceptors retain their individual characteristics The microstructure of such a supramolecular porphyrin should favour high local concentrations of the light-harvesting chromophores without forming intermolecular aggregates which are notorious energy-wasting sinks.[11] Furthermore, for a realistic description of the photosynthetic antenna function, a porphyrin-based model system should exhibit an electron transfer reaction [12-14] All of these considerations indicate that a molecular pentad system, in which a porphyrin acceptor is linked, *via* spacers, to four appropriately positioned donor hydrocarbons, forms a suitable choice for the demonstration of a biomimetic antenna function

This chapter describes the synthesis and results on photophysical studies of a pentad system in which a 5,10,15,20-(tetraphenyl)porphyrin (H_2TPP) is linked, *via* ether bridges, to four anthracene donor moieties (5,10,15,20-tetra(3-(9-methyloxy-anthracenyl)phenylporphyrin, a D_4-A pentad **2**, Scheme 5 1) A detailed analysis of the spectroscopic, electrochemical and solvent-dependent fluorescence data indicates the occurrence of both energy- and electron transfer reactions in this supramolecular porphyrin The photophysical properties of **2** are compared with those of the molecular dyads described in chapter 4

5.2 Experimental

5.2.1 Synthesis of meso-5,10,15,20-tetra(3-(9-methyloxyanthracenyl) porphyrin (2)

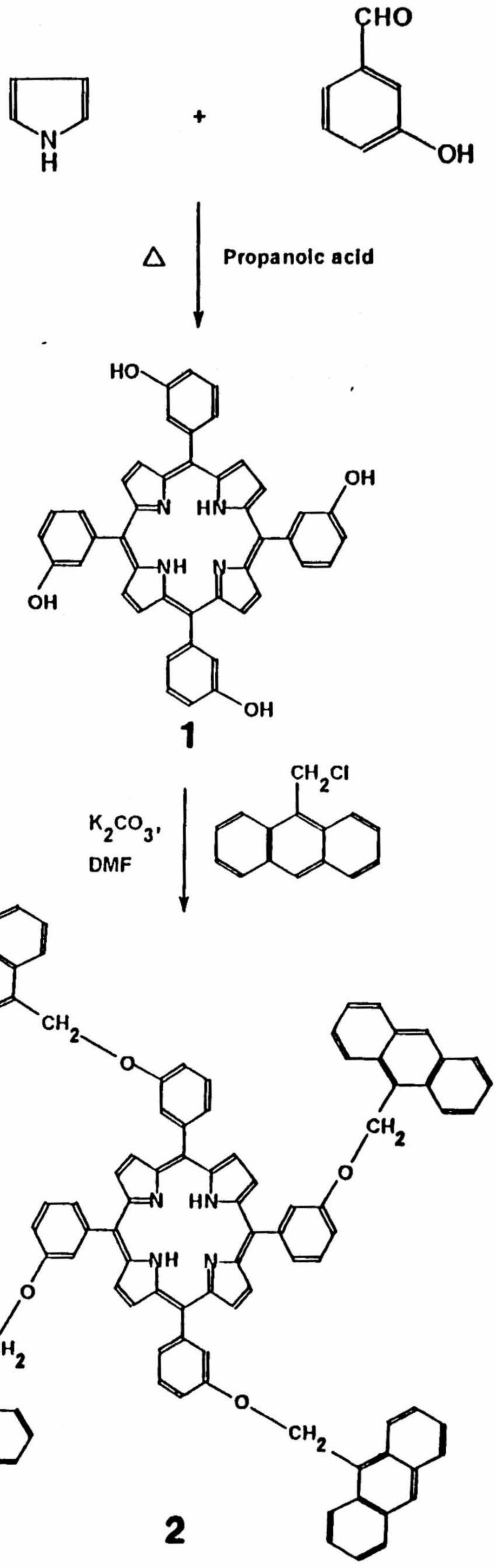
CHO
OH
+
N
H
Δ
Propanoic acid
HO
OH
N
HN
NH
N
OH
OH
1
K_2CO_3,
DMF
CH_2Cl
CH_2
O
CH_2
O
CH_2
O
CH_2
O
2

Scheme 5.1

Compound **2** was synthesized by condensing 1 mol equivalent of **1**[15] with an excess of 9-chloromethylanthracene in dimethylformamide using K_2CO_3 as a base. Reaction conditions and the work-up procedure were similar to those employed for the synthesis of porphyrin-anthracene dyads described in Chapter 4. The compound was purified on an alumina column using $CHCl_3$-CH_3OH (10.1 V/V) as an eluent (yield· ≅60%) Purity of the sample was checked by thin layer chromatography, analytical data and ^1H NMR methods. Analytical data· obsd.: C, 84.68; H,4.84, N, 3 76. calcd. for $C_{104}H_{70}N_4O_4$: C, 86.60, H,4 87, N, 3.88 ^1H NMR ($CDCl_3$, TMS δ_H (ppm) 8.96 (s, 8H; pyrrole), 8.45 (m, 10H, 1,8-anthryl and o-phenyl porphyrin), 7.98 (m, 14H; 4,5-anthryl and m-and p-phenyl porphyrin), 6 15 (s, 2H, -OCH_2, spacer), -2.76 (br, s, 2H, -NH porphyrin).

Zinc(II) and copper(II) derivatives of **2** were prepared, in quantitative yields, by refluxing a $CHCl_3$·CH_3OH solution of the compound in the presence of excess metal salts, and were purified by column chromatography on alumina ($CHCl_3$ eluent)

Synthesis of the reference compound 9-methoxyphenyl anthracene, **3** has been described in chapter 4.

5.2.2 Metallation kinetics

To a 5 x 10^{-5} M of **2** or H_2TPP dissolved in $CHCl_3$ CH_3OH (1 1, V/V) mixture were added 5 x 10^{-4} - 3 x 10^{-3} M zinc(II) acetate solutions in separate experiments and the metalltion rates were monitored spectrophotometrically by observing the decrease of absorbance at 515 nm in each case The derived pseudo-first order rate constants were plotted against [Zn^{2+}] to obtain the second order rate constants

5.2.3 Fluorescence quenching by 2,4-dinitrobenzene (DNB)

Fluorescence intensities were measured (600 -750 nm), for $CHCl_3$ solutions of **2** or H_2TPP (2×10^{-6} M) with and without added DNB (2×10^{-6} - 1×10^{-3} M), by exciting at 420 nm Plots of I_o/I (I_o and I are fluorescence intensities in the absence and the presence of DNB) versus [DNB] was found to be linear in each case.

Each investigated porphyrin was purified on a short alumina column before spectral measurements were made. All the spectroscopic and electrochemical experiments have been carried out as described in chapter 2.

5.3 Results and discussion

5.3.1 Ground state properties

The UV-visible spectral data of the supramolecular pentad **2** along with its individual constituents (H_2TPP and **3**) are summarized in Table 5 1. Fig. 5.1 shows the spectrum of **2** in CH_2Cl_2. As seen, **2** shows bands due to both porphyrin (400-600 nm) and anthracene (200-400 nm) absorptions. Furthermore, the spectrum is similar to the one obtained for a solution containing 1 mole equivalent of H_2TPP and 4 mole equivalents of anthracene. A comparison of the ^1H NMR spectrum of **2** (Fig. 5 2) with the spectra of H_2TPP and **3**, suggests that, except for the spacer-OCH_2 protons (which are slightly deshielded for **2** in comparison with **3**), the peak positions of all the other protons in **2** are not altered significantly with respect to those of the corresponding protons in the constituent partners. Moreover, the EPR spectrum of the copper(II) derivative of **2** showed g and A values ($g_{||} = 2\ 204 \pm 0\ 001$, $g_{\perp} = 2\ 033 \pm 0\ 001$, $A_{||}^{Cu} = (199 \pm 4) \times 10^{-4}$ cm^{-1}, $A_{||}^{N} = (14 \pm 1) \times 10^{-4}$ cm^{-1}) similar to those observed for CuTPP[16] ($g_{||}$

= 2.203 ± 0.001, $g_{\perp}$ = 2.027 ± 0.001, A_{II}^{Cu} = (198 ± 1) x 10^{-4} cm^{-1}, A_{II}^{N} = (14 ± 1) x 10^{-4} cm^{-1}) (toluene, 100 ± 3 K)

Table 5.1 : UV-visible spectral data in CH_2Cl_2.

Compound	λ_{max}, nm (log ε)							
	Porphyrin transitions					Anthracene transitions		
	Q_1	Q_2	Q_3	Q_4	B	I	II	III
H_2TPP	645 (3.67)	590 (3 6)	548 (3 7)	514 (4 22)	417 (5 5)			
Anthracene						378 (3 8)	359 (3 8)	255 (5 19)
2	649 (3 75)	590 (3.7)	550 (3.8)	515 (4 27)	420 (5 6)	387 (4.8)	350 (4 6)	257 (5 79)
3						387 (3 8)	359 (3 8)	257 (5.29)

The differential pulse voltammetric experiments reveal that the electrochemical redox potentials of **2** do not vary significantly from those of its individual constituents, (Fig 5.3) The porphyrin part of **2** is oxidized and reduced at (1.08 ± 0.03) V and (-1 19 ± 0.03) V respectively, and all four of

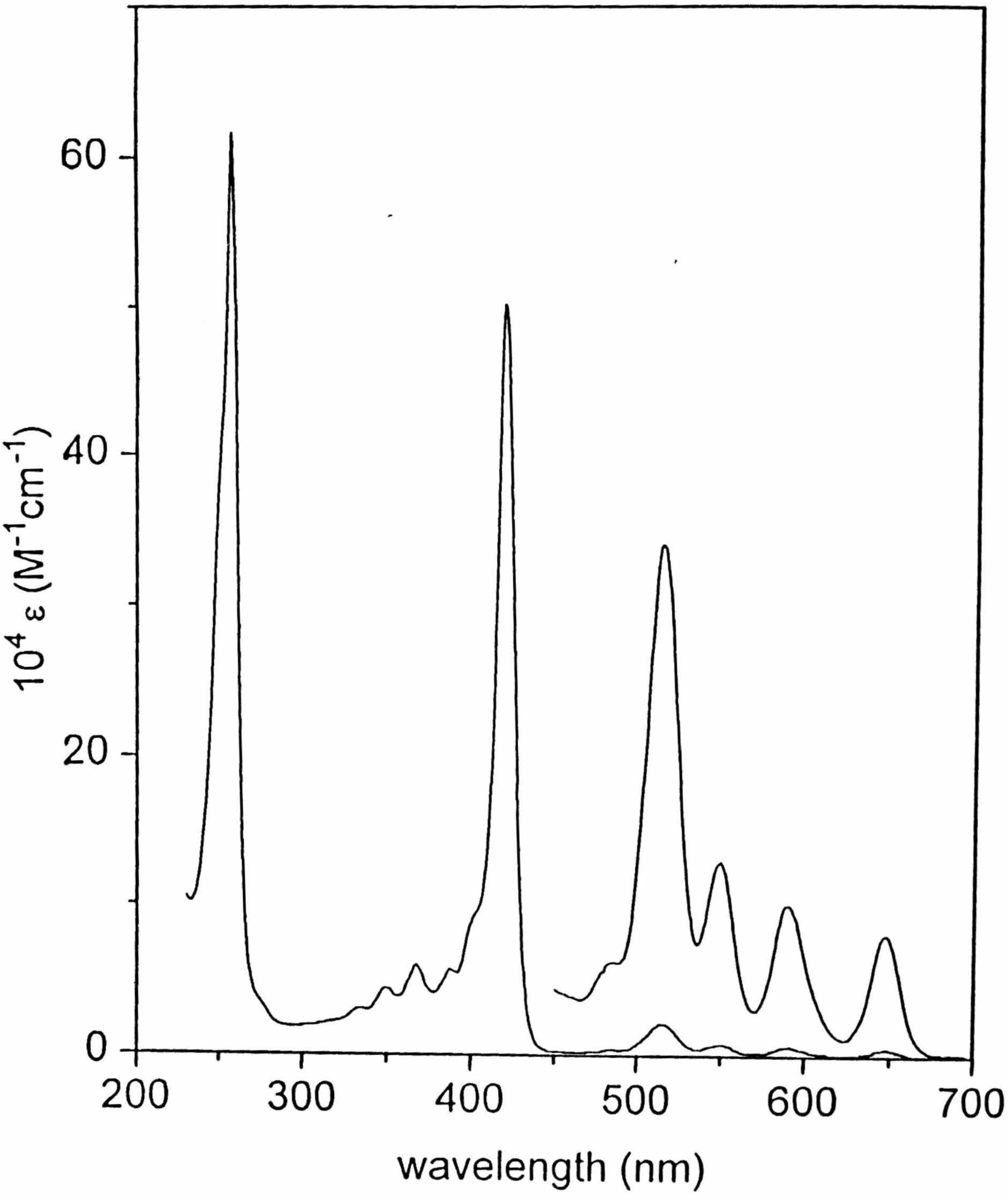

Fig. 5.1. UV-visible spectrum of **2** in CH_2Cl_2. (The Q-band region is expanded 15 times for clarity).

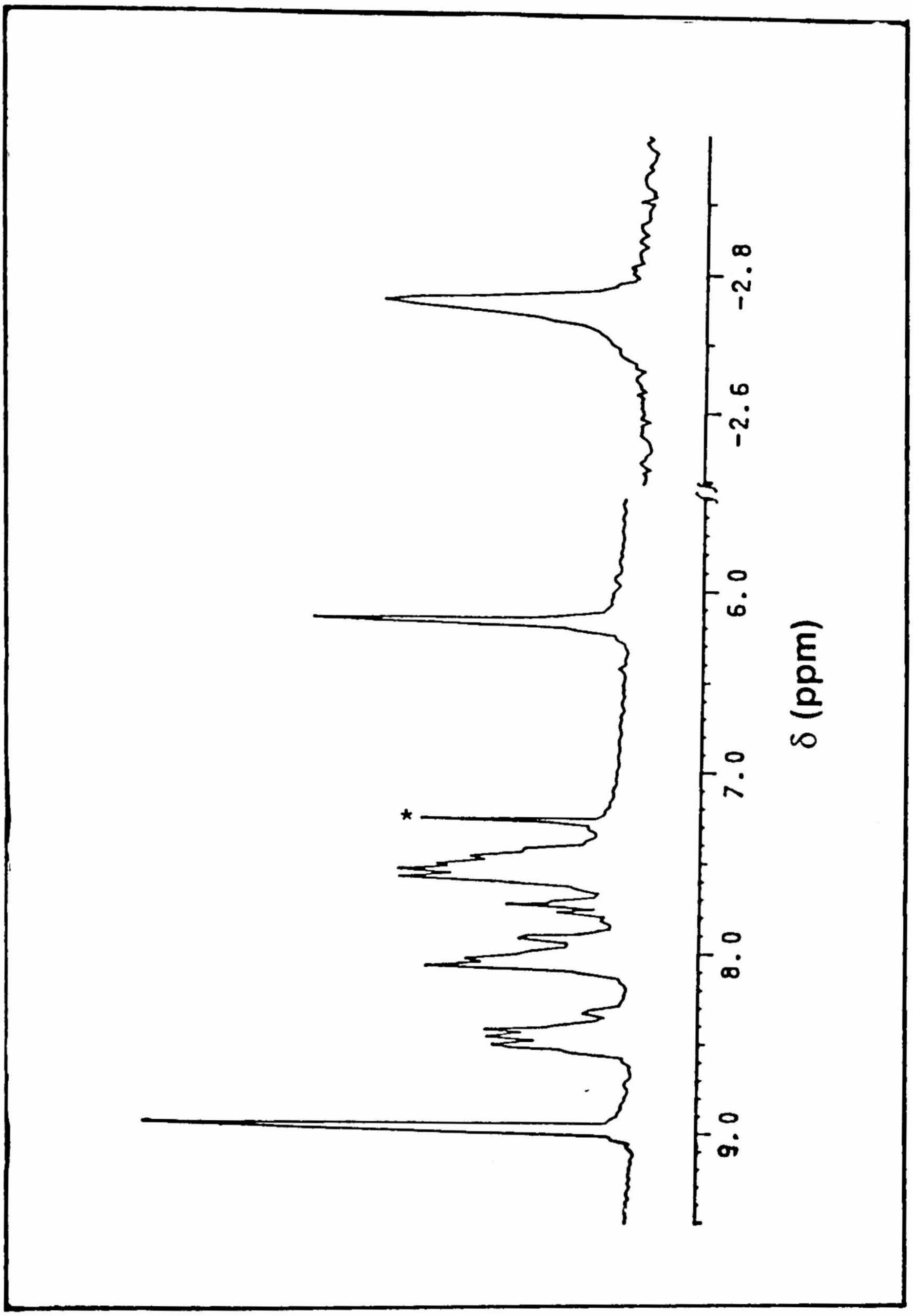

Fig. 5.2. ^{1}H NMR spectrum of 2.

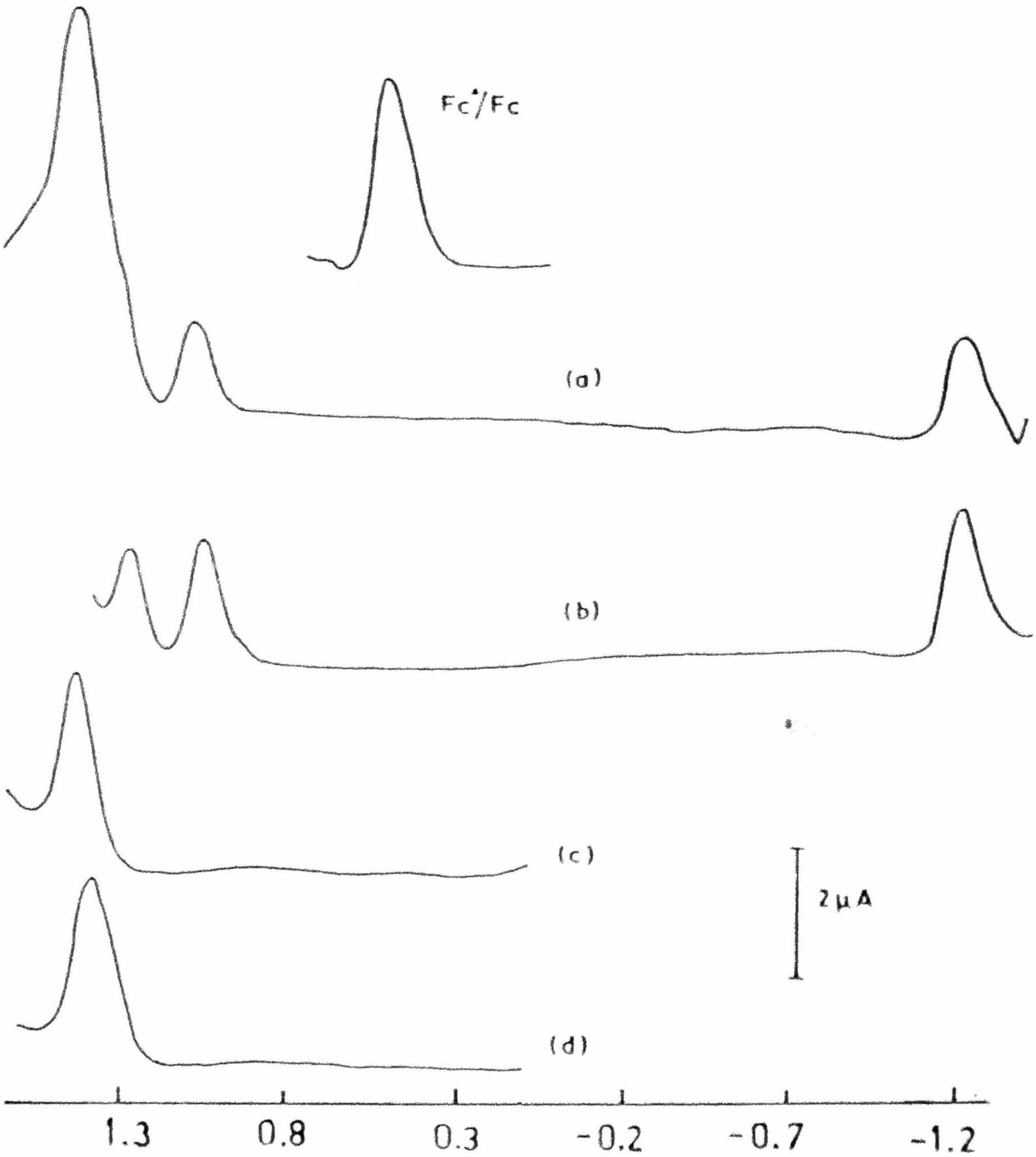

Fig. 5.3. Differential pulse voltammograms of **2** (a), H_2TPP (b), **3** (c), and anthracene (d) in CH_2Cl_2, 0.1 M TBAP (scan rate, 10 mV s^{-1}, modulation amplitude ΔE = 10 mV) The potential axis is referenced with respect to SCE Fc, ferrocene

the anthracene subunits are oxidized in a single step at (1 51 ± 0 04) V (the peak having a large current value in Fig 5.3). Thus, UV-visible, ^{1}H NMR, EPR and redox potential data of **2** suggest that there is no appreciable interaction between the porphyrin and the anthracenes in this molecule Therefore, the microstructure around the porphyrin is sufficiently "porous" and is devoid of perturbations arising from either crowding of the four anthracene subunits or π-π interactions between the porphyrin and anthracenes.

The above proposition is further substantiated by metallation reaction kinetics, excited state intermolecular electron transfer kinetics of the porphyrin part of **2** and structure simulation studies employing molecular mechanics (MMX) calculations In CH_3OH-$CHCl_3$ (1·1, V/V) mixtures, the second-order rate constants for zinc(II) insertion into **2** and H_2TPP are (0 28 ± 0.03) $M^{-1}s^{-1}$ and (0 35 ± 0 04) $M^{-1}s^{-1}$ respectively. The bimolecular rate constants (k_q) for the steady state fluorescence quenching of **2** and H_2TPP (excitation at 420 nm where only the porphyrin part absorbs) by 2,4-dinitrobenzene (DNB) are (4 3 ± 0.4) x 10^9 and (5 4 ± 0 6) x 10^9 $M^{-1}s^{-1}$ (τ (H_2TPP) = 8.00 ns, λ_{exc} = 515 nm) [17] It has been proposed that quenching of H_2TPP by DNB involves a photoinduced electron transfer (PET) reaction,[18] and the similarity between the k_q values observed for H_2TPP and **2** indicates that an intermolecular PET mechanism is also operative in the quenching of **2**. Thus, both metallation and bimolecular fluorescence quenching experiments strongly indicate that the attached anthracene subunits do not physically hinder the approach of small molecules such as Zn^{2+} or DNB to the core porphyrin part of **2**. This situation is similar to that observed for a tetraporphyrin-substituted tetraphenylporphyrin [2] Finally, MMX calculations and Corey-Pauling-Kolton models of **2** suggest that the

anthracene subunits on this molecule are tilted away from the face of the porphyrin, thus avoiding mutual repulsions. The average centre-to-centre *(ctc)* distance, R_c between the anthracenes and the porphyrin is 10.5 A^o and the average dihedral angle encompassing $C_{3\text{-phenyl}}$-O-C_{CH_2}-$C_{9\text{-anthryl}}$ is 162 ± 30.

5.3.2 Singlet state properties

In CH_2Cl_2 solutions, excitation into the porphyrin (420 nm) and the anthracene (250 nm) band maxima of **2** gave the fluorescence spectra which are shown in Fig. 5.4. The corresponding fluorescence peak maxima are given in Table 5.2. The spectral shape and band maxima observed when **2** was excited at 420 nm are similar to the corresponding parameters for H_2TPP. However, the maxima of the fluorescence bands observed in the anthracene emission region of **2** (excitation at 250 nm) are slightly red shifted in comparison with the fluorescence maxima of anthracene itself. The 0-0 spectroscopic transition energies ($E_{0\text{-}0}$) of the anthracene moiety (3 25 ± 0.05 eV) and the porphyrin moiety (2 02 ± 0 05 eV) of the molecule are similar to the $E_{0\text{-}0}$ values of anthracene[19] and H_2TPP,[20] respectively. All of these observations are similar to what was observed for the porphyrin-anthracene dyads described in the previous chapter

Although, the fluorescence quantum yield (ϕ_f) value for excitation into the porphyrin moiety of the molecule (ϕ_f = 0 11) is similar to that for H_2TPP (ϕ_f = 0 11),[21] ϕ_f for excitation into the anthracene moiety of the molecule (ϕ_f = 0.012) is strongly quenched in comparison with the fluorescence of anthracene (ϕ_f = 0 24) in CH_2Cl_2 solution.[19] These observations are illustrated in Fig 5 4 The fluorescence spectra were also

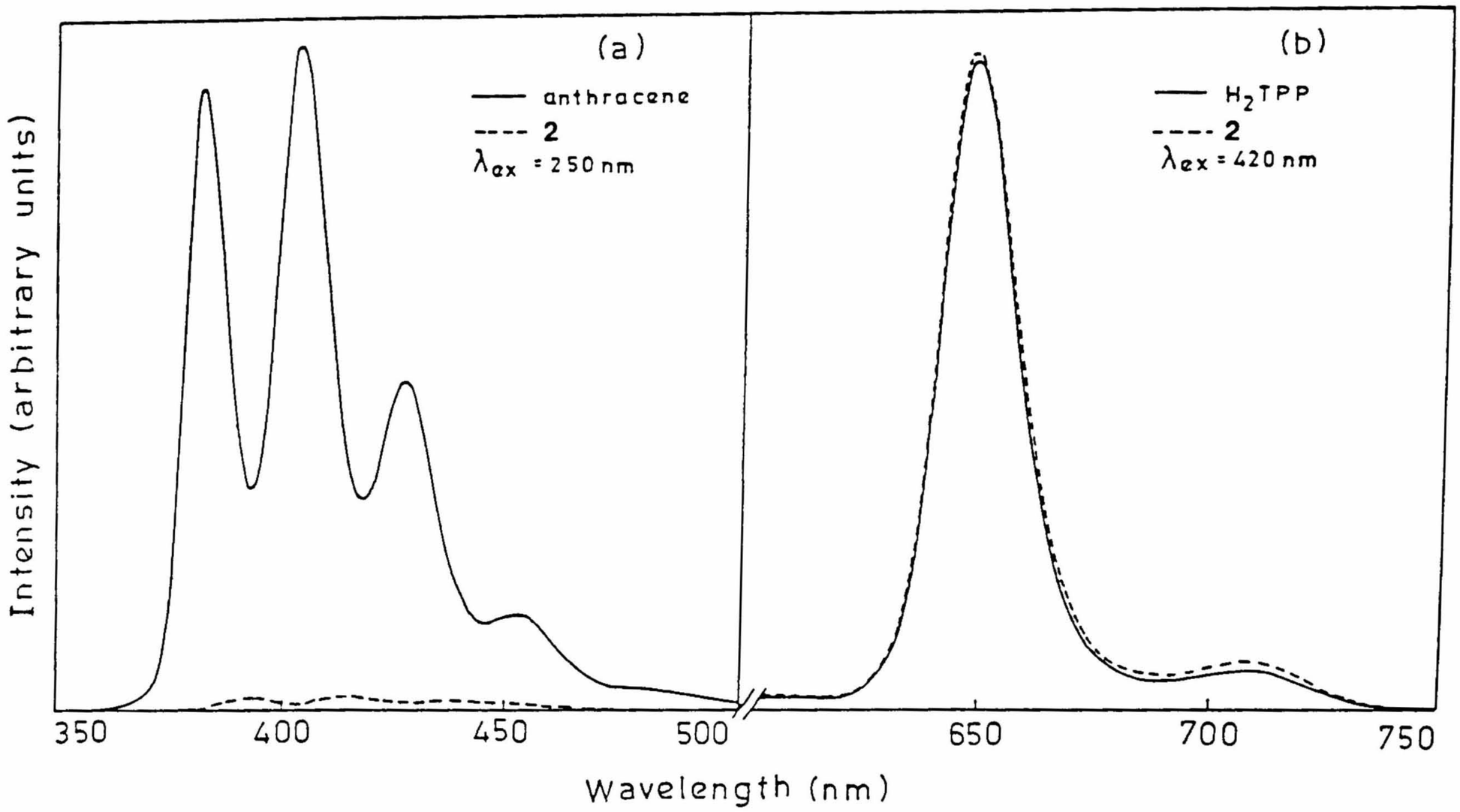

Fig. 5.4. Comparison of the fluorescence spectra of equi-absorbing solutions (optical density at $\lambda_{ex} = 0.11$) of (a) anthracene and **2** and of (b) H_2TPP and **2**.

taken in hexane and CH_3CN and the spectral data obtained in all the three sovlents are summarized in Table 5.2.

Table 5.2 Steady state fluorescence data.

Compound	**Hexane**		**CH_2Cl_2**		**CH_3CN**	
	λ_{max} (nm)	**ϕ_f**	**λ_{max}** (nm)	**ϕ_f**	**λ_{max}** (nm)	**ϕ_f**
	Porphyrin band excitation (λ_{ex} = 420 nm)					
H_2TPP	650,713	0 11	648,708	0.11	648,707	0 12
2	653,713	0 11	648,709	0.11	647,707	0.11
	Anthracece band excitation (λ_{ex} = 250 nm)					
Anthracene	377,398, 421,447	0.27	382,403, 427,452	0.24	379,401, 424,449	0 35
2	388,410,	0.02	393,413,	0.01	391,412, 436,465	0.005

From the ϕ_f values given in this Table, the quenching efficiencies of **2** in the three solvents were calculated using the eq 5.1.

$$Q = \frac{\phi_f(\text{anthracene}) - \phi_f(\mathbf{2})}{\phi_f(\text{anthracene})} \qquad (5.1)$$

and these values follow the order 99%(CH_3CN) > 95%(CH_2Cl_2) > 93%(hexane). As was the case with the dyads described previously, this quenching is not due to the competitive absorption by the porphyrin part of **2**, as the contribution of the porphyrin absorption at 250 nm is insignificant for this molecule.

Fig.5.5 shows a considerable overlap between the emission of anthracene moieties in **2** and the absorption of H_2TPP. As suggested earlier for the porphyrin-anthracene dyads (chapter 4), fluorescence quenching of the anthracene moieties in **2** may be due to an intramolecular energy transfer from the excited singlet anthracenes to the porphyrin Indeed, excitation of **2** at 250 nm results in the appearance of porphyrin emission bands in the 600-750 nm region in all three solvents

Further evidence of intramolecular EET in **2** comes from the excitation spectral data. An overlay of the corrected and normalised excitation spectra of **2** with the corresponding absorption spectra in the three investigated solvents is shown in Fig 5.6. A comparison of the excitation and absorption spectra in the 45 5 x 10^3 to 37.0 x 10^3 cm^{-1} (220-270 nm) region suggests energy transfer efficiencies (T_{obs}) of (76 ± 7)%, (64 ± 6)%, and (36 ± 4)% in hexane, CH_2Cl_2 and CH_3CN, respectively It should be noted here that, in each solvent, the T_{obs} values are lower than the Q values given above and that opposite trends are obtained for T_{obs} (CH_3CN < CH_2Cl_2 < hexane) and Q (CH_3CN > CH_2Cl_2 > hexane) in this solvent series

That the intermolecular energy transfer between the porphyrin and the anthracene is not obvious from the steady state spectral measurements has been demonstrated in the previous chapter Consistent with this is the

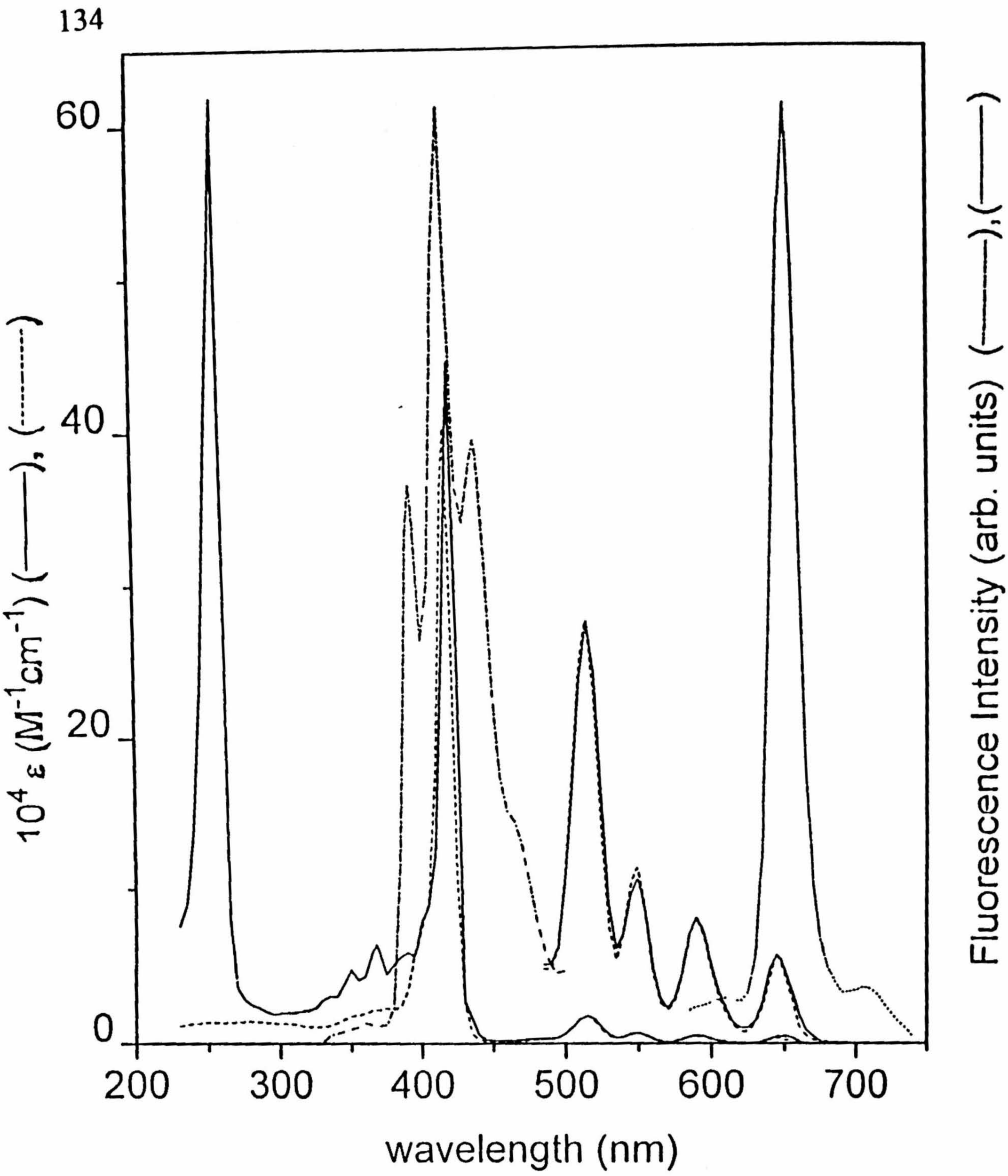

Fig. 5.5. UV-visible spectra of H_2TPP (--------) and **2** (———) and fluorescence spectra of **2** obtained on excitation at the anthracene (250 nm) absorption peak (–·–·–·–) and porphyrin (420 nm) absorption peak (·····). The solvent was CH_2Cl_2. The spectra were regenerated using absorption/fluorescence data obtained at 5 nm intervals. The spectra were normalized for clarity.

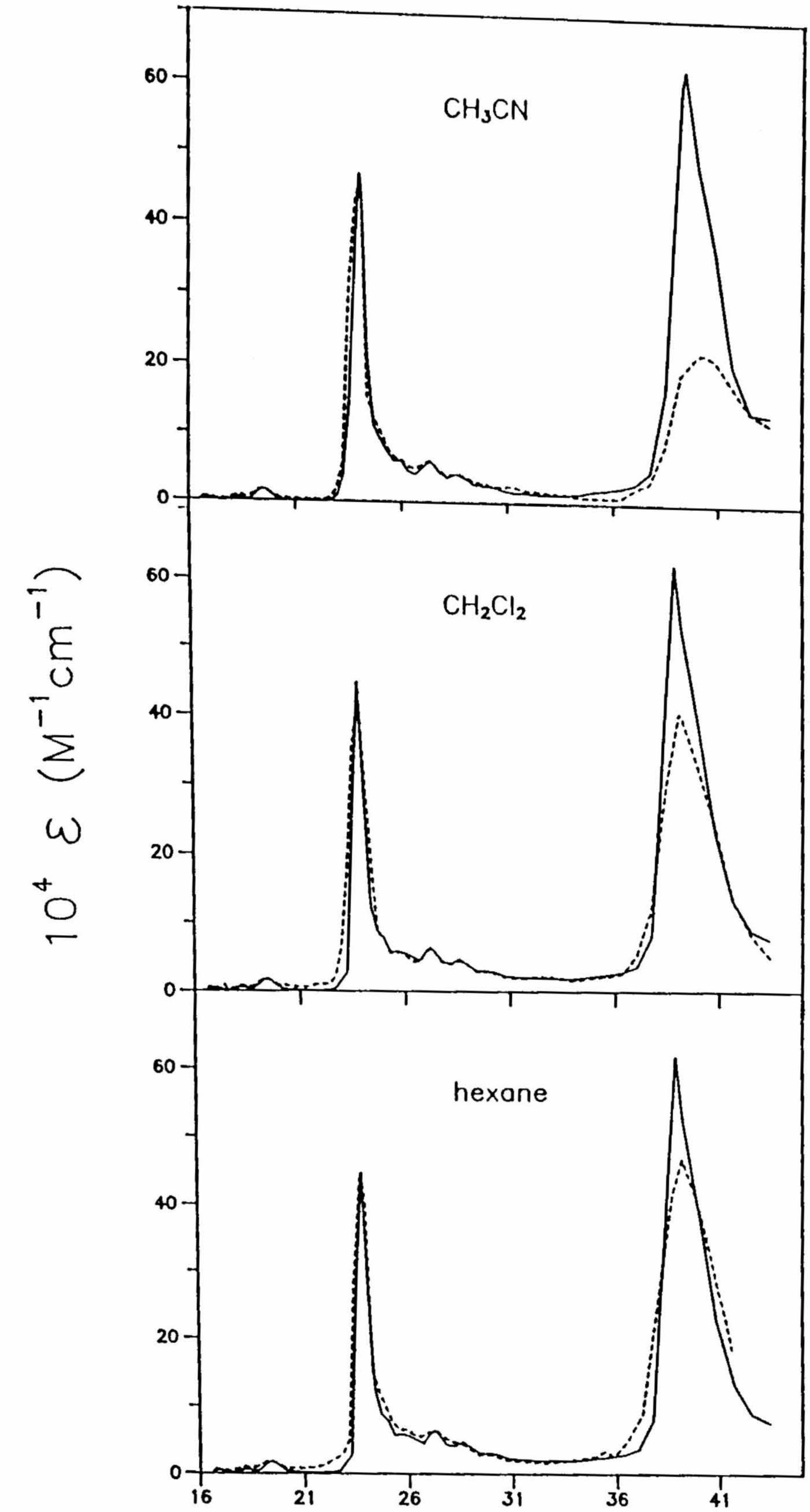

Fig. 5.6. Overlay of the excitation (·····) and the absorption (——) spectra ot **2** in CH_3CN, CH_2Cl_2 and hexane (λ_{em} = 650 nm). The excitation spectra were corrected for the instrument response function and were normalized with respect to the absorption spectra between 16.6 x 10^3 cm^{-1} 600 nm and 20.0 x 10^3 cm^{-1} (500 nm).

observation made in this study that the excitation spectra (λ_{exc} = 650 nm) obtained for 4:1 and 1:1 (mol/mol) mixtures of anthracene and H_2TPP are indistinguishable from the spectrum obtained for H_2TPP alone. In addition, it was also observed that the emission of both anthracene and porphyrin moieties is independent of the concentration of **2**. This latter observation not only shows that concentration quenching does not occur in **2**, but also rules out trivial reabsorption in this supramolecular complex.

Having noted the occurrence of intramolecular energy transfer in **2**, it is of interest to investigate the possible mechanisms of energy transfer and to rationalize the opposite trends obtained for T_{obs} and Q values in the three solvents. In principle, singlet-singlet energy transfer can proceed through either Forster's dipole-dipole mechanism[22] or Dexter's electron exchange mechanism.[23] As most experimental observations of singlet-singlet energy transfer reactions in porphyrin-based D-A systems similar to **2** have been interpreted in terms of Forster's mechanism,[12,24] we consider this first.

Key parameters for the Forster type energy transfer in **2** have been obtained as described in the previous chapter for the porphyrin-anthracene dyads (eqs. 4.1-4.7) and the data are summarized in Table 5.3 It should be noted here that the value of κ^2 has been taken to be equal to 0 66 assuming average orientation of anthracenes with respect to the porphyrin plane in the excited state of **2**. This assumption is valid for this compound as both ^1H NMR and structure simulation studies (see above) show average orientation of four anthracenes around the porphyrin In particular, the results do not indicate the presence of atropisomers (or rotamers) for **2** that are quite common for ortho-substituted tetraphenylporphyrins but not for meta-substituted tetraphenylporphyrins such as **2**

Table 5.3 Energy transfer data [a]

	Hexane	CH_2Cl_2	CH_3CN
n [b]	1.375	1.425	1 344
ε [b]	1.88	8 93	37.50
Q (%)	93	95	99
R_0 (A°)	15.6	14.4	16.0
T_{cal} (%)	91	87	92
T_{obs} (%)	76	64	36
ΔG_{PET} [c] (eV)	-0.21	-0 70	-0 80
k_{EN} (cal) (10^9 s^{-1})	2 1	1.3	2 3
k_{EN} (obs) (10^9 s^{-1})	0 65	0 34	0.11
k_{obs} (10^9 s^{-1})	2 7	3 7	18 7
k_{obs}-k_{EN} (obs) (10^9 s^{-1})	2 1	3.4	18 6

(a) Error limits : Q, ΔG_{PET} and k_{obs}, ±5%, R_0, T_{cal} and k_{EN}(cal), ±7%, T_{obs} and k_{EN}(obs), ±10%.

(b) n and ε are the refractive index and dielectric constant of the solvent respectively.

c) $\Delta G_{PET} = E_{1/2}(ox) - E_{1/2}(red) - E_{0\text{-}0} + \Delta G_{Solv}$

where

$\Delta G_{Solv} = e^2/2[(1/r_D) + (1/r_A)]\ [(1/4\pi\varepsilon_0\varepsilon) - (1/4\pi\varepsilon_0\varepsilon_r)] - e^2/4\pi\varepsilon_0\varepsilon R.$

$E_{1/2}(ox)$ and $E_{1/2}(red)$ are the potentials for one-electron oxidation of the donor (anthracene) and one-electron reduction of the acceptor (porphyrin) moieties of **2** respectively. r_D (4.8 A°) and r_A (7A°) are the radii of the donor and the acceptor respectively and ε_r and ε are the dielectric constants of CH_2Cl_2 and other solvents respectively It should be noted that the compound is insoluble in CH_3CN, 0 1M TBAP in electrochemical experiments. It should also be noted thtat incorporation of solvent correction terms to low polarity situation is rather risky and hence the values of ΔG_{PET} in hexane can be taken as only a rough estimate.[25]

An inspection of the data presented in Table 5 3 suggests the following.

i) The estimated R_0 values are in the range 14.4-16 0 A° and these distances are somewhat longer than the *ctc* distance (R) in **2** (10 5 A°). The estimated value of the overlap integral (donor emission and acceptor absorption), $J_{Forster}$ is (2.64 ± 0 2) x 10^{-16} cm^6 $mmol^{-1}$.

ii) Although the Q and T_{cal} values are similar, the T_{obs} values are consistently lower than both of these parameters in each solvent

iii) Similarly, the observed energy transfer rate constants (k_{EN} (obs)) are lower than the calculated rate constant (k_{EN} (cal)) in each solvent.

iv) Moreover, the k_{obs} values that are calculated on the basis of the quenching efficiencies are higher than both k_{EN} (cal) and k_{EN} (obs) in each solvent.

v) The T_{obs} (k_{EN} (obs)) values bear no obvious relationship with the refractive index (n) of the solvent.

The above analysis indicates that quenching of the anthracene fluorescence in **2** is not entirely due to excitation energy transfer by Forster's dipole-dipole mechanism This is substantiated by the facts that the T_{obs} (k_{EN} (obs)) values are consistently lower than the T_{cal} (k_{EN} (cal)) and Q (k_{obs}) values and that there is no obvious correlation between T_{obs} (k_{EN} (obs)) and n values [22] Possibly, other mechanisms may also be operative in the observed fluorescence quenching of **2**

The similarity of the redox potentials of **2** and the covalently linked dyads described in the previous chapter suggests the possibility of Dexter's electron-exchange mediated EET process[23] to be operative in the fluorescence quenching of this pentad system. By the same token, a PET reaction from the singlet anthracenes to the porphyrin is also, in principle, possible in **2**. Indeed, inspection of Table 5.3 indicates that the (k_{obs} - k_{EN} (obs)) values correlate with the dielectric constant of the solvent Assuming that the rates of other non-radiative processes of anthracene do not alter on attachment to the porphyrin in **2**, the (k_{obs} - k_{EN} (obs)) values can be correlated to the PET rate constants Moreover, as mentioned earlier, the Q (k_{obs}) and T_{obs} (k_{EN} (obs)) values show opposite trends with ε of the solvent. Collectively, these observations can be rationalized in terms of a competition between energy transfer and electron transfer reactions in **2**

(Fig. 4.7b); the electron transfer pathway taking over with an increase in the polarity of the medium.

The presence of four anthracene subunits in close proximity to each other in **2** can, in principle, open up several other avenues of fluorescence quenching in this supramolecular compound. For example, it is possible that the anthracene moieties in **2** may associate into a nonfluorescent excited state complex and that the amount of complex formation may be solvent dependent. In principle, this possibility can explain the additional quenching obeserved over and above that rationalized solely on the basis of energy transfer in **2**. Although this mechanism seems to be an attractive proposition, there are no spectral or other data to substantiate this viewpoint Therefore, the oxidative quenching mechanism described above, most certainly, contributes to the low fluorescence quantum yield observed for the anthracene moieties in **2**

As the singlet state activity of the present pentad **2** has much in common with that of the dyads described in chapter 4 , a comparison between the two can be attempted here Such a comparison suggests that, as was the case with the dyads, invoking both energy and electron transfer processes is essential to explain the fluorescence quenching of the anthracene chromophores in **2**. However, $\%T_{obs}$ for the pentad porphyrin **2** is lower, (hexane, 76%; CH_2Cl_2, 64%; and CH_3CN, 36%) than that for the meta linked dyad (i.e. compound **2b** in chapter 4) which shows about 82-85% efficiency in the solvents investigated. It is possible that the D-A orientation is conducive for an EET in the dyad whereas, the presence of several D-A orientations that are a consequence of linking four anthracene subunits might promote excited-state processes other than the EET in this supramolecular porphyrin

5.4. Summary

A tetraphenylporphyrin bearing four anthracene donor moieties (meso-5,10,15,20-tetra(3-(9-methyloxyphenyl)phenyl)porphyrin, **2**) is synthesized and fully characterized Spectroscopic and electrochemical data and results of metallation and intermolecular fluorescence quenching experiments suggest that there is no appreciable interaction between the porphyrin and anthracene moieties in **2**. Although intermolecular quenching of anthracene fluorescence by H_2TPP is not obvious, the fluorescence of the anthracene donors in **2** is quenched by more than 90% On the basis of the fluorescence excitation spectral data, the observed quenching has been attributed to an intramolecular singlet-singlet energy-transfer from the anthracenes to the porphyrin. However, neither Forster's dipole-dipole formalism nor Dexter's electron exchange mechanism can explain adequately this intramolecular energy transfer Thermodynamic considerations and solvent-dependent fluorescence data indicate that photoinduced electron transfer from singlet anthracene to the porphyrin can compete with energy transfer in this supramolecular system A comparison of the singlet state activity of the dyads described in chapter 4 and compound **2** suggests that, invoking both energy and electron transfer processes is essential to explain the fluorescence quenching of the anthracene/s in these cases

5.5 References

1. Wennerstrom, O ; Erricsson, H , Ratson, I , Svensson, S.; Pimlott, W. *Tetrahedron Lett* **1989**, 30, 1129
2. Davila, J.; Harriman, A , Milgrom, L R *Chem Phys Lett* **1987**, 136, 427.

3. Prathapan, S ; Johnson, T. E ; Lindsey, J. S. *J Am. Chem. Soc.* **1993,** 115, 7519.
4. Abraham, R. J.; Hawkes, G. E.; Hudson, M. F.; Smith, K. M. *J. Chem. Soc., Perkin Trans. II* **1975**, 204
5. Fonda, H. N.; Gilbert, J. V.; Cormier, R. A.; Sprague, J. R.; Kamioka, K.; Connolly, J. S *J. Phys. Chem.* **1993**, 97, 7024
6. Cense, J. M.; Le Quax, R. M. *Tetrahedron Lett.* **1979**, 39, 3725.
7. Toeibs, A.; Haeberle, N. *Justus Liebigs Ann. Chem.* **1968**, 718, 183.
8. Suriyanarayanan, P., Krishnan, V. *Photochem. Photobiol.* **1983**, 38, 533.
9. Harriman, A.; Davila, J *Tetrahedron* **1989**, 45, 4737.
10. Lin, Z. -M.; Feng, W. -Z.; Leung, H. -K *J. Chem. Soc , Chem. Commun.* **1991**, 209
11. White, W I In *The Porphyrins;* Dolphin, D , Ed; Academic: New York, 1978, Vol 5, chapter 7
12. Gust, D.; Moore, T A , Moore, A. L *Acc Chem. Res.* **1993**, 26, 198.
13. Gust, D.; Moore, T. A.; Moore, A. L.; Devadoss, C.; Liddell, P. A.; Hermant, R.; Niemann, R. A.; Demanche, L. J.; DeGraziano, J. M.; Gouri, I. *J. Am. Chem Soc.* **1992**, 114, 3590.
14. Hermant, R. M.; Liddel, P A.; Lin, S , Alden, R. G , Kang, H. K ; Moore, A. L.; Moore, T. A.; Gust, D *J. Am Chem Soc.* **1993**, 115, 2980.
15. Berenbaum, M C.; Akande, S. L ; Bonnett, R , Kaur, H ; Ioannou, S.; White, R. D.; Winfield, U. -J *Br J. Cancer* **1986**, 54, 717
16. Lin, W. C.; In *The Porphyrins;* Dolphin, D. Ed.; Academic: New York, 1978, Vol. 4, Chapter 7

17. D. Birch, IBH Consultants, UK, personal communication of lifetime data, 1993.

18. Chandrashekhar, T. K.; Krishnan, V *Inorg. Chem.* **1981**, 20, 2782.

19. Murov, S. L. In *Handbook of Photochemistry;* Marcel Dekker: New York, 1973.

20. Bergkamp, M. A., Dalton, J.; Netzel, T. L. *J. Am Chem. Soc.* **1982**, 104, 253.

21. Quimby,D. J.; Longo, F R *J Am Chem. Soc.* **1975**, 97, 5111.

22. Forster, Th. *Disc. Faraday Soc* **1959**, 27, 7.

23. Dexter, D. L. *J Chem Phys.* **1953**, 21, 836.

24. Lindsey, J. S; Brown, P. A , Siesel, D A. *Tetrahedron* **1989**, 45, 4845

25. Schmidt, J. A.; Liu, J. -Y.; Bolton, J. R.; Archer, M. D.; Gadzekpo, V. P. V. *J. Chem. Soc., Faraday Trans. 1.* **1989**, 85, 1027.

CHAPTER 6

Design, Synthesis and Singlet State Activity of a Porphyrin-Anthracene Supramolecular System Assembled by Nucleic Acid Base-Pairing

6.1 Introduction

A critical perusal of the literature cited in chapters 3-5 suggests that a majority of porphyrin-based donor-acceptor (D-A) systems that are built to mimic the photosynthetic electron and energy transfer systems utilise the covalent bond linkage between the donor and the acceptor [1,2] On the other hand, D-A systems bound by noncovalent interactions can be expected to provide a better understanding of the biological energy/electron transfer processes as these processes in biological systems proceed through complex noncovalently bound protein pathways [3-5] This consideration has led to the construction of porphyrin-based systems that are characterised by either H-bonding or nucleic acid base-pairing interaction between the donor and the acceptor. However, studies on such noncovalently bound, photochemically active D-A systems are relatively new and only a few such systems have been reported so far.

Recently, Ogoshi and co-workers[6-11] have utilized the hydrogen bonding interactions to construct supramolecular assemblies in which bis- or tetrakis-(2-hydroxynaphthyl)porphyrin spontaneously forms face-to-face adducts with various quinones through one-, two-, or multi-point hydrogen bonding depending on the substrate Results of steady state fluorescence spectroscopy have indicated the possibility of occurrence of a photoinduced electron transfer (PET, porphyrin— quinone) in these systems More recently, Nocera and co-workers[12,13] have synthesized various porphyrin-based D-A

complexes *via* carboxylate-carboxylate or amidinium-carboxylate salt bridge and have established the occurrence of a PET reaction from the porphyrin donor to the nitroaromatic acceptor in these novel systems. An interesting and probably, biologically 'more relevant' approach for the construction of photosynthetic model systems involves nucleic acid base-pairing. This approach has been exploited in the synthesis of porphyrin-porphyrin (P-P) and porphyrin-quinone (P-Q) energy and electron transfer systems.[14-16] For example, Sessler, Harriman and their co-workers[17-20] and Lehn and co-workers[21] have demonstrated the occurrence of energy- or electron transfer reactions in P-P and P-Q systems wherein the complementary base-pairing between cytosine (C) and guanine (G) or self-association of C, G or uracil residues have been employed to assemble individual donor and acceptor subunits. Porphyrin arrays assembled *via* complementary base-pairing between adenine (A) and thymine (T) residues are also known in the literature but the photochemical function of these systems has not been investigated.[22-24]

During the course of investigations on the covalently linked porphyrin-anthracene (P-A) systems described in the previous two chapters, the possibility of building nucleic acid base-paired P-A systems appeared to be attractive. This has been realized in this study and, the present chapter describes the design, construction, spectroscopic characterization and singlet state activity of a new supramolecular P-A system **3** (scheme 6.1) which is obtained from a self assembly of meso-5(4-(9-(2-oxyethyl)adenine)phenyl)10,15, 20-tritolylporphyrin, **1**, and 1-(9-methylanthracene)thymine, **2**

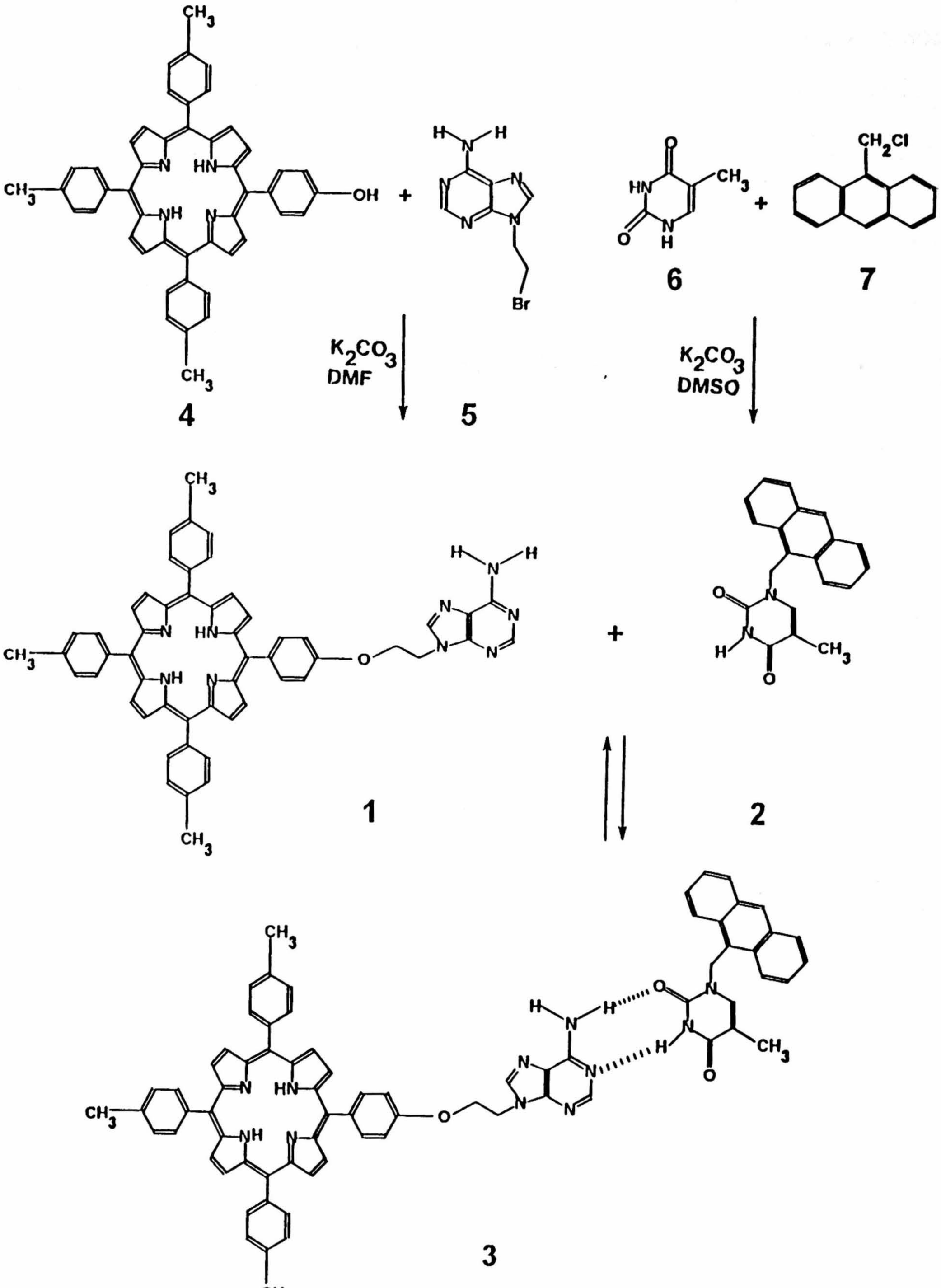
CH3
CH3
OH
CH3
HN
NH
N
H
N
H
N
N
N
N
Br
4
K2CO3
DMF
5
O
HN
CH3
N
H
O
6
CH2Cl
7
K2CO3
DMSO
O
N
N
H
O
CH3
1
2
3

Scheme 6.1

6.2 Experimental

6.2.1 Synthesis of meso-5,10,15,20-tetratolylporphyrin (H_2TTP)[25]

A solution of 4-tolualdehyde (12.0 g, 100 mmol) in propanoic acid (200 ml) was warmed to 120 °C with vigorous stirring in 30 min Pyrrole (6.9 ml, 100 mmol) was added and the resulting mixture was refluxed for 1 h. The solution was then cooled and allowed to stand at room temperature overnight. The residue was filtered off, washed with methanol and dried The resulting solid was dissolved in CH_2Cl_2 and subjected to column chromatography (basic alumina, activity I) with CH_2Cl_2 as the eluent The fast moving first fraction was collected and the solvents evaporated to get the desired product Yield : ≅ 10%.

UV-visible spectral data in $CHCl_3$: λ_{max}, nm (log ε)

417 (5.34), 514 (4.26), 549 (3 90), 590 (3.74), 647 (3 73)

6.2.2 Synthesis of meso-5(4-hydroxyphenyl)10,15,20-tritolyl porphyrin (4)[26]

A solution of 4-hydroxy benzaldehyde (4g, 33 mmol) in propanoic acid (200 ml) was warmed to 120 °C with vigorous stirring in 30 min. 4-tolualdehyde (7.7 ml, 66 mmol) and pyrrole (6.8 ml, 99 mmol) were added and the resulting mixture was refluxed for 1 h. The solution was then cooled to room temperature and the precipitate was filtered off, washed with ethanol and dried. The solid was dissolved in CH_2Cl_2 and subjected to column chromatography (basic alumina, activity 1) with CH_2Cl_2 as the eluent The fast moving first fraction was identified as H_2TTP The desired compound was eluted out when the eluent was changed to CH_2Cl_2-CH_3OH (95·5 V/V). The solvents were evaporated to get **4**. Yield : ≅ 6%.

UV-visible spectral data in $CHCl_3$ λ_{max}, nm (log ε)

419 (5.32), 516 (4.25), 550 (3.92), 592 (3.76), 649 (3.75).

6.2.3 Synthesis of 5-(4-(2-bromoethylphenyl)10,15,20-tritolylpor-phyrin (8)

A mixture of porphyrin **4** (0.067g, 0.1 mmol), and anhydrous K_2CO_3 (0.15g, 1.5 mmol) in dry dimethylformamide (10 ml) was stirred under nitrogen for 24 h. The solvent was removed under vacuo and the residue was dissolved in $CHCl_3$ and loaded on an alumina column. Using $CHCl_3$ as the eluent, the desired product was eluted out as the first band. Yield: ≅ 70%.

UV-visible spectral data in $CHCl_3$: λ_{max}, nm (log ε)

419 (5.77), 517 (4.27), 553 (4.04), 593 (3 76), 649 (3.75).

6.2.4 Synthesis of 9-(2-bromoethyl)adenine (5)

A mixture of adenine (2 5g, 18 5 mmol), 1,2-dibromoethane (15g, 79.8 mmol), and K_2CO_3 (6g, 43 4 mmol) in dry dimethylformamide (100 ml) was stirred at room temperature under nitrogen atmosphere for 48 h. The reaction mixture was filtered and the filtrate was evaporated to dryness. The resulting yellow solid was washed with water and dried Purity of the compound was checked by comparing the IR, UV-visible and ^{1}H NMR spectra with the reported spectra.[26] Yield: 77%. m.p 198-200 °C .

6.2.5 Synthesis of meso-5(4-(9-(2-oxyethyl)adenine)phenyl)-10,15, 20-tritolylporphyrin (1)

A mixture of **4** (0 063g, 0.1 mmol), **5** (0 022g, 0.11 mmol) and K_2CO_3 (1.5g, 1.0 mmol) in dry dimethylformamide (10 ml) was stirred at room temperature for 48 h. The solvent was removed under vacuum after which the residue was dissolved in $CHCl_3$ and loaded on an alumina column Using

$CHCl_3$ as the eluent, the desired product was eluted out as the first band. Yield: ≅ 70%. M/Z: obsd. 834. Calcd. for $C_{54}H_{43}N_9O$. 834 (Fig. 6.1). Analytical data: obsd. C, 77.74; H, 5.20, N, 15.12. Calcd. for $C_{54}H_{43}N_9O$: C, 77.75; H, 5.20; N, 15.13.

6.2.6 Synthesis of 1-(9-methylanthracene)thymine (2)[28]

To a solution of thymine (1.25g, 10 mmol) in 135 ml of dry dimethylsulfoxide were added 9-chloromethylanthracene (0 57g, 3.3 mmol) and anhydrous K_2CO_3 The resulting suspension was stirred at room temperature for 2 h, after which it was filtered. The filtrate was evaporated to dryness and the resulting solid was washed with water thoroughly Recrystalization in absolute ethanol yielded yellow crystals of **2** Yield. ≅ 50%. M/Z: obsd. 317. calcd for $C_{20}H_{16}O_2$: 316 (Fig 6.2) Analytical data obsd. C, 75.90, H, 5 12, N, 8 89 Calcd for $C_{20}H_{16}N_2O_2$ C, 75 94, H, 5 10, N, 8 86.

Each investigated porphyrin was purified on a short alumina column before spectral measurements were made All the spectroscopic and electrochemical experiments have been carried out as described in chapter 2

6.2.7 ^{1}H NMR titration

A 0.5 ml of 0.005 M (C_1) solution of **1** in $CDCl_3$ and a 1 ml of 0 05 M solution of **2** in $CDCl_3$ containing 0.005 M of **1** were prepared in two separate NMR tubes **A** and **B**, respectively. ^{1}H NMR spectra were recorded by adding successive 10 µl (C_2 being the concentration of **2**) fractions of solution from tube **B** to tube **A** For each successive addition $\Delta\delta_{obsd}$ values for adenine amino-Hs of **1** were calculated by subtracting the chemical shift

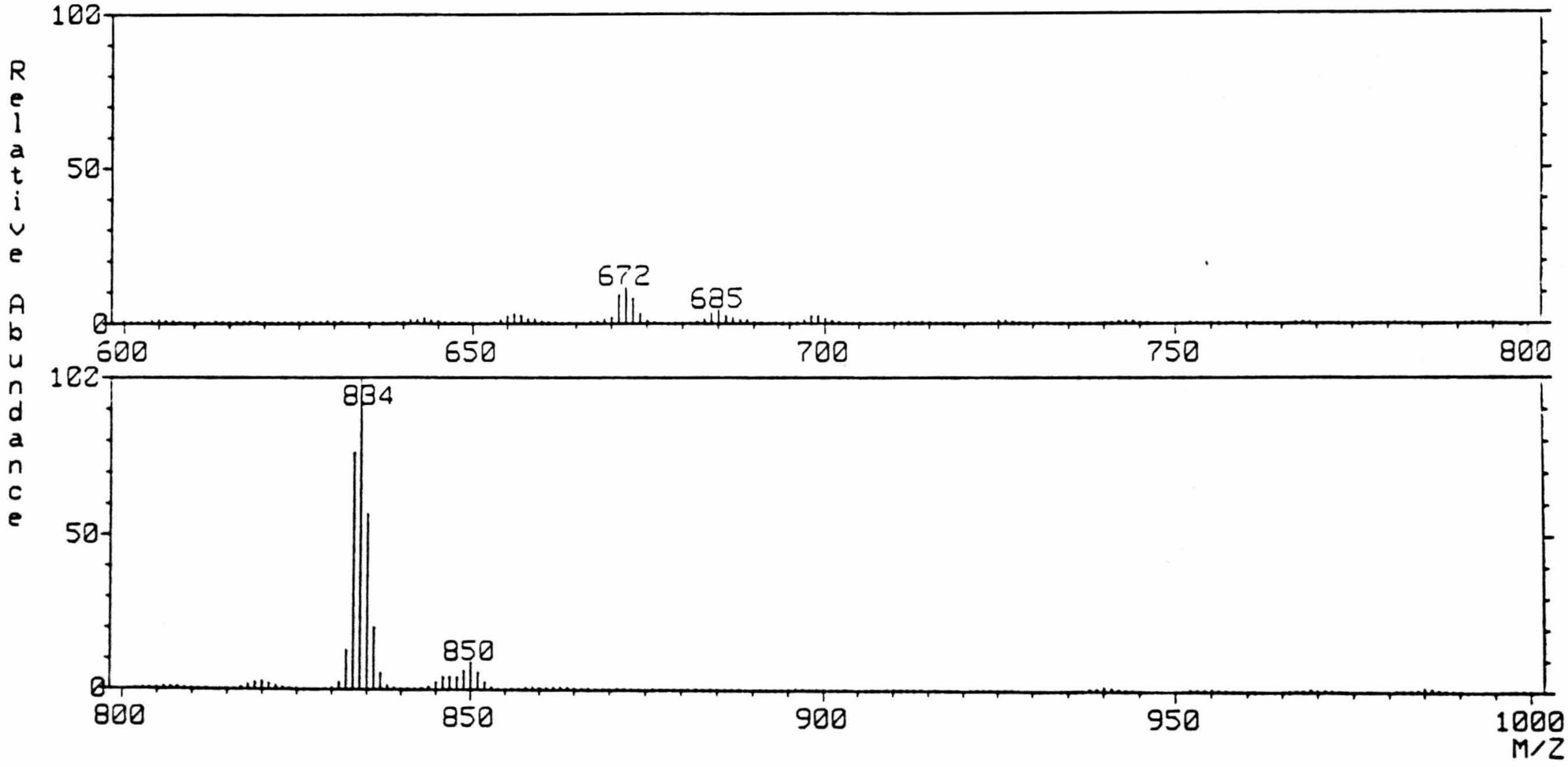

Fig. 6.1. Mass spectrum of **1**.

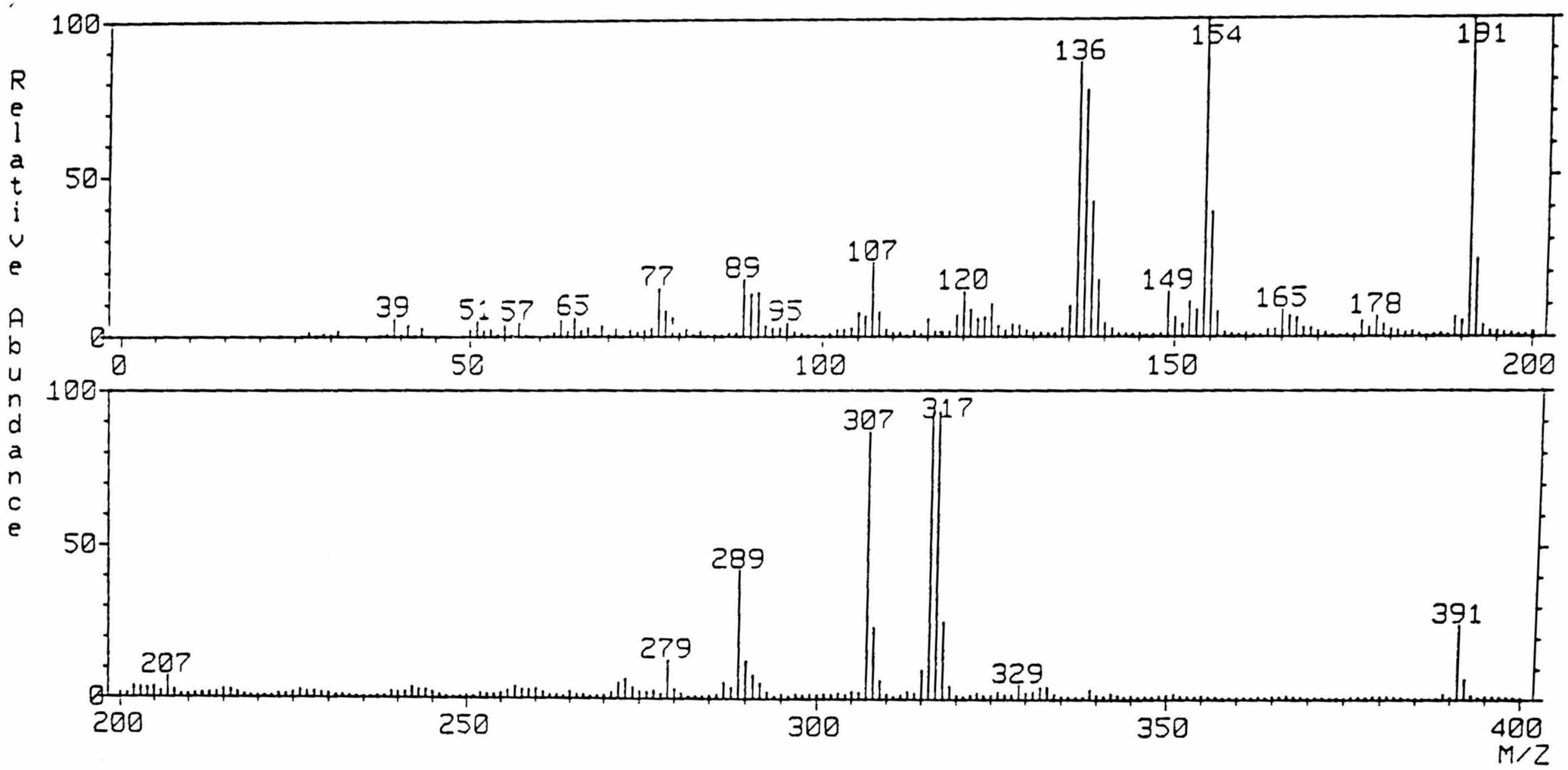

Fig. 6.2. Mass spectrum of **2**.

of interest in the successive addition, δ_{obsd} from the adenine amino-H resonance δ_1 in the spectrum of solution **A** alone

6.2.8 Time-resolved fluorescence experiments

Fluorescence lifetimes for 2 μM solutions (CH_2Cl_2) of **2** were measured both in the absence and in the presence of increasing concentrations (upto 70 μM) of **1** Similar experiments were also carried in the presence of **8** as the quencher Competing absorption at the excitation wavelength by **1** and **8** rendered the lifetime measurements difficult for solutions containing > 70 μ M of these porphyrins and 2 μM of **2** In another set of experiments, fluorescence lifetimes were measured for solutions containing equimolar (0.001 mM to 2 mM) mixtures of **2** and **1** or **8**

The samples were excited at 290 ± 10 nm and the emission was monitored at 430 ± 10 nm in each case Analysis of the lifetime data was carried out as described in chapter 2

6.3 Results and discussion

6.3.1 Ground state properties

The UV-visible spectra of **1** and **2** are shown in Fig 6.3 and the spectral data of **1**, **2** , **8** and anthracene are summarized in Table 6.1 As seen from the figure, spectrum of **1** shows bands due to the porphyrin chromophore's absorption between 700-400 nm and a band due to absorption of the adenine moiety at 260 nm Spectrum of **2** shows bands due to anthracene and thymine moieties between 200-400 nm The logε values at the peak maxima in the spectra of **1** and **2** are close to those of their individual constituents

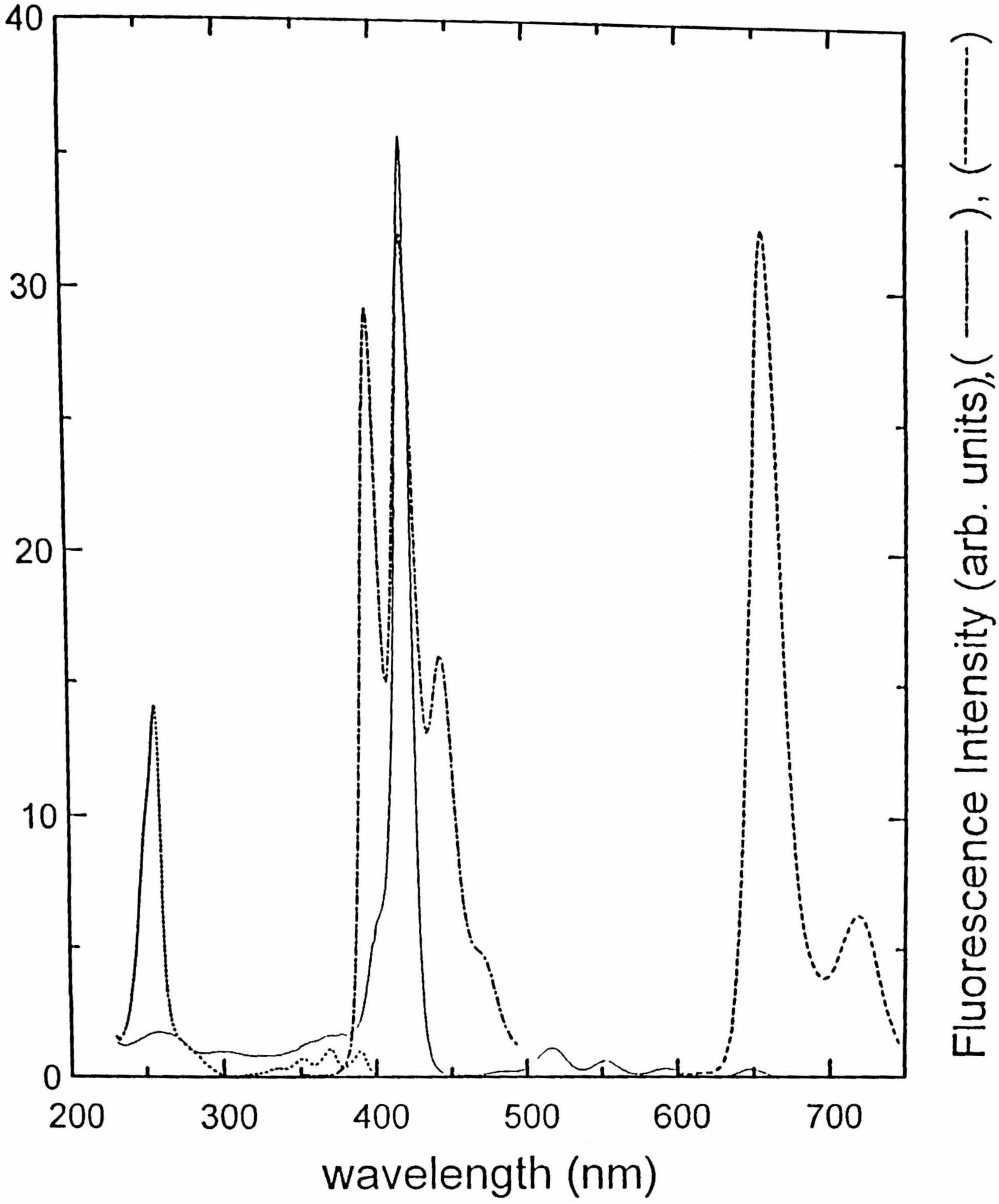

Fig 6.3. UV-visible spectra of **1** (———) and **2** (·····) and fluorescence spectra of **2** obtained on excitation at the anthracene (250 nm) absorption peak (–·–·–·–) and the porphyrin (420 nm) absorption peak (-------). The solvent was CH_2Cl_2.

Table 6.1 UV-visible data in CH_2Cl_2.

Compound	λ_{max}, nm (logε)							
	Porphyrin transitions					Anthracene transitions		
	Q_1	Q_2	Q_3	Q_4	B	I	II	III
8	647 (3 68)	589 (3 69)	549 (3 85)	512 (4 22)	417 (5 67)			
1	648 (3 51)	592 (3 52)	553 (3 79)	517 (4.05)	419 (5 55)			260 (4 24)
Anthracene						378 (3 84)	359 (3 88)	255 (5.19)
2						389 (4 00)	369 (4 04)	257 (5.55)

Compound **1** is reversibly oxidized and reduced at 0.99 and -1.19 V, respectively and these potentials are close to those at which H_2TTP undergoes one-electron oxidation and one-electron reduction reactions under similar experimental conditions. Similarly, compound **2** undergoes a quasi-reversible one-electron oxidation at 1 43 V, a potential at which free anthracene can be oxidized. In addition, the redox potentials measured for an

1:1 mixture of **1** and **2** did not show any deviation from the redox potentials mentioned above.

Fig. 6.4 shows the ^{1}H NMR spectra of **1** and **2** (5 mM) measured in $CDCl_3$. The spectra show characteristic resonances and, the peak positions as well as their integrated intensities are consistent with the structures of these conjugates. The resonances due to the 'ring' protons of porphyrin and anthracene moieties on **1** and **2** occur in the aromatic region, as expected Whereas the resonances due to spacer methylinic protons of **1** occur between 4-5 ppm (m), the corresponding resonance of **2** occur at 5.93 ppm (s) Similarly, the resonances due to amino, C_2- and C_8-Hs on the adenine moiety of **1** occur at 5.63 ppm (s), 8 46 (s) and 8 48 (s) ppm respectively, and the imido- and C_6-H resonances on the thymine moiety of **2** are seen at 8.31 (s) and 6.55 (s) ppm, respectively A comparison of the spectra of **1** and **2** with those of **4**, **5**, 9-methyloxyphenylanthracene and thymine suggests that no major changes have occurred in the resonance positions of the protons on these conjugates with respect to those on the reference compounds Therefore, interaction between the aromatic rings and the nucleobases is minimum in these conjugates

Thus, UV-visible, ^{1}H NMR and redox potential data indicate that both porphyrin in **1** and anthracene in **2** retain their individual characteristics even after coupling with the bases

Upon mixing in $CDCl_3$ solutions, the nucleobases **1** and **2** may associate by way of complementary two-point hydrogen bonding to produce bichromophoric assemblies in which the subunits are separated by < 18 A^o (edge-to-edge, as derived from CPK models) with many conformations being possible. Indeed ^{1}H NMR experiments have suggested that, when **1** and **2** are mixed in $CDCl_3$ at 293 ± 3 K, both adenine amino-Hs and the thymine imido

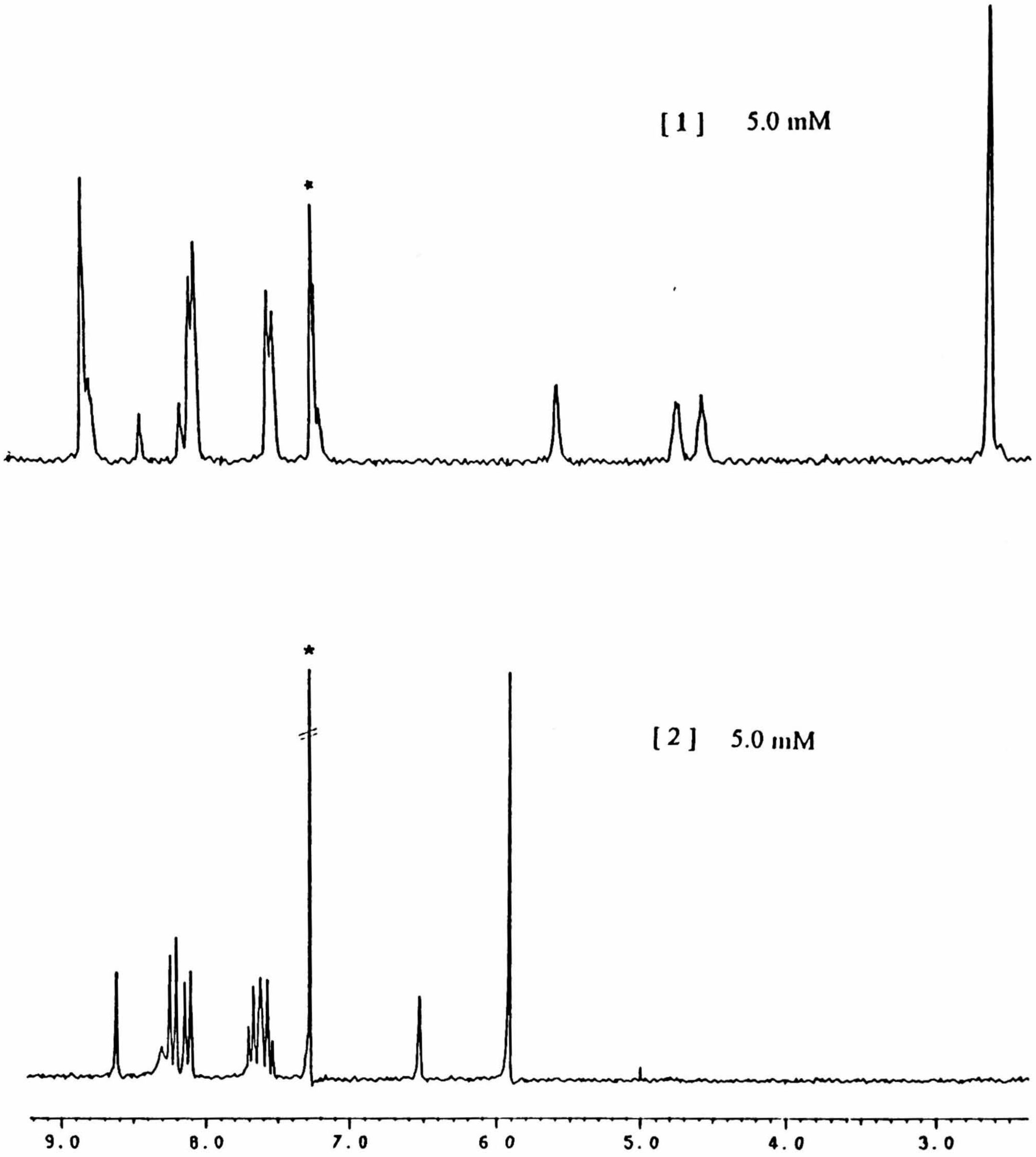

Fig. 6.4. ^{1}H NMR spectra of **1** and **2**.

H are shifted downfield indicating the formation of the hydrogen-bonded ensemble **3** (see Scheme 6.1). The details of complexation between **1** and **2** and the method of calculation of the equilibrium constant are described below.

6.3.1.1 Calculation of equilibrium constant by the ^{1}H NMR method[29-31]

If **1** and **2** interact reversibly in solution to form the 1:1 complex **3** according to

$$\mathbf{1} + \mathbf{2} \underset{}{\overset{K_3}{\rightleftharpoons}} \mathbf{3} \qquad (6.1)$$

the equilibrium constant, K_3 can be expressed as

$$K_3 = C_3 / (C_1 - C_3)(C_2 - C_3) \qquad (6.2)$$

where C_1 and C_2 are the added concentrations of **1** and **2**, respectively, and C_3 is the concentration of the complex **3** at equilibrium

Since this equilibrium is fast with respect to the NMR time scale,[29] the observed chemical shift of the protons on **1**, δ_{obsd}, will be the time-weighted average of the chemical shift of the protons in the complexed form, δ_3, and that in the uncomplexed form, δ_1 [26] Therefore, δ_{obsd} is related to δ_1 and δ_3 by eq. 6.3.

$$\delta_{obsd} = \frac{C_3\,\delta_3}{C_1} + \frac{C_1 - C_3\delta_3}{C_1} \qquad (6.3)$$

Eqs. (6.2) and (6.3) can be rearranged to give eqs. (6.4) and (6.5), respectively.

$$C_3 = \frac{\delta_{obsd} - \delta_1}{\delta_3 - \delta_1} C_1 \qquad (6.4)$$

$$K_3 C_1 C_2 - K_3 C_3 (C_1 + C_2 - C_3) = C_3 \qquad (6.5)$$

From eq. (6 4) and (6 5), eq (6 6) is obtained

$$\frac{C_2}{\Delta\delta_{obsd}} = \frac{1}{\delta_3 - \delta_1}(C_1 + C_2 - C_3) + \frac{1}{K(\delta_3 - \delta_1)} \qquad (6.6)$$

where $\Delta\delta_{obsd} = \delta_{obsd} - \delta_1$. Eq (6 6) contains two unknowns, C_3 and δ_3, which can be calculated by means of a simple iterative procedure based on successive approximations

A plot of $C_2/\Delta\delta_{obsd}$ *vs* $(C_1 + C_2)$ would yield, according to eq (6.6), a straight line with a slope value approximately equal to $1/(\delta_3 - \delta_1)$ Substitution of this slope into eq. (6.4) would give the first approximate values of C_3. These values thus obtained can be reemployed in eq. (6.6) to calculate the improved values. These steps can be repeated, using a computer program, until two successive cycles yield essentially identical convergent values for the slope. Finally, the equilibrium constant, K_3, can be calculated from the limiting slope and intercept values. The chemical shift of the H-bonded proton in the complex (δ_3) can also be obtained form the final slope.

6.3.1.2 Complexation of 1 and 2

Figs. 6.5 and 6.6 show the spectra of **1**, **2** and also the mixtures of **1** and **2**. Inspection of these figures reveals that the two amino protons of the adenine moiety on **1** resonate as a singlet and that this resonance is gradually downfield shifted with successive additions of **2** This later observation is clearly demonstrated in Fig 6 7a, which gives a plot of adenine proton resonance *vs* concentration of **2**. The observation is similar to those made earlier for the A-T base paired P-P systems[22,24] and constitutes a strong evidence in favour of the formation of the A-T base-paired P-A complex **3** in solutions containing **1** and **2** (scheme 6 1)

Analysis of the data shown in Fig. 6.7a to obtain the association constant (K_3) was carried out as described above, a plot of $C_2/\Delta\delta_{obsd}$ *vs* (C_1 + C_2 - C_3) is given in Figure 6 8. The derived value of K_3 is (47 ± 5) M^{-1} for the A-T base-pairing in this system and it is consistent with the low association constants (ca < 100 M^{-1}) reported earlier for the A-T base pairing in $CDCl_3$.[32,33] The base pairing in these two-point H-bonded systems including **3** is far too weak in comparison with that in a three-point H-bonded, G-C base-paired P-Q complex for which an association constant of (3100 ± 470) M^{-1} has been reported.[19] The low value of K_3 observed for **3** might also be a reflection of its flexible structure

It should be noted here that presence of other complexes such as self associated forms of **1** (A-A) and **2** (T-T) can also be expected in solutions containing **1** and **2** However, because of their low association constants (the self association constant of 9-ethyladenine in chloroform is 3 1 M^{-1} and that of thymine is 2.2 - 4.2 M^{-1} [32.33]), the contribution of these forms to the overall equilibrium, and hence, to the observed ^1H NMR chemical shifts, are expected to be insignificant

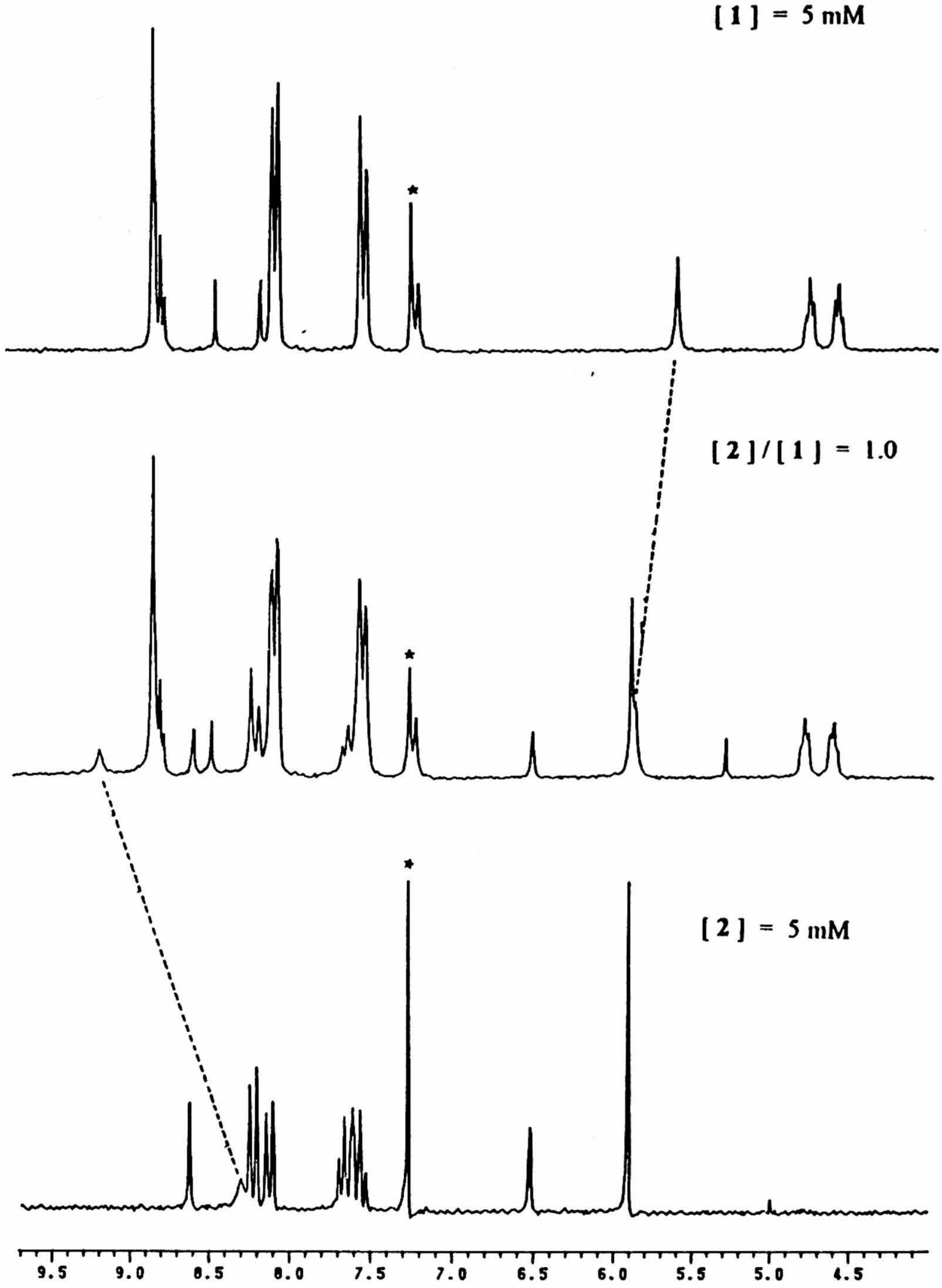

Fig. 6.5. ^{1}H NMR spectra of **1** (5 mM), **2** (5 mM) and **[2] / [1]** = 1 0. The dashed lines indicate the downfield shifts observed for amino and imido protons of **1** and **2**, respectively.

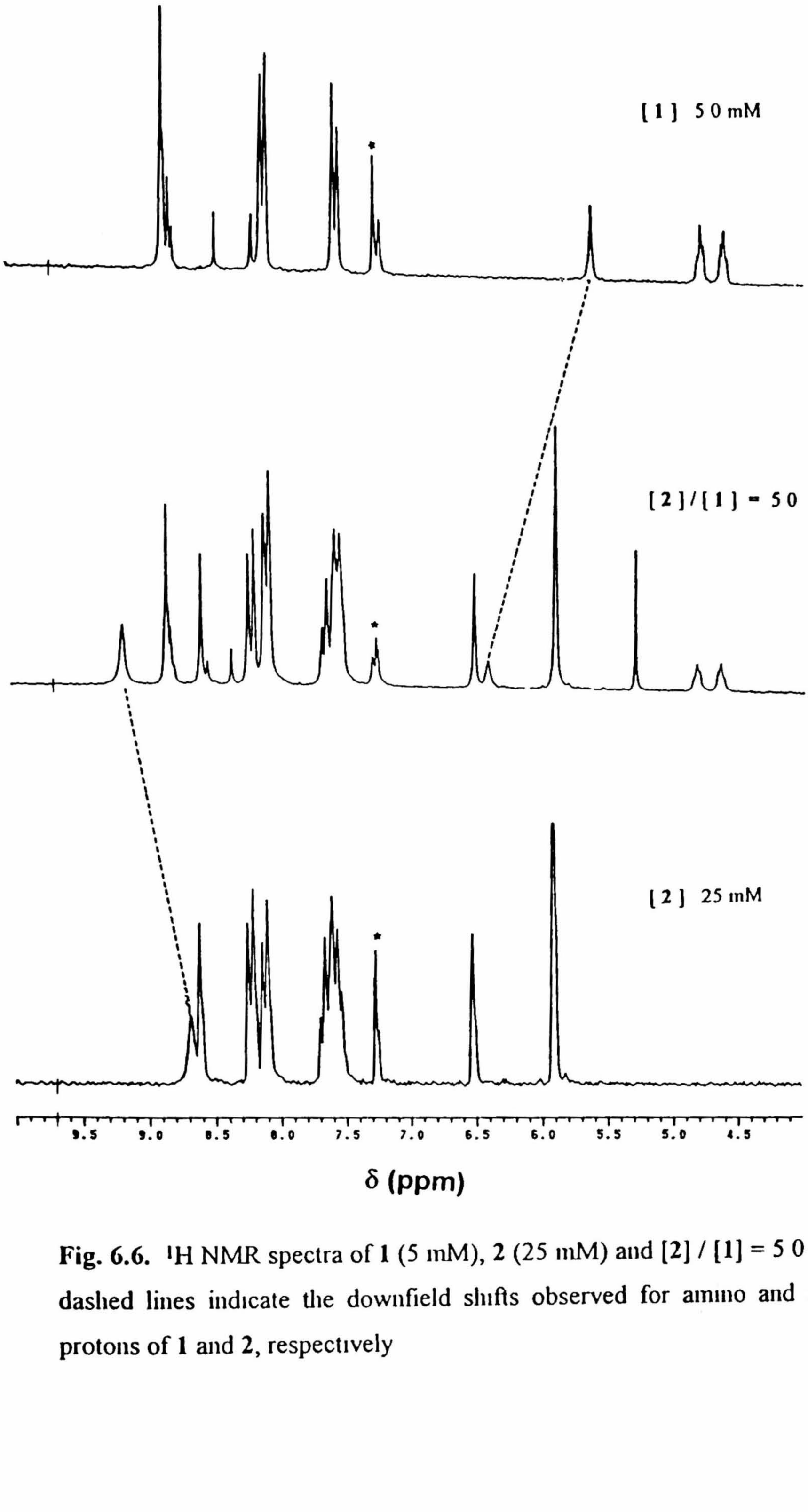

Fig. 6.6. ^{1}H NMR spectra of **1** (5 mM), **2** (25 mM) and [2] / [1] = 5 0 The dashed lines indicate the downfield shifts observed for amino and imido protons of **1** and **2**, respectively

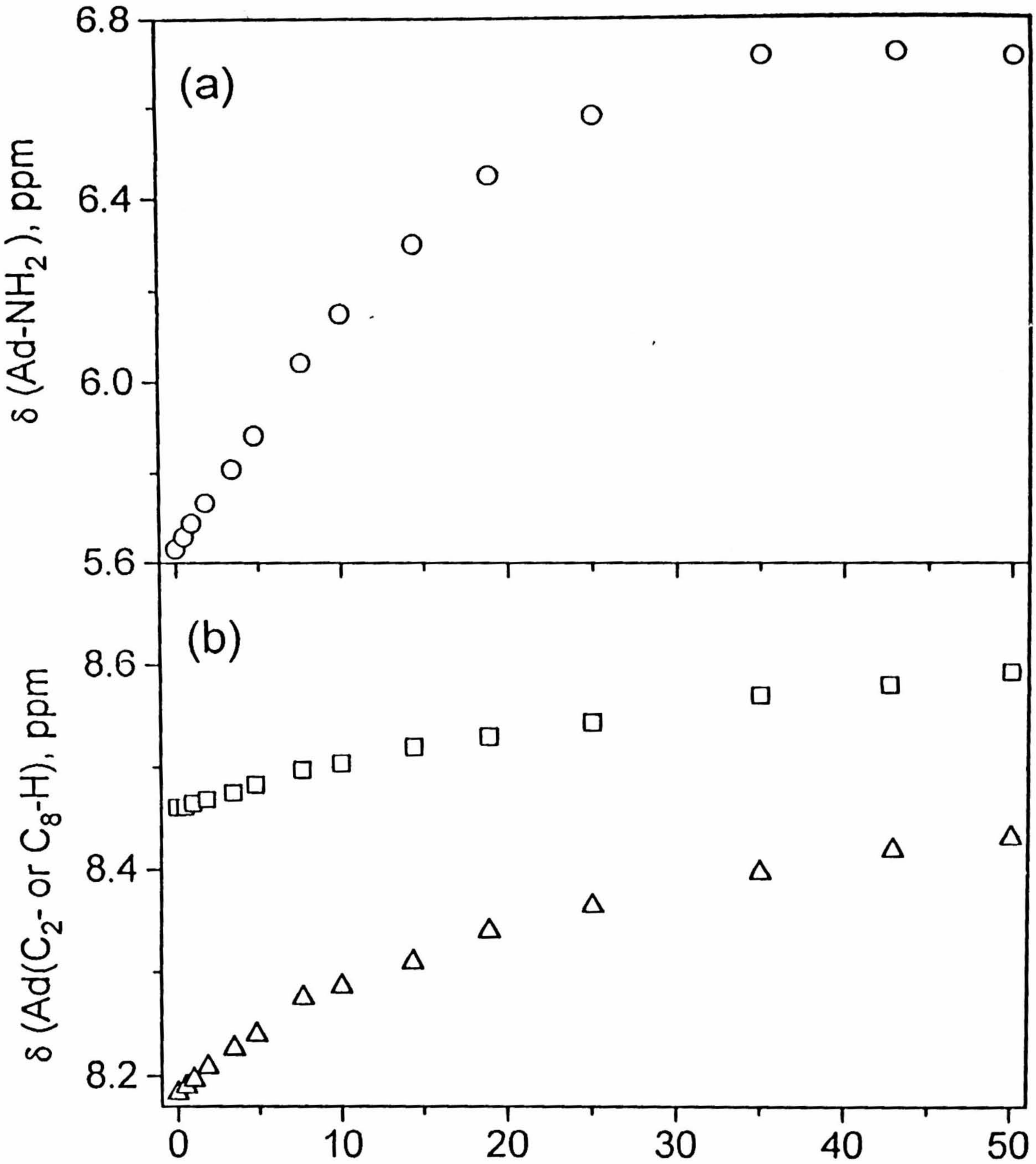

Fig. 6.7. Plot showing the downfield shifts of adenine (**a**) -NH_2, and (**b**) C_2- or C_8-H of **1** (5 mM) in the presence of **2** (0.5 - 50 mM).

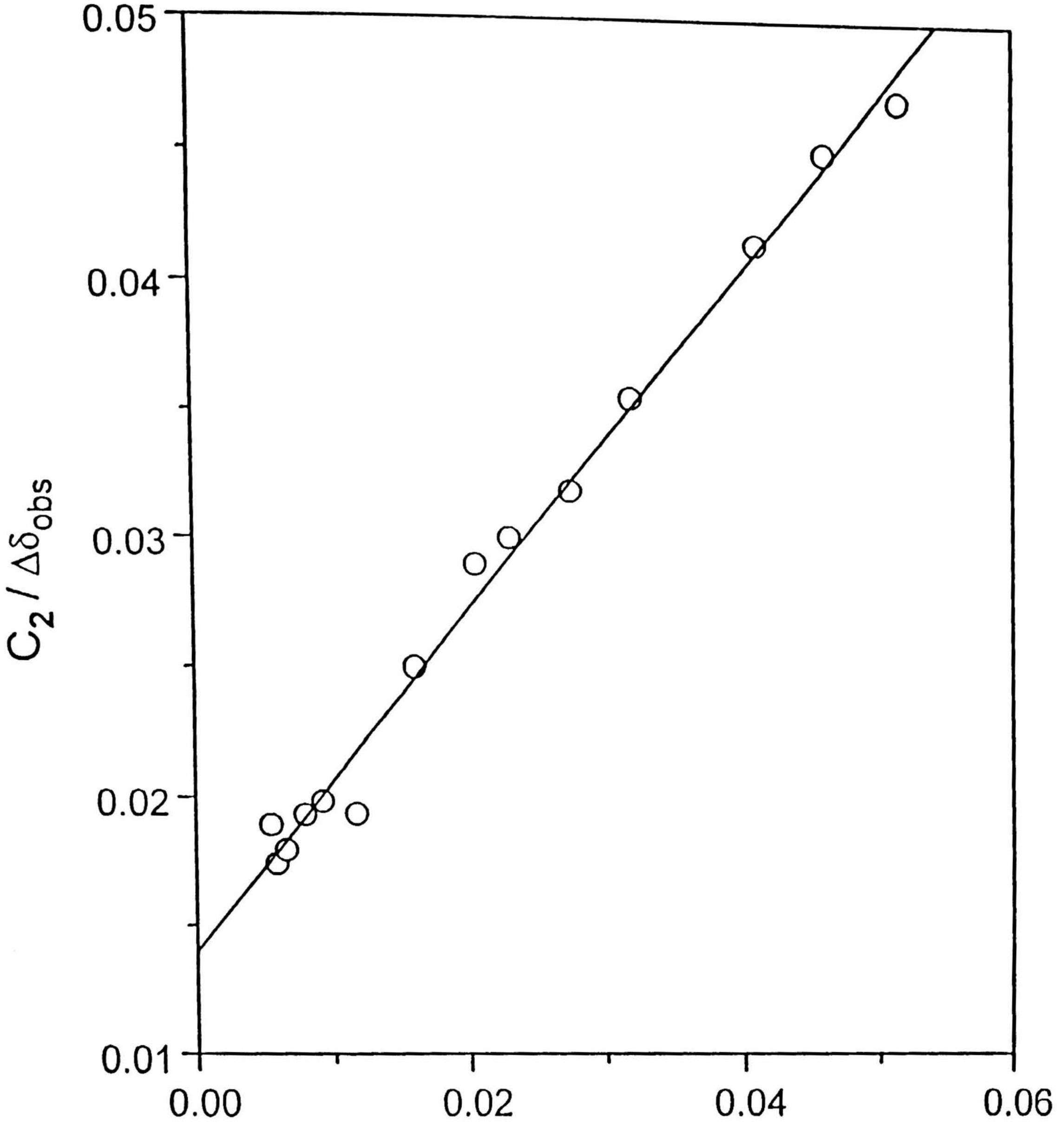

Fig. 6.8. Plot of $C_2 / \Delta\delta_{obsd}$ vs $(C_1 + C_2 - C_3)$ for the adenine-NH_2 proton resonance. $\Delta\delta_{obsd}$ is the difference in the chemical shift for the adenine-NH_2 of **1** in the absence and in the presence of **2**. C_1 (5mM), C_2 (0 - 50 mM) and C_3 are the concentrations of **1**, **2** and **3**, respectively. The data were analyzed as a per a procedure given in ref. 27. The derived equilibrium constant is (47 ± 5) M^{-1}.

Interestingly, downfield shifts have also been noticed for adenine C_8-H (max. shift : 0.116 ppm at **[2] / [1]** = 10) and C_2-H (max. shift : 0.193 ppm at **[2] / [1]** = 10) of **1** (see Fig 6.7b). As these two protons are attached to carbon atoms, and therefore are not expected to participate in the H-bonding, the observed downfield shifts seen for them can be interpreted in terms of the existence of more than one form of H-bonding complex that is possible in this A-T base paired supramolecular complex.[34,35] It is now well known that a significant C_2-H downfield shift implies the formation of Watson-Crick[36] hydrogen bonds and that a C_8-H downfield shift implies interactions of the Hoogsteen type.[37-39] As seen from the structures given in Figure 6 9, the C_2-H of adenine becomes highly polarized in contact with the C_2-carbonyl function of thymine in the Watson-Crick base pair and a similar situation exists with the C_8-H on the Hoogsteen edge Thus, based on the previous studies, the observed downfield shifts can be attributed to the existence of both Watson-Crick[36] and Hoogsteen[37] type hydrogen bonds in the complex **3**.[40-42]

It should be noted here that, in contrast to the downfield shifts noticed for the adenine C_2- and C_8- protons in complex **3**, upfield shifts have been reported for the same protons in previously studied porphyrin-nucleobase (P-N) complexes. In these P-N complexes, the base moieties are linked, *via* amido or ether bridges at the phenyl ortho positions of 5,15-diphenylporphyrin and, as the bases are located on the 'upper zone' of the macrocycle, the high field shifts have been interpreted as due to the ring current effect of the porphyrin.[22,24] Clearly, the situation is quite different for **3** as explained below.

Unlike the case with the P-N complexes, the adenine moiety in **1** is linked to the porphyrin at the para position of the phenyl ring and the CPK

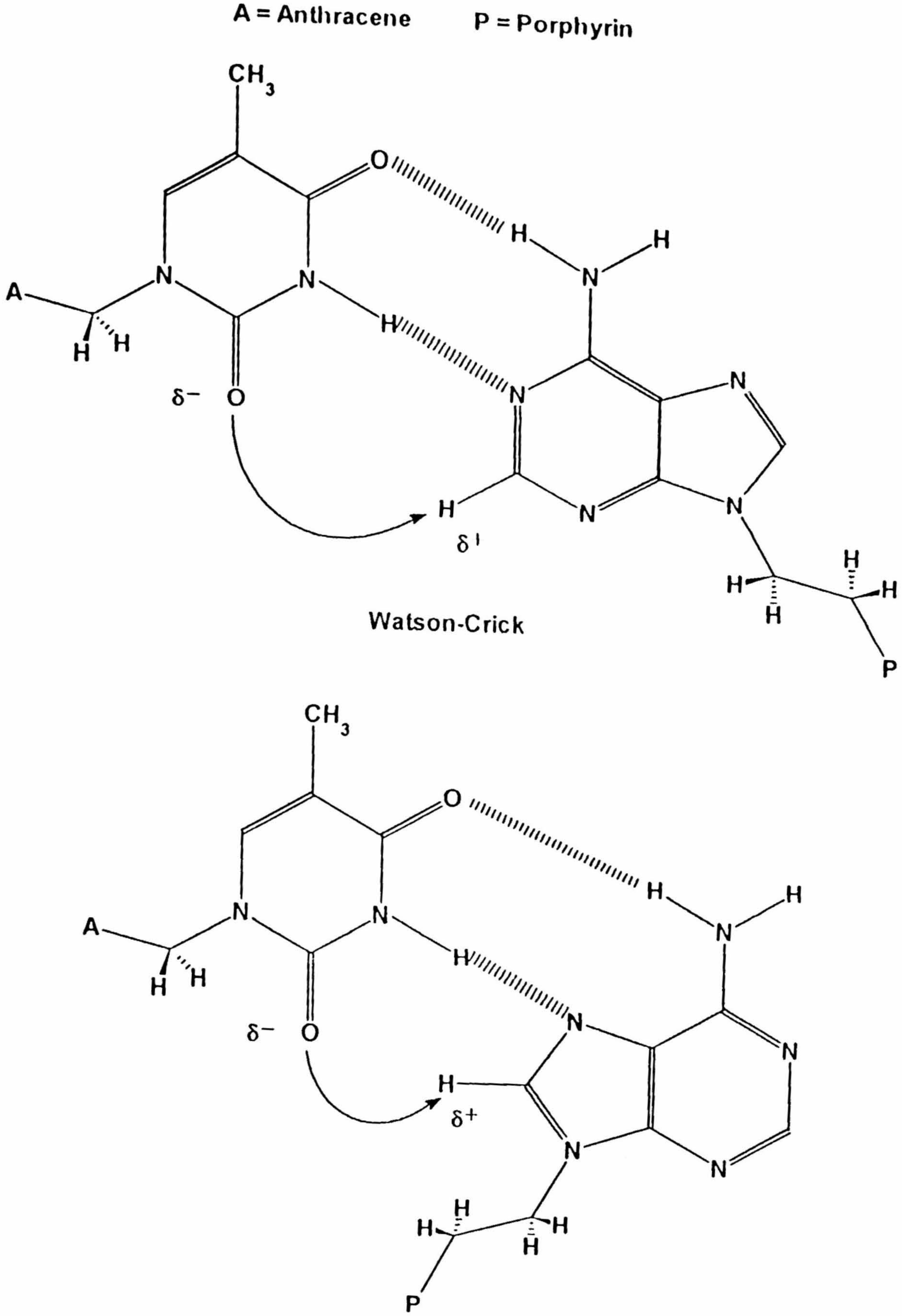

Fig. 6.9 Structures of Watson-Crick and Hoogsteen base-paired complexes that are possible in **3**.

molecular models (and also MMX minimized structures) suggest that the nucleobase prefers to be away from the porphyrin ring current. Consistent with this are the observations that no porphyrin-adenine interaction was discernible in **1** and nor was there any spectral evidence for a π- π interaction between the porphyrin and anthracene in the supramolecular complex **3** *(vide supra)*. In addition, and more importantly, other than the resonances due to adenine amine, C_2 and C_8 protons, no other resonance due to protons on **1** was seen to be downfield shifted to > ca 0 03 ppm during the NMR titration of **1** with **2** Also, spectral shifts observed for these adenine protons of **1** were not more than 0 02 ppm when **8**, which lacks the H-bonding ability, was titrated against the former conjugate Finally, in contrast to the observation made here for the A-T base paired ensemble **3**, only the Watson-Crick[36] assemblies have been reported for the previously studied G-C base-paired P-Q systems as expected.[19]

Collectively, ^{1}H NMR investigations carried out here suggest that the supramolecular D-A complex **3** is self-assembled *via* Hoogsteen and Watson-Crick type H-bonding interactions and that the association constant between **1** and **2** is low

6.3.2 Singlet state properties

Steady state flourescence spectra of **1** and **2** measured in CH_2Cl_2 are shown in Fig. 6 3 As seen from this figure, excitation of **1** at 420 nm results in a spectrum that is similar to the one obtained for H_2TTP in the same solvent Analogously, excitation of **2** at 250 nm, results in a spectrum that is similar in shape to that of free anthracene or 9-methyloxyphenylanthracene The quantum yields of porphyrin (0 11) and the anthracene (0 24) parts of **1**

and **2** are also found to be in the same range of **8** and free anthracene, respectively. These observations, together with the fact that the UV-visible and electrochemical data of **1** and **2** are quite similar to those of their corresponding reference compounds *(vide supra)* suggest that linking of nucleobases does not have any adverse effect on the photophysical attributes of porphyrin and anthracene chromophores in **1** and **2**, respectively. Accordingly, the 0-0 spectroscopic transition energies ($E_{0\text{-}0}$) and the fluorescence quantum yields of **1** and **2** are in the same range as those of the corresponding unlinked compounds

Spectra given in Fig 6.3 show a clear overlap between the emission of **2** and the absorption of **1** between 400 - 500 nm suggesting the possibility of energy transfer from the singlet state of anthracene in **2** to porphyrin in **1** As discussed in chapters 4 and 5, both Forster and Dexter mechanisms can be involved in this energy transfer Furthermore, the free energy change for the electron transfer (ΔG_{PET}) from the singlet state of **2** to **1** as derived from the redox potential and the singlet state energy data (eq 4 9) is also exoergic by (0.66 ± 0.05) eV for this system Thus, both electron- and energy transfer reactions can participate in the singlet state decay of **2** in this supramolecular P-A complex as was the case with the analogous covalently linked P-A systems described earlier

Application of the steady state fluorescence spectroscopy to probe the singlet state activity of **2** in the presence of varying amounts of **1** was found to be difficult owing to the competing absorption by the porphyrin chromophore of **1** at the excitation wavelengths (250 - 350 nm) This is not unexpected in view of a similar situation that had been encountered earlier when the intermolecular quenching of anthracene by the porphyrin was attempted (see section 4.3 2) On the other hand, the time-resolved

fluorescence method has been found to be useful to monitor the singlet state of **2** in complex **3** and also in the presence of **8** as described below.

6.3.2.2 Time-resolved fluorescence

Fig. 6 10 shows the fluorescence decay curve for a 2 μM solution of **2** (λ_{ex} = 290 nm, λ_{em} = 430 nm) in CH_2Cl_2. The decay was found to fit to a single exponential function ($f(t) = Aexp(-t/\tau)$) and gave a lifetime of 7 3 ns (χ^2 = 0.95). Addition of increasing concentrations of **1** or **8** (0 - 70 μM) to **2** (2 μ M) caused the decrease in the fluorescence lifetime of **2** with the decay being seen to fit to a monoexponential function in each case (χ^2 = 0 99 - 1 06) An analysis of the quenching data gave the Stern-Volmer constants (K_{SV}) of (1600 ± 150) and (2100 ± 300) M^{-1} for the quenching by **1** and **8**, respectively. The estimated quenching rate constants (= K_{SV}/τ, where τ is the lifetime of anthracene, 5.2 ns, or **2**, 7 3 ns), which are faster (> ca. 1 5 x 10^{11} $M^{-1}s^{-1}$) than the diffusi limit (≅ 1.4 x 10^{10} $M^{-1}s^{-1}$ in CH_2Cl_2) suggest that the electron exchange processes might play a dominant role in the quenching of **2** by **1** and **8** [43] Similarly, experiments carried out for the solutions containing equimolar mixtures of **2** and **8** or **1** at varying concentrations (0 001 - 2 mM in each case) gave slightly shorter lifetimes for solutions containing **2** and **8** (τ(**2/8**) =

Concentration (mM)	τ (ns)		
	2 /8	**2 /1**	**Δ**
0 003	7 09	7 09	0 00
0 016	6 95	6 97	0 02
0 080	6 54	6 78	0 24
0 400	4 96	5 65	0 69
0 700	3.77	4 47	0 70
1 000	3 53	4 24	0 71

Table 6.2 Time-resolved fluorescence data of equimolar mixtures of 2/8 and 2/1 in CH_2Cl_2.

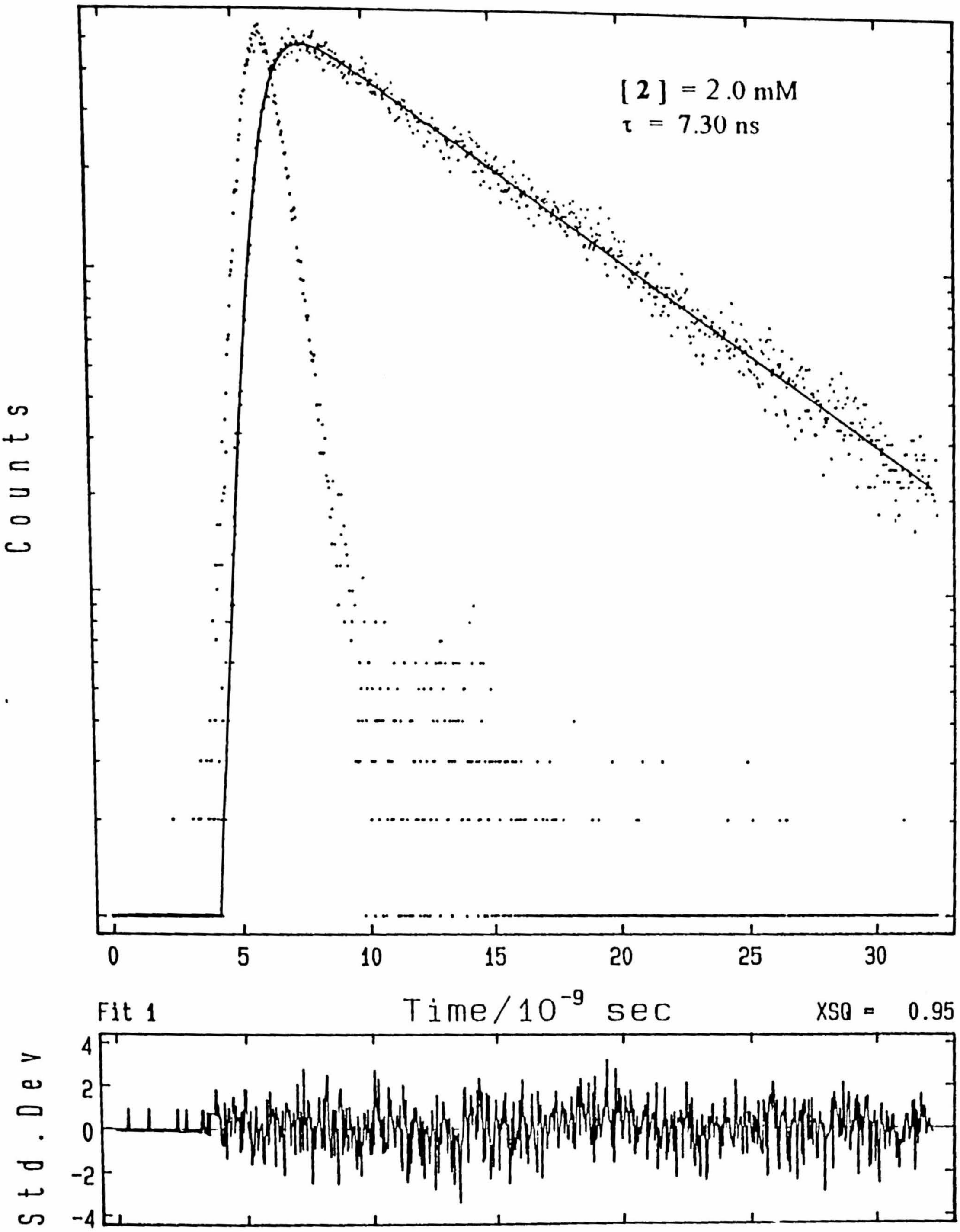

Fig. 6.10. Time-resolved fluorescence decay curve for **2**.

7 30 - 3.53 ns) in comparison with those obtained for solutions containing **2** and **1** (τ(**2**/**1**) = 7 30 - 4 24 ns) Representative decays showing this behaviour are given in Figs. 6 11 and 6 12 and Table 6 2 gives the relevant lifetime data. It can be noted here that lifetime measurements for solutions more concentrated than 2 mM could not be carried out due to a strong reabsorption by the sample. It can also be noted that addition of **5** does not quench the fluorescence of **2**

The lower Stern-Volmer constant and the shorter fluorescence lifetimes observed when **2** was titrated against **1** in comparison with the corresponding parameters obtained when **8** was titrated against **1** can, in principle and to a first approximation, be interpreted in terms of an exclusive intermolecular quenching reaction between **2** and **8** and of an additional and slightly less efficient intramolecular pathway involving the H-bonded complex **3** in the quenching reaction between **2** and **1** However, a careful analysis of the time-resolved data in the light of data obtained for the previously studied H-bonded chromophoric assemblies does not seem to suggest the same In contrast to the monoexponential decays observed in this study for solutions containing **2** and **1**, dual exponential decays, with one short- ($\leq$ 20%) and one long-lived component, have been noticed for C-C and G-G H-bonded free-base porphyrin-zinc(II) porphyrin energy-transfer systems (K = 45 $\pm$ 15 M^{-1}) [12,13] The dual exponential behaviour observed for these porphyrin ensembles can be attributed to the co-existence of H-bonded and free species that do not equilibrate within the lifetime of the zinc(II) porphyrin On the other hand, the observed monoexponential decay of **2** in the presence of **1** seem to suggest that all possible conformations of **3** might equilibrate within the lifetime of the fluorophore However, it is not realistic to assume that the Watson-Crick and the Hoogsteen type H-bonded ensembles and also the

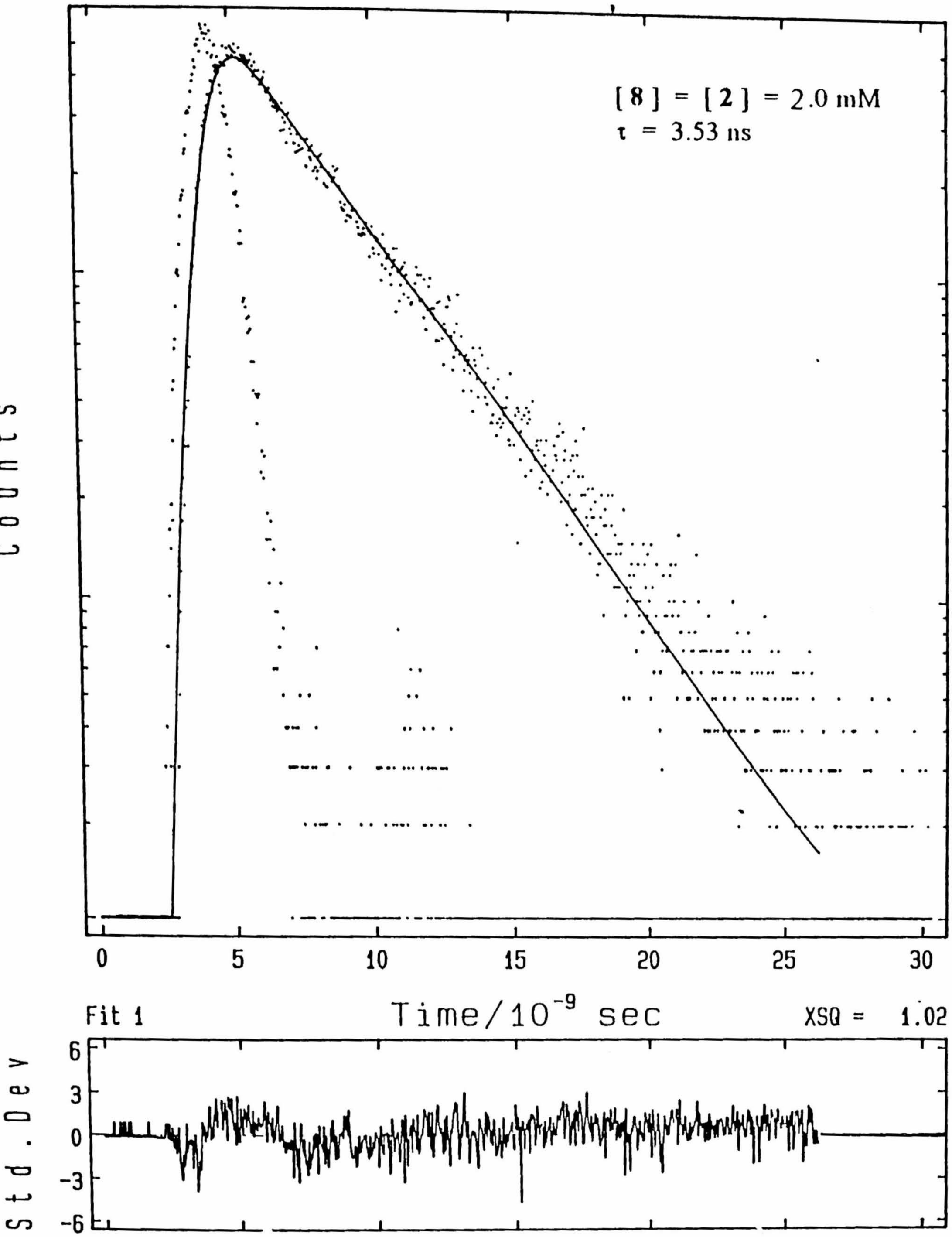

Fig. 6.11. Time-resolved fluorescence decay curve for an equimolar (2 mM) solution of **2** and **8**.

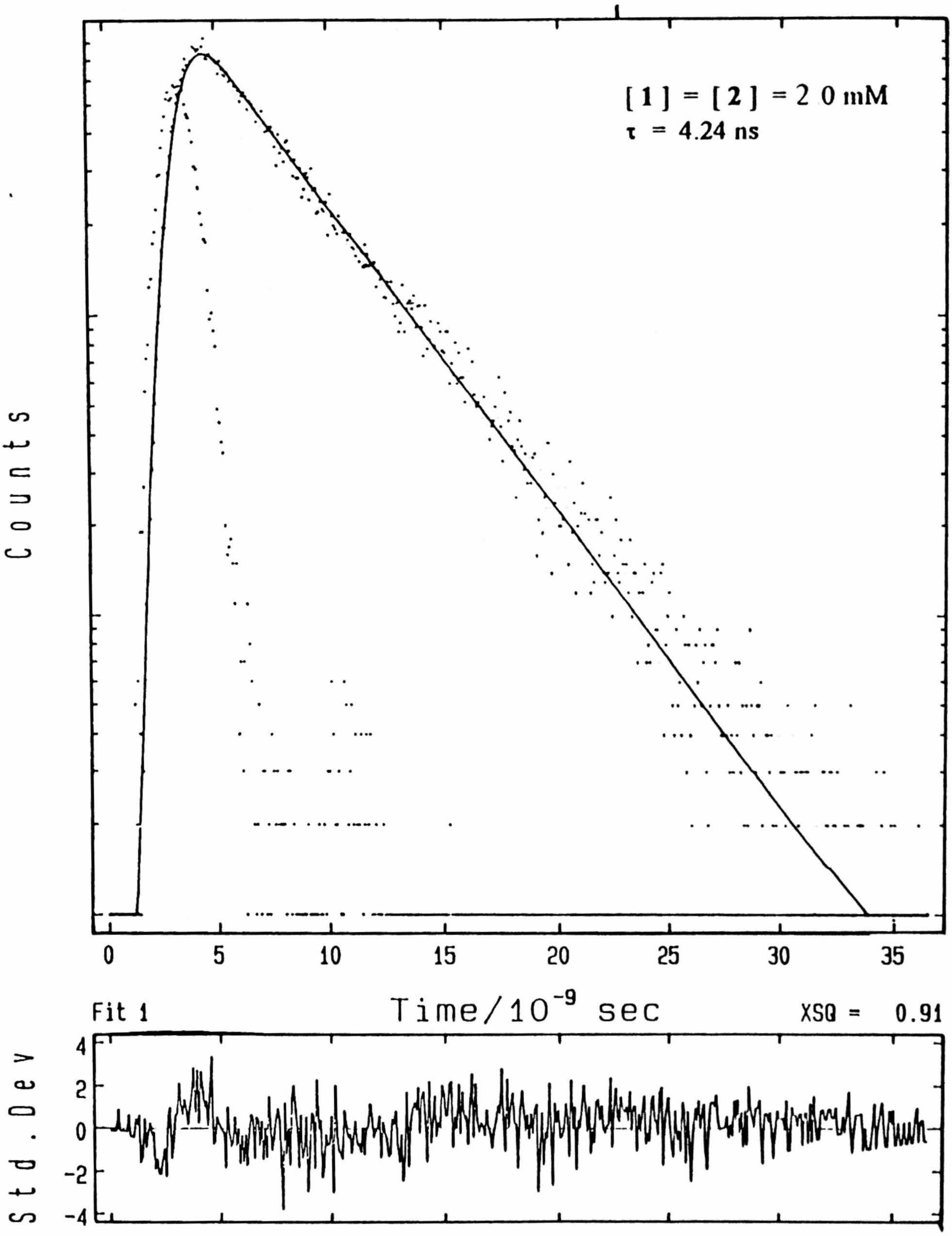

Fig. 6.12. Time-resolved fluorescence decay curve for an equimolar (2 mM) solution of **2** and **1**.

various conformations that are possible due to the presence of methylinic spacers present in these ensembles can equilibrate within the nanoseconds lifetime of the excited state of **3**.

Therefore, these data can be interpreted if one considers that the quenching of fluorescence of **2** by **1** and **8** proceed with similar rates. A comparison of the structures and the properties of the covalently linked P-A dyads (chapter 4) with those of **3** suggests that this consideration is quite reasonable. The center-to-center distance between the donor (anthracene) and the acceptor (porphyrin) for the linked dyads described in chapter 4 ranges between 12.5 - 7 A^{o}, whereas that for **3** lies at 23 ± 2 A^{o} (MMX). Accordingly, while fluorescence of the anthracene moiety in the covalently linked dyads is quenched by more than 90% that of the anthracene in **2** by the porphyrin in **1** under similar conditions (i e at [**2**]/[**1**] = 1) is quenched by only < 5%. Moreover, the fact that similar efficiencies are observed for the fluorescence quenching of anthracene by **8** and that of **2** by **1** indicates that the effective quenching distances in both the intermolecular and the H-bonded cases are also similar

6.4 Summary

A non-covalently bound supramolecular D-A system **3** has been assembled by mixing $CHCl_3$ (or $CDCl_3$) solutions of meso-5(4-(9-ethyloxyadenyl)phenyl))-10,15,20-tritolyl)porphyrin (**1**) and 1-(9-methyl-anthracenyl) thymine (**2**). Binding studies carried out by monitoring the ^1H NMR resonance due to adenine amino-Hs of **1** in the presence of **2** gave the association constant, K, to be equal to (47 ± 5) M^{-1} for the A-T base-pairing The ^1H NMR data have also suggested the presence of both Watson-Crick and Hoogsteen type H-bonded ensembles in **3** Time-resolved fluorescence

studies carried out for **2** in the presence of **1** and **8** suggest that there exist minimal influence due to the base pairing on the singlet state activity of **2**. This is in contrast to what was seen for the covalently linked P-A systems described in chapters 4 and 5 wherein the intramolecular quenching was seen to be more efficient in comparison with the intermolecular situation

6.5 References

1 Moser, C C , Keske, J M , Warncke, K , Farid, R S , Dutoon, P L *Nature* **1992**, 355, 796

2 Pelletier, H , Kraut, J *Science* **1992**, 258, 1748

3 Beratan, D N , Onuchic, J N , Winkler, J R , Gray, H B *Science* **1992**, 258, 1740

4 Wasielewski, M R *Chem Rev* **1992**, 15, 435

5 Kurreck, H , Huber, M *Angew Chem , Int Ed Engl* **1995**, 34, 849

6 Aoyama, Y , Asakawa, M , Matsui, Y , Ogoshi, H *J Am Chem Soc* **1991**, 133, 6223

7 Hayashi, T , Asai, T , Hokazono, H , Ogoshi, H *J Am Chem Soc* **1993**, 115, 1220

8 Hayashi, T , Miyahara, T , Hashizume, N , Ogoshi, H *J Am Chem Soc* **1993**, 115, 2049

9 Hayashi, T , Miyahara, T , Aoyama, Y , Nonoguchi, M , Ogoshi, H *Chem Lett* **1994**, 1749

10 Hayashi, T , Miyahara, T , Aoyama, Y , Kobayashi, M , Ogoshi, H *Pure and Appl Chem* **1994**, 66, 797

11 Mizutani, T , Murakami, T , Matsumi, N , Kurahashi, I , Ogoshi, H *J Chem Soc , Chem Commun* **1995**, 1257

12. Turro, C.; Chang, C. K.; Leroi, G. E.; Cukier, R. I.; Nocera, D. G. *J. Am. Chem. Soc.* **1992**, 114, 4013.

13. Kirby, J. P.; van Dantzig, N. A.; Chang, C. K ; Nocera, D. G. *Tetrahedron Lett.* **1995**, 36, 3477.

14. *Supramolecular photochemistry,* Balzani, V.; Reidel, D.; Ed ; Dordrecht, 1987

15. Bissell, R. A.; de Silva, A P.; Gunaratne, H. Q. N.; Lynch, P. L. M.; Maguire G. E M.; Sandanayake, K R. A. S. *Chem. Soc. Rev.* **1992**, 187.

16. *Frontiers in supramolecular organic chemistry and photochemistry,* Schneider, H.-J.; Durr, H., Ed ; VCH : Weinheim, 1991

17. Harriman, A ; Magda, D J , Sessler, J L *J Chem Soc , Chem Commun.* **1991**, 345.

18. Harriman, A ; Magda, D J., Sessler, J L *J. Phys Chem* **1991**, 95, 1530.

19. Harriman, A.; Kubo, Y.; Sessler, J. L *J. Am Chem Soc* **1992**, 114, 388

20. Sessler, J. L., Wang, B , Harriman, A. *J. Am Chem Soc* **1993**, 115, 10418.

21. Drain, M.; Fischer, R.; Nolen, E. G.; Lehn, J -M. *J. Chem. Soc , Chem Commun.* **1993**, 243.

22. Hisatome, M.; Maruyama, N ; Furutera, T.; Ishikawa, T , Yamakawa, K *Chem. Lett.* **1990**, 2251.

23. Kus, P.; Knerr, G.; Czuchajowski, L *Tetrahedron Lett.* **1990**, 36, 5133

24. Hisatome, M.; Ikeda, K.; Kishibata, S.; Yamakawa, K. *Chem Lett* **1993**, 1357.

25 Adler, A D , Longo, F R , Finarelli, J D , Goldmacher, J , Assour, J , Korsakoff, L *J Org Chem* **1967**, 32, 476

26 Esternad-Moghadam, G , Ding, L , Tadj, F , Meunier, B *Tetrahedron* **1989**, 45, 2641

27 Fkyerat, A , Demeunynck, M , Constant, J -F , Michon, P , Lhomme, J *J Am Chem Soc* **1993**, 115, 9952

28 Brown, D T , Eisinger, J ; Leonard, N J *J Am Chem Soc* **1968**, 90, 7302

29 Nakano, M , Nakano, N I , Higuchi, T *J Phys Chem* **1967**, 71, 3954

30 Wilcox, C S , Cowart, M D *Tetrahedron Lett* **1986**, 27, 5563

31 Zimmerman, S C , Wu, W , Zeng, Z *J Am Chem Soc* **1991**, 113, 196

32 Kyogoku, Y , Lord, R C , Rich, A *Proc Natl Acad Sci USA* **1967**, 57, 250

33 Iwahashi, H , Kyogoku, Y *J Am Chem Soc* **1977**, 99, 7765

34 Jeffrey, G A , Saenger, W *Hydrogen Bonding in Biological Structures*, Springer-Verlag Heidelberg, 1991, Chapter 16

35 Saenger, W *Principles of Nucleic Acid Structure*, Springer-Verlag New York, 1984, Chapter 6

36 Watson, J D , Crick, F H C *Nature* **1953**, 171, 737

37 Hoogsteen, K *Acta Crystallogr* **1959**, 12, 822 , **1963**, 16, 907

38 Jeong, K S , Muehldorf, T A , Deslongchamps, G , Famulok, M , Rebek, J Jr *J Am Chem Soc* **1991**, 113, 201

39 Jorgensen, W L , Severance, D L *J Am Chem Soc* **1991**, 113, 209

40 Gutowsky, G S , Saika, A *J Chem Phys* **1953**, 21, 1688

41 Angel, D , von Hippel, P H *Biochemistry* **1974**, 13, 4143

42 Schall, O F , Gokel, G W *J Am Chem Soc* 1994, 116, 6089

43. See *Modern molecular photochemistry;* N. J. Turro, Ed.; Benjamin/Cummings: Menlo Park, 1978, p 323

CHAPTER 7

Photophysical and DNA Cleavage Studies of Porphyrin-Based Photosensitizers for Photodynamic Therapy

7.1 Introduction

A recently emerging application of porphyrin and related macrocyclic chromophores is concerned with their role as sensitizers in the photodynamic therapy (PDT) of malignant tumors. A brief introduction to this aspect of porphyrin chemistry has already been given in Chapter 1, Section 1.2.

The haematoporphyrin derivative (HpD), a first generation photosensitizer, and its commercial variant Photofrin® have been extensively employed both in experimental and clinical studies of PDT.[1-4] However, the uncertainty about the chemical structure and mechanism of action of HpD combined with the fact that HpD absorbs weakly in the red region of the visible spectrum (where the greatest penetration of light into tissue occurs) necessitated the development of other porphyrin and related macrocycles as PDT photosensitizers.[5-7] A plethora of new photosensitizers including modified phthalocyanines,[8-11] chlorins and bacteriochlorins,[12-16] purpurins[17], benzoporphyrin derivatives,[18,19] expanded porphyrins,[20-22] and picket fence porphyrins[23-25] have been reported recently. However, many of these new generation photosensitizing drugs suffer from their inability to accumulate selectively in tumors, leading to lower levels of tumor necrosis.

One possible way to circumvent the problem of low accumulation of a given porphyrin-based drug in the cells is to equip the drug with an intracellular recognition element *viz.* a DNA or membrane binding agent. This approach has the potential to deliver a better tumor-targetting device as

the appended intracellular recognition element can, in principle, enhance the tumor accumulation ability of the drug. The modified drug is also expected to be more effective, even at low concentrations, in cleaving the DNA by either photochemical or other means Thus, porphyrin conjugates endowed with oligonucleotide,[26-29] monoclonal antibody,[30,31] ellipticene,[32-34] or other intracellular recognition element[35-38] have been reported recently It is interesting to note that most of the hitherto reported such porphyrin conjugates effect the DNA cleavage only *via* chemical means and that very little effort seems to have been done to induce the photocleavage of DNA utilizing these modified photosensitizers This has been realized in the present study and this chapter presents results of photochemical and photoinitiated DNA cleavage studies carried out on a series of new, porphyrin-based photosensitizers that are linked to either a DNA intercalator or a DNA cross-linking agent as an intracellular recognition element

The structures of these new hybrid porphyrins are shown in Fig 7 1 As seen in this figure, 5-(4-hydroxyphenyl)10,15,20-tritolylporphyrin has been linked to acridone (**1a-e**), 9-amino-acridine (**2a-c**), phenothiazine (**3a-j**) and chlorambucil (**4a-f**) derivatives, by alkyl or aryl spacers *via* ether, ester or amide bridges All these compounds were obtained as a kind gift from Professor G. Mehta, University of Hyderabad It can be noted here that while the choice of acridone, acridine and phenothiazine derivatives for linking to the porphyrin has been based on their known DNA intercalating ability,[39-42] chlorambucil, a currently marketed anti-cancer drug, has been utilized on account of its DNA cross-linking ability [43-45] A set of reference compounds 5(4-hydroxyphenyl)10,15,20-tritolylporphyrin, **5a**, 5(4-(3-aminopropyl) phenyl) 10,15,20-tritolylporphyrin, **5b**, N-propylacridone, **1f**, 9-propylaminoacridine, **2d**, N-propylphenothiazine, **3k**, N(1-propylpiperazine)-

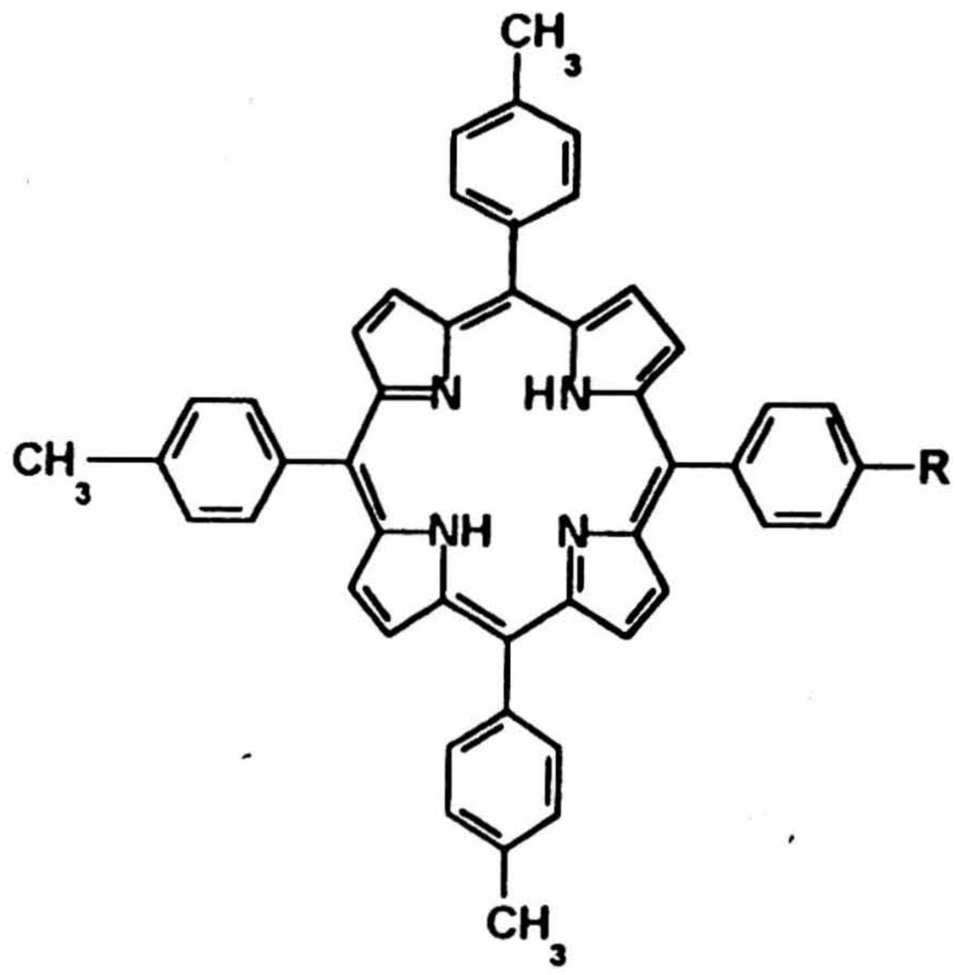

R =

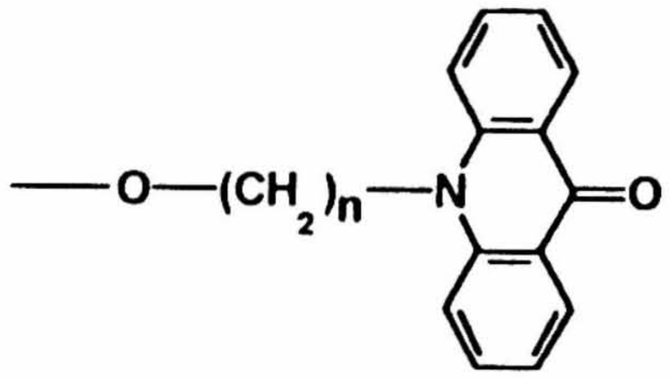

n = 2 1a
n = 3 1b
n = 4 1c
n = 5 1d
n = 6 1e

R =

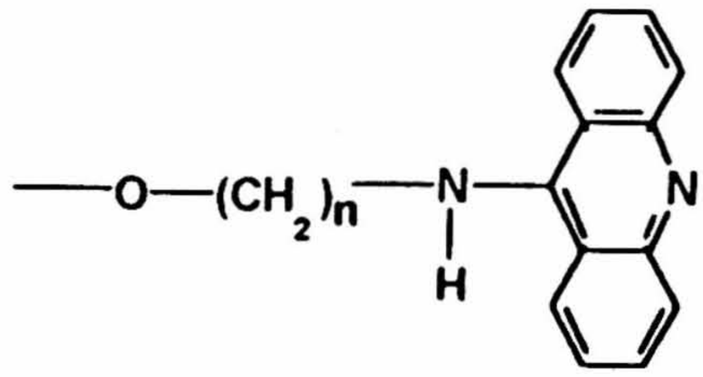

n = 2 2a
n = 3 2b
n = 4 2c

R =

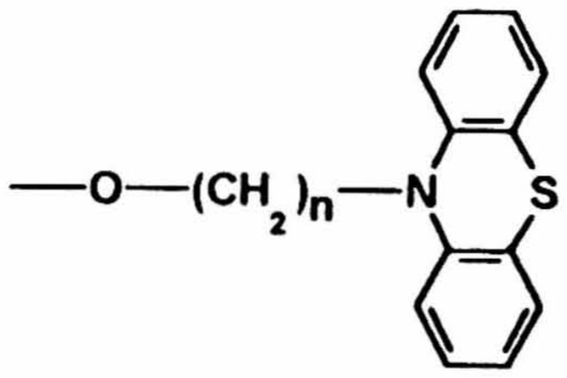

n = 3 3a
n = 4 3b
n = 5 3c
n = 6 3d

R =

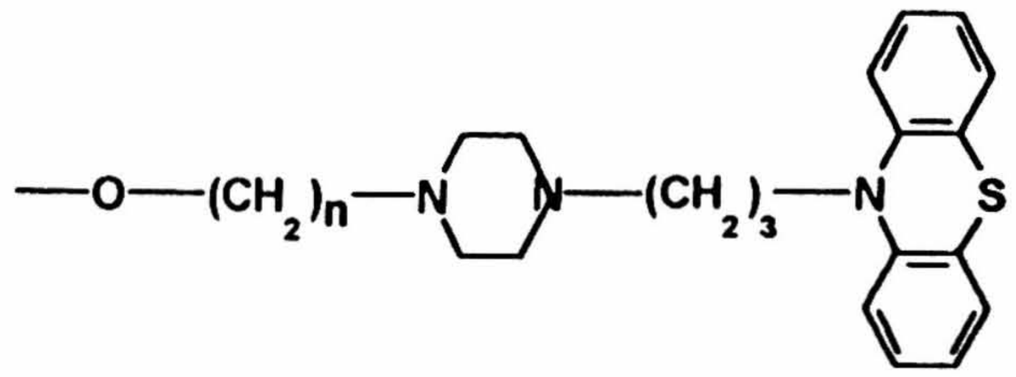

n = 3 3e
n = 4 3f
n = 5 3g

R =

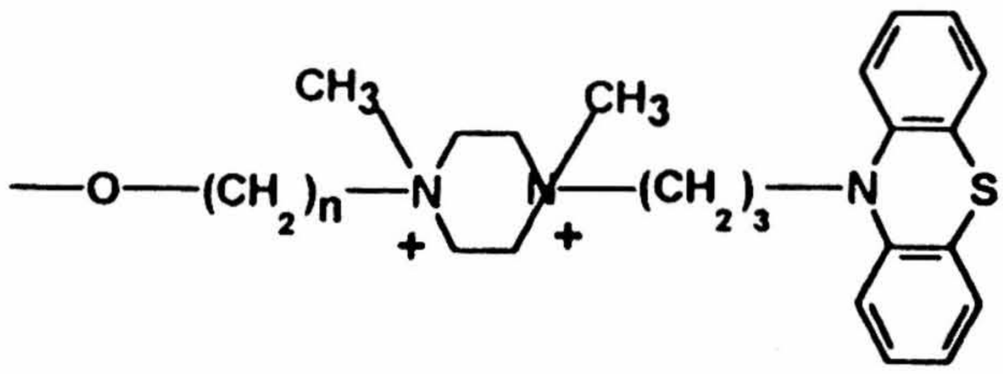

n = 3 3h
n = 4 3i
n = 5 3j

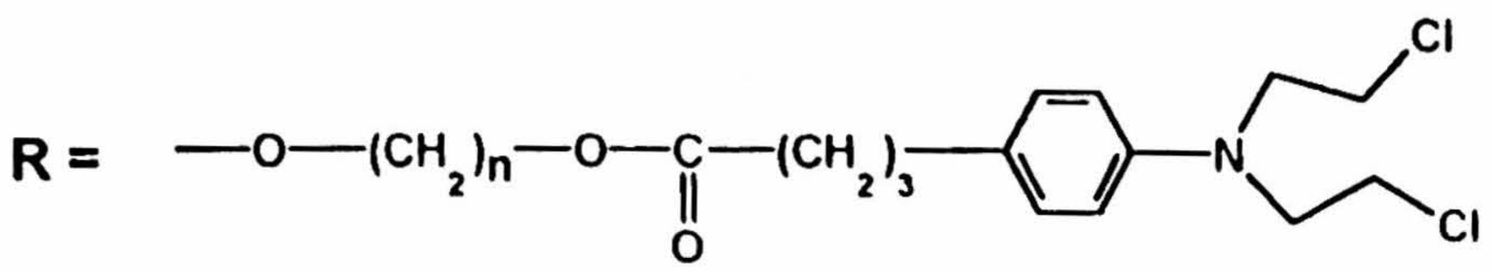

n = 3 4a
n = 4 4b
n = 5 4c
n = 6 4d

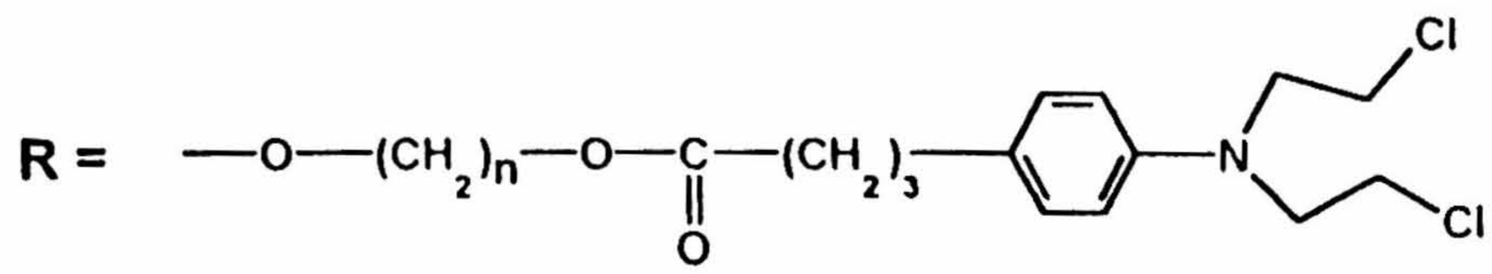

4e

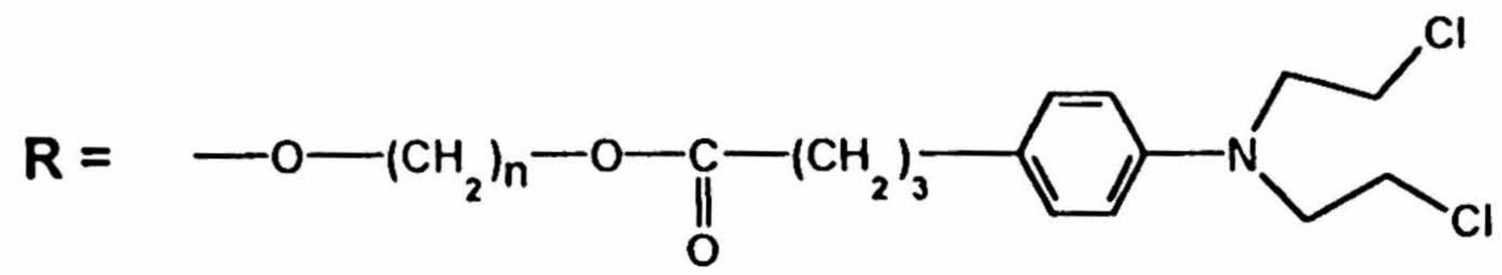

4f

R = OH 5a

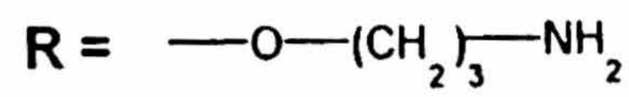

5b

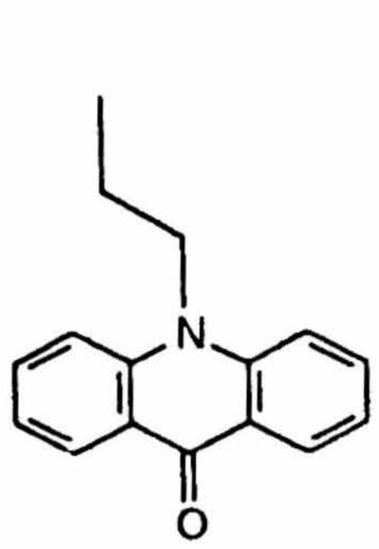

1f

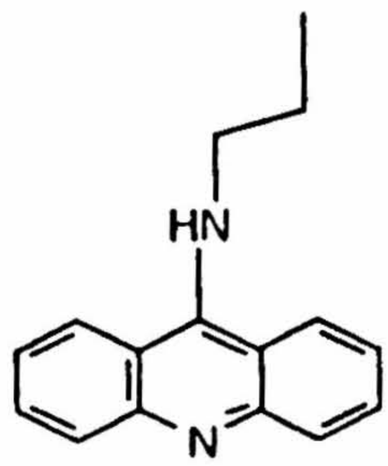

2d

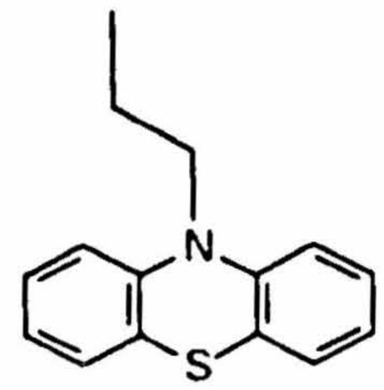

3h

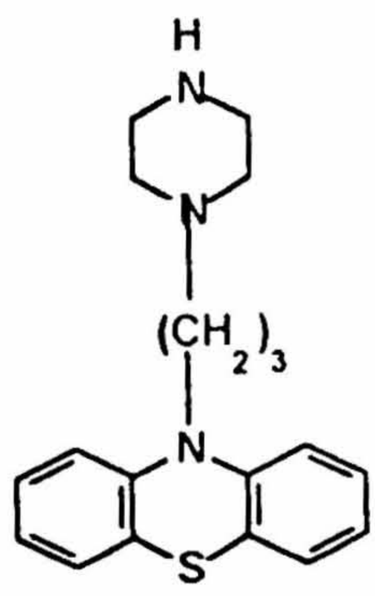

3i

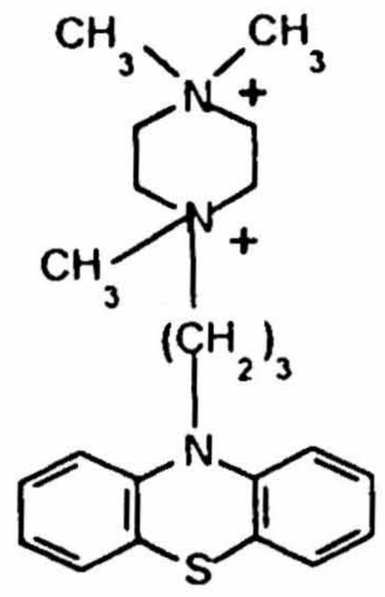

3j

Fig. 7.1. Molecular structures of "porphyrin-intracellular recognition element" conjugates

phenothiazine, **3l**, its dimethyl derivative **3m** and chlorambucil **4g** were also available or were freshly prepared. For purpose of the discussion in this chapter, these compounds have been classified into four series: series-I, porphyrin-acridone derivatives; series-II, porphyrin-aminoacridine derivatives; series-III, porphyrin-phenothiazine derivatives and series-IV, porphyrin-chlorambucil derivatives.

It can be expected that porphyrins in combination with these anti-cancer agents as intracellular recognition elements would acquire dual action capabilities - i.e. they can bind with DNA by virtue of possessing the intracellular recognition element and they can cleave DNA, probably *via* a $^1O_2$-based mechanism, when irradiated into the porphyrin absorption maximum. Indeed, as will be shown in this chapter only the hybrid porphyrins, and not the reference compounds mentioned above, are able to cleave the supercoiled pBR 322 DNA when irradiated by the visible light.

7.2 Experimental

Each investigated porphyrin was purified on a short alumina column before spectral measurements were made. All the spectroscopic and electrochemical experiments have been carried out as described in chapter 2.

Each investigated new photosensitizer has been fully characterized by elemental analysis as well as by UV-visible and ^{1}H NMR spectral methods. The ^{1}H NMR spectral data of a few selected compounds is given below.

7.2.1 ^{1}H NMR DATA

1a: -2.77(2H, s), 2.69(9H, s), 4 73(2H, t), 5 00(2H, t), 7 20-7.38(4H, m), 7.52-7 56(8H, m), 7.81-7 85(2H, m), 8.05-8.11(8H, m), 8 65(2H, dd) and 8.85-8.77(8H, m). **1b**: -2.76(2H, s), 2 62(2H, m), 2.70(9H, s), 4.41(2H, t), 4 81(2H, t), 7 26-7.36(4H, m), 7 53-7 57(8H, m), 7.77-7.80(2H, m), 8.05-

8.17(8H, m), 8.65(2H, dd) and 8 85(8H, m) **1c**: -2 76(2H, s), 2.41(4H, m), 2.69(9H, s), 4.31(2H, t), 4.50(2H, t), 7.23-7.33(4H, m), 7.51-7.62(8H, m), 7.69-7.80(2H, m), 8.06-8.13(8H, m), 8.61(2H, dd) and 8.85(8H, m) **1d**: -2.75(2H, s), 1.96(2H, m), 2.14(4H, m), 2 71(9H, s), 4.32(2H, t), 4.48(2H, t), 7.26-7.38(4H, m), 7.54-7.62(8H, m), 7.75-7.84(2H, m), 8.08-8 15(8H, m), 8.63(2H, dd) and 8.86(8H, m). **1e**: -2.76(2H, s), 1.81(4H, m), 2 06(4H, m), 2.70(9H, s), 4.30(2H, t), 4 45(2H, t), 7 26-7.37(4H, m), 7.54-7.60(8H, m), 7.73-7.80(2H, m), 8.08-8.15(8H, m), 8.63(2H, dd) and 8.86(8H, m). **1f** 1.15(3H, t), 1 90(m, 2H), 4 29(2H, t), 7 68(m, 4H), 7 74(2H, m), 8 58(2H, dd). **3a**: -2.75(2H, s), 2.45(2H, q), 2 71(9H, s), 4.27(2H, t), 4 38(2H, t), 6 97-7.07(4H, m), 7.18-7 25(6H, m), 7.56(8H, d), 8 10(8H, d), 8 86(8H, s) **3b** -2.74(2H, s), 2 13(4H, m), 2 70(9H, s), 4 07(2H, t), 4 25(2H, t), 6 95-6 99(4H, **ma**), 7.17-7.25(6H, m), 7.55(6H, d), 8 10(8H, d), 8 86(8H, s) **3c**. -2 74(2H, s), 1.80(2H, m), 2 00(4H, m), 2 71(9H, s), 3 98(2H, t), 4 19(2H, t), 6 93-7.00(4H, m), 7 16-7.23(6H, m), 7.55(6H, d), 8.10(8H, d), 8 87(8H, s) **3d** -2.76(2H, s), 1.65(2H, m), 1.94(4H, m), 2 74(9H, s), 3.95(2H, t), 4 20(2H, t), 6.86-6.90(4H, m), 7.12-7 22(6H, m), 7 53(6H, d), 8 08(8H, d), 8.85(8H, s) **3e**: -2.75(2H, s), 2 03(2H, q), 2 72(9H, m), 3 00(2H, t), 3 97(2H, t), 4 39(2H, t), 6.91-6.96(4H, m), 7.16(4H, m), 7 28(2H, d), 7 56(6H, d), 8 10(8H, s), 8.85(8H, s). **3f** -2 75(2H, s), 2.01(2H, m), 2 17(2H, m), 2.57(12H, m), 2.71(9H, s), 3.96(2H, t), 4 30(2H, t), 6.92-6 95(4H, m), 7.28(2H, d), 8.10(8H, d), 8.86(8H, s). **3g** -2 74(2H, s), 1 85(2H, m), 1.99(4H, m), 2.53(12H, m), 2.72(9H, s), 3 94(2H, t), 4 27(2H, t), 6.91-6.95(4H, m), 7.15(2H, d), 7 27(2H, d), 7.56(6H, d), 8 11(8H, d), 8.87(8H, s) **3k** 1 40(4H, m), 1.83(4H, m), 3.30(2H, t), 3.80(2H, t), 6 87(4H, m) 7.13(4H, m) **3l** 1.90(2H, m), 2 42(8H, m), 2 80(2H, t), 3.90(2H, t), 6 89(4H, d), 7 11(4H, d), 8.0(1H, s). **4a**: -2.77(2H, s), 1.92(2H, q), 2.31(2H, q), 2 42(2H, t), 2.61(2H,

t), 2.70(9H, s), 3.55(8H, m), 4.34(2H, t), 4 44(2H, t), 6.59(2H, d), 7.10(2H, d), 7.26(2H, d), 7 55(6H, d), 8 10(8H, d), 8.85(8H, s). **4b**: -2.78(2H, s), 1.97(6H, m), 2.37(2H, t), 2 59(2H, t), 2.70(9H, s), 3.59(8H, m), 4.27(4H, t), 6.60(2H, d), 7.10(2H, d), 7 26(2H, d), 7 54(6H, d), 8.10(8H, d), 8.85(8H, s). **4c**: -2.77(2H, s), 1.76(2H, m), 1.99(6H, m), 2.38(2H, t), 2.59(2H, t), 2.70(9H, s), 3.59(8H, m), 4 20(2H, t), 4.25(2H, t), 6.60(2H, d), 7 08(2H, d), 7 25(2H, d), 7 55(6H, d), 8 10(8H, d), 8 85(8H, s). **4d**: -2 75(2H, s), 1 69(4H, m), 1.95(6H, m), 2.36(2H, t), 2.58(2H, t), 2.70(9H, s), 3.61(8H, m), 4.16(2H, t), 4.23(2H, t), 6 60(2H, d), 7 07(2H, d), 7.25(2H, d), 7 54(6H, d), 8.10(8H, d), 8.85(8H, s). **4e**: -2 78(2H, s), 2 16(2H, q), 2 61-2 81(4H, m), 2.70(9H, s), 3.61(8H, m), 3 67(8H, t), 6 65(2H, d), 7.14(2H, d), 7.38(2H, d), 7.54(6H, d), 8.10(6H, d), 8.13(2H, d), 8 85(8H, s). **4f**: -2.76(2H, s), 1 99(2H, q), 2.17(2H, t), 2.26(2H, q), 2 65(2H, t), 2 70(9H, s), 3 49(8H, m), 3 63(2H, m), 4 31(2H, t), 6 57(2H, d), 7 10(2H, d), 7 22(2H, d), 7 55(8H, d), 8 10(6H, d), 8.13(2H, d), 8.85(8H, s) **4g** 1 92(2H, t), 2 38(2H, m), 2 58(2H, t), 3.68(2H, m), 6.63(2H, d), 7 08(2H, d) **5a**· -2 71(2H, s), 2 76(9H, s), 7 16(2H, d), 7 76(6H, d), 8.12(8H, d) 8 85(8H, s). **5b**: -2 75(2H,s), 2.70(9H, s), 4 00(2H, s), 7.24(2H, s), 7.54(6H, d), 8 09(8H, d), 8 85(8H, m).

7.3 Results and discussion

7.3.1 Ground state properties

The ^{1}H NMR spectra of the hybrid porphyrins are highly characteristic of each compound with the integrated intensities of the proton resonances being in conformity with the proposed structures (Fig. 7.1). The proton resonances due to the porphyrin moiety of these linked compounds occur at positions similar to those of unlinked meso-5,10,15,20(tetratolyl)porphyrin (H_2TTP) or **5a** The spacer alkyl protons in

the linked compounds resonate between 1.5-5 ppm whereas the aryl proton resonances occur at the normal aromatic region. Moreover, the proton resonances of the appended intracellular recognition moieties occur at positions similar to those of the corresponding unlinked derivatives indicating the absence of porphyrin ring current effect on these protons

The UV-visible spectral data of these hybrid porphyrins are summarized in Table 7.1 and the spectra of porphyrins **1d** and **3d** are given in Fig. 7.2. As seen from this figure and Table 7 1, porphyrin moiety in each compound shows absorption bands between 700 - 400 nm and the appended intercalator/cross-linking moiety absorbs below 400 nm The λ_{max} and logε values of the linked compounds are in the same range as those of the corresponding unlinked compounds

Table 7.2 summarizes the redox potential data of the hybrid porphyrins measured in CH_2Cl_2, 0 1 M TBAP (with respect to SCE) by the cyclic voltammetric method and representative voltammograms showing the current-voltage responses of H_2TTP, **4e** and **4f** are shown in Fig 7.3 Inspection of this figure and Table 7 2 reveals that the porphyrin part of each compound is oxidised and reduced at (1 00 ± 0 03) V and (-1 22 ± 0 05) V While the oxidations of acridone and 9-aminoacridine moieties occurs at (1.72 ± 0.03) V in series-I and II porphyrins, those of the phenothiazine and chlorambucil moieties occur at (0 80 ± 0 02) and (1 16 ± 0 02) V in series-III and IV porphyrins, respectively In the case of dicationic porphyrins of series III, **3h-j**, the cyclic voltammetric peaks ascribable to oxidation of the iodide counter ions were observed in the potential range of 0 40-0.43 V and no redox activity has been observed for the N-methylated dicationic piperazine moiety. Reduction of the appended acridine, phenothiazine and chlorambucil moieties has not been observed within the cathodic limit (-1 8 V for CH_2Cl_2)

Table 7.1 UV-visible spectral data of porphyrin-intracellular recognition element conjugates.

Compound	λ_{max},nm (log ε)							
	Porphyrin transitions					Int[a] transitions		
	Q_1	Q_2	Q_3	Q_4	B	I	II	III
1a	649 (3.76)	592 (3 73)	552 (3.99)	517 (4.25)	420 (5.67)	303 (4.26)	277 (4.53)	255 (4.80)
1b	649 (3.67)	592 (3 63)	552 (3 91)	517 (4.15)	419 (5.59)	305 (4.22)	276 (4 60)	255 (4.75)
1c	649 (3.70)	592 (3.64)	552 (3.92)	517 (4.16)	419 (5.59)	305 (4.22)	276 (4.60)	255 (4 68)
1d	649 (3.70)	592 (3.59)	552 (3.89)	517 (4.10)	420 (5 57)	306 (4.18)	277 (4.41)	254 (4.67)
1e	648 (3.56)	592 (3.59)	553 (3.87)	517 (4.10)	420 (5.54)	301 (4.18)	277 (4.41)	256 (4 67)
1f						400 (4.05)	382 (3.91)	257 (4.63)
2a	648 (3 53)	592 (3.53)	552 (3.82)	517 (4.06)	419 (5.52)			265 (5 02)
2b	648 (4 11)	592 (4 10)	553 (4.59)	517 (4.62)	419 (5 81)			266 (5.23)
2c	648 (3.77)	592 (3.78)	553 (4.07)	517 (4.31)	420 (5.75)			266 (5.24)

	2d						416 (4.25)	-----	267 (5 16)
	3a	648 (3.73)	592 (3.70)	553 (3.96)	517 (4.22)	420 (5.71)		304 (4.35)	257 (4.82)
	3b	650 (3.87)	593 (3.73)	553 (4.10)	517 (4.25)	419 (5.75)		308 (4.31)	258 (4.58)
	3c	649 (3 81)	593 (3.68)	553 (3.97)	517 (4.20)	420 (5.73)		305 (4.32)	257 (4.72)
	3d	649 (3 88)	593 (3.75)	553 (4.04)	517 (4.27)	420 (5 77)		308 (4.35)	258 (4 76)
	3e	649 (3.98)	592 (3.84)	552 (4.13)	516 (4.36)	419 (5.81)		304 (4 43)	258 (4 72)
	3f	649 (3 79)	592 (3.66)	552 (3 94)	516 (4 17)	420 (5 60)		305 (4 26)	258 (4 64)
	3g	649 (3.97)	592 (3 83)	552 (4.12)	516 (4 35)	420 (5 76)		306 (4 48)	259 (4 71)
	3h	649 (3 88)	592 (3 78)	552 (4.05)	516 (4 31)	419 (5 63)		299 (4.35)	254 (4 73)
	3i	649 (3 93)	593 (3 78)	552 (4 05)	517 (4 27)	419 (5 58)		300 (4.35)	253 (4 70)
	3j	649 (3.54)	592 (3.44)	552 (3 72)	516 (3 95)	419 (5 29)		299 (4.02)	253 (4 34)
	3k							312 (3 57)	258 (4 40)
	3l							310 (3 10)	257 (3 87)
	3m							303 (3.06)	250 (4 18)

4a	647 (3.68)	591 (3.69)	552 (3.97)	516 (4.22)	419 (5.68)	303 (4.20)	260 (4.45)
4b	648 (3.68)	592 (3.70)	552 (3.98)	516 (4.22)	419 (5.68)	303 (4.20)	259 (4.46)
4c	648 (3.75)	591 (3.75)	552 (4.03)	516 (4.27)	419 (5.73)	303 (4.24)	260 (4.49)
4d	648 (3.65)	591 (3.65)	552 (3.94)	516 (4.18)	420 (5.65)	303 (4.16)	259 (4.41)
4e	648 (3.74)	591 (3.63)	551 (3.88)	515 (4.16)	419 (5.60)	303 (4.15)	259 (4.49)
4f	647 (3.76)	591 (3.73)	552 (4.00)	516 (4.18)	420 (5.68)	303 (4.19)	260 (4.49)
4g						303 (3.31)	260 (4.15)
5a	647 (3.73)	590 (3.74)	549 (3.90)	514 (4.26)	417 (5 34)		
5b	650 (3.64)	593 (3.54)	552 (3.71)	517 (3.87)	420 (5.38)		

(a) Int = Intracellular recognition element.

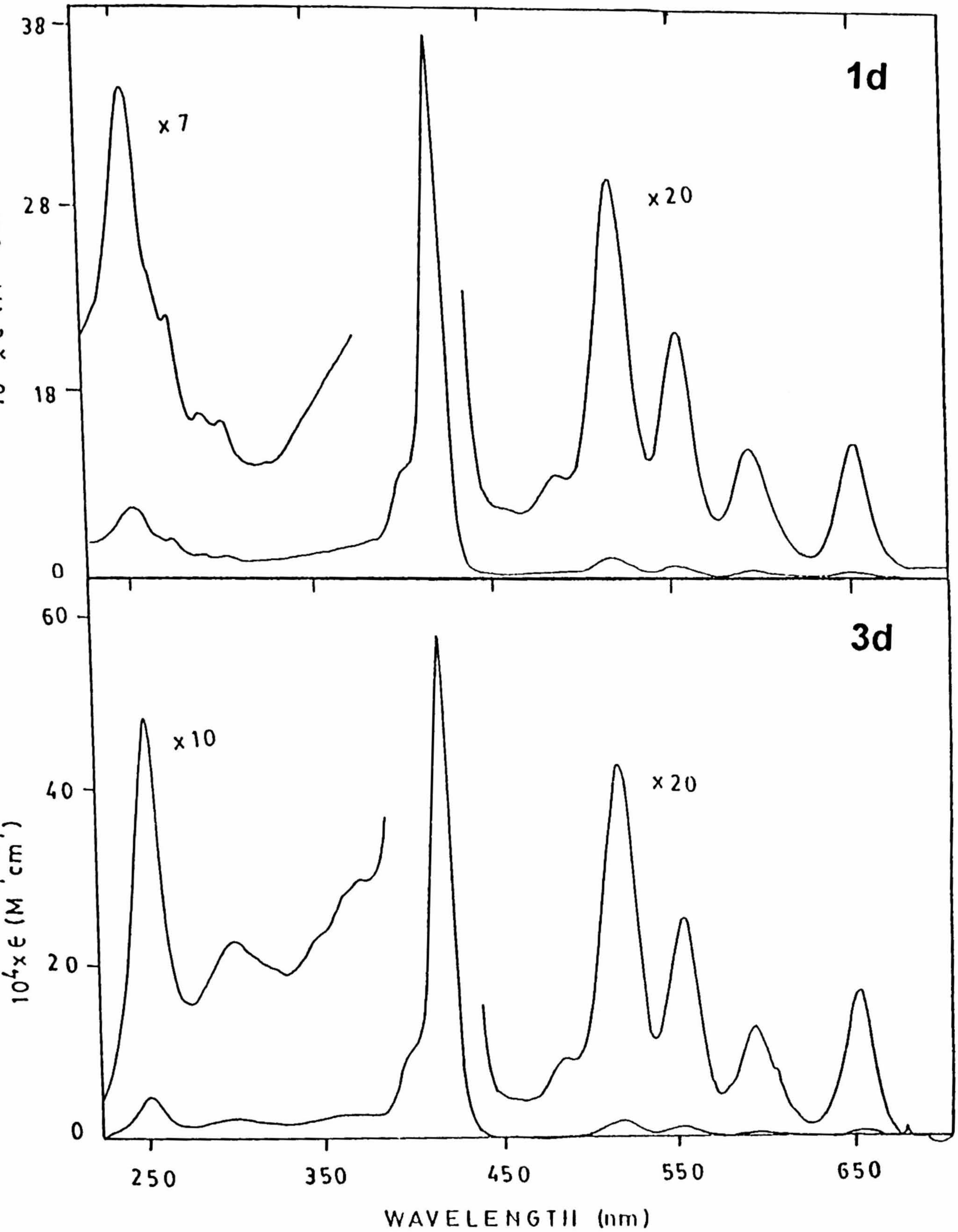

Fig. 7.2. UV-visible spectra of **1d** and **3d** in CH_2Cl_2.

Table 7.2: Redox potential data in CH_2Cl_2, 0.1 M TBAP.

Compound	$Int^a \rightarrow Int^+$	$P \rightarrow P^+$ (V)	$P \rightarrow P^-$
5a	——	0 99	-1.25
5b	——	0.99	-1.21
1a	1.70	1.00	-1.23
1b	1.72	1.02	-1.21
1c	1.70	0.99	-1.20
1d	1.69	0.98	-1.25
1e	1.70	1.01	-1.22
1f	1 68	——	——
2a	1 75	0 93	-1 21
2b	1 74	0 94	-1 22
2c	1 73	0 95	-1 22
2d	1.74	——	——
3a	0 81	0 98	-1 21
3b	0.80	0 98	-1 21
3c	0 80	0 97	-1 20
3d	0.79	0 97	-1 21
3e	0.81	0 98	-1 20
3f	0 78	0 95	-1 21
3g	0.80	0 98	-1 21
3h	0.80	0.98	-1 17
3i	0 81	0 97	-1 19
3j	0.77	0 94	-1.20
3k	0.79	——	——
3l	0.85	——	——
3m	0.76	——	——
4a	1.15	1 00	-1 19
4b	1 18	1 02	-1 19
4c	1.18	1 02	-1 18
4d	1.17	1.02	-1 20
4e	1.15	1 06	-1 18
4f	1 15	1 06	-1.19
4g	1 18	——	——

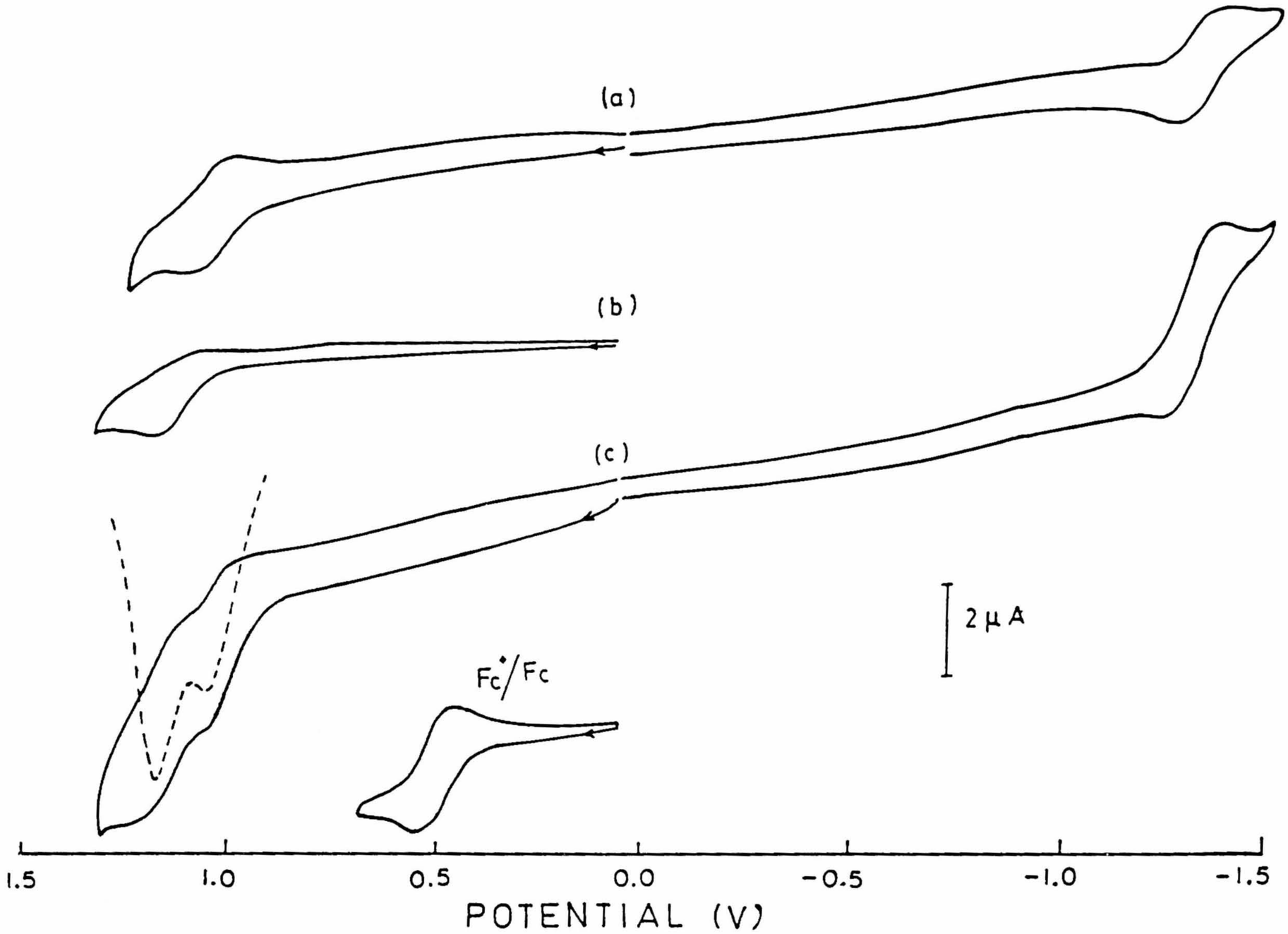

Fig. 7.3. Cyclic voltammograms (scan rate, 100 mV s^{-1}) of (a) H_2TTP, (b) **4g** and (c) **4c** in CH_2Cl_2, 0.1 M TBAP. The potential axis is referenced with SCE. The dotted line for **4c** corresponds to the differential pulse

under these experimental conditions. Thus, the redox potentials of these hybrid porphyrins are similar to those of the corresponding individual constituents. This fact coupled with the ^{1}H NMR and UV-visible data *(vide supra)* suggest that there exists no appreciable interaction between the porphyrin ring and the appended intracellular recognition element in these hybrid porphyrins.

7.3.2 Singlet state properties

When excited with light of wavelength corresponding to the porphyrin absorption maximum (420 nm), all of the hybrid porphyrins exhibited a characteristic porphyrin fluorescence spectrum in CH_2Cl_2 solutions with peak maxima appearing at (650 ± 2) and (710 ± 2) nm in each case The peak maxima and the quantum yield (ϕ = 0 13 ± 0 02) values of these porphyrins are similar to the corresponding values observed for the reference porphyrins **5a** or **5b**. On the other hand, when excited at 255 nm, where the acridone or the aminoacridine moieties absorb strongly, compounds **1a-e** (series-I) and **2a-c** (series II) although showed fluorescence spectra that are similar in shape to those of acridone or aminoacridine, the intensities of these fluorescence bands were found to be decreased in comparison with those of free acridone or aminoacridine. This observation is illustrated as a representative example in Fig. 7.4 which shows the fluorescence spectra of series-I porphyrins. The ϕ_f values of these compounds have been estimated using the standard method (Chapter 2) with reference to N-propylacridone (ϕ_f = 0 65), and the relevant data are summarized in Table 7 3 From the ϕ_f values given in Table 7 3, the quenching efficiencies (%Q) have been calculated using eq 7 2

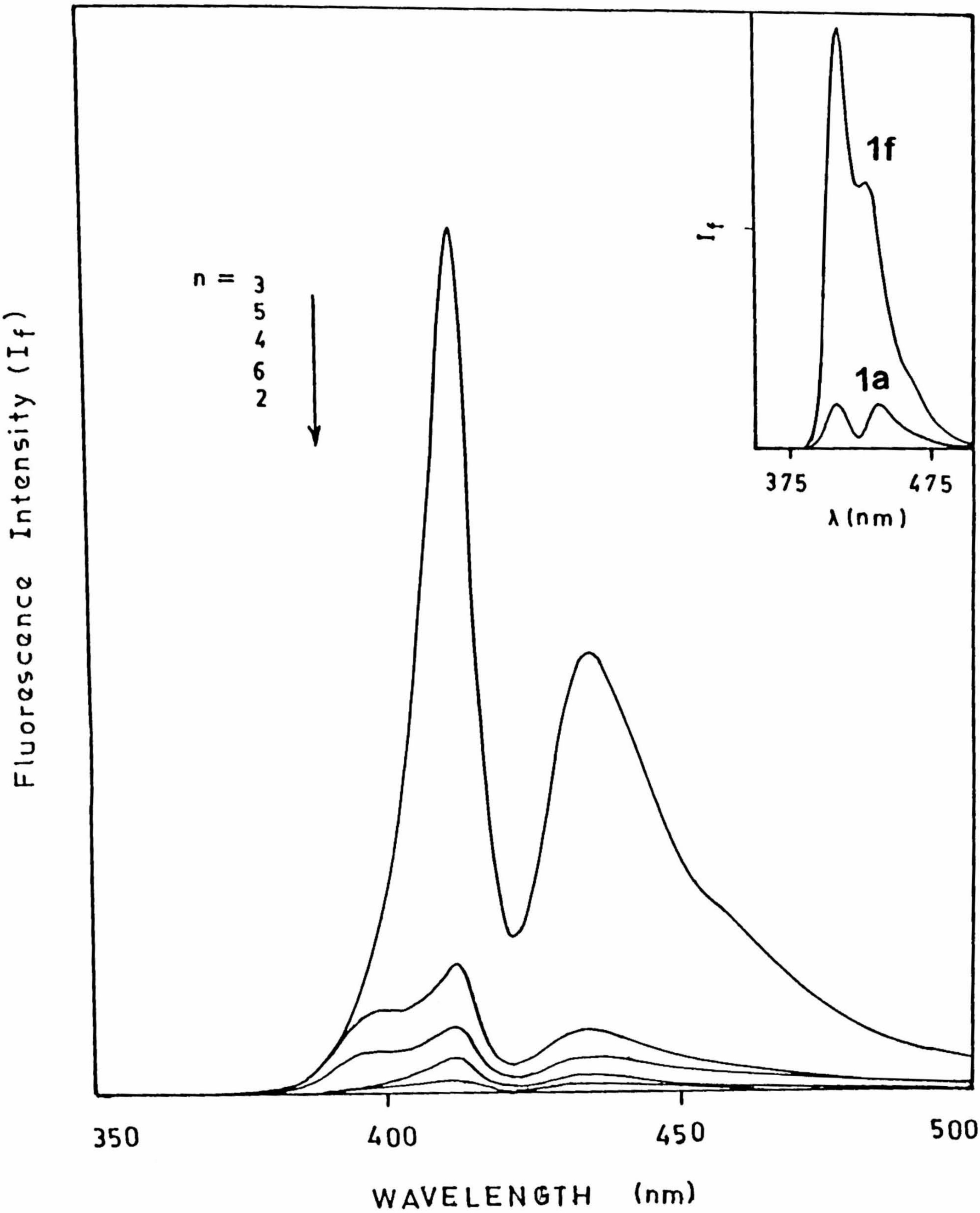

Fig. 7.4. Fluorescence sepctra of series I porphyrins in CH_2Cl_2 Inset shows the flourescence spectra of **1f** and **1a**. Solutions were excited at 255 nm.

$$Q = \frac{\phi_f(\textbf{1f or 2d}) - \phi_f(\textbf{1a-e or 2a-c})}{\phi_f(\textbf{1f or 2d})} \qquad (7.2)$$

Table 7.3 : Steady state fluorescence data in CH_2Cl_2.

Compound	**Porphyrin emission (λ_{ex} = 420 nm)**		**Int[a] emission (λ_{ex}= 260 nm)**	
	λ_{max} (nm)	ϕ_f	λ_{max} (nm)	ϕ_f
1a	651,711	0.14	412,433	0.0013
1b	651,712	0.13	412,435	0.09
1c	652,712	0.14	412,434	0.014
1d	651,712	0.12	412,434	0.007
1e			412,434	0 004
1f			413,433	0.61
2a	650,711	0.13	399, 452	0.04
2b	651,712	0.13	399, 442	0.007
2c	651,711	0.13	396	0.007
2d			413, 456, 476	0.10
5a	651,712	0.13		
5b	651,711	0 14		

(a) Int · Intracellular recognition element

The Q values for both series I and series II porphyrins are given in Table 7.3. The fluorescence from phenothiazine and chlorambucil moieties of series III and series IV hybrids was found to be too low to be measured with any accuracy ($\phi_f < 10^{-4}$).

Fig. 7.5 shows the fluorescence spectrum of 9-propylacridone (**1f**), and the absorption spectrum of H_2TTP. There is a strong overlap of the acridone's emission into the absorption of H_2TTP suggesting a possibility of intramolecular energy transfer from the acrodone to the appended porphyrin. The emission of 9-aminopropylacridine (**2d**) also shows a similar overlap with the absorption spectrum of H_2TTP. Thus, the fluorescence quenching observed for the acridone/acridine moieties in series I and series II hybrids might be due to intramolecular EET from these intercalators to the porphyrin Indeed, fluorescence excitation spectra of compounds **1a-e** and **2a-c** obtained when the emission was monitored at the porphyrin emission maximum (650 nm) showed absorptions due to the acridone/acridine moieties in the UV region. A comparison of the overlay of normalized excitation spectrum of these hybrids with the corresponding absorption spectra in the region of 45 5 x 10^3 - 37.0 x 10^3 cm^{-1} (220-270 nm), gave the energy transfer efficiencies (T_{obs}) of 74% (**1a**), 85% (**1b**), 98% (**1c**), 80% (**1d**) and 77% (**1e**) for series I hybrids and 79% (**2a**), 89% (**2b**) and 65% (**2c**) for series II porphyrins

No attempt has been made here to investigate on the exact mechanism of the observed intramolecular EET occurring in the hybrid porphyrins However, the excitation spectra obtained when emission was collected at the porphyrin emission maximum (650 nm) for mixtures containing 1:1 mole equivalents of H_2TTP and **1f** or **2d** did not show any absorption due to the latter chromophores This rules out the possibility of intermolecular energy transfer in series I and series II porphyrins under these experimental

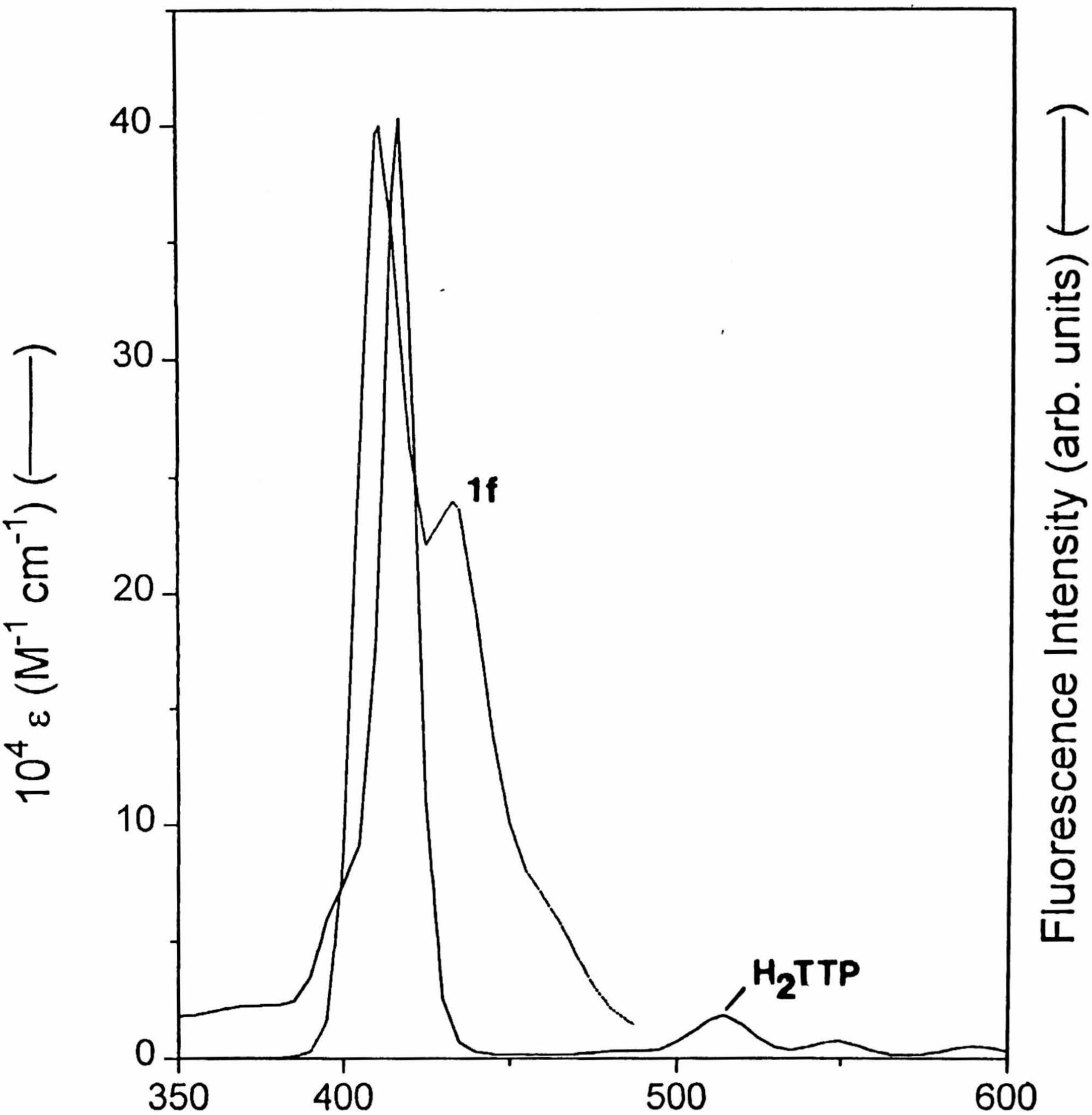

Fig. 7.5. UV-visible sepctrum of H_2TTP (———) and the fluorescence spectrum (λ_{ex} = 250 nm) of **1f** (------). The spectra were regenerated using absorption /fluorescence data obtained at 5 nm interval. The peak heights of the two spectra are normalized for clarity.

conditions. Thus, the efficient intramolecular EET from the appended intracellular recognition elements to the porphyrin part of these hybrids is a positive feature as it provides flexibility of irradiation anywhere inside the absorption envelope of **1a-e** and **2a-c** and yet eventuates in the excited state of the porphyrin sensitizer.

The possibility of a photoinduced electron transfer (PET) reaction from the singlet excited state of the appended acridine/acridone moiety to the porphyrin is also discernible in these hybrid porphyrins as was the case with the porphyrin-anthracene systems described in the earlier chapters Based on the redox potential data and the singlet state energies of acridone and 9-aminoacridine moieties, the free energy changes involved in the PET reactions from the singlet states of the appended intracellular recognition element to the porphyrin in both series I and series II photosensitizers have been estimated to be -0 20 ± 0 02 V. Thus, these systems can show both EET and PET reactions as illustrated in Fig 7.6. The free energy changes involved in the PET reactions that are possible in series III and series IV porphyrins were also found to be exoergic (-0 80 ± 0.02 (series III) and -1 52 ± 0 02 V (series IV)) and these might rationalize the low fluorescence quantum yields observed for the chlorambucil or the phenothiazine group in these systems

7.3.3 Singlet oxygen generation

Many porphyrin sensitized *in vivo* and *in vitro* photoreactions appear to be mediated by $^1O_2$ which is produced by collisional energy transfer from the porphyrin triplet state followed by spin exchange [46,47] The $^1O_2$ being a highly reactive species, diffuses a small distance before it reacts with biomolecules, such as cell membranes, nucleotide bases, unsaturated lipids, α-amino-acid residues etc to give photooxidation products resulting in

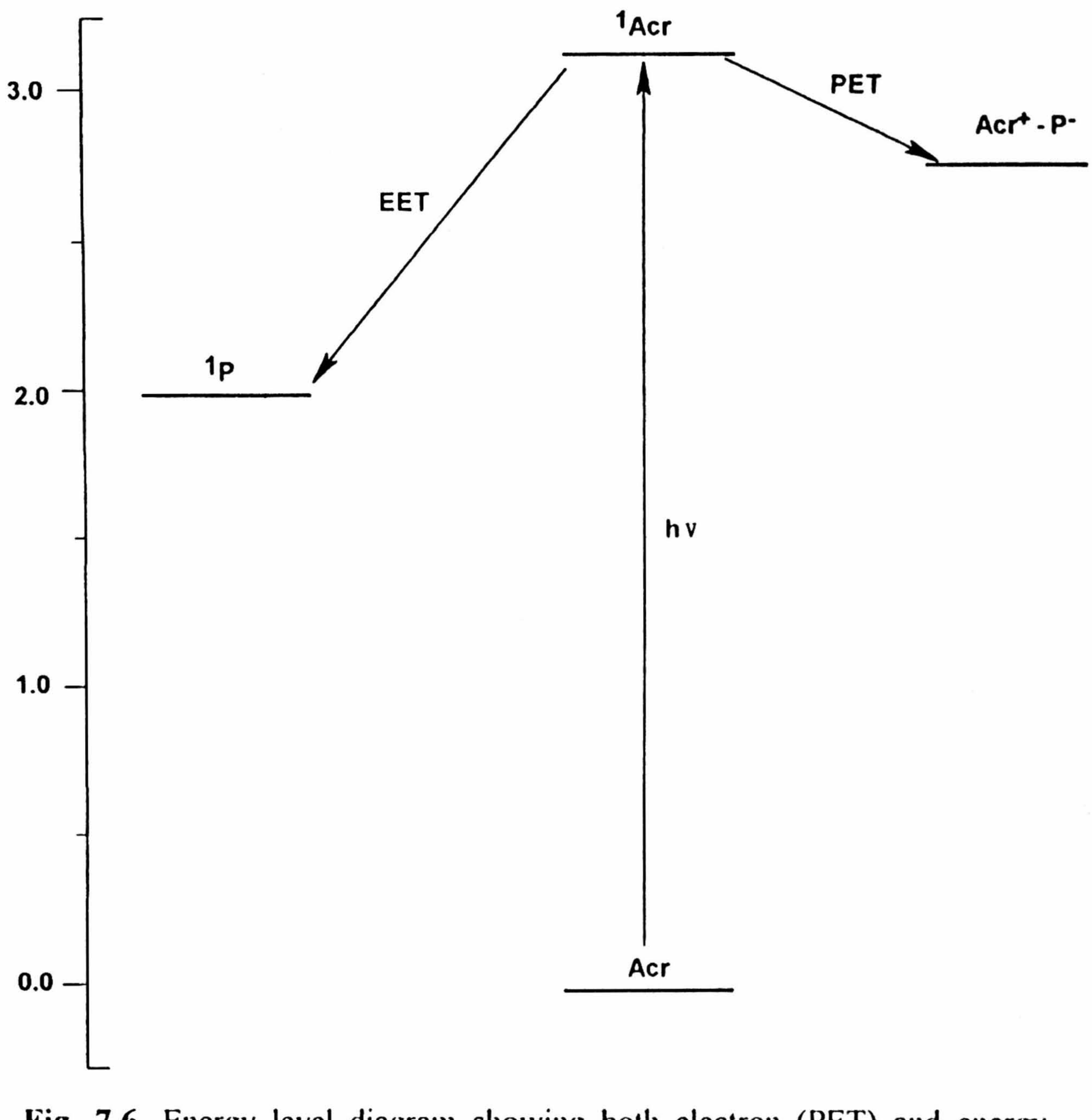

Fig. 7.6. Energy level diagram showing both electron (PET) and energy (EET) transfer reactions from the excited singlet state of the acridone/aminoacridine moiety of series I and series II porphyrins. Here, P = Porphyrin and Acr = acridone/aminoacridine.

DNA/membrane damage leading to photo-necrosis.[48,49] The quantity which defines the efficiency of the photosensitizer with regard to PDT is the quantum yield of singlet oxygen (ϕ_Δ). Measurements of ϕ_Δ have been carried out using both steady state and time-resolved techniques [50] Steady state methods, by and large, have employed chemical traps, *viz* the molecules that react with $^1O_2$ resulting in loss of the starting material. Because of its largely chemical quenching of $^1O_2$ and the high reaction rate constant, 1,3-diphenylisobenzofuran (DPBF) has been employed as the $^1O_2$ scavenger in most of the studies and this study has also employed DPBF as the $^1O_2$ scavenger. The mechanism of $^1O_2$ production by the photosensitizers and the decay of it *via* reactions with DPBF are given in eqs 7 2 - 7 7

$$^1S_0 \xrightarrow{h\nu/I_{abs}} {}^1S^* \qquad (7\ 2$$

$$^1S^* \xrightarrow{k_{isc}} {}^3S^* \qquad (7.3$$

$$^3O_2 + {}^3S^* \xrightarrow{k_\Delta} {}^1O_2 + {}^1S_0 \qquad (7\ 4$$

$$DPBF + {}^1O_2 \xrightarrow{k_r} DBB \qquad (7.5$$

$$DPBF + {}^1O_2 \xrightarrow{k_q} DPBF + {}^3O_2 \qquad (7.6$$

$$^1O_2 \xrightarrow{k_d} {}^3O_2 \qquad (7.$$

Here, I_{abs} is the intensity of the light absorbed, k_d is the rate of $^1O_2$ production, k_r and k_q are the rates of chemical reaction and physical quenching of DPBF with $^1O_2$, respectively, and k_d is the solvent initiated $^1O_2$ decay.

Thus,

$$\frac{d[^1O_2]}{dt} = I_{abs}\ \phi_\Delta \qquad (7.8)$$

Eq. 7. 9 can be obtained from eq. (7.5),

$$-\frac{d[DPBF]}{dt} = k_r\,[DPBF]\ [^1O_2] \qquad (7.9)$$

and, from eqs. (7.4), (7.5), (7 6) and (7.7), it follows that

$$\frac{d[^1O_2]}{dt} = I_{abs}\ \phi_\Delta - [^1O_2]\,(k_r\,[DPBF] + k_q\,[DPBF] + k_d) \qquad (7\ 10)$$

At steady state conditions,

$$\frac{d[^1O_2]}{dt} = 0 \qquad (7.11)$$

Therefore, the eq.(7.10) becomes

$$I_{abs}\,\phi_{\Delta} = [^1O_2]\,(k_r + k_q)\,[DPBF] + k_d \qquad (7.12)$$

Rearranging, the above equation gives

$$[^1O_2] = \frac{I_{abs}\,\phi_{\Delta}}{k_d + (k_r + k_q)\,[DPBF]} \qquad (7.13)$$

Substitution of eq 7.13 into eq 7.9, gives

$$-\frac{d[DPBF]}{dt} = I_{abs}\,\phi_{\Delta}\,\frac{k_r\,[DPBF]}{k_d + (k_r + k_q)\,[DPBF]} \qquad (7.14)$$

Since, at low concentrations,[68] k_q for DPBF is insignificant as compared to k_d,[51] it can be assumed that $(k_r + k_q)\,[DPBF] << k_d$ and thus eq (7.14) becomes

$$-\frac{d[DPBF]}{dt} = \frac{I_{abs}\,\phi_{\Delta}\;k_r\,[DPBF]}{k_d} \qquad (7.15)$$

Integration of eq (7.15) gives,

$$-\ln\frac{[DPBF]_t}{[DPBF]_0} = \frac{I_{abs}\,\phi_{\Delta}\;k_r}{k_d}\;x\;t \qquad (7.16)$$

Thus, a plot of $-\ln(A_t / A_0)$ (A is the absorbance of DPBF at 326 or 415 nm) versus time of irradiation, t, will give a straight line passing through the origin, whose slope equals to $I_{abs}\,\phi_\Delta k_r / k_d$ By knowing k_r, k_d and I_{abs}, the ϕ_Δ can be calculated In this study, the values of k_r and k_d were taken to be 1 1 x 10^9 M^{-1} s^{-1} and 1 40 x 10^5 s^{-1} respectively [52] I_{abs} for a given photosensitizer was calculated from the slope by substituting the values of k_r, k_d and ϕ_Δ of H_2TPP (ϕ_Δ = 0 60) taken as the standard The experimental details are given in chapter 2, section 2 5

Representative spectra showing the depletion of DPBF with time in the presence of H_2TPP and **4c** are given in Fig 7 7 and the ϕ_Δ values of hybrid porphyrins are summarized in Table 7 4 Inspection of Table 7 4 reveals that, within the experimental error, ϕ_Δ values of all the hybrid porphyrins are in the same range as that of H_2TPP This fact suggests that appending an intracellular recognition element has no adverse effect on the photosensitizing ability of the porphyrin in all these hybrid molecules

7.3.4 Nuclease activity

Among the various methods developed to detect single- and double-strand cleavage of DNA, the most convenient one is the agarose gel electrophoresis method [53] Single strand breaks in supercoiled DNA (form I) lead to open circular DNA (form II) and double strand breaks lead to linear DNA (form III)[54-56] (Fig 7 8) In an agarose gel, form I DNA migrates faster compared to other two forms, whereas form II migrates slower because of the decrease in the superhelical density Form III, however, moves at an intermediate rate relative to form I and form II Thus, three forms of DNA can be readily separated by the agarose gel electrophoresis method and they can easily be visualized by staining with a fluorescent dye (ethidium bromide) and

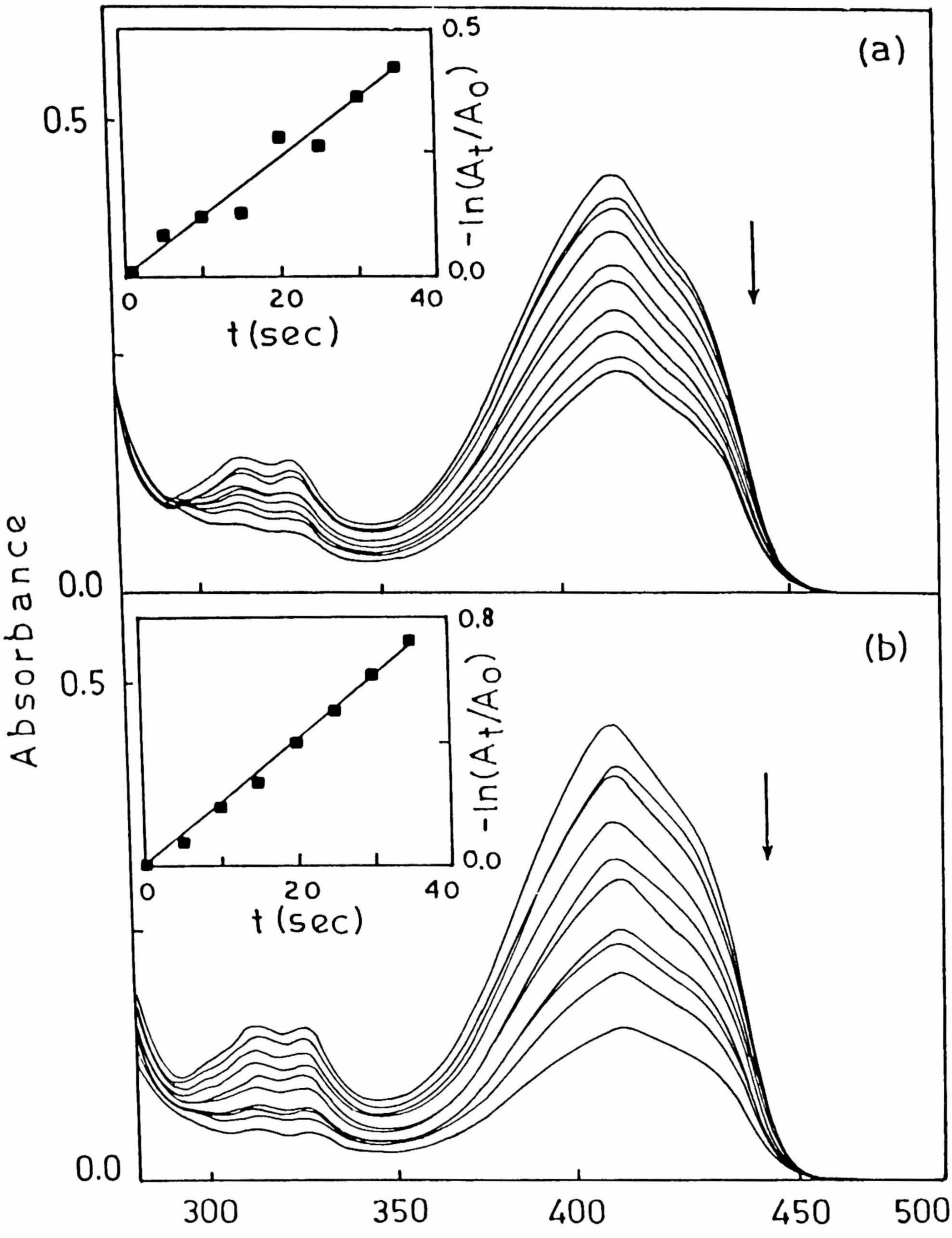

Fig. 7.7. UV-visible spectra of DPBF (5 x 10^{-5} M) in presence of (a)H_2TPP (1.0 x 10^{-6} M) and (b) **4e** (1.0 x 10^{-6} M) recorded after each 5 s of irradiation (lines 1 to 10), (λ_{irrd} 530 nm). The inset shows plot of $-\ln(A_t/A_0)$ vs. t (sec) in each case where A_0 is the absorbance of DPBF at time t = 0

subsequent illumination with UV light [57] The nuclease activity of the hybrid porphyrins has been studied by this method using the plasmid DNA pBR 322 in the presence and in the absence of light. The experimental details of the assay are given chapter 2, section 2.6 2

Table 7.4 : Singlet oxygen quantum yield (ϕ_Δ) data in DMF.

Compound	ϕ_Δ	Compound	ϕ_Δ
1a	0 56	**3g**	0 60
1b	0 69	**3h**	0 71
1c	0 66	**3i**	0 80
1d	0 70	**3j**	0 79
1e	0 60	**3k**	0 30
1f	0 45	**3l**	0 13
2a	0 77	**3m**	0 15
2b	0 70	**4a**	0 70
2c	0 68	**4b**	0 57
2d	0 40	**4c**	0 64
3a	0 66	**4d**	0 62
3b	0 64	**4e**	0 65
3c	0 77	**4f**	0 57
3d	0 76	**4g**	0 35
3e	0 41	**5a**	0 66
3f	0 67	**5b**	0 60

Figures 7 9-7 12 summarize the results of irradiation/electrophoresis experiments. Upon irradiation by the visible light ($\lambda > 400$ nm), compounds **1a-e**, **3a-d** and **4a-f** all effected relaxation of the supercoiled form I to

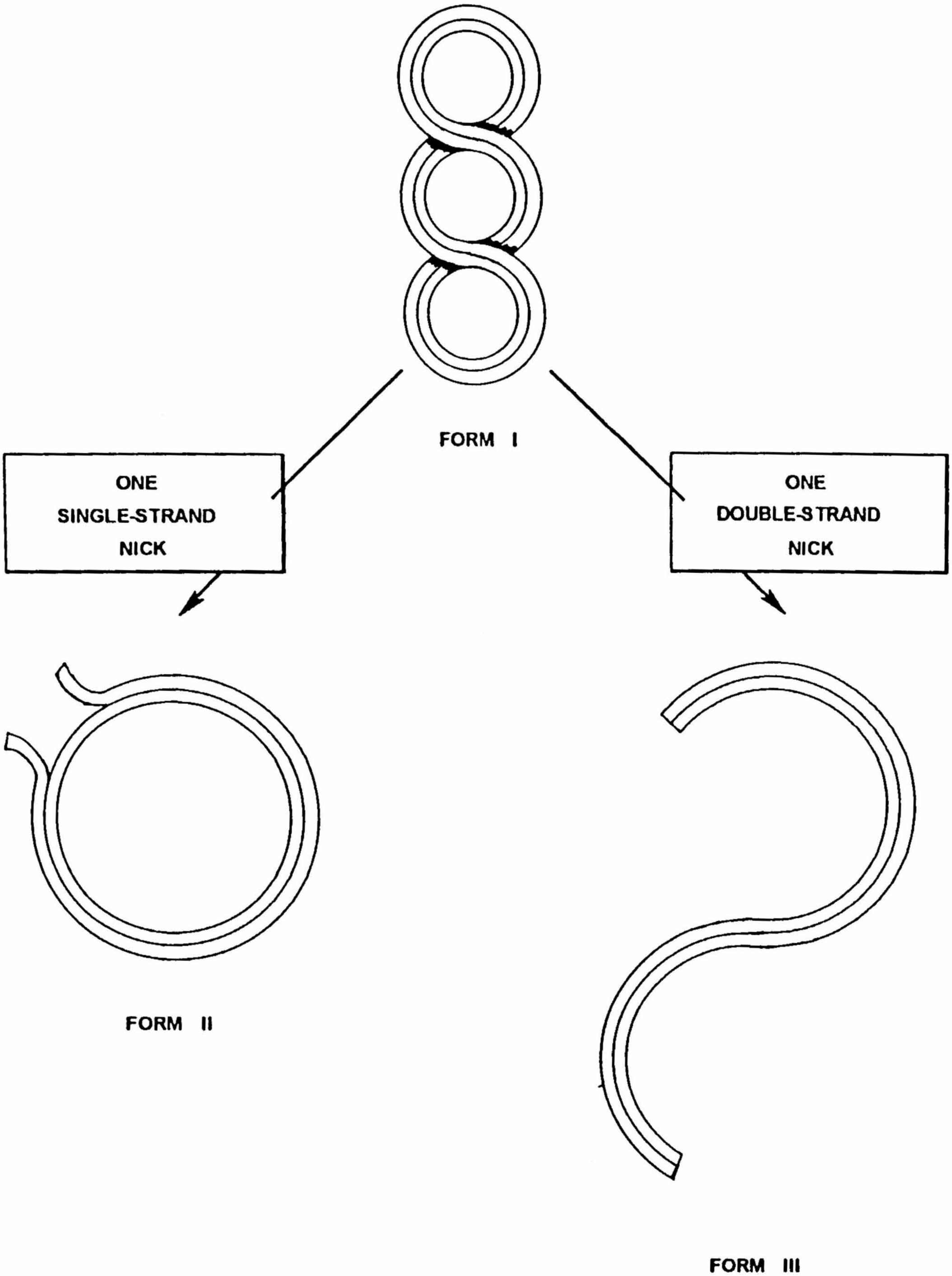

Fig. 7.8. Pictorial representation of the three forms of DNA: Form I (supercoiled), Form II (open circular) and Form III (linear)

generate open circular form II (Fig. 7.9 and 7.10). The cationic porphyrins **3h-j** displayed DNase activity (data not shown). While little or no photocleavage activity has been observed when compounds **2a-c** and **3e-g** were used (Fig 7.11 and 7.12), all of the hybrid porphyrins investigated in this study did not effect the DNA cleavage in the absence of irradiation. The latter observation has been illustrated in photographs of representative gels (**3a-d** and **4a-f,** in the dark) shown in Figs. 7.13 and 7.14. Finally, it is important to note that reference compounds **5a**, **5b**, **1f**, **2d**, **3k**, **3l** and **3m**, which either lack the intracellular recognition element or the porphyrin, all showed no nuclease activity either in the presence or in the absence of light.

The fact that the present series of drugs, upon irradiation, cause only a single-strand nick and not a double strand nick is demonstrated in Fig. 7.15. In this gel, one of the lanes has been loaded with a Hind III digested pBR 322 DNA and the other, with a sample of pBR 322 DNA that had previously been irradiated with **4b.** Hind III, a restriction enzyme, recognizes specific sequences within the double-stranded DNA and causes two coincident nicks on it leading to an exclusive generation of the linear form III. As seen in Fig. 7.15, while the lane corresponding to the Hind III digested pBR 322 DNA shows a complete relaxation of the supercoiled form I to linear form III, that corresponding to the drug-digested DNA shows no sign of form III in it.

Recent studies have shown that among the various reactive species that are responsible for the photocleavage of DNA by the porphyrin-based sensitizers, $^1O_2$ is of importance.[58-63] While it is tempting to invoke a $^1O_2$-based mechanism for the observed nuclease activity of the present series of hybrid porphyrins, especially in the context of the observed high ϕ_Δ values, other mechanisms including those based on electron transfer reactions can not be altogether neglected.[64,65] As discussed earlier, intramolecular PET is

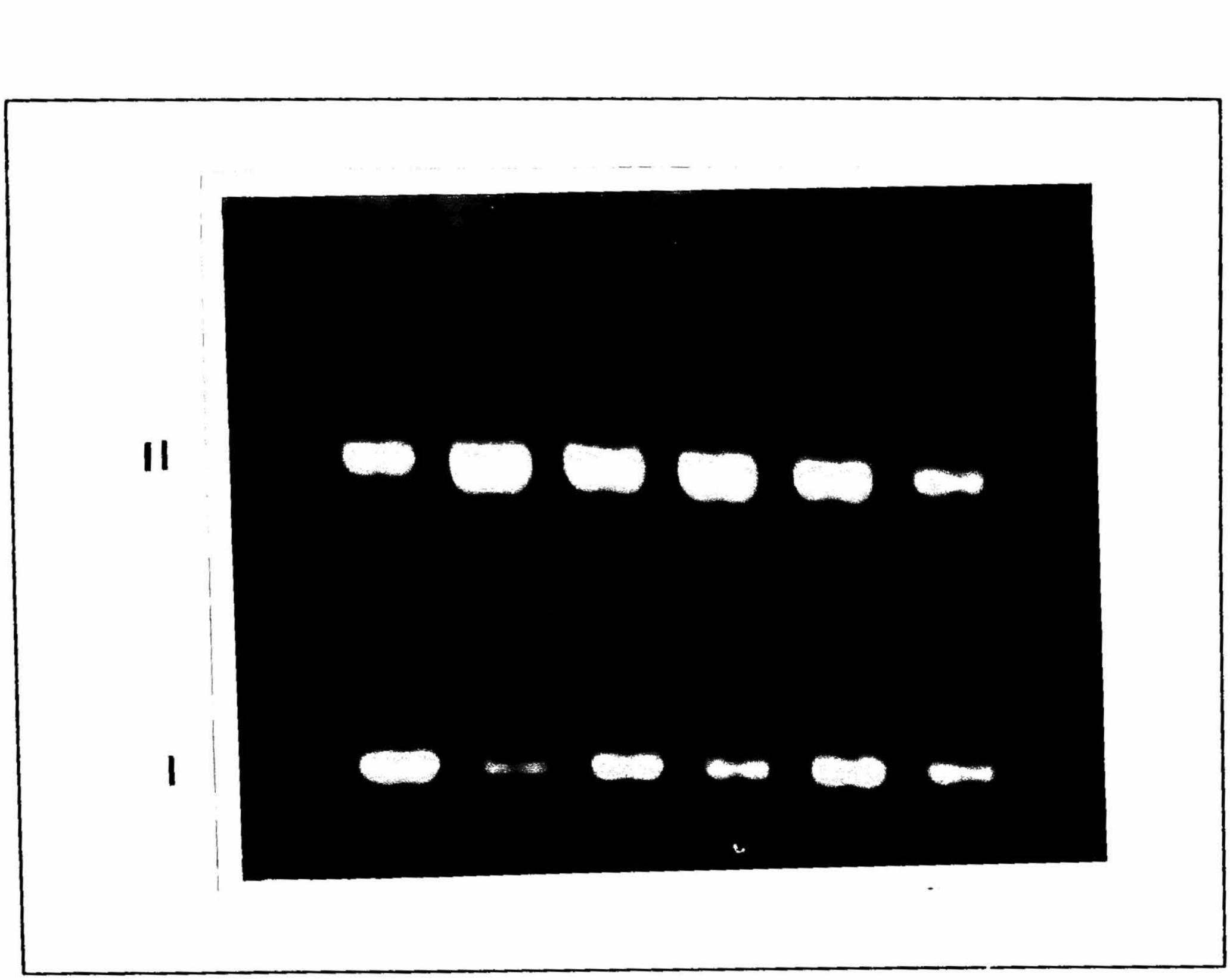

Fig. 7.9. Light induced nuclease activity of series III porphyrins, **3a-d** (left to right) Lane 1 Untreated pBR 322, Lanes 2, 3, 4, 5 and 6 pBR 322 + **3a**, **3b**, **3c**, **3d** and **5a** In each case [DNA]/[Drug] = 1 and samples were incubated for 1h before being irradiated with visible light ($\lambda > 400$ nm) for 2.5 h Electrophoresis experiment was carried out as described in section 2 6

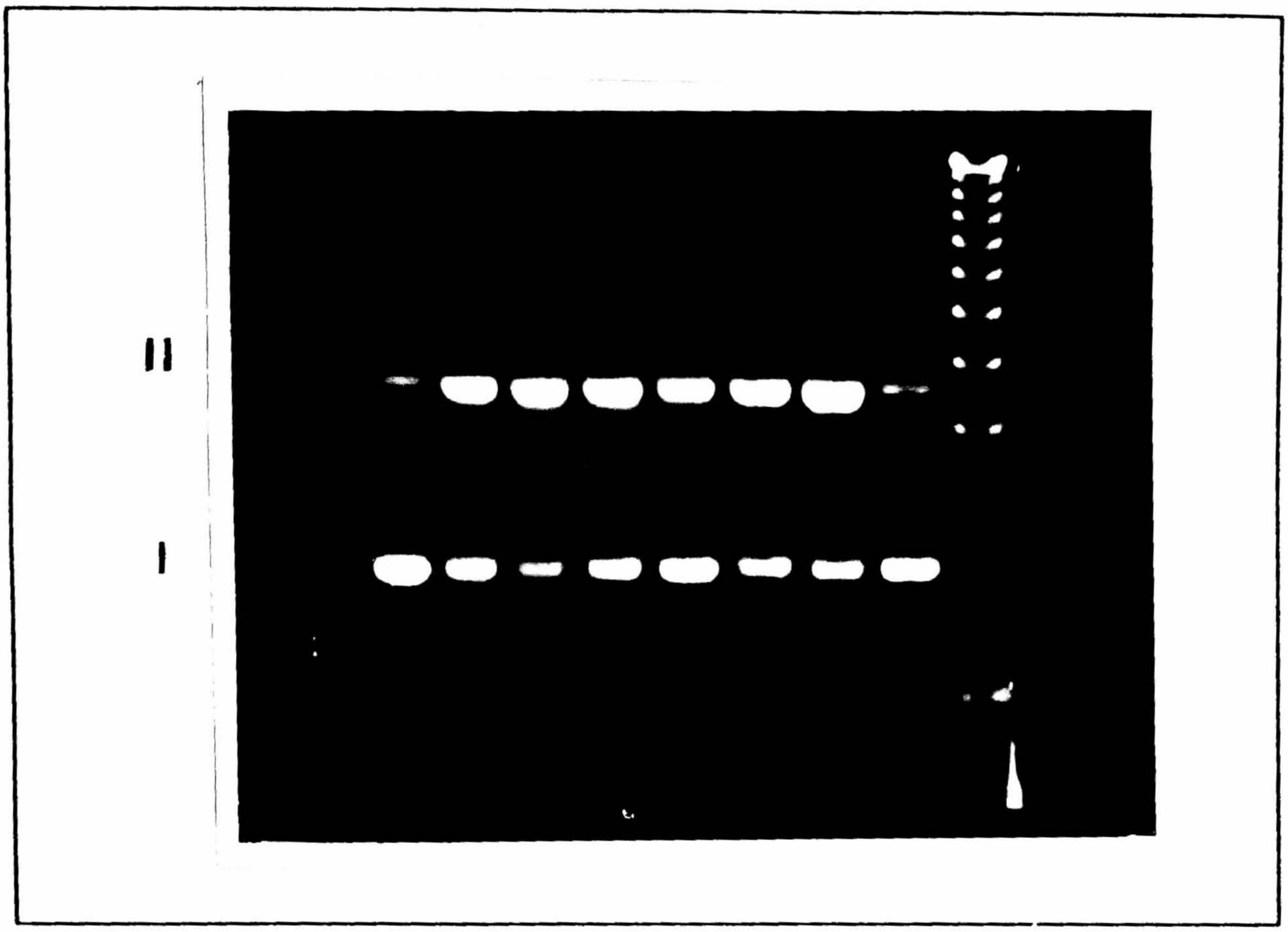

Fig. 7.10. Light induced nuclease activity of series IV porphyrins (left to right) Lane 1 Untreated pBR 322, Lanes 2, 3, 4, 5, 6, 7 and 8 pBR 322 + **4e**, **4a**, **4b**, **4c**, **4d**, **4f** and **4g** Lane 9 DNA molecular weight marker In each case [DNA]/[Drug] = 1 and samples were incubated for 1h before being irradiated with visible light ($\lambda > 400$ nm) for 2.5 h Electrophoresis experiment was carried out as described in section 2 6.

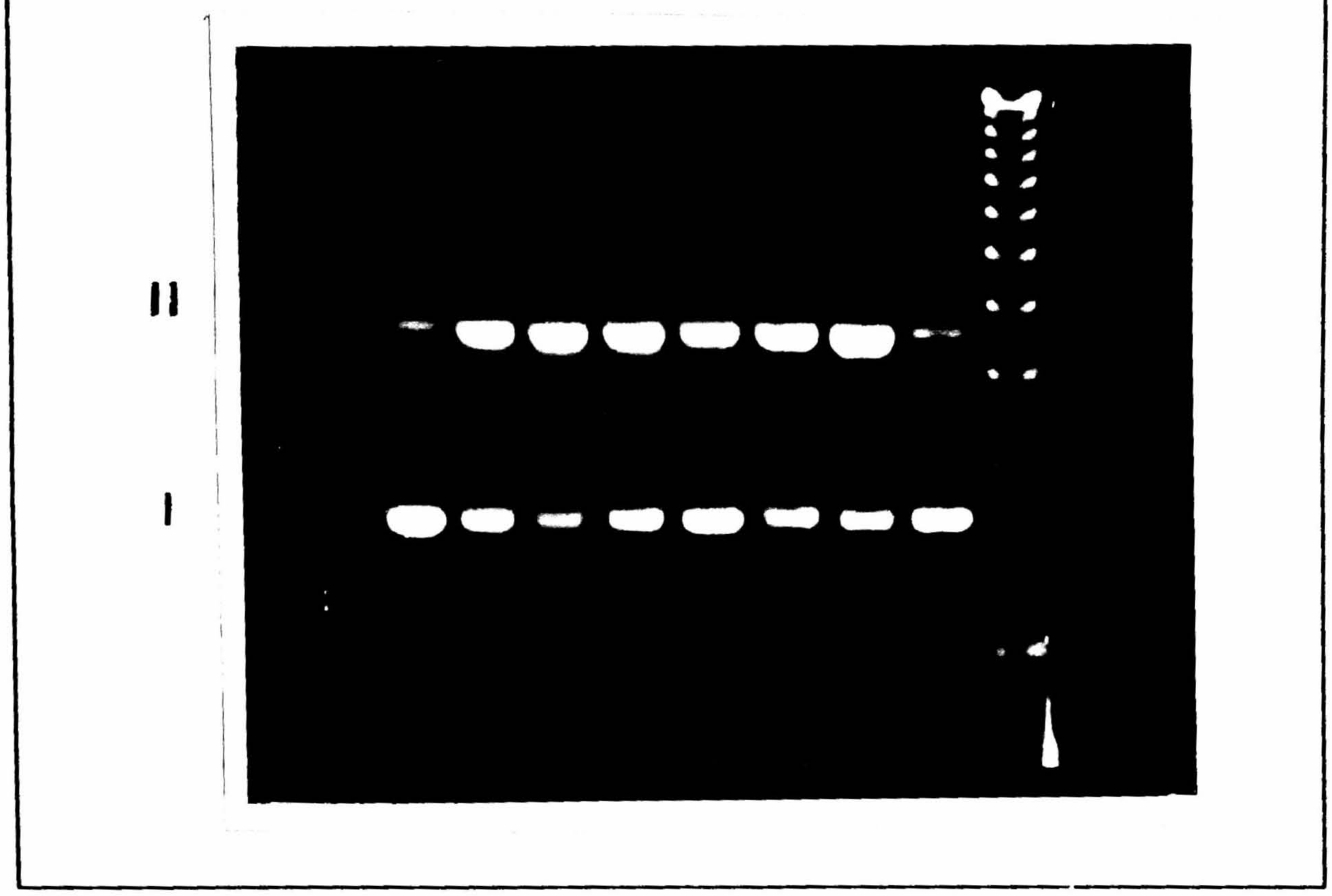

Fig. 7.10. Light induced nuclease activity of series IV porphyrins (left to right) Lane 1: Untreated pBR 322, Lanes 2, 3, 4, 5, 6, 7 and 8 pBR 322 + **4e**, **4a**, **4b**, **4c**, **4d**, **4f** and **4g** Lane 9 DNA molecular weight marker In each case [DNA]/[Drug] = 1 and samples were incubated for 1h before being irradiated with visible light ($\lambda > 400$ nm) for 2.5 h Electrophoresis experiment was carried out as described in section 2 6.

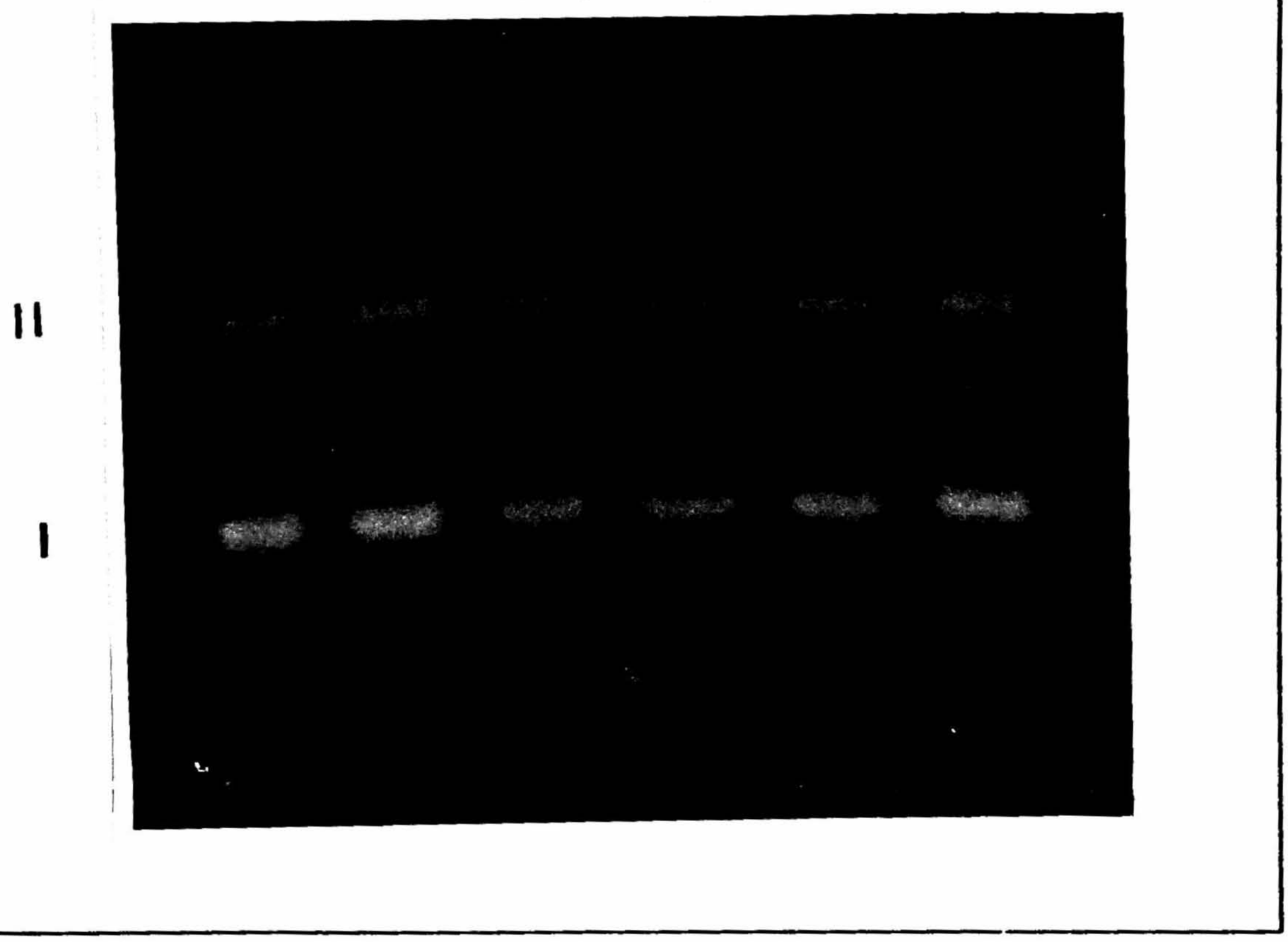

Fig. 7.11. Light induced nuclease activity of series II porphyrins, **2a-c** (left to right) Lane 1: Untreated pBR 322, Lanes 2, 3, 4, 5 and 6. pBR 322 + **2a**, **2b**, **2c**, **2d** and **5b** In each case [DNA]/[Drug] = 1 and samples were incubated for 1h before being irradiated with visible light ($\lambda > 400$ nm) for 2.5 h. Electrophoresis experiment was carried out as described in section 2.6

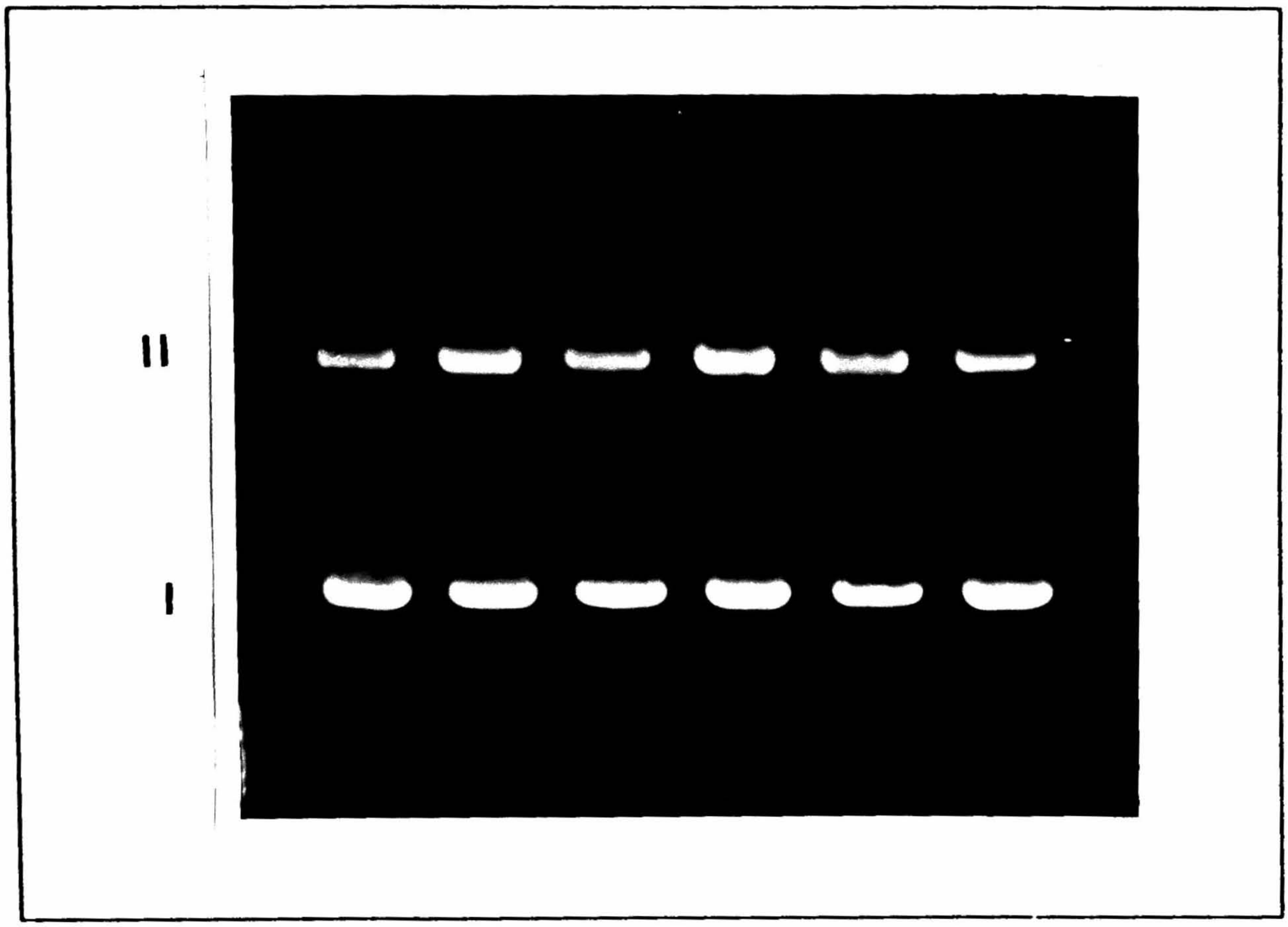

Fig. 7.12. Light induced nuclease activity of series III porphyrins, **3e-g** (left to right) Lane 1. Untreated pBR 322, Lanes 2, 3, 4, 5 and 6: pBR 322 + **3e**, **3f**, **3g**, **3l** and **5a** In each case [DNA]/[Drug] = 1 and samples were incubated for 1h before being irradiated with visible light ($\lambda > 400$ nm) for 2.5 h. Electrophoresis experiment was carried out as described in section 2.6.

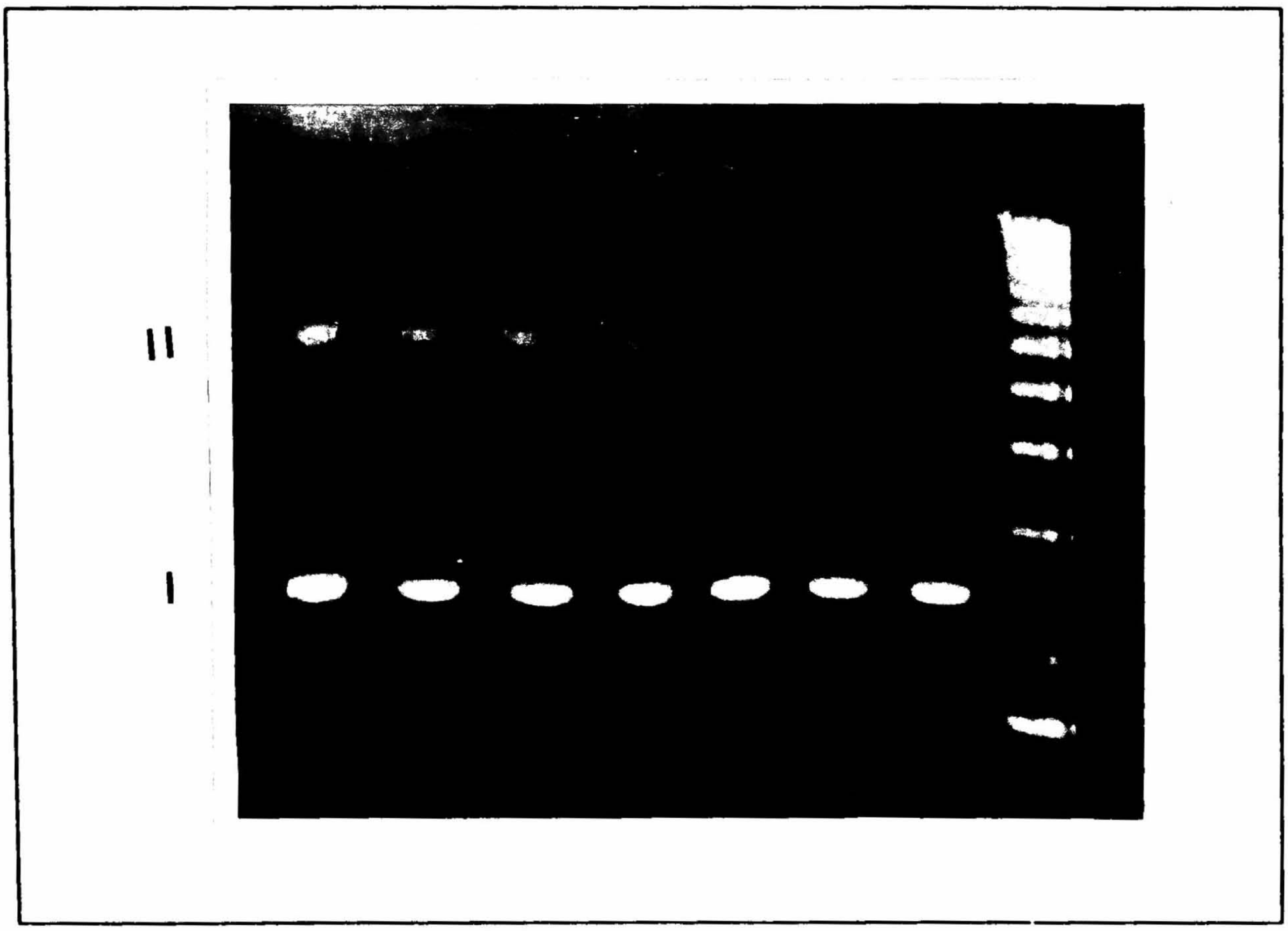

Fig. 7.13. Photograph showing the electrophoretic behaviour of pBR 322 in the presence of compounds **3a-d** in dark (left to right) Lane 1 Untreated pBR 322; Lanes 2, 3, 4, 5, 6, 7 and 8 pBR 322 + **3a**, **3b**, **3c**, **3d**, **3l**, **5a**, and DNA mol wt. marker. In each case [DNA]/[Drug] = 1 and samples were incubated for 1h before electrophoresis

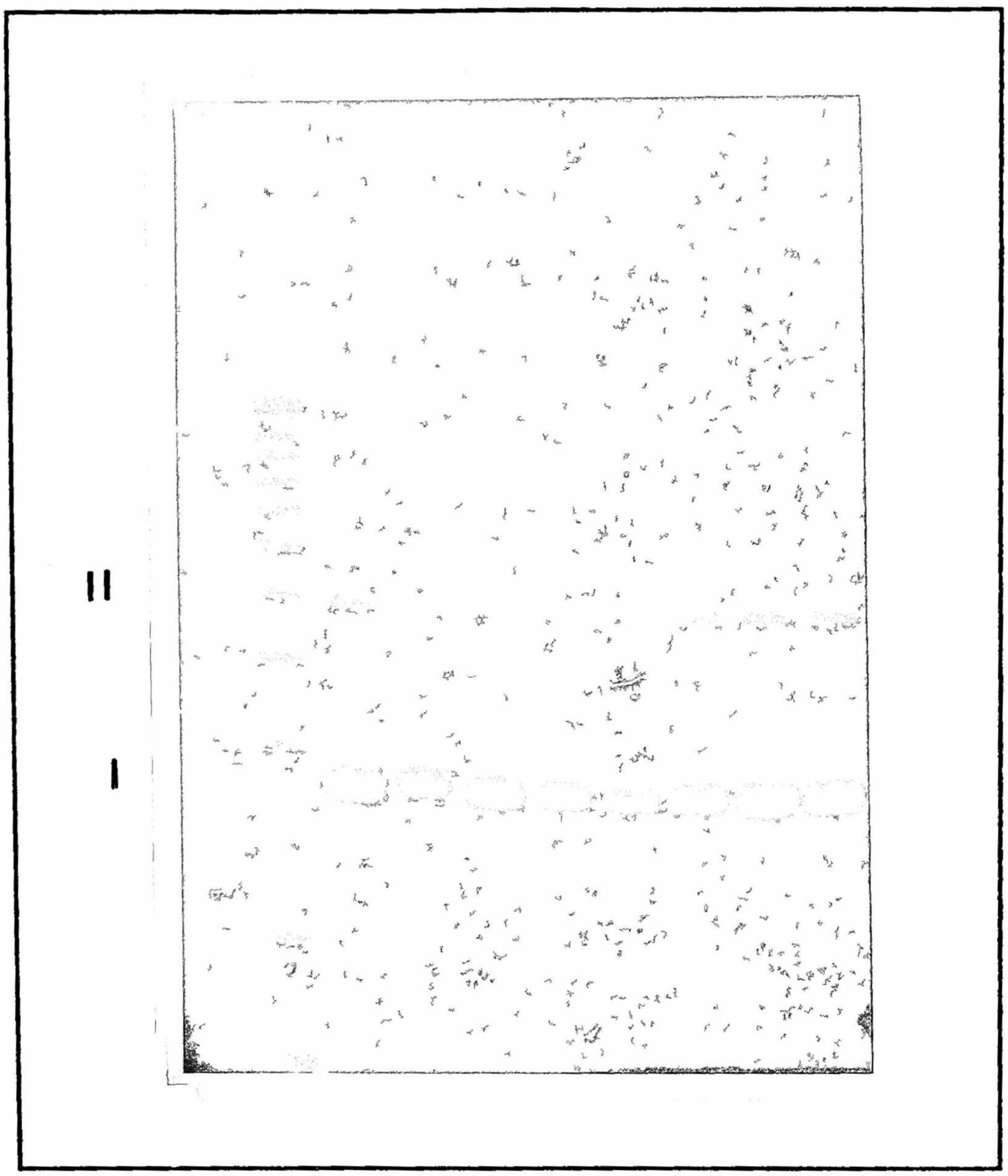

Fig. 7.14. Photograph showing the electrophoretic behaviour of pBR 322 in the presence of compounds **4a-g** in dark (left to right) Lane 1: DNA mol. wt. marker. Lanes 2, 3, 4, 5, 6, 7, 8, and 9: pBR 322 + Untreated pBR 322, **4a**, **4b**, **4c**, **4d**, **4e**, **4f**, **4g** and **5b**. In each case [DNA]/[Drug] = 1 and samples were incubated for 1h before electrophoresis.

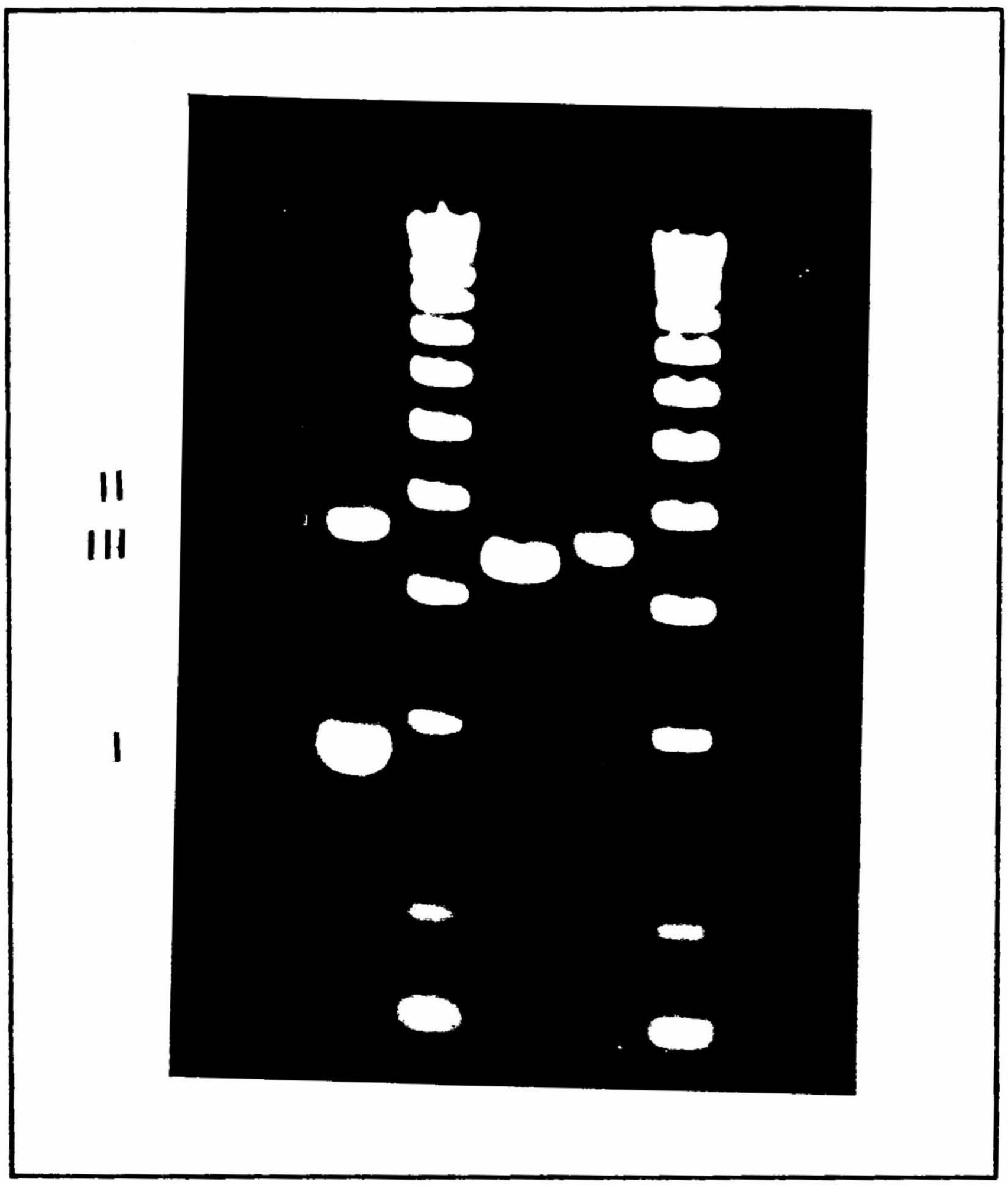

Fig. 7.15. Generation of form II DNA upon photoirradiation of form I pBR 322 solutions containing porphyrin-intracellular recognition element conjugates. (from left to right) Lane 1 : Untreated pBR 322 DNA. Lane 2: DNA marker; Lane 3 : pBR 322 digested with HIND III; Lane 4: pBR 322 digested with **4c** and Lane 5: DNA marker.

prevalent in all these drugs and the possibility of the generation of radical species is imminent during irradiation of aqueous, oxygenated solutions of these photosensitizers containing DNA.

A closer examination of the results obtained during the irradiation/gel-electrophoresis experiments carried out using these hybrid porphyrins (Figs. 7.10 -7.13) reveals several interesting features with regard to their nuclease activity. Firstly, no definite trend is discernible in the nicking efficiencies of these photosensitizers as a function of the linker group in compounds **1a-e** and **4a-e** On the other hand, the linker moiety is seen to have a marked influence on the nuclease activity of series III porphyrins The observed highest cleavage efficiency for **3a** (see Fig 7.14) compared to the cleavage ability of any other porphyrin and the DNAse activity of compounds **3h-j** are revealing. The shorter chain length between the porphyrin and the intracellular recognition element in **3a** might be responsible for a better cleavage ability of this hybrid photosensitizer. Indeed, observations similar to this have been made earlier. For example, higher efficiencies towards DNA-binding, cross-linking and cytotoxicity have been noticed for 'bifunctional' DNA cleaving agents having short chain lengths (n = 3, 5) between a DNA alkylating agent and methyl viologen [66] In addition, recent *in vivo* PDT studies carried out with ethers derived from haematoporphyrin species or with some methylene-linked diporphyrin systems have suggested a dependence of tumor damage on length of the alkyl chain; the longer the alkyl chain, the lower is the activity.[67] It can be supposed that, an increase in the alkyl chain length of the linker group, in principle, increases the hydrophobicity within the molecule and lowers its solubility. This can cause a decline in the cellular uptake of the drug leading to lower cleavage efficiencies.[65] While such a situation might also hold good for the porphyrin-spacer-intracellular

recognition element systems investigated in this chapter when they will be used in *in vivo* experiments, the strong nuclease activity observed here for the n=3 system has to be analyzed only at the molecular level. In this regard, it can be noted that singlet oxygen has to diffuse within its lifetime to effect the DNA cleavage and the feasibility of this process is more in the case of hybrids with n=3, where the distance between the porphyrin moiety (the $^1O_2$ generator) and the appended DNA intercalator is short. Thus, a proximity of the porphyrin moiety and the appended intracellular recognition element could play a critical role in the cleavage efficiency of the drug. Finally, the DNAse activity is observed for the dicationic species **3h-j** possibly due to their hydrophilic nature and additional involvement of Coulombic interactions with the phosphate backbone of DNA.

7.4 Summary

The ground state properties as well as photochemical and photoinitiated DNA cleavage reactions of various porphyrin-based photosensitizers, in which a porphyrin is linked to an intracellular recognition element such as acridone (**1a-e**), 9-aminoacridine (**2a-c**), phenothiazine (**3a-j**) or chlorambucil (**4a-f**) have been reported. The ^1H NMR, UV-visible, and electrochemical data of these hybrids suggests that there is no appreciable ground state interaction between the porphyrin and the appended intracellular recognition element. Although, the fluorescence quantum yield for the porphyrin part of each hybrid molecule is similar to that of H_2TTP, flourescence from the acridone/acridine moiety is quenched in compounds **1a-e** and **2a-c** Detailed fluorescence studies have revealed the occurrence of intramolecular energy transfer between the acridone/acridine and the porphyrin in these hybrids. The singlet oxygen quantum yields of these linked

compounds are similar to those of unlinked reference compounds H_2TPP, **5a** or **5b**. All of these results suggest that appending an intracellular recognition element has no adverse effect on the photosensitizing ability of the porphyrin in these compounds. The nuclease activity of these hybrid molecules measured using the supercoiled plasmid DNA pBR 322 suggests that upon irradiation by the visible light, compounds **1a-e**, **3a-d** and **4a-e** cleave the supercoiled DNA (form I) to the open circular form II. While no photocleavage has been observed when compounds **2a-c** and **3e-g** are used, compounds **3h-j** are seen to display DNase activity upon photoirradiation

7.4 References

1. Diamond, I.; McDonagh, A. F.; Wilson, C B ; Granelli, S. G.; Nielsen, S.; Jaenicke, R *Lancet* **1972**, 2, 1175
2. Dougherty, T. J.; Kaufman, J. E.; Goldfarb, A. Weishaupt, K. R , Boyle, D. G.; Mittlemam, A. *Cancer Res.* **1978**, 38, 2628
3. (a) Kessel, D , Cheng, M -L *Photochem Photobiol* **1985**, 41, 277 (b) Kessel, D , Thompson, P.; Musselman, B., Chang, C K *Cancer Res* **1987**, 47, 4642
4. Byrne, C. J ; Marshallsay, L V.; Sek, S Y., Ward, A D. In *Photodynamic therapy of neoplastic disease,* Kessel D., Ed ; CRC: Boca Raton, 1990, Vol. 2, p 131.
5. Henderson, B W.; Dougherty, T. J. *Photodynamic Therapy Basic Principles and Clinical Applications;* Marcel Dekker. New York, 1992.
6. Moan, J.; Berg, K. *Photochem. Photobiol* **1992**, 55, 931.
7. Pandey, R. K ; Shiau, F. -Y.; Ramachandran, K , Dougherty, T. J.; Smith, K. M. *J. Chem. Soc. Perkin Trans. 1* **1992**, 1377 and references therein

8. Shopova, M.; Mantareva, V.; Krastev, K.; Hadjiolov, D.; Milev, A.; Spirov, K.; Jor, G.; Ricchelli, F. J. *Photochem. Photobiol., B. Biol.* **1992**, 16, 83.
9. Bishop, S. M.; Khoo, B. J.; MacRobert, A. J.; Simpson, M. S. C.; Phillips, D.; Beeby, A *J. Chromatogr.* **1993**, 646, 345.
10. Boyle, B. W.; Leznoff, C. C.; van Lier, J. E. *Br. J. Cancer* **1993**, 67, 1177.
11. Segalla, A.; Milanesi, C.; Jori, G.; Capraro, H. -G.; Isele, U.; Schieweck;, K. *Br. J. Cancer* **1994**, 69, 817.
12. Kostenich, G. A ; Zhuravkin, I. N.; Zhavrid, E. A. *J. Photochem. Photobio B. Biol.* **1994**, 22, 211.
13. Bonnett, R.; Benzie, R.; Grahn, M. F.; Salgado, A.; Valles, M. A. *Proc. SPIE* **1994**, 2078, 171.
14. Leach, M. W.; Higgins, R. J ; Autrey, S. A.; Bogganim J. E.; Lee, S. -J. H.; Smith, K. M. *Photochem. Photobiol.* **1993**, 58, 653.
15. Pandey, R. K.; Bellnier, D. A.; Smith, K. M.; Dougherty, T. J. *Photochem. Photobiol.* **1991**, 53, 65.
16. Richter, A. M.; Kelly, B.; Chow, J.; Liu, D. J.; Towers, G. M. N.; Dolphin, D.; Levy, J. G. *J. Natl. Cancer Inst.* **1987**, 79, 1327.
17. Morgan, A. R.; Garbo, G. M., Keck, R W., Skalkos, D.; Selman, S. H. *Photochem Photobiol.* **1990**, 6,133.
18. Ritcher, A. M.; Watterfield, M. E., Jain, A. K.; Allison, B.; Sternberg, E. D.; Dolphin, D.; Levy, J. G. *Br. J. Cancer* **1991**, 63, 87.
19. Hunt, D. W. C.; Jiang, J. -H.; Levy, G. J.; Kabn. A. H. *Photochem. Photobiol.* **1995**, 61, 417.
20. Vogel, E.; Kocher, M.; Schmickler, H.; Lex, J. *Angew. Chem., Int. Ed. Engl.* **1986**, 25, 197.

21. Leung, M.; Richert, C.; Gamarra, F.; Lumper, W.; Voge E.; Jochanji, D.; Goetz, A. E. *Br. J. Cancer* **1993**, 68, 225.

22. Sessler, J. L.; Hemmi, G.; Mody, T. D.; Murai, T.; Burrell, A.; Young, S. W. *Acc. Chem. Res.* **1994**, 27, 43 and references therein.

23. Hegan, W. J.; Barber, D. C.; Whitten, D. G.; Kelly, M.; Albrecht, F.; Gibson, S. L.; Hilf, R. *Cancer Res.* **1988**, 48, 1148.

24. Barber, D. C.; Van Der Meid, K. R.; Gibson, S. L.; Hilf, R.; Whitten, D. G. *Cancer Res.* **1991**, 51, 1836.

25. Lawrence, D S., Gibson, S L; Nguyen, M L.; Whittemore, K R, Whitten, D. G.; Ressell, H. *Photochem. Photobiol.* **1995**, 61, 90.

26. Bigey, P.; Pratviel, G.; Meunier, B. *J Chem. Soc, Chem. Commun* **1995**, 181.

27. Mastruzzo, L , Woisard, A.; Ma, D. D. F., Rizzarelli, E.; Favre, A.; Doan, T. L *Photochem. Photobiol* **1994**, 60, 316.

28. Le Doan, T. Praseuth, D.; Perrouault, L.; Chassignol, M , Thuong, N T ; Helene, C. *Bioconjugate Chem.* **1990**, 2, 108.

29. Fedorova, O S.; Savitskii, A. P.; Shoikhet, K. G ; Ponomarev, G. V. *FEBS Lett.* **1990**, 259, 335.

30. Milgrom, L. R.; O'Neill, F. *Tetrahedron* **1995**, 51, 2137.

31. Harada, A.; Shiotsuki, K ; Fukushima, H.; Yamaguchi, H ; Kamachi, M *Inorg Chem.* **1995**, 34, 1070.

32. Ding, L.; Moghadam, G E.; Cros, S ; Auclair, C.; Meunier, B. *J. Chem Soc., Chem. Commun.* **1989**, 1711.

33. Moghadam, G. E.; Ding, L., Tadj, F.; Meunier, B. *Tetrahedron* **1989**, 45, 2641.

34. Ding, L.; Moghadam, G. E.; Meunier, B. *Biochemistry* **1990**, 29, 7868.

35. Perreee-Fauvet, M ; Gresh, N. *Tetrahedron Lett* **1995**, 36, 4227.

16 [illegible] Thorntgill, M D [illegible] **1995** [illegible]

17 [illegible] Pereira-Faca, M [illegible] Holmes, P Rowell, N [illegible] **1993** 15 [illegible]

18 Hashimoto, Y Lee, C S Shoda, K Okamoto, T [illegible] **1993** 24 [illegible]

19 Dyer, R T [illegible] Hall, D D [illegible] Noble, M Osborne, C K [illegible] **1989** 19 [illegible]

20 Fujioka, H Nishiyama, Y Tomikawa, H Kawada, N [illegible] **1989** 33 [illegible]

21 (a) Takeuchi, S Ohara, T Takagi, M Fukuoka, H [illegible] **1992** (b) Su, T [illegible] Chen, T C Kim, J Y Hong, J T Czarnecka, E R Nash, A V Cyr, M G Sowinski, P M Watanabe, K A [illegible] **1995** 18 [illegible] and references therein

22 *Physicochemical and Pharmacokinetic Aspects of Drug Formulation*; Gupta, P P Ed Elsevier: Amsterdam, 1986

23 Cohen, G M Collis, P M Hartley, J A Mather, A Spencer, M C R Wheelhouse, R T [illegible] **1992** [illegible]

24 Kuwano, J V Gumpper, H R Hall, A A Mayer, R P [illegible] **1993** [illegible]

25 Collis, P M Chapot, J M Weaver, R [illegible] **1995** [illegible]

26 Wardleworth, K P Forster, C J Donaghue, T F [illegible] **1976** 16 [illegible]

27 Pollacco, D A Donaghue, T J [illegible] **1978** [illegible]

28 Box, G Spiers, J D In *Statistics in Pharmaceutical Research*; Smith, D C Ed Pergamon: New York, 1981

49. Pooler, J. P.; Valenzeno, D. P. *Photochem. Photobiol.* **1979**, 30, 581.

50. Tanielian, C.; Wolf, C. *J Phys. Chem.* **1995**, 99, 9825 and references therein.

51. Stevens, B.; Ors, J. A.; Christy, C. N. *J. Phys. Chem.* **1981**, 85, 210.

52. Reddi, E.; Jori, G.; Rodgers, M. A. J.; Spikes, J. D. *Photochem Photobiol.* **1983**, 38, 639.

53. Maniatis, T.; Fritsch, E. F.; Sambrook, J. *Molecular Cloning A Laboratory Manual;* CSH: New York, 1984.

54. Vinograd, J.; Lebowitz, J.; Radloff, R.; Watson, R.; Laipis, P *Proc. Natl. Acad. Sci. USA* **1965**, 53, 1104.

55. Spotheim-Maurizot, M ; Charlier, M.; Sabattier, R. *Int. J Radiat Biol.* **1990**, 57, 301.

56. Masnyk, T. W.; Minton, K. W. *Photochem Photobiol* **1991**, 54, 99.

57. Dugaiczyk, A.; Boyer, H W.; Goodman, H. M *J. Mol. Biol.* **1975**, 96, 171.

58. Fiel, R. J.; Datta-Gupta, N.; Mark, E. H , Howard, J C. *Cancer Res* **1981**, 41, 3453

59. Munson, B. R ; Fiel, R. J. *Nucleic Acids Res* **1992**, 20, 1315.

60. Nicotera, T. M.; Munson, B. R.; Fiel, B. J. *Photochem. Photobiol.* **1994**, 60, 295.

61. Bohm, F.; Marston, G.; Truscot, T. G.; Wayne, R. P. *J. Chem Soc., Faraday Trans* **1994**, 90, 2453

62. Ma, L.; Moan, J.; Berg, K. *Int. J. Cancer* **1994**, 57, 883

63. Shinozuka, K.; Seto, Y.; Sawaki, H. *J. Chem. Soc., Chem. Commun.* **1994**, 1377.

64. Takenaka, S.; Ihara, T.; Takagi, M. *Chem. Lett.* **1992**, 1.

65. Shinozuka, Seto, Y.; Sawai, H. *J. Chem. Soc., Chem. Commun.* **1994,** 1377.

66. Bose, D. S.; Thompson, A. S.; Smellie, M.; Berardini, M. D.; Hartley, J. A.; Jenkins, T. C.; Neidle, S.; Thurston, D. E. *J. Chem. Soc., Chem. Commun.* **1992,** 1518.

67. Bellnier, D. A.; Henderson, B. W.; Pandey, R. K.; Potter, W. R.; Dougherty, T. J. *J. Photochem. Photobiol., B. Biol.* **1993,** 20, 55.

68. Gandin, E.; Lion, Y.; Van der Vorst, A. *Photochem. Photobiol.* **1983,** 37, 271.

CHAPTER 8

Conclusions

Figure 8.1 summarizes the main experimental results that were obtained upon probing the excited states of various porphyrin-based D-A compounds described in the previous chapters of this thesis.

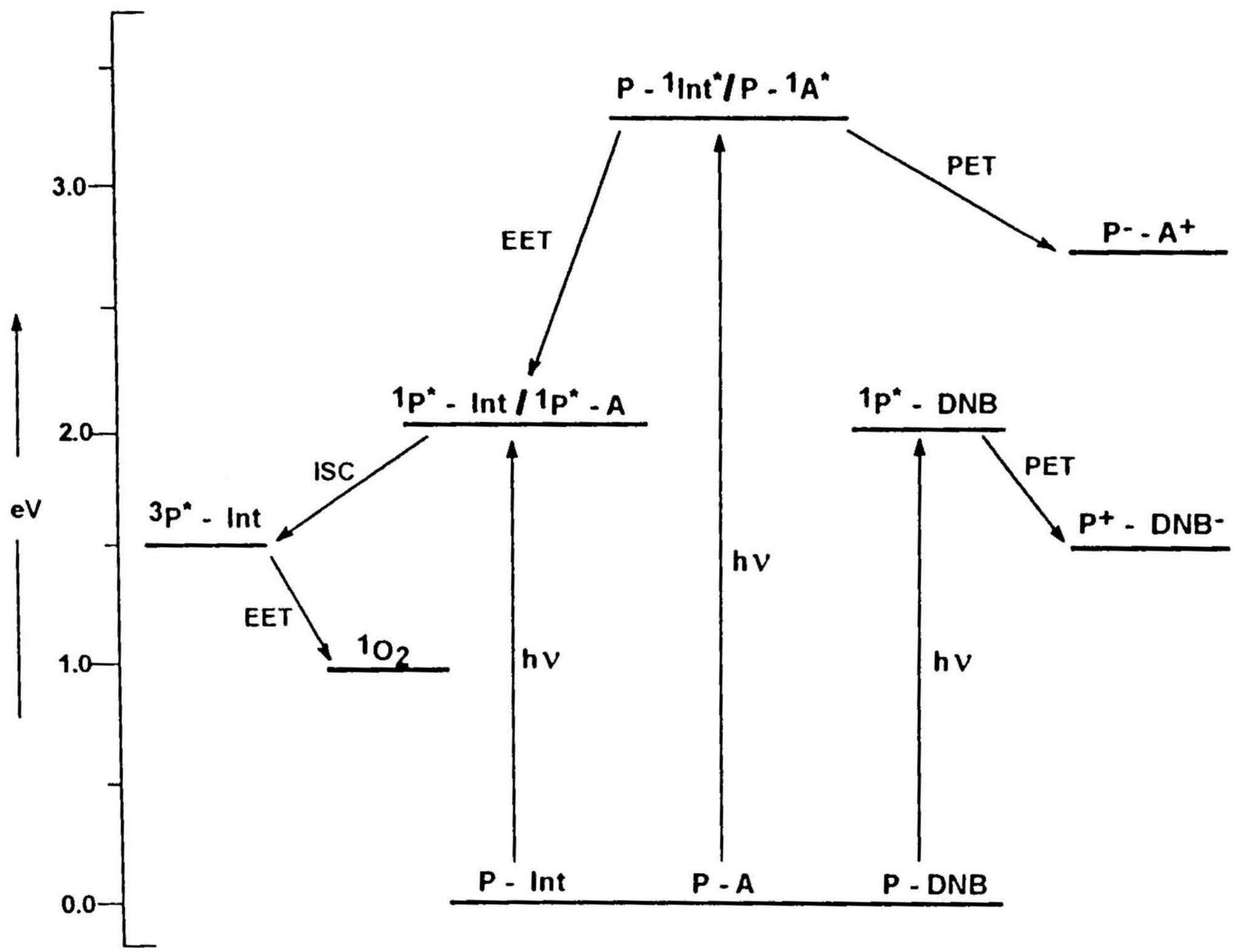

Fig. 8.1

As seen in this figure, excited state chemistry of the D-A compounds investigated in this study is characterized by both PET and EET reactions. The porphyrin subunit which is a customary component in each of these bichromophoric compounds can act as either a donor or an acceptor of energy/electron. For example, porphyrin excited states which are electron donors in the isomeric porphyrin-dinitrobenzene (P-DNB) complexes (chapter 3), also take the role of energy donors, to $^3O_2$, in the porphyrin-intracellular recognition element (P-Int) conjugates (chapter 7). On the other hand, electron and energy accepting ability of the porphyrin species has been clearly demonstrated in the covalently- and non-covalently linked porphyrin-anthracene (P-A) dyads (chapters 4 and 6), P-A_4 pentad (chapter 5) and P-Int conjugates (chapter 7).

Obviously, possibility of occurrence, efficiency and direction (i. e. whether to or from the porphyrin) of the individual electron and energy transfer reactions are dependent on the spectroscopic features and redox potentials of a given D-A compound. In this regard, the choice of chromophores as well as the simplistic design element involved in the synthesis of the D-A compounds using these chromophores have ensured that there exists no 'overlap' of the spectral bands or redox potentials between the donor and the acceptor in each case. Among the other things, one of the main advantages in having a porphyrin as a component in all these D-A compounds is that this aromatic macrocycle possesses well-defined spectral features with the major absorption and emission peaks occurring mostly in the 'red-region' of the visible range. On the other hand, almost all of the non-porphyrinic species that are linked to the porphyrins in these compounds absorb and fluoresce below ca. 400 nm. Thus, it was possible to selectively excite the required chromophore in each D-A compound to

initiate and monitor the required PET or EET reaction. Likewise, the redox potential data of the porphyrin and the non-porphyrinic species in these D-A compounds could also be analyzed easily so as to arrive at the exact location of the charge-transfer (CT) states. The CT state energies could be further fine-tuned either by inserting the zinc(II) ion into the macrocycles and/or by varying the solvent dielectric constant.

As far as the mechanisms of the PET reactions are concerned, the results suggest that a 'through bond' electron mediation is less likely in these covalently- and 'non-covalently' bound D-A systems having flexible or 'semi-flexible' spacers.[1] Thus, most of the PET reactions have to be interpreted in terms of a 'through space' electron mediation. The EET reactions, on the other hand, have been interpreted by invoking both dipole-dipole and electron-exchange mechanisms. An incisive analysis of the results presented in various chapters of this thesis has aided in identifying various determinants of EET and PET reactions in these D-A systems and a few important ones will be discussed below.

8. 1 Determinants of EET and PET efficiencies

The effect due to the free energy change (ΔG^0) on the rates of PET reactions (k_{et}) has been clearly discernible in the P-DNB compounds. The k_{et} values for the free-base derivatives of these systems are, in general, lower than those for the corresponding zinc(II) analogues and this fact is consistent with the more positive ΔG^0 values for the former compounds. The effect of the solvent dielectric constant on the k_{et} values has been noted for P-DNB compounds, P-A dyads and P-A_4 pentad. Interestingly, for the P-A dyads and the pentad, observed competition between the EET and PET reactions is critically dependent on the solvent polarity.

Another important determinant of EET and PET reaction efficiencies that has been specifically addressed in this study is concerned with the D-A distance and orientation. It should be noted here that, owing to the flexible nature of the spacers separating the donor and the acceptor, only a combined effect due to changes in both these parameters was obvious here. EET (and also PET) rates varied as o > m > p for the P-A dyads and this order is in-line with the estimated D-A distances in these isomeric compounds. On the other hand, PET rates for the isomeric P-DNB dyads varied as o > p > m; an order that is inconsistent with the distance dependence of electron transfer reaction. Thus, it was suggested that the D-A orientation is not so conducive for an efficient electron transfer to occur in the meta linked P-DNB dyad.[1] A similar situation has been encountered earlier in the case of covalently linked porphyrin-trinitrobenzene dyads wherein the k_{et} for the ortho isomer was seen to be less than that for the meta isomer.[2]

The nature of spacer groups utilized in this study also has a profound influence on the PET and EET reactions. The 'short', albiet flexible, ether or ester spacer utilized here for the construction of P-A and P-DNB compounds has been responsible for a close proximity of the donor and the acceptor subunits and also for the consequent unusual features observed for these systems that are otherwise rare in D-A compounds bridged by either rigid or long, flexible spacers. Firstly, the 'short' spacers have permitted π-π interactions between the donor and the acceptor as suggested by the UV-visible and ^{1}H NMR spectroscopic results. The π-π interaction between the anthracene and the porphyrin in the P-A dyads has also been implicated in promoting the electron exchange mediated EET. Secondly, as mentioned above, k_{et} for the meta linked P-DNB dyad is less than that for the para analogue. Here, if one considers that PET is following a 'through space'

mechanism, the above feature is, most probably, a consequence of the 'short' chain length of the spacer rather than an electronic effect due to the presence of an ester group at the meta position.[1] Another observation, that highlights the role of spacers in the EET and PET reactions of the D-A systems investigated here, is that the fluorescence quenching observed for the meta linked P-A dyad is lower than that observed for the P-A_4 pentad. This observation is curious and may have an explanation that is based on statistical considerations. Nonetheless, it is possible that the differences in the D-A orientations between the dyad and the pentad can also cause the observed disparity in their quenching efficiencies. Finally, EET efficiencies of the P-Int (where Int = acridone or acridine) conjugates wherein the donor and the acceptor are separatred by long, flexible alkyl chains are all nearly equal to one another. Thus, overall, an important outcome of this study is the realization that the PET and EET reaction rates in the isomeric D-A compounds can be fine-tuned by separating the donor and the acceptor by a 'short' spacer.

DNA nicking efficiencies of the P-Int conjugates have been seen to be markedly influenced by the nature of the spacer group. This can be illustrated for porphyrin-phenothiazine conjugates having alkyl (with or without interspersed piperzine) and 'qurternized' piperzine groups in the spacers. As seen in Fig 8.2(a), a porphyrin-phenothiazine conjugate having an alkyl chain (with or without the interspersed piperizine) as the spacer binds to DNA by intercalation of the phenothiazine moiety and, the porphyrin part of the molecule lies outside keeping a certain distance with the helix. The DNA nicking efficiency of these conjugates has been shown to depend on the length of the spacer between the intercalator and the photosensitizer. On the other hand, a porphyrin-phenothiazine conjugate

having a 'quarternized' piperzine in the spacer showed DNAse activity. As seen in Fig. 8.2(b), these conjugates can bind to DNA by both intercalation of the phenothiazine and Coulombic interaction between the positive charges on the spacer and the negative 'back bone' of DNA resulting in not only a stronger binding but also a closer approach of the photosensitizer with DNA. Thus, a spacer-induced change in the distance between the porphyrin and DNA in these compounds is responsible, in part, for the observed variation in their DNA nicking efficiencies *via* a $^1O_2$ mediated mechanism; larger the distance between the photosensitizer and the helix, more is the diffusion distance for $^1O_2$ and hence less is the DNA nicking efficiency.[3]

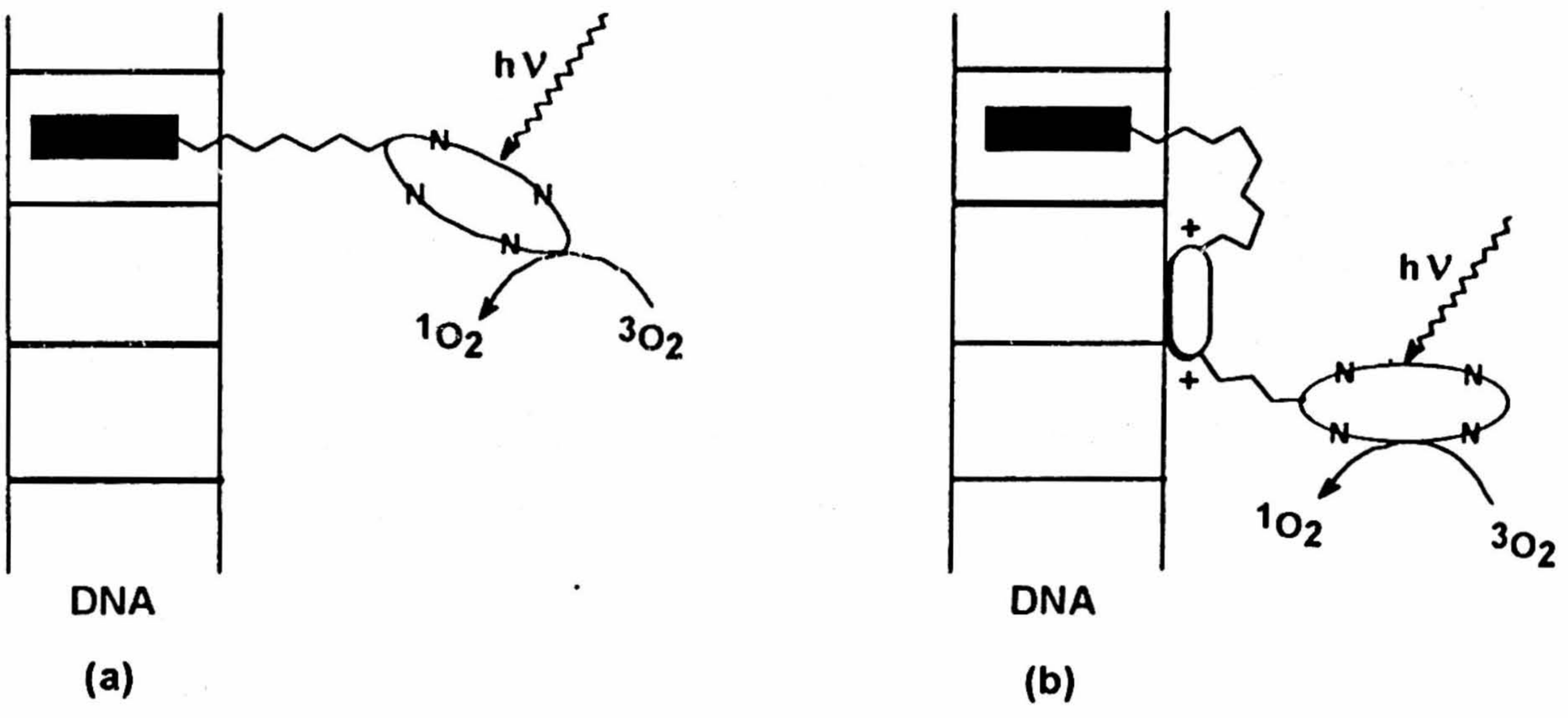

Fig. 8.2

8.2 Biological relevance

Although this study is not aimed at building the 'photosynthetic model systems', it is instructive to compare and contrast the results obtained for the P-DNB, P-A and P-Int compounds with those obtained earlier for various porphyrin-based D-A compounds that have been specifically designed to mimic certain key features of the initial events of

photosynthesis. Firstly, in stark contrast to the prevalent use of a quinone as an electron acceptor and a carotenoid as an energy donor in porphyrin-based, biomimetic compounds, this study utilizes dinitrobenzene and anthracene as electron acceptor and energy donor, respectively. On the other hand, ΔG^0, distance and orientation as well as solvent effects on the PET reactions observed in this study for the covalently linked P-DNB systems are similar to those observed earlier for various porphyrin-quinone compounds. Similarly, the details of the EET reactions and the light-harvesting abilitiy of the P-A dyads and the P-A_4 pentad are reminiscent of those reported earlier for porphyrin-anthracene, porphyrin-carotene and porphyrin-cyanine dye bichromophoric systems[4] and for the directly linked porphyrin-tetra(anthracene) systems[5] and novel pentameric porphyrins, respectively.[6] It is interesting that direction of the PET reaction (anthracene porphyrin) in the P-A dyads and the P-A_4 pentad is also similar to that observed in the antenna function of the carotenoids (eq. 1.13)[7] and in the covalently linked porphyrin-carotene dyads (carotenoid → chlorophyll or porphyrin).[8] However, while PET occurs from the excited state of anthracene to the ground state of the porphyrin in the P-A systems investigated in this study, it occurs from the ground state of the carotenoid to the singlet state of the chlorophyll or the porphyrin in the latter two cases Finally, singlet state activity of the non-covalently bound P-A system is found to be different from that observed for other comparable porphyrin-based, base-paired, D-A systems.

Results of photophysical and DNA cleavage experiments carried out in this study on the P-Int conjugates are noteworthy in many respects. In this regard, it can be noted that notwithstanding the recent reports which suggest that the current clinical PDT agents target the cell membrane and bring

about the photoinitiated cell necrosis,[9] it is essential to examine the effect of photoirradiation on DNA in the presence of porphyrins. Such studies might be useful in the development of new and efficient PDT agents. The approach which involves a combination of a porphyrin and an intracellular recognition element, as utilized here for the synthesis of novel PDT agents, is interesting and, this strategy should be able to impart a higher level of bioavailbility for the drug. In addition, the 'dual action' theme as exemplified in studies with the porphyrin-chlorambucil conjugates should be very useful in the 'combination therapy' (e.g. chemotherapy + phototherapy) against cancer.

8.3. Future scope

Notwithstanding the fact that the present study has been helpful, to some extent, in probing certain intricacies involved in the PET and EET reactions of the porphyrin-based D-A compounds, an in-depth analysis of the results described in various chapters of this thesis suggests that a lot more remains to be done to arrive at a better understanding of the EET and PET mechanisms and to generate more sophisticated D-A compounds and PDT agents. For example, more elaborate photophysical experiments involving the time-resolved absorption and fluorescence techniques can be carried out to learn more about the mechanistic details of the PET and EET reactions. PET and EET reactions of the P-DNB and P-A systems that are linked by flexible spacers can be compared with those of the analogous systems having rigid spacers so as to have a better understanding of the role of spacers in mediating the PET and EET reactions. The experience gained in this study while working on various D-A compounds can be advantageously used for the construction of covalently or noncovalently bound triads of the type D-A_1-A_2, D_1-A-D_2 etc Non-covalently bound P-A

systems with higher propensity for the self-assembly and shorter D-A distances than those which characterize the A-T base-paired P-A system described in chapter 6, can be built and H-bonding effects on the PET and EET reactions in them can be studied. Finally, water-soluble PDT agents for *in vitro* and probably, *in vivo* applications can be devised by linking porphyrins having peripheral positive or negative charges with various intracellular recognition elements.

8.4 References and notes

1. A 'through space' mechanism has been proposed for the EET and PET reactions of many porphyrin-based, isomeric D-A systems wherein the donor or the acceptor groups have been linked at, para, meta or ortho positions of one of the phenyl rings of a porphyrin. An exception is that of porphyrin-carotene dyads (compounds **2**, chapter 1) for which 'through bond' mediated EET reactions and internal conversion processes have been reported (Ref. 32, chapter 1). Here, if one considers the partial double bond nature of the amide, there exists a possibility for the porphyrin π-electron system to be formally conjugated, through the amide, with the carotenoid. Such a possibility is less likely in the case of ester or ether bridged D-A compounds investigated in the present study.
2. Maiya, B. G.; Krishnan, V. *J. Phys. Chem.*, **1985**, 89, 5225.
3. It should be noted here that the variation of DNA nicking efficiencies observed for these conjugates need not necessarily be dependent only on the porphyrin-DNA distance and that the illustration in Fig. 8.2 is only tentative as it is largely intuitive.

4. (a) Gust, D., Moore, T. A.; Moore A. L. *Acc. Chem. Res.*, **1993**, 26, 1988 and references therein. (b) Lindsey, J. S.; Brown, P. A.; Siesel, D. A. *Tetrahedron* **1989**, 45, 4845. (c) Osuka, A.; Yamada, H.; Maruyama, K.; Mataga, N.; Asahi, Ohkouchi, M. T.; Okada, T.; Yamazaki, I.; Nishimura, Y. *J. Am. Chem. Soc.* **1993**, 115, 9439. (d) Effenberger, F.; Schlosser, H.; Bauerle, P.; Maier, S.; Port, H.; Wolf, H. C. *Angew Chem., Int. Ed. Engl.* **1988**, 27, 281.

5. (a) Harriman, A.; Davila, J. *Tetrahedron* **1989**, 45, 4737. (b) Nakajima, S.; Osuka, A. *Tetrahedron Lett.* **1995**, 36, 8457.

6. (a) Davila, J.; Harriman, A.; Milgrom, L. R. *Chem. Phys. Lett.* **1987**, 136, 427. (b) Prathapan, S.; Johnson, T. E.; Lindsey, J. S. *J. Am. Chem. Soc.* **1993**, 115, 7519.

7. Hermant, R.; Liddell, P. A.; Lin, S.; Alden, R. G.; Kang, H. K.; Moore, A. L.; Moore, T. A.; Gust, D. *J. Am. Chem. Soc.* **1993**, 115, 2080.

8. (a) Beddard, G. S.; Davidson, R. S.; Trethewey, K. R. *Nature* **1977**, 267, 373. (b) Deming-Adams, B. *Biochim. Biophys. Acta* **1990**, 1020, 1.

9. Levy, J. G. *Tibtech.* **1995**, 13, 14

Appendix I

List of Publications

1. Sirish, M.; Kache, R.; Maiya, B. G. "Intramolecular excitation energy transfer in isomeric porphyrin-anthracene dyads", *J. Photochem. Photobiol. A:Chemistry*, **1995**, 99, 000.

2. Sirish, M.; Maiya, B. G. "Fluorescence studies on a supramolecular porphyrin bearing anthracene donor moieties", *J. Photochem. Photobiol. A: Chemistry*, **1995**, 88, 127.

3. Mehta, G.; Sambaiah, T.; Maiya, B. G.; Sirish, M.; Dattagupta, A. "Porphyrin-phenothiazine hybrid molecules: Marked dependence of light induced nuclease activity on the linker chain" *J. Chem. Soc. Perkin Trans. I*, **1995**, 295.

4. Sirish, M.; Maiya, B. G. "Quenching of fluorescence in a series of covalently linked porphyrin dinitrobenzene compounds" *J. Photochem. Photobiol. A: Chemistry*, **1994**, 77, 189.

5. Mehta, G.; Sambaiah, T.; Maiya, B. G.; Sirish, M.; Dattagupta, A. "Porphyrin-chlorambucil conjugates: Synthesis and light-induced nuclease activity" *Tetrahedron Lett.* **1994**, 35, 4201.

6. Mehta, G.; Sambaiah, T.; Maiya, B. G.; Sirish, M.; Chatarjee, D. "Synthesis and nuclease activity of "porphyrin-acridone" hybrid molecules" *J. Chem. Soc., Perkin Trans. 1*, **1993**, 2667.

Erratum

p14, L7 "violegens" → "viologens"

p28, L1 : although are .. → . although they are .. ,

p28, L3 suffer severly .. → ....suffer severely....

p50, L5 A 2.5 ml of DMF → DMF (2.5 ml)

p51, L15 . A 48 4 g of tris base .. → Tris base (48.4 g)..., A 7.44 g of EDTA disodium salt .. → EDTA disodium salt (7.44 g)...

p51, L22 A 0.25% bromophenol blue.... → Bromophenol blue (0.25%)....

p52, L4 : A 100 mg of ethidium bromide.... → Ethidium bromide (100 mg)....

p52, L18 A 400 mg of low-melt, fine quality agarose.... → Low-melt fine quality agarose (400 mg)...

p53, L5 : A 200 ml of working buffer (TAE) .... → Working buffer (TAE, 200ml).....

p90, L5 .... only examples.... → .....the only examples....

p91, L16 A 0.063 g (0.1 mmol) of compound **1a**.... → **1a** (0.063g, 0.1 mmol)...

p91, L16 0.025 g (0.11 mmol) of 9-chloromethylanthracene.... → 9-chloromethyl-anthracene (0.025 g, 0.11 mmol)...,

p91, L18 ...0.5 g (0.5 mmol) of K_2CO_3.... → K_2CO_3 (0.5 g, 0.5 mmol)....

p99, L15 . Upon incorporating Coulombic correction terms, the ΔG_{PET} values in Table 4.3 can be transformed to those given Table 4.3a

Table 4 3a

Compound	ΔG_{PET}		
	Hexane	CH_2Cl_2	CH_3CN
2a	0.38	-0.39	-0 53
2b	0.26	-0.43	-0.56
2c	-0.09	-0.53	-0 63

p107, L21 . ...among the other.... → ....among other ...

p113, L6 . Despite these, .. → ....Despite these considerations, .

p123, L22 .metalition.....→..... metallation..

p132, L10 Anthracece . → Anthracene....

p158, L13 · ..these values of C_3.... → . .this value of C_3.

p159, L17 . ... **3** is far too weak... . → .... **3** is weak.....

p166, L20 · flourescence..... → .....fluorescence. ...

p178, L1 CHPATER 7 → CHAPTER 7

P179, L9 have been done.... → . . . have been spend . .

p195, L21 · investigate on the . → . . . investigate the

p197, L22 collisional ... → .. .. triplet-triplet .

p199, L6 .largely. → .. . efficient... .

p199, L15 DBB = Oxidised product of DPBF.

p202, L2 . . .irradiation . → . .. irradiation (λ_{ex} = 550 nm where only porphyrin absorbs)